THE PRODUCTION OF ELLIPTIC INTERFERENCES IN RELATION TO INTERFEROMETRY

By CARL BARUS

Hazard Professor of Physics, Brown University

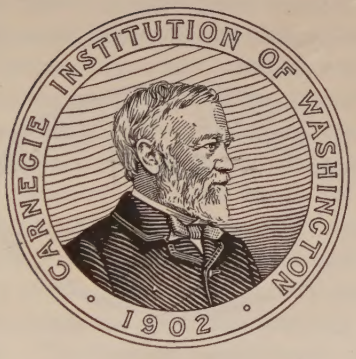

WASHINGTON, D. C.

Published by the Carnegie Institution of Washington

1911

CARNEGIE INSTITUTION OF WASHINGTON

PUBLICATION NO. 149

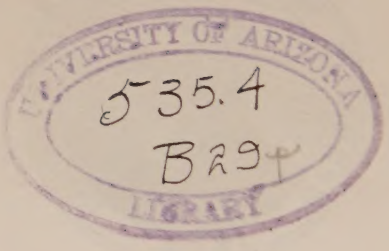

535.4
B29

PRESS OF J. B. LIPPINCOTT COMPANY
PHILADELPHIA, PA.

PREFACE.

In connection with my work on the coronas as a means for the study of nucleation, I came across a principle of interferometry which seemed of sufficient importance to justify special investigation. This has been undertaken in the following chapters, and what appears to be a new procedure in interferometry of great promise and varied application has been developed. In case of the coronas there is a marked interference phenomenon superposed on the diffractions. The present method is therefore to consist in a simplification or systematization of this effect, by bringing two complete component diffraction spectra, from the same source of light, to interfere. This may be done in many ways, either directly, or with a halved transmission or reflecting grating, or by using modifications of the devices of Jamin, Michelson, and others for separating the components.

In the direct method, chapters II and III, a mirror immediately behind the grating returns the reflected-diffracted and diffracted-reflected rays, to be superimposed for interference, producing a series of phenomena which are eminently useful, in addition to their great beauty. In fact the interferometer so constructed needs but ordinary plate glass and replica gratings. It gives equidistant fringes, rigorously straight, and their distance apart and inclination are thus measurable by ocular micrometry. The fringes are duplex in character and an adjustment may be made whereby ten small fringes occupy the same space in the field as one large fringe, so that sudden expansions within the limits of the large fringe (as for instance in magnetostriction) are determinable. This has not been feasible heretofore. Length and small angles (seconds of arc) are thus subject to micrometric measurement. Finally the interferences are very easily produced and are strong with white light, while the spectrum line may be kept in the field as a stationary landmark. The limiting sensitiveness is half the wave-length of light.

The theory of these phenomena has been worked out in its practical bearings, advantageous instrumental equipment has been discussed, and a number of incidental applications to test the apparatus have been made. In much of this work, including that of the first chapter on a modification of Rowland's spectrometer, I had the assistance of my son, Mr. Maxwell Barus, before he entered into the law.

The range of measurement of an instrument like the above is necessarily limited to about 1 cm. and the component rays are not separated. To increase the range indefinitely and to separate the component rays, the grating may replace the symmetrically oblique transparent mirror of

23278

Michelson's adjustment, for instance. In this way transmitted-reflected-diffracted and reflected-transmitted-diffracted spectra, or two corresponding diffracted spectra returned by the opaque mirrors M and N, may be brought to interfere. In both cases the experiments as detailed in chapters IV and V have been strikingly successful. The interference pattern, however, is now of the ring type, extending throughout the whole spectrum from red to violet with the fixed spectrum lines simultaneously in view. These rings closely resemble confocal ellipses, and their centers have the same position in all orders of spectra; but the major axes of the ellipses are liable to be vertical in the first and horizontal in all the higher orders of spectra.

Again there is an opportunity for coarse and fine adjustment, inasmuch as the rings have the usual sensitive radial motion, as the virtual air-space increases or decreases, while the centers simultaneously *drift* as a whole, across the fixed lines of the spectrum, from the red to the violet end.

Drift and radial motion may be regulated in any ratio. The general investigation shows that three groups, each comprising a variety of interferences, are possible and I have worked out the practical side of the theory of the phenomenon. Transparent silvered surfaces are superfluous, as the ellipses are sufficiently strong to need no accessory treatment. Considerable width of spectrum slit is also admissible. Finally, the ellipses may be made of any size and the sensitiveness of their lateral motion may be regulated to any degree by aid of a compensator. In this adjustment the drift may be made even more delicate than the radial motion, thus constituting a new feature in interferometry.

The interesting result follows from the work that the displacement of the centers of ellipses does not correspond to the zero of path difference, but to an adjustment in which $\mu - \lambda d\mu/d\lambda$ (where μ is the index of refraction and λ the wave-length) is critical.

It is obvious that the transparent plate grating may be replaced by a reflecting grating. Thus the grating may be replaced by a plate of glass, as in Michelson's case, and the function of the two opaque mirrors may be performed by two identical plane *reflecting* gratings, each symmetrically set at the diffraction angle of the spectrum to the incident ray. In this case the undeviated reflection is thrown out, whereas the spectra overlap in the telescope. Finally the grating may itself be cut in half by a plane parallel to the rulings, whereupon the two overlapping spectra will interfere elliptically, if by a micrometer one-half is slightly moved, parallel to itself, out of the original common vertical plane of the grating.

Throughout the editorial work and in the drawings I have profited by the aptitude and tireless efficiency of my former student, Miss Ada I. Burton. But for her self-sacrificing assistance it would have been difficult to bring the present work to completion.

CARL BARUS.

BROWN UNIVERSITY, PROVIDENCE, RHODE ISLAND.

CONTENTS.

CHAPTER I.—*On an Adjustment of the Plane Grating Similar to Rowland's method for the Concave Grating.* By C. BARUS AND M. BARUS.

Page

1. Apparatus. Figs. 1 and 2 1–2
2. Single focussing lens in front of grating 2–3
3. Adjustments. Figs. 3 and 4, A, B, C 3–6
4. Data for single lens in front of grating. Table 1 6
5. Single focussing lens behind grating 6
6. Data for single lens behind grating. Table 2 6
7. Collimator method 7
8. Data for collimator method. Table 3 7
9. Discussion 8–9
10. Reflecting plate grating 9
11. Rowland's concave grating. Table 4 10–11
12. Summary 11

CHAPTER II.—*The Interference of the Reflected-Diffracted and the Diffracted-Reflected Rays of a Plane Transparent Grating, and on an Interferometer.* By C. BARUS AND M. BARUS.

13. Introductory. Figs. 5, 6, 7 13–15
14. Observations. Table 5 16–17
15. Equations 17–19
16. Differential equations 19–20
17. Normal incidence or diffraction, etc 20
18. Comparison of the equations of total interference with observation 20–21
19. Interferometer. Figs. 8 and 9; table 6 21–25
20. Secondary interferences 25
21. Summary of secondary interferences 26
22. Convergent and divergent rays 26–27
23. Measurement of small horizontal angles 27–28
24. Summary 28

CHAPTER III.—*The Grating Interferometer.* By C. BARUS AND M. BARUS.

25. Introductory. Figs. 10 and 11 29
26. Apparatus 30
27. Adjustments 31–32
28. Angular extent of the fringes. Tables 7 and 8 32–34
29. Test made by magneto-striction. Figs. 12 to 14; table 9 34–38
30. Summary 38

CHAPTER IV.—*The Use of the Grating in Interferometry; Experimental Results.*

31. Introductory. Fig. 15 39–41
32. Special properties. Fig. 16 41–44
33. Elementary theory. Fig. 17 44–47
34. Compensator. Table 10 47–48

CHAPTER V.—*Interferometry with the Aid of the Grating; Theoretical Results.*

PART I. INTRODUCTION.

35. Remarks on the phenomena. Figs. 18 and 19 49–51
36. Cause of ellipses 51–53
37. The three principal adjustments for interference. Figs. 20, 21, 22, 23 53–55

PART II. DIRECT CASES OF INTERFERENCE. DIFFRACTION ANTECEDENT.

38. Diffraction before reflection..... 55–56
39. Elementary theory. Figs. 24 and 25..... 56–58
40. Equations for the present case. Fig. 26; table 11..... 58–61
41. Interferometer..... 61
42. Discrepancy of the table..... 62

PART III. DIRECT CASES OF INTERFERENCE. REFLECTION ANTECEDENT.

43. Equations for this case. Tables 12, 13, and 14; figs. 27 and 28..... 62–66
44. Divergence per fringe. Tables 15 and 16; fig. 29..... 66–70
45. Case of $d\theta/dy$, $d\lambda/dy$, etc. Fig. 30..... 70–72
46. Interferometry in terms of radial motion..... 72
47. Interferometry by displacement..... 72

PART IV. INTERFERENCES IN GENERAL, AND SUMMARY.

48. The individual interferences. Figs. 31, 32, 33..... 73–75
49. The combined interferences. Table 17..... 75–76
50. Special results..... 76–77

CHAPTER I.

ON AN ADJUSTMENT FOR THE PLANE GRATING SIMILAR TO ROWLAND'S METHOD FOR THE CONCAVE GRATING. By C. Barus and M. Barus.

1. Apparatus.—The remarkable refinement which has been attained (notably by Mr. Ives and others) in the construction of celluloid replicas of the plane grating makes it desirable to construct a simple apparatus whereby the spectrum may be shown and the measurement of wave-length made, in a way that does justice to the astonishing performance of the grating. We have therefore thought it not superfluous to devise the following inexpensive contrivance, in which the wave-length is strictly proportional to the shift of the carriage at the eyepiece; which for the case of a good 2-meter scale divided into centimeters admits of a measurement of wave-length to a few Angström units and with a millimeter scale should go much further.

Observations are throughout made on both sides of the incident rays and from the mean result most of the usual errors should be eliminated by symmetry. It is also shown that the symmetrical method may be adapted to the concave grating.

In fig. 1 A and B are two double slides, like a lathe bed, 155 cm. long and 11 cm. apart, which happened to be available for optical purposes, in the laboratory. They were therefore used, although single slides at right angles to each other, similar to Rowland's, would have been preferable. The carriages C and D, 30 cm. long, kept at a fixed distance apart by the rod ab, are in practice a length of ¼-inch gas pipe, swiveled at a and b, 169.4 decimeters apart, and capable of sliding right and left and to and fro, normally to each other.

The swiveling joint, which functioned excellently, is made very simply of ¼-inch gas-pipe tees and nipples, as shown in fig. 2. The lower nipple N is screwed tight into the T, but all but tight into the carriage D, so that the rod ab turns in the screw N, kept oiled. Similarly the nipple N'' is either screwed tight into the T (in one method, revolvable grating), or all but tight (in another method, stationary grating), so that the table tt, which carries the grating g, may be fixed while the nipple N'' swivels in the T.

Any ordinary laboratory clamp K and a similar one on the upright C (screwed into the carriage D) secures a small rod k for this purpose. Again a hole may be drilled through the standards at K and C and provided with set screws to fix a horizontal rod k or check. The rod, k, should be long enough to similarly fix the standard on the slide S, carrying the slit, and be prolonged further toward the rear to carry the flame or Geissler tube appa-

ratus. The table *tt* is revoluble on a brass rod fitting within the gas pipe, which has been slotted across so that the conical nut *M* may hold it firmly. The axis passes through the middle of the grating, which is fastened centrally to the table *tt* with the usual tripod adjustment.

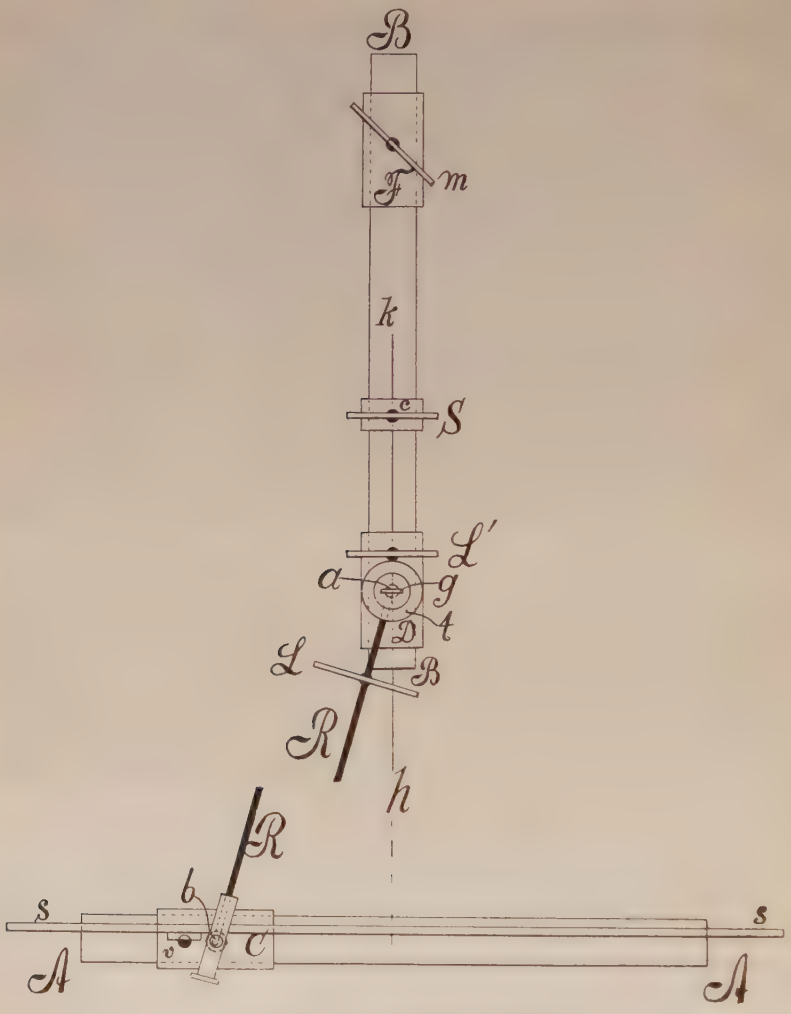

FIG. 1.—Plan of the apparatus.

2. Single focussing lens in front of grating.—I shall describe three methods in succession, beginning with the first. Here a large lens *L*, of about 56 cm. focal distance and about 10 cm. in diameter, is placed just in front of the grating, properly screened and throwing an image of the slit *S* upon the cross-hairs of the eyepiece *E*, the line of sight of which is always parallel to the rod *ab*, the end *b* swiveled in the carriage *C*, as stated. (See fig. 2.) An ordinary lens of 5 to 10 cm. focal distance, with an appropriate

diaphragm, is adequate and in many ways preferable to stronger eyepieces. The slit, S, carried on its own slide and capable of being clamped to C when necessary, as stated, is additionally provided with a long rod hh lying underneath the carriage, so that the slit S may be put accurately in focus by the observer at C. F is a carriage for the mirror or the flame or other source of light whose spectrum is to be examined; or the source may be adjustable on the rear of the rod by which D and S are locked together.

Finally, the slide AB is provided with a scale ss and the position of the carriage C read off by aid of the vernier v. A good wooden scale, graduated in centimeters, happened to be available, the vernier reading to within one millimeter. For more accurate work a brass scale in millimeters with an appropriate vernier has since been provided.

Eyepiece E, slit S, flame F, etc., may be raised and lowered by the split tube device shown as at M and M' in fig. 2.

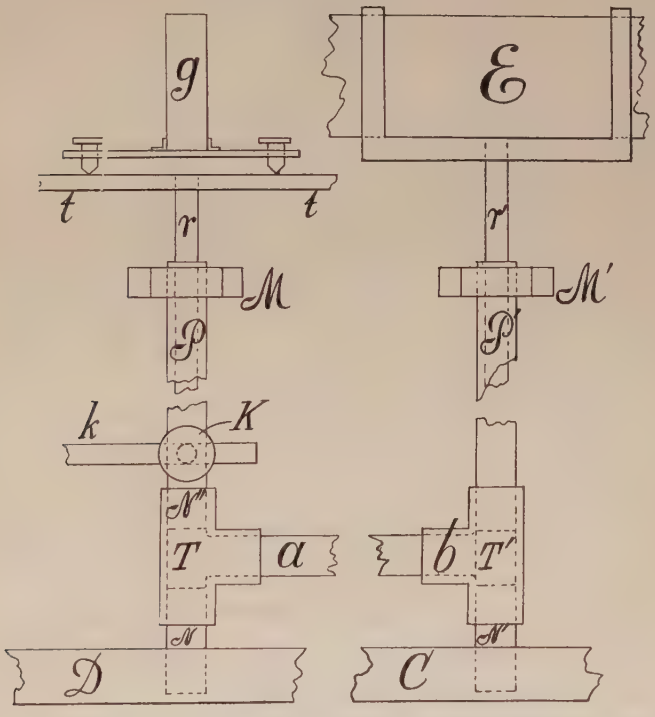

FIG. 2.—Elevation of standards of grating (g) and eyepiece (E).

3. Adjustments.—The first general test which places slit, grating and its spectra, and the two positions of the eyepiece in one plane, is preferably made with a narrow beam of sunlight, though lamplight suffices in the dark. Thereafter let the slit be focussed with the eyepiece on the right, marking the position of the slit; next focus the slit for the eyepiece on the left; then place the slit midway between these positions and now focus by slowly

rotating the grating. The slit will then be found in focus for both positions and the grating which acts as a concave lens counteracting L will be symmetrical with respect to both positions. Let the grating be thus adjusted when fixed normally to the slide B or parallel to A. Then for the first order of the spectra the wave-length $\lambda = d \sin \theta$, where d is the grating space and θ the angle of diffraction. The angle of incidence i is zero.

Again let the grating adjusted for symmetry be free to rotate with the rod ab. Then θ is zero and $\lambda = d \sin i$.

In both cases, however, if $2x$ be the distance apart of the carriage C, measured on the scale ss, for the effective length of rod $ab = r$ between axis and axis,

$$\lambda = dx/r \text{ or } (d/2r)2x$$

so that in either case λ and x are proportional quantities.

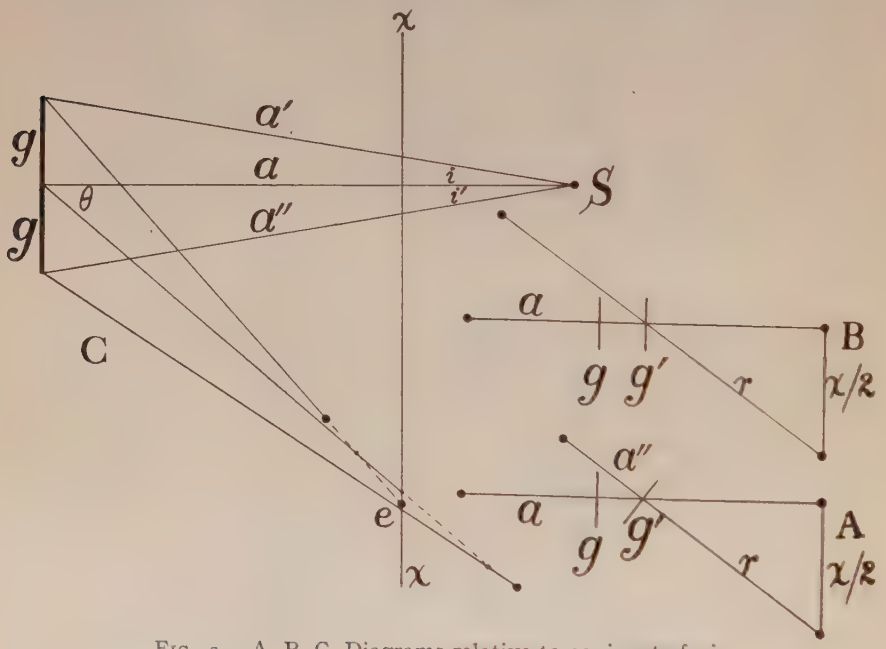

FIG. 3.—A, B, C, Diagrams relative to conjugate foci.

The whole spectrum is not, however, clearly in focus at one time, though the focussing by aid of the rod hh is not difficult. For extreme positions a pulley adjustment, operating on the ends of h, is a convenience, the cords running around the slide AA. In fact if the slit is in focus when the eyepiece is at the center ($\theta = o$, $i = o$), at a distance a from the grating, then for the fixed grating, fig. 4,

$$a' = a \frac{r^2}{r^2 - x^2}$$

where a' is the distance between grating and slit for the diffraction corresponding to x. Hence the focal distance of the grating regarded as a concave lens is $f' = ar^2/x$. For the fixed grating and a given color, it frequently

happens that the undeviated ray and the diffracted rays of the same color are simultaneously in focus, though this does not follow from the equation.

Again for the rotating grating, fig. 3A, if a'' is the distance between slit and grating $a''=a\frac{r^2-x^2}{r^2}$, so that its focal distance is $f''=a\frac{r^2-x^2}{x^2}$. It follows also that $a'\times a''=a$. For $a=80$ cm. and sodium light, the adjustment showed roughly $f'=650$ cm., $f''=570$ cm., the behavior being that of a weak concave lens. The same $a=80$ cm. and sodium light showed furthermore $a'=91$ and $a''=70.3$.

Finally there is a correction needed for the lateral shift of rays, due to the fact that the grating film is inclosed between two moderately thick

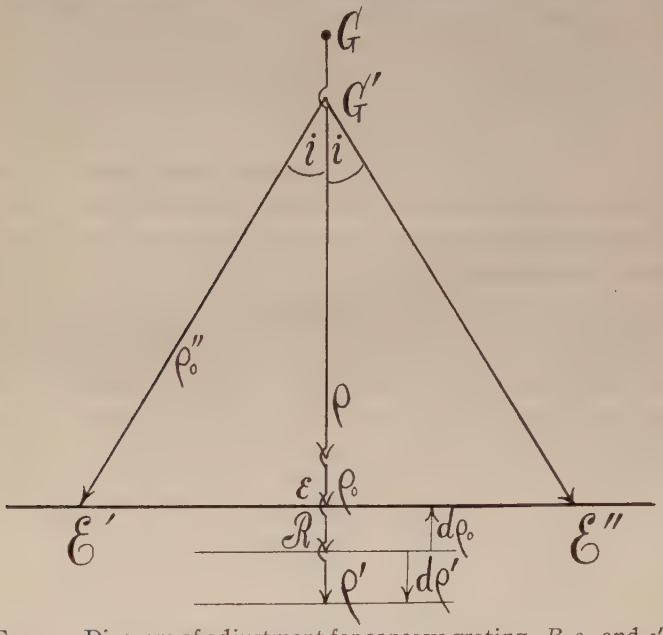

FIG. 4.—Diagram of adjustment for concave grating. R, ρ_0, and ρ' are measured from G, ρ and ρ_0'' from G'.

plates of glass (total thickness $t=.99$ cm.) of the index of refraction n. This shift thus amounts to

$$e=\frac{tx}{r}\left(\frac{1}{\sqrt{1-x^2/r^2}}-\frac{1}{\sqrt{n^2-x^2/r^2}}\right)\begin{matrix}b\\a\end{matrix}$$

But since this shift is on the rear side of the lens L, its effect on the eyepiece beyond will be (if f is the principal focal distance and b the conjugate focal distance between lens and eyepiece, remembering that the shift must be resolved parallel to the scale ss)

$$e=\frac{tx}{r}\left(\frac{1}{\sqrt{1-x^2/r^2}}-\frac{1}{\sqrt{n^2-x^2/r^2}}\right)\left(\frac{b}{f}-1\right)$$

where the correction e is to be added to $2x$, and is positive for the rotating grating and negative for the stationary grating.

Hence in the mean values of $2x$ for stationary and rotating grating the effect of e is eliminated. For a given lens at a fixed distance from the eyepiece $(b/f-1)$ is constant.

4. Data for single lens in front of grating.—In conclusion we select a few results taken at random from the notes.

TABLE 1.

Stationary grating.				Rotating grating.			
Line.	Observed $2x'$	Shift.	Corrected $2x$	Line.	Observed $2x'$	Shift.	Corrected $2x$
C.....	132.60	−.26	132.34	C.....	132.10	+.26	132.36
D_2.....	118.90	−.23	118.67	D_2.....	118.45	.23	118.68
F.....	98.23	−.19	98.04	F.....	97.90	.19	98.09
Hydrogen violet..	87.87	−.16	87.71	Hydrogen violet..	87.50	.16	87.66

The real test is to be sought in the corresponding values of $2x$ for the stationary and rotating cases, and these are very satisfactory, remembering that a centimeter scale on wood with a vernier reading to millimeters only was used for measurement.

5. Single focussing lens behind the grating.—The lens L, which should be achromatic, is placed in the standard C. The light which passes through the grating is now convergent, whereas it was divergent in §2. Hence the focal points at distances a', a'' lie in front of the grating; but in other respects the conditions are similar but reversed. Apart from signs,

$$a' = a\frac{r^2 - x^2}{r^2}, \text{ for the stationary grating}$$

$$a'' = a\frac{r^2}{r^2 - x^2}, \text{ for the rotating grating}$$

The correction for shift loses the factor $(b/f-1)$ and becomes

$$e = \frac{tx}{r}\left(\frac{1}{\sqrt{1-x^2/r^2}} - \frac{1}{\sqrt{n^2-x^2/r^2}}\right)$$

As intimated, it is negative for the rotating grating and positive for the stationary grating. It is eliminated in the mean values.

6. Data for single lens behind the grating.—An example of the results will suffice. Different parts of the spectrum require focussing.

TABLE 2.

Grating.	Line.	$2x'$	Shift.	$2x$
Stationary.....	D_2	118.40	+.13	118.53
Rotating.....	D_2	118.65	−.13	118.52

The values of $2x$, remembering that a centimeter scale was used, are again surprisingly good. The shift is computed by the above equation. It may be eliminated in the mean of the two methods. The lens L' at C may be more easily and firmly fixed than at L.

7. Collimator method.—The objection to the above single-lens methods is the fact that the whole spectrum is not in sharp focus at once. Their advantage is the simplicity of the means employed. If lenses at L' and at L are used together, the former as a collimator (achromatic) and with a focal distance of about 50 cm., and the latter (focal distance to be large, say 150 cm.) as the objective of a telescope, all the above difficulties disappear and the magnification may be made even excessively large. The whole spectrum is brilliantly in focus at once and the corrections for the shift of lines due to the plates of the grating vanish. Both methods for stationary and rotating gratings give identical results. The adjustments are easy and certain, for with sunlight (or lamplight in the dark) the image of the slit may be reflected back from the plate of the grating on the plane of the slit itself, while at the same time the transmitted image may be equally sharply adjusted on the focal plane of the eyepiece. It is therefore merely necessary to place the plane of spectra horizontal. Clearly a' and a'' are all infinite.

In this method the slides S and D are clamped at the focal distance apart, so that flame, etc., slit, collimator lens, and grating move together. The grating may or may not be revoluble with the lens L on the axis a.

8. Data for the collimator method.—The following data chosen at random may be discussed. The results were obtained at different times and under different conditions. The grating nominally contained about 15,050 lines per inch. The efficient rod-length ab was $R = 169.4$ cm. Hence if $1/C = 15{,}050 \times .3937 \times 338.8$, the wave-length $\lambda - C = 2x$ cm.

TABLE 3.—Stationery rotating grating.

Lines.	$2x'$	$2x$
D_2	{ 118.30 / 118.08 }	118.19
D_2	{ 118.27 / 118.05 }	118.16

Rowland's value of D_2 is 58.92×10^{-6} cm.; the mean of the two values of $2x$ just stated will give 58.87×10^{-6} cm. The difference may be due either to the assumed grating-space, or to the value of R inserted, neither of which was reliable absolutely to much within 0.1 per cent.

Curiously enough, an apparent shift effect remains in the values of $2x$ for stationary and rotating grating, as if the collimation were imperfect. The reason for this is not clear, though it must in any case be eliminated in the mean result. Possibly the friction involved in the simultaneous motion of three slides is not negligible and may leave the system under slight strain equivalent to a small lateral shift of the slit.

9. Discussion.—The chief discrepancy is the difference of values for $2x$ in the single-lens system (for D_2, 118.7 and 118.5 cm., respectively) as compared with a double-lens system (for D_2, 118.2 cm.) amounting to 0.2 to 0.4 per cent. For any given method this difference is consistently maintained. It does not therefore seem to be mere chance.

We have for this reason computed all the data involved for a fixed grating 5 cm. in width, in the two extreme positions, fig. 3, C, the ray being normally incident at the left-hand and the right-hand edges, respectively, for the method of § 6. The meaning of the symbols is clear from fig. 3, C, S being the virtual source, g the grating, e the diffraction conjugate focus of S for normal incidence, so that $b=r$ is the fixed length of rod carrying grating and eyepiece. It is almost sufficient to assume that all diffracted rays b' to b'' are directed toward e, in which case equation (1) would hold; but this will not bring out the divergence in question. They were therefore not used. Hence the following equations (2) to (5) successively apply where d is the grating space.

$$\cot\theta'=(b/g+\sin\theta)/\cos\theta;\quad \cot\theta''=(b/g-\sin\theta)/\cos\theta \tag{1}$$

$$a=b/\cos^2\theta;\quad a'=a''=\sqrt{g^2+a^2} \tag{2}$$

$$\sin i'=\sin i''=g/a' \tag{3}$$

$$-\sin i'+\sin(\theta+\theta')=\lambda/d;\ \sin\theta=\lambda/d;\ \sin i''+\sin(\theta+\theta'')=\lambda/d \tag{4}$$

$$\cos^2 i'/a'=\cos^2(\theta+\theta')b';\quad \cos^2 i''/a''=\cos^2(\theta+\theta'')/b'' \tag{5}$$

Since θ, g, λ, d, b are given, θ' and θ'' are found in equation (4), apart from signs. If δ_1' and δ_1'' be the distance apart of the projections of the extremities of b' and b, b and b'', respectively, on the line x,

$$\delta_1'=g+(b-b')\sin\theta-b'\sin i' \qquad \delta_1''=g+(b''-b)\sin\theta-b''\sin i'' \tag{6}$$

If δ_2' and δ_2'' be the distance apart of the intersections of the prolongation of b' and b, b and b'', respectively, with the line x

$$\left.\begin{aligned}\delta_2'&=\sin(\theta+\theta')(b\cos\theta/\cos(\theta+\theta')-b')\\ \delta_2''&=\sin(\theta-\theta'')(b''-b\cos\theta/\cos(\theta-\theta''))\end{aligned}\right\} \tag{7}$$

Given $b=169.4$ cm., $\theta=20^\circ\ 22'$, about for sodium, $g=5$ cm., the following values are obtained:

$\theta'=1^\circ 36'$ $\quad a=192.7$ cm. $\quad \theta''=1^\circ 34'$ $\quad a'=a''=192.8$ cm.
$i'=i''=1^\circ 30'$ $\quad b'=166.0$ cm. $\quad r=b=169.4$ cm. $\quad b''=172.4$ cm.

whence

$$\delta_1'=1.92\text{ cm.} \qquad \delta_2''=1.74\text{ cm.}$$

These limits are surprisingly wide. If, however, they should be quite wiped out on focussing, for any group of rays and symmetrical observations on the two sides of the apparatus, this would be no source of discrepancy. The effect of focussing the two parts of the grating may, in the first instance, be considered as a prolongation of b' till it cuts x, together with the corre-

sponding points for the intersection of b'' with x. Thus the values δ_2' and δ_2'' are here in question and they are

$$\delta_2' = 1.97 \text{ cm.} \qquad \delta_2' - \delta_1' = .05 \text{ cm.}$$

whence

$$\delta_2'' = 1.65 \text{ cm.} \qquad \delta_1'' = \delta_2 = .09 \text{ cm.}$$

are the conjugate foci for the extreme rays of the grating, respectively, beyond the conjugate focus of the middle or normal rays b, on x. Hence the mean of the extreme rays lies at .07 cm. beyond (greater θ) the normal ray, and the λ found in the first instance is too large as compared with the true value for the normal ray.

The datum .07 cm. may be taken as the excess of $2x$, corresponding to the excess of angle for a grating one-half as wide and observed on both sides ($2x$), as was actually the case. Finally, since not the whole of the grating is not in focus at once a correction less than .07 cm. for $2x$ must clearly be in question. This is quite below the difference of several millimeters brought out in §§4 and 6.

To make this point additionally sure and avoid the assumption of the last paragraph, we will compute the conjugate focus of the central ray (different angles θ) on the b' focal plane parallel to the grating and to x and on the b'' focal plane parallel to x. The computation is simpler if the central ray is thus focussed than if the extreme rays are focussed on the x plane. The distance apart will be

$$\delta_3' = g - b' \cos(\theta + \theta')(\tan(\theta + \theta') - \tan\theta)$$
$$\delta_3'' = g - b'' \cos(\theta - \theta'')(\tan\theta - \tan(\theta - \theta''))$$

Inserting the results for $\theta \quad \theta_1' \quad \theta_1'' \quad b' \quad b'' \quad g$

$$\delta_3' = .06 \qquad \delta_3'' = -.04$$

Both the b foci thus correspond to large angles. Their mean, however, may be considered as vanishing on the intermediate x plane.

Thus it is clear that the effect of focussing is without influence on the diffraction angle and much within the limits of observation. It is therefore probable that the residual discrepancy in the three methods is referable to a lateral motion of the slit itself, due to insufficient symmetry of the slides AA and BB in the above adjustment. This agrees, moreover, with the residual shift observed in the case of parallel rays in §8. The remedy should present no difficulty.

10. Reflecting plate grating.—The adjustment of the plane grating if cut on specular metal is nearly identical to the above, except that the collimator is fixed as a whole in front of the grating, either to the slide carrying the standard of the grating, B, or else quite in front of the cross slide AA, fig. 1 above, so as to give clearance for the to-and-fro motion of the rail, R. This admits of measurement of x on both sides of the slit, so that $2x$, the distance apart of the two symmetrical positions for a given spectrum line, is again observed.

11. Rowland's concave grating.—For the case of the *concave* grating, the accurate adjustment for symmetrical measurement on *both* sides of the slit is not feasible, because the slit and eyepiece would have to pass through each other. It is possible, however, to find conjugate foci at different distances from the grating in the normal position, which approximately answer the purposes of measurement. Rowland's equation

$$(\cos i/\rho - 1/R)\cos i + (\cos\theta/\rho' - 1/\rho')\cos\theta = 0$$

where ρ and ρ' are the conjugate focal distances for angles of incidence and deviation i and θ, may for $\theta = 0$ be written

$$\frac{1}{\rho/\cos^2 i} - \frac{1}{R/\cos i} = \frac{1}{\rho_0} - \frac{1}{R}$$

where ρ_0 is the normal distance of the eyepiece, so that

$$\frac{1}{\rho_0} - \frac{1}{\rho_0'} = \frac{2}{R}$$

If in fig. 4 (page 5) the slit S is put at $\rho' > R$ from the grating G (normal position), the image is at E at the end of ρ_0 from G, where $\rho_0 < R < \rho'$. If ρ_0 be used as a rail instead of R and put at an angle of incidence i, for the eyepiece at E' or E'', $\rho_0 \cos i > \rho$. But this excess need not be so large as to interfere with adequately sharp focussing.

Table 4 gives an example, in which the difference of ρ_0 and ρ_0' in the normal position is even over 1 foot, an excessive amount, as the distance necessary for clearance need not be more than a few inches. The grating has 14,436 lines to the inch and a radius about $R = 191$ cm.

TABLE 4.—Conjugate foci of the concave grating. $R = 191$ cm., 14,436 lines to inch, 5683 lines to cm. $D = .000{,}176$. $\rho_0 = 166$ cm., $\rho = 198$ cm., $\rho - \rho_0 = 32$ cm. $1/\rho_0 - 1/R = .000{,}788$, $\theta = 0$, $\sin i = \lambda/D$.

$i°$	ρ	$\rho_0 \cos i$	Diff.	$(\rho/\cos i)^2$	Fraunhofer lines.	i
	cm.		*cm.*			
0°	166.0	166.0	.0	27500	B	22° 59′
5	165.3	165.3	.0	27500	C	21° 54′
10	163.2	163.5	.3	27400	D	19° 34′
15	159.6	160.3	− .7	27300	E	17° 26′
20	154.7	156.0	−1.3	27100	F	16° 02′
25	148.5	150.4	−1.9	26800	G	14° 10′
30	140.9	143.7	−2.8	26500	....	....
35	132.2	136.0	−3.8	26000	....	....
40	122.3	127.1	−4.8	25500	....	....

The greater part of the visible spectrum is thus contained between $i = 15°$ and $i = 20°$. It follows that the excess of $\rho_0 \cos i - \rho$ lies between 7 and 13 mm. Hence the eyepiece may be placed at a mean position corresponding to 10 mm. and give very good definition of the whole spectrum without refocussing, as I found by actual trial. Within 1 cm. the focus is sharp enough for most practical purposes. If the distances ρ_0 and ρ_0' are selected so that eyepiece and slit just clear each other the definition is quite sharp.

The diffraction equation is not modified and if $2x$ corresponds to the positions $+i$ and $-i$ for the same spectrum line,

$$2\lambda = (D/R)\,2x$$

It is therefore not necessary to touch the eyepiece and this is contributory to accuracy.

If Rowland's equation is differentiated relatively to ρ and ρ', $-d\rho = \left(\frac{\rho}{\rho_0' \cos i}\right)^2 d\rho_0'$ where the factor $d\rho_0'/\rho_0'^2$ is constant. Hence $-d\rho$ varies as $(\rho/\cos i)^2$, given in the table. If, furthermore, a comparison is made between $d\rho_0$ and $d\rho$ this equation reduces to

$$\sqrt{d\rho_0/d\rho} = (R - \rho_0(1 - \cos i))/R \cos i$$

which becomes unity either for $i = 0$ or for $\rho_0 = R$ (Rowland's case).

12. Summary.—By using two slides symmetrically normal to each other and observing on both sides of the point of interference, it is shown that many of the errors are eliminated by the symmetrical adjustments in question. The slide carrying the grating may be provided with a focussing lens in front or again behind it, if the means are at hand for actuating the slit which is not sharply in focus on the plane of the eyepiece carried by a second slide throughout the spectrum at a given time. It is thus best to use both lenses conjointly, the latter as a collimator and the former as an objective of the telescope in connection with the eyepiece. It is shown that a centimeter scale parallel to the eyepiece slide with a vernier reading to millimeters is sufficient to measure the wave-lengths of light to few Angström units, while the wave-lengths are throughout strictly proportional to the displacements along the scale. The errors of the three available methods and their counterparts are discussed in detail. The method is applicable both to the transparent and the reflecting grating.

It is furthermore shown that, in case of Rowland's concave grating, observation may be made symmetrically on both sides of the slit, by providing for reasonable clearance of slit and eyepiece passing across each other, although one conjugate focal distance is now not quite the projection of the other.

CHAPTER II.

THE INTERFERENCE OF THE REFLECTED-DIFFRACTED AND THE DIFFRACTED-REFLECTED RAYS OF A PLANE TRANSPARENT GRATING, AND ON AN INTERFEROMETER. By C. Barus and M. Barus.

13. Introductory.—If parallel light, falling on the front face of a transparent plane grating, is observed through a telescope after reflection from a rear parallel face (see fig. 5), the spectrum is frequently found to be intersected by strong, vertical interference bands. Almost any type of grating will suffice, including the admirable replicas now available, like those of Mr. Ives. In the latter case one would be inclined to refer the phenomenon to the film and give it no further consideration. On closer inspection, how-

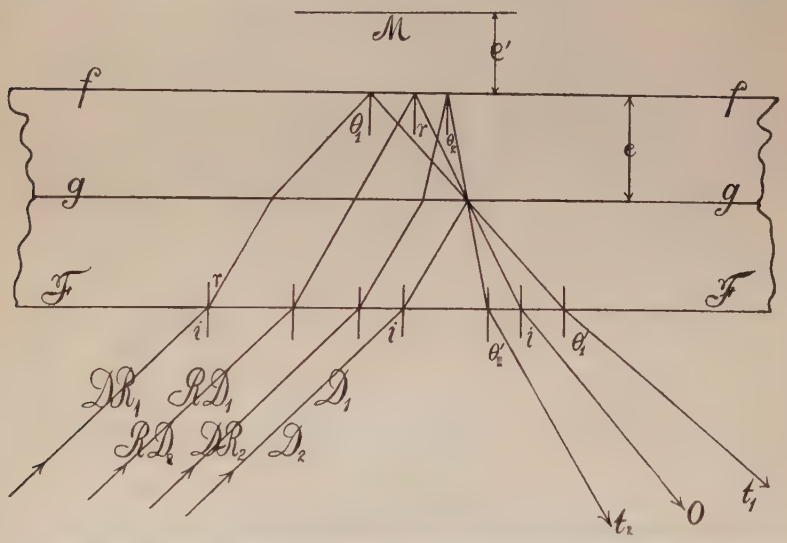

FIG. 5.—Showing the three incident rays interfering in the diffracted ray t_1, $(\theta_2' > i)$, and the three rays interfering similarly in the ray t_2, $(\theta_1' < i)$. DR is first diffracted and then reflected, and the reverse is true for RD. D is diffracted only.

ever, it appears that the strongest fringes certainly have a different origin and depend essentially on the reflecting face behind the grating. If, for instance, this face is blurred by attaching a piece of rough, wet paper, or by pasting the face of a prism upon it with water, so as to remove most of the reflected light, the fringes all but disappear. If a metal mirror is forced against the rear glass face, whereby a half wave-length is lost at the mirror but not at the glass face in contact, the fringes are impaired, making a rather interesting experiment. With homogeneous light the fringes of

the film itself appear to the naked eye, as they are usually very large by comparison.

Granting that the fringes in question depend upon the reflecting surface behind the grating, they must move if the distance between them is varied. Consequently a phenomenon so easily produced and controlled is of much greater interest in relation to micrometric measurements than at first appears and we have for this reason given it detailed treatment. It has the great advantage of not needing monochromatic light, of being applicable for any wave-length whatever, and admitting of the measurement of horizontal angles. In chapter 5 it will be shown that these interferences may also be produced by Michelson's or by Jamin's apparatus.

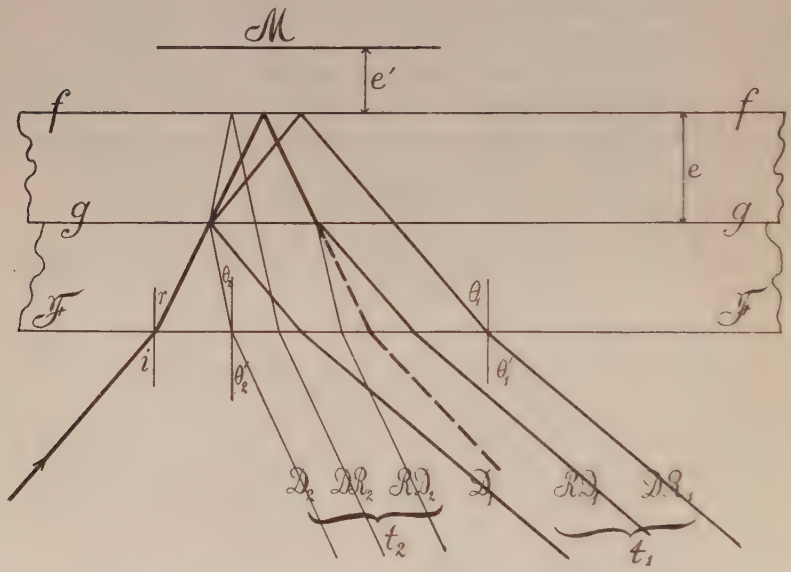

FIG. 6.—Showing corresponding triplets of diffracted rays for a single incident ray, and each of the cases $\theta_1' > i$ and $\theta_2' < i$ of fig. 5.

When the phenomenon as a whole is carefully studied it is found to be multiple in character. In each order of spectrum there are different groups of fringes of different angular sizes and usually in very different focal planes. Some of these are associated with parallel light, others with divergent or convergent light, so that a telescope is essential to bring out the successive groups in their entirety. At any deviation the diffracted light is necessarily monochromatic, but the fringes need not and rarely do appear in focus with the solar spectrum. If the slit of the spectroscope is purposely slightly inclined to the lines of the grating, certain of the fringes may appear inclined in one way and others in the opposite way, producing a cross pattern like a pantograph. The reason for this appears in the equations.

In any case the final evidence is given when the reflecting face behind the grating is movable parallel to it. The interferometer so obtained is

subject to the equation (air space e, wave-length λ, angle of incidence i, of diffraction θ'), $\delta e = \lambda/2(\cos\theta' - \cos i)$, and is therefore less unique as an absolute instrument than Michelson's classic apparatus or the device of Fabry and Perot. Its sensitiveness per fringe, δe, depends essentially upon the angle of incidence and diffraction and it admits of but 1 cm. (about) of air-space between grating face and mirror before the fringes become too fine to be available. But on the other hand it does not require monochromatic light (a Welsbach burner suffices), it does not require optical plate glass, it is sufficient to use but a square cm. of grating film, and it admits of very easy manipulation, for painstaking adjustments as to normality, etc., are superfluous. In fact it is only necessary to put the sodium lines in the spectrum reflected from the grating and from the mirror into coincidence

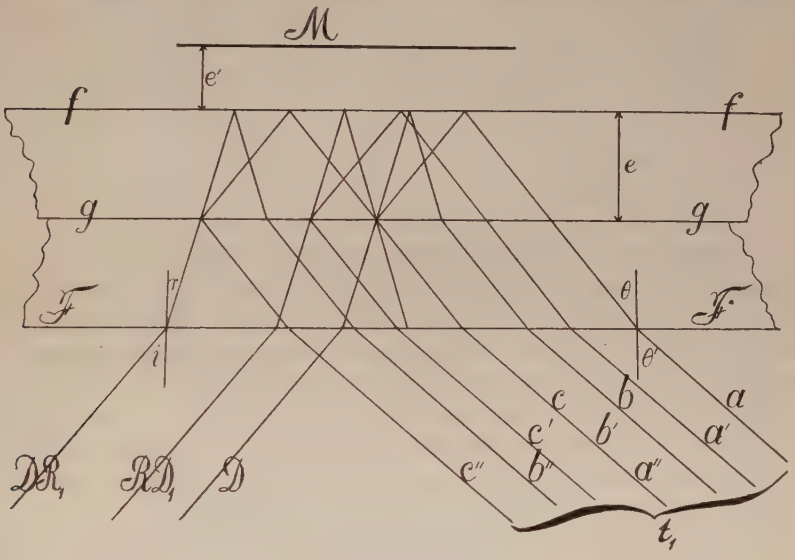

FIG. 7.—Superposition of the cases of figs. 5 and 6 for $\theta' > i$.

both horizontally and vertically with the usual three adjustment screws on grating and mirror. Naturally sunlight is here desirable. Thereupon the fringes will usually appear and may be sharply adjusted upon a second trial at once.

When the air-space is small, coarse and fine fringes (fluted fringes) are simultaneously in focus, one of which may be used as a coarse adjustment on the other. Finally, the sensitiveness per fringe to be obtained is easily a length of one-half wave-length in the fine fringes and one wave-length in the coarse fringes, though the latter may also be increased almost to the limit of the former. The fine fringes compatibly with their greater sensitiveness vanish within about a millimeter. Their occurrence with the coarse fringes makes it possible to investigate sudden displacements within the latter.

TABLE 5.—Interferences. Grating between plates of glass each 0.48 cm. thick. Additional rear plate (mirror) 0.29 cm. thick. Index of refraction of glass $\mu = 1.527$.

Side.	Order.	Color.	Rays.	i	Mean θ'	Observed $\delta\theta'$ Minutes.	Computed $\delta\theta'$ Minutes.	Remarks.
				°	° ′			
$\theta > r$								
$r = 0$	1	C.....	Convergent*....	0	24 8	1.87	1.81	About double divergence, but not clear.
$\theta = 15° 49'$....	2							
$r > \theta$	1	D to E...	Less convergent.	45	21 1	1.80	1.70	Strong. Total.
$r = 27° 35'$....	1	Do....	Parallel.....	45	21 21	.35	....	Estimated.†
$\theta = 13° 35'$....	1	Do....	Divergent.....	45	21 32	.70	....	Estimated.†
	1	Do....	More divergent..	45	22 40	.87	....	
$r > 0$	2	Do....	Convergent.....	45	31	3.32	....	Clear, but faint.
	2	Do....	Convergent.....	45	....	.8	....	Very fine and close.
	2	Do....	Parallel.....	45	31	1.20	....	
	2	Do....	Divergent.....	45	....	....	....	Not clear. $\delta\theta' = 2.0'$?
	2	Do....	Very divergent..	45	....	....	....	Not clear. $\delta\theta' = 3.0'$?
$r < \theta$	1	D to E...	Very divergent..	22.5	1 30	4.7	....	Faint, but certain.
$r = 14° 31'$....	1	Do....	Divergent.....	22.5	....	....	....	Faint. $\delta\theta' = 2'$?
$\theta = 1° 23'$.....	1	Do....	Nearly parallel..	22.5	....	....	....	Faint. $\delta\theta' = 1.5'$?
	1	Do....	Parallel.....	22.5	....	....	....	Fine, close, and strong
	1	Do....	Convergent.....	22.5	2 6	1.85	1.84	Strong. Total.
Interferometer:								
	1	D to E...	.....	22.5	....	1.83	1.84	$e = .48$ cm. Total.
	1	Do....	.....	22.5	....	1.13	1.15	$e' = .77$ cm. Total.

* Color not definite, only end of red spectrum seen.

† Lines strong, but too fine and close together.

14. Observations.—The following observations were made merely to corroborate the equations used. The general character of the results will become clear on consulting the preceding abbreviated table chosen at random from many similar data. An Ives replica grating with 15,000 lines to the inch (film between plates of glass .46 cm. thick) was mounted as usual on a spectrometer admitting of an angular measurement within one minute of arc. Parallel light fell on the grating, fig. 5, *gg* (see p. 13), under different angles of incidence, i, and the spectrum lines were observed by reflection (after reflection from *gg* and the rear face *ff*) at an angle of diffraction θ' in air, both in the first and second order of spectra, and so far as possible on both sides of the directly reflected beam. In view of the front plate, the angle i corresponds to an angle of refraction r, within the glass and the angle θ' similarly to an angle of diffraction θ, respectively. Hence $r > \theta_2$ or $\theta_1 < r$ denote the sides of the ordinary ray on which observation is made. As a rule these were as nearly as possible in the region of the D line passing toward E. Finally $\delta\theta$ denotes the angle between two consecutive dark fringes, observed and computed as specified. Similarly δe will be reserved for changes of thickness e of the glass and $\delta e'$ for changes of the air space in case of an auxiliary mirror M.

For $i = 0°$ the number of groups of lines was a single set in each order; but only the end of the spectrum could be seen. Measurements refer (about) to the C line. For $i = 45°$ several groups were too close together, or too faint for measurement, and the same is true for $i = 22.5°$. An estimate of divergence is all that could be attempted on the given spectrometer. The case $\theta_1 > r$ was usually not available, but for $i = 22.5°$ two sets were found in the first order, one being the normal set. The fringes in all cases decrease in size from red to violet, but less rapidly than wave-length.

Whether they are convergent or divergent for a given set of fringes, as for instance for the strong set, depends on the position of the grating. Thus the divergent rays become convergent when the grating is rotated 180° about its normal. It is therefore definitely wedge-shaped. In fact when the auxiliary mirror M is used, the fringes may be put anywhere, either in front of or behind the principal focal plane, by suitably inclining the mirror.

15. Equations.—If we suppose the film of the grating *gg* to be sandwiched in between plates of glass each of thickness e, it will be seen that triplicate rays pass in the direction t_1, ($\theta_1' > i$) or of t_2, ($\theta_2' < i$), which will necessarily produce interference either partial or total. With respect to t_1, the only light received comes either from D_1 by direct diffraction at *gg*, or from RD_1, by reflection from the lower face *ff*, and thereafter by diffraction at *gg*; or from DR_1, by diffraction at *gg* and reflection at *ff*. Similarly the light along t_2 comes in like manner either from D_2 or DR_2 or RD_2. With regard to the angles of incidence and refraction or of diffraction within the glass or outside of it, we have the equations for the first and second order of spectra (D being the grating space).

$$\sin i_1 = \mu \sin r_1 \tag{1}$$
$$\sin \theta_1' = \mu \sin \theta_1 \tag{2}$$
$$\sin \theta_2' = \mu \sin \theta_2 \tag{3}$$
$$\sin r - \sin \theta_2 = \lambda/D\mu, \text{ or } = 2\lambda/D\mu \tag{4}$$
$$\sin \theta_1 - \sin r = \lambda/D\mu, \text{ or } = 2\lambda/D\mu \tag{5}$$
$$\sin i - \sin \theta_2' = \lambda/D, \text{ etc.} \tag{4'}$$
$$\sin \theta_1' - \sin i = \lambda/D, \text{ etc.} \tag{5'}$$

where μ is the index of refraction of the glass, found to be equal to 1.5265 for sodium light, by breaking off a small corner of the glass of the grating and using Kohlrausch's total reflectometer.

Furthermore, for the occurrence of interference along t_1 we shall have, for the case of the three rays in question, respectively combined in pairs, if the wave fronts be taken in the glass plate *FFgg*

$$n\lambda = 2e\mu \cos r \tag{6''}$$
$$n\lambda = 2e\mu(1 - \sin \theta_1 \sin r)/\cos \theta_1 \tag{7''}$$
$$n\lambda = 2e\mu(1 - \cos (\theta_1 - r))/\cos \theta_1 \tag{8''}$$

where n is the order of interference and a whole number, e the thickness of the lower glass plate, as may be found from a consideration of wave fronts and need not be deduced here. It will be seen that, whereas equations 6 and 7 present cases of partial interference, equation 8, which is virtually the difference of 6 and 7, should be a case of total interference, giving strong fringes and possibly useful for interferometry.

Again for t_2 the equations will be similar if corresponding wave fronts be taken in the glass plate *FFgg*

$$n\lambda = 2e\mu \cos r \tag{6'}$$
$$n\lambda = 2e\mu(1 - \sin \theta_2 \sin r)/\cos \theta_2 \tag{7'}$$
$$n\lambda = 2e\mu(1 - \cos (r - \theta_2))/\cos \theta_2 \tag{8'}$$

the same as in the preceding case when θ_1 is replaced by θ_2 and $\theta_1 - r$ by $r - \theta_2$. To this extent there is no essential difference between the cases. Therefore θ may be used indiscriminately for either.

If, however, the wave fronts be taken in the glass plate *ffgg* the equations become

$$n\lambda = 2e\mu \cos r \tag{6}$$
$$n\lambda = 2e\mu \cos \theta_1 \tag{7}$$
$$n\lambda = 2e\mu (\cos r - \cos \theta_1) \tag{8}$$

with three other corresponding forms for $\theta < r$, as before. The latter are the true equations and equation 8 is the case of total interference.

These circumstances are at first quite puzzling, but they are due to the fact that in the cases 6', 7', 8', 6'', 7'', 8'', the wave fronts taken correspond to the refracted ray only, whereas the diffracted rays subsequently undergo

sudden changes of deviation on leaving gg. We have nevertheless carried both groups of equations 6′ to 8′ and 6 to 8 in mind, though the latter are alone certain of application.

For an air-space between gg and M the equations would be

$$n\lambda = 2e\cos i \qquad n\lambda = 2e\cos\theta' \qquad n\lambda = 2e(\cos\theta' - \cos i), \text{ etc.}$$

16. Differential equations.—The quantity measured on the spectrometer is essentially angular and preferably $d\theta'/dn$, the angular distance apart of the fringes, in radians. Later we shall measure δe or the linear displacement of the parallel faces per fringe. In any measurement, however, we meet with embarrassment, inasmuch as n, λ, μ, r, θ, θ', are all variable. The angle i and the thickness e and the grating space D are alone given. Among these, the variation of r with μ and λ must be found by experiment. Fortunately, in case of the interferometer all these variables are eliminated and e alone changes, subject to a given i and θ'. The μ used need not be known. (See paragraph 19.)

For the present purpose, as the variation of μ enters only as a correction, we have been satisfied with the usual results in physical tables.* If from the C to the D line

$$(d\mu/\mu)/(d\lambda/\lambda) = -.016$$

and from the B to the C line, $= -.013$, we may write

$$-\frac{d\mu}{\mu} = .015\frac{d\lambda}{\lambda}$$

and therefore

$$d\left(\frac{\lambda}{\mu}\right) = 1.015\frac{d\lambda}{\mu} \tag{9}$$

We shall write $a = .015$, $b = 1 + a$.

The case $\theta > r$ in the present paper is not of much experimental interest, and may be omitted here. For the case of $r > \theta$ we shall have successively and for the total interferences RD, DR, equation 8,

$$-\frac{d\lambda}{d\mu} = \frac{\lambda\cos\theta}{\sin r - b\sin\theta}\frac{d\theta}{dn} \tag{11}$$

$$-\frac{dr}{dn} = a\frac{\tan r\cos\theta}{\sin r - b\sin\theta}\frac{d\theta}{dn} \tag{12}$$

$$\frac{d\mu}{dn} = \frac{a\mu\cos\theta}{\sin r - b\sin\theta}\frac{d\theta}{dn} \tag{13}$$

$$\frac{d\theta'}{dn} = \frac{\mu\cos\theta(\sin r - \sin\theta)}{\cos\theta'(\sin r - b\sin\theta)}\frac{d\theta}{dn} \tag{14}$$

* See Kohlrausch's Leitfaden, 11th edition, 1910, p. 712, light crown glass being taken.

and finally corresponding to equations 6, 7, 8,

$$\frac{d\theta'}{dn}=\frac{\cos\theta}{2e\cos\theta'}\ \frac{\lambda(\sin r-\sin\theta)}{b-\sin r\sin\theta} \tag{15}$$

$$\frac{d\theta'}{dn}=\frac{\cos\theta}{2e\cos\theta'}\ \frac{\lambda(\sin r-\sin\theta)}{b\cos r\cos\theta+a\sin r\tan r\cos\theta} \tag{16}$$

$$\frac{d\theta'}{dn}=\frac{\cos\theta}{2e\cos\theta'}\ \frac{\lambda(\sin r-\sin\theta)}{b(1-\cos(r-\theta))+a\sin r\sin\theta(1-\cot\theta\tan r)} \tag{17}$$

the last term in the denominator being corrective. Here $d\theta'/dn$ is the observed angular deviation of two consecutive fringes, so that

$$\frac{dn}{d\theta_1'}-\frac{dn}{d\theta_2'}=\frac{dn}{d\theta_3'}$$

The equation corresponding to the incorrect equation 8′ would have been

$$\frac{d\theta'}{dn}=\frac{\cos\theta}{2e\cos\theta'}\ \frac{\lambda\cos^2\theta(\sin r-\sin\theta)}{b\cos^2\theta(1-\cos(r-\theta))-(\sin r-\sin\theta)(\sin r-b\sin\theta)-a\tan r\cos^2\theta\sin(r-\theta)}$$

17. Normal incidence or diffraction, etc.—For the case of normal incidence $i=r=0$, the equations corresponding to 6, 7, and 8 take a simplified form and are respectively

$$-\frac{d\theta_0'}{dn}=\frac{\lambda\sin\theta\cos\theta}{2be\cos\theta'} \tag{15'}$$

$$-\frac{d\theta_0'}{dn}=\frac{\lambda\sin\theta}{2be\cos\theta'} \tag{16'}$$

$$-\frac{d\theta_0'}{dn}=\frac{\cos\theta}{2be\cos\theta'}\ \frac{\lambda\sin\theta}{1-\cos\theta} \tag{18'}$$

If $\theta'=\theta=0$, for normal diffraction, which is particularly useful in Rowland's adjustments as well as on the spectrometer

$$-\left[\frac{d\theta'}{dn}\right]_{\theta=0}=\frac{\lambda}{2e}\ \frac{\sin r}{b(1-\cos r)-a\sin r\tan r}$$

for the case of total interference corresponding to equations 8 and 17. If $i=-\theta'$ or $r=-\theta$

$$\left[\frac{d\theta'}{dn}\right]_{r=-\theta}=\frac{\lambda}{2e}\ \frac{1}{\tan\theta\cos\theta'}$$

18. Comparison of the equations of total interference with observation.—The partial interferences corresponding to equations 6 and 7 are usually too fine to be seen unless e is very small. They amount in cases of equations 15 and 16 for $e=.48$ cm. to the following small angles

	(15)	(16)
$i=0°$	$d\theta'/dn=.060'$	$d\theta'/dn=.062'$
$22.5°$	$.048'$	$.050'$
$45°$	$.057'$	$.058'$

usually less than four seconds of arc and are therefore lost. The origin of the fine interferences actually seen in the table is thus still open to surmise. With small e and the interferometer they are obvious.

The total interferences as computed in the above table agree with the observations to much within 0.1 minute of arc and these are experimental errors; particularly so as it was not possible to use both verniers of the spectrometer. The interesting feature of the experiment and calculation is this, that $\delta\theta'$ has about the same value for all incidences i from 0° to 45° and even beyond. The equations do not show this at once, owing to the entrance of μ and r. But apart from a and b equation 17 is nearly

$$\frac{d\theta}{dn} = \frac{\lambda}{2e\mu} \frac{\lambda/D}{1-\cos(r-\theta)} \tag{19}$$

which is independent of r to the extent in which $\cos(r-\theta)$ is constant. The dependence of $d\theta'/dn$ on wave-length is borne out. (See paragraph 19.) Finally, $d\theta'/dn$ is independent of μ except as it occurs in a and b.

If the glass plate *ffgg* is removed and a mirror M used, as in the interferometer, the fringes may be enormously enlarged by decreasing e and the measurements made with any degree of accuracy; but such measurements were originally impracticable and have little further interest in this place since the interferometer itself is tested in the next chapter.

19. Interferometer.—The final test of the above equation is given by the last part of the table for different thicknesses of glass, $e = .48$ and $e = .77$ cm. The results are in perfect accord.

These data suffice to state the outlook for the interferometer. In this case n and e are the only variables, so that equation 8 becomes

$$\delta e = \lambda/2\mu(\cos\theta - \cos r) \tag{20'}$$

where δe is the thickness of glass corresponding to the passage of one fringe across the cross-hairs of the telescope or a definite spectrum line.

If instead of glass in the grating above, an air-space intervenes between the film of the grating and the auxiliary mirror M, fig. 5, the equation reduces to

$$\delta e = \frac{\lambda}{2(\cos\theta' - \cos i)} = \frac{\lambda}{2\left(\sqrt{1-(\sin i - \lambda/D)^2} - \cos i\right)} \tag{20}$$

where i and θ' are the angles of incidence and diffraction in air.

These equations 20 embody a curious circumstance. Inasmuch as θ and θ' change as i increases from 0° to 90° from negative to positive values at about $i = 13°$ and $i = 20°$, respectively, the denominator of either equation 20 will pass through zero (for air at about $i = 10°$). Hence at this value of i the motion of the mirror M produces no e effect (stationary fringes), while on either side of it the fringes travel in opposite directions in the telescope when e changes by the same amount. In the negative case the sensitiveness for air-spaces passes from $\delta e = -.000\,489$ to $\delta e = -\infty$, per

fringe. In the positive case from $\delta e = +\infty$ to $\delta e = .000\,039$, per fringe or to a limit of about a half wave-length in case of 15,000 lines to the inch. This limiting sensitiveness may be regarded as practically reached even at $i = 40°$ where $\delta e = .000\,155$ cm. per fringe and an angle of about $i = 45°$ is most convenient in practice.

In addition to the large fringes the fine set appears when e is small or not more than a few tenths of a millimeter. The sensitiveness of these is naturally much more marked. In the two cases

$$\delta e = \lambda/2 \cos i \qquad (20')$$

$$\delta e = \lambda/2 \cos \theta' \qquad (20'')$$

so that nearly $\lambda/2$ per fringe is easily attained, but the available thickness of air-space within which they are visible is decreased.

At $i = 20°$ about, and in case of an air-space θ' is nearly 0°. We suggested above that these fine fringes may be used as a fine adjustment in connection with the large fringes, on which they are superimposed. In appearance these large fluted fringes are exceedingly beautiful. The fine fringes have the limiting sensitiveness of the coarse fringes, *i.e.*, the cases for $i = 90°$ or θ' equal to maximum value. In different focal planes both sets of fine fringes may be seen separately for small e (air wedge).

Equation 20 shows that for smaller grating spaces D, and consequently also in the second order of spectra there must be greater sensitiveness, *caet. par.*; but as a rule we have not found these fringes as sharp and useful as those in the first order.

The limiting sensitiveness per fringe, however, follows a very curious rule. If in equation 20 we put $i = 90°$,

$$2\delta e = \sqrt{\lambda D/(2 - \lambda/D)} = \lambda/\sqrt{r(2 - r)} \text{ in the first order}$$

if $r = \lambda/D$, and

$$2\delta e = \sqrt{\lambda D/4(1 - \lambda/D)} = \lambda/2\sqrt{r(1 - r)} \text{ in the second order}$$

D is the grating space. Both equations have a minimum, $\delta e = \lambda/2$, at $\lambda/D = 1$ in the first order and $\lambda/D = .5$ in the second order, beyond which it would be disadvantageous to decrease the grating space. These minimum conditions are as good as reached even when D corresponds to 15,000 lines to the inch, as above, where roughly $10^6 \delta e = 38$ cm. in the first order and $10^6 \delta e = 33$ cm. in the second order.

All the conditions discussed above are summarized in fig. 8 and fig. 9 for the first and second orders of spectrum.

To view the stationary fringes of the first order was not practicable, since they occurred for $i = 10°$, whereas the telescopes were in contact at about 20°. In the second order of spectra they may be approached more nearly as they occur when i is roughly 20°. If the distance e is made small enough, so that the three cases of equations 20, 20', 20'', are visible, the appearance is very peculiar. The fringes of equation 20 are very slow-

moving. They are intersected by the small fringes of equation 20′, producing the fluted pattern already discussed. Over all travel the rapidly moving fringes of equation 20″, producing a kind of alternation or flickering which it is very difficult to analyze or interpret until e is very small, when all three sets are broad and easily recognized. Sunlight should be used. Nothing like these alternating fringes was seen in the first order, but we used a film grating only.

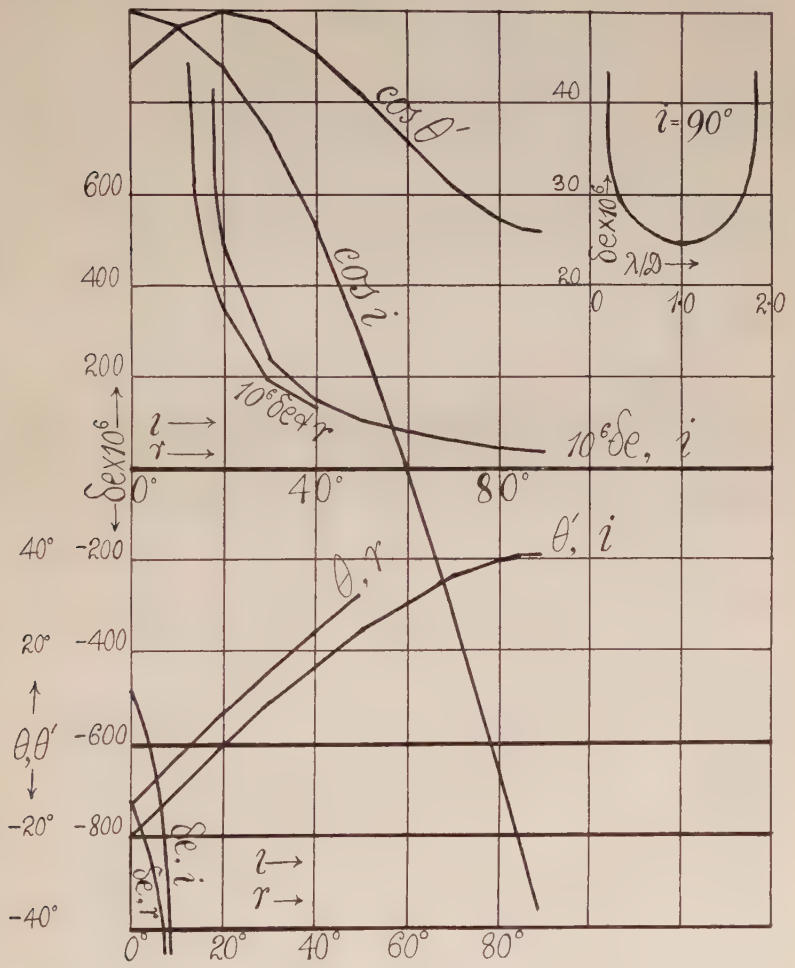

FIG. 8.—Charts showing dependence of θ on r, θ' on i, cos θ' and cos i on i, δe on r and δe on i, δe on λ/D for the first order of spectrum.

The above equation shows finally that δe is not exactly proportional to wave-length, though the former decreases with the latter, as shown above.

The three equations 20 indicate finally that for $i > \theta'$ all fringes travel in the same direction with increasing e; whereas if $\theta' > i$, the set corresponding to equation 20 travel in a direction opposite to that of the sets 20′ and 20″.

This is strikingly borne out by making the experiment for $\theta > i$ with a small angle i, both in the first and second order.

Table 6 contains a few data obtained by carrying the mirror on a Fraunhofer micrometer, reading to .0001 cm., toward a stationary grating film.

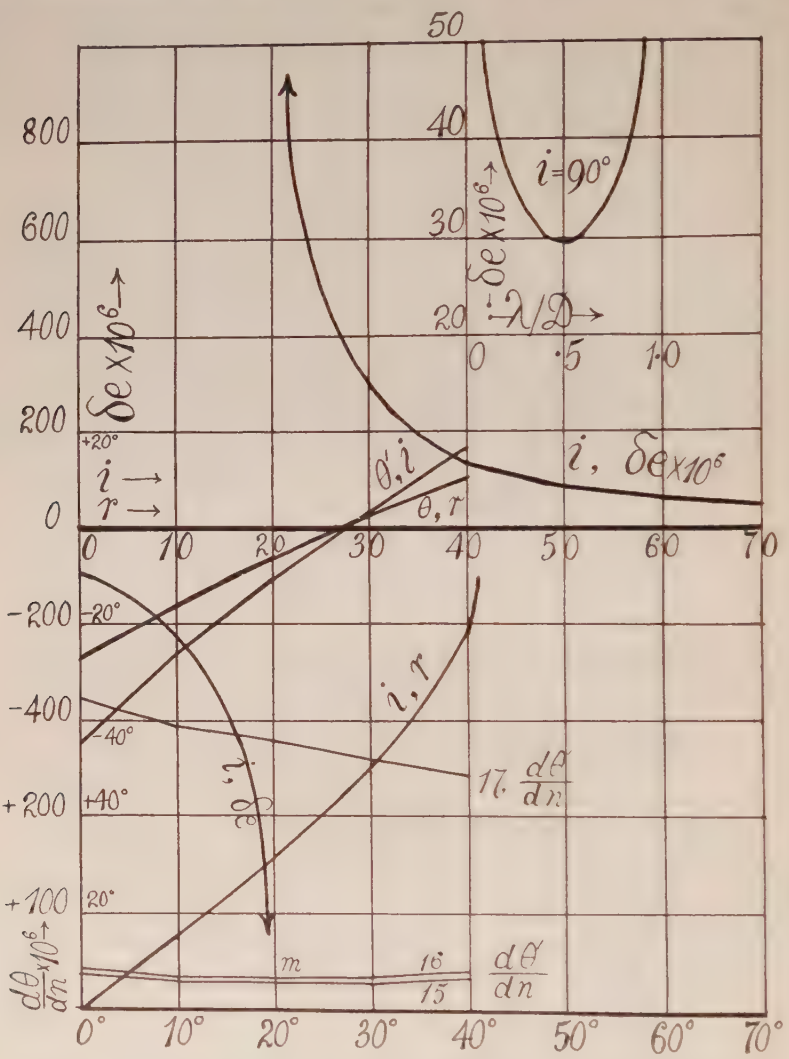

FIG. 9.—Similar data to those of fig. 8, for the second order of spectrum. In addition, $d\theta'/dn$ is shown as given by equations 15, 16, 17.

Observations were made in the region of the D lines. The grating was originally between plates of glass $c = .48$ cm. thick. Finally the plate between grating and mirror was removed, the whole distance now being an air-space. This has no effect on δc, but c may then be reduced to zero and the fringes enlarged.

These data merely test the equations, as no special pains were taken for accurate measurement, which neither the micrometer screw nor the special adjustments warranted. Usually the micrometer equivalent of 50 fringes was observed on the screw. The maximum distance e between grating and mirror was .48 cm. of glass and .25 cm. of air conjointly, or within 1 cm. In case of fine fringes mere pressure on table or screw impaired the adjustment. Moreover these fine fringes run through the shadow of the coarse fringes, and their size in consecutive spaces between the latter seems to vary periodically as if they alternated between the two equations 15 and 16.

TABLE 6.—Interferometer measurements. Replica grating. Air-space, often in addition to glass space, $e = .46$ cm.

i	θ'	Coarse fringes. Air-space.*	Coarse fringes. Observed. $\delta e \times 10^6$	Coarse fringes. Computed. $\delta e \times 10^6$	Fine fringes. Air-space.	Fine fringes. Observed. $\delta e \times 10^6$	Fine fringes. Computed. $\delta e \times 10^6$
		cm.	cm.	cm.	cm.	cm.	cm.
22° 30′	2° 6′	.02 to .33	390	Co., 391	....	....	....
45 0	21 1	.03	131	130	....	....	....
67 30	35 1	.03	72	68	....	....	....
25 0	4 7	....	322	324	....	....	....
30 2	8 37	.013 to .250	241	240	....	....	....
Glass removed between mirror and grating.							
22° 25′	1° 40′	.013 to .054	387	392	.006 to .025	34	{32 30
45 0	20 49	.032 to .064	129	130	.000 to .007	33	{42 32

* Approximate; contact endangering adjustment.

20. Secondary interferences.—We come now to consider the minor interferences which are either weaker, finer, or more diffuse than the strong forms discussed. In the interpretation of these we have not met with success, but some reference to them is essential. We assume that after two reflections the fringes can no longer be seen.

In fig. 6 if there is light reinforcement passing in any direction t_1 or t_2; then each incident ray I, at an angle i with the normal n, will after refraction be represented by the six rays $D_1\,RD_1\,DR_1$ $(\theta_1 > r)$, $D_2\,DR_2\,RD_2$ $(\theta_2 < r)$, as shown in the figure, under a notation similar to the preceding case. If these rays are brought to a focus by a telescope there must be interferences between pairs of which the fringes of D, RD, and D, DR, will usually be too fine to be visible, whereas RD, and DR, will be large enough to be seen.

As the lines are not quite sharp, measurement is difficult and no other fringes were therefore computed, and we have not thus far been at pains to discover a reason for the large fringes in table 1, either in the first order $(i = 22.5°,\ \delta\theta' = 4.7')$ or in the second order $(i = 45°,\ \delta\theta' = 3.3')$.

21. Summary of secondary interferences.—The possible partial interferences are naturally numerous. If we superimpose the case of fig. 5 on fig. 6 and draw all the rays of the first reflection for $\theta > r$ only (to avoid complications), *i. e.*, for a single direction, it will be seen that nine rays are included, of which a, b, c, a', b', c', a'', b'', c'', come from a single incident ray each. Thus we can assemble these interferences from a determinant like

$$\begin{matrix} a & b & c \\ a' & b' & c' \\ a'' & b'' & c'' \end{matrix}$$

and there should be 18 cases. Most of these are identical in path difference, but they have not led us to any satisfactory identification. They may therefore be omitted here.

Other difficulties enter. Fringes which may be invisible if observed for the glass plate may be visible if arising in the collodion film, as this is very thin. Possibly some of the finer lines may arise in this way, but not probably.

The tendency of certain groups of interferences to travel in opposed directions with rotation of the slit has suggested to us the possible occurrence of zone-plate action, where there would be multiple foci. But we have not succeeded in establishing coincidences either for the virtual or real foci in such a case. Moreover this opposition in motion has already been accounted for in paragraph 19.

22. Convergent and divergent rays.—What finally characterizes the above groups of interferences is the difference in position of their focal planes. They rarely coincide with the spectrum (parallel rays) and hence do not always destroy it. If present with the spectrum the latter is wholly wiped out. If the strong fringes are convergent for a given adjustment of grating they become divergent when the grating is rotated 180° about its normal. Hence the plates of glass are sharply wedge-shaped and to these differences the location of focal planes is to be referred.

In addition to this the three regular reflections are not in the same focus which shows the surfaces (collodium film) to be slightly curved. The above experiments succeed best when two of the reflections are yellowish, which probably means that the grating face is from the observer.

Suppose the remote glass face makes an angle $dr/2$ with the surface of the grating. Then the DR ray of the strong interferences has its angle incremented by $d\theta = dr$, whereas the RD ray receives an increment of but $d\theta = \frac{\cos r}{\cos \theta} dr$. Hence if the DR and RD rays were parallel for parallel surfaces they would be at an angle corresponding to

$$\frac{d\theta - dr}{dr} = \frac{\cos r - \cos \theta}{\cos \theta} \qquad (21)$$

where $dr/2$ is the angle of the wedge. Thus for the partial case of single incidence, fig. 6, $d\theta > dr$ if $\theta > r$, or the issuing rays would converge; and $d\theta < dr$ and $r > \theta$, or the issuing rays would diverge. If DR is negative the

opposite conditions will hold, since dr and $d\theta$ change signs together. For the case of triple incidence, fig. 5, there will be similar relations with less liability to convergence. The interferences are further modified by the change of thickness of glass or the variable e implied.

Fig. 7 shows that rays all but parallel will cross each other in front (convergent) or behind (divergent) the grating, depending on their mutual lateral positions. As a ray moves from the right to the left of the normal, the phenomenon may change from divergence to convergence and vice versa.

23. Measurement of small horizontal angles.—These relations are very well brought out by the interferometer, in which the mirror M may be inclined at pleasure. If small values of deviation only are in question, this instrument becomes a means of measuring small horizontal angles γ between mirror and grating as these involve less change of focus. In fact if h is the vertical height of the illumination at the mirror M and the corresponding obliquity of fringes is equivalent to an excess of N fringes crossing the bottom of the cross-hairs as compared with the top for a wave-length λ, $\gamma = N\delta e/h$; or

$$\gamma = \frac{N\lambda}{2h\,(\cos\theta' - \cos i)}$$

The question next at issue is thus the value of h. It will be noticed that if parallel rays fall upon the slit, they will be brought to a focus by the collimator objective first, and thereafter by the telescope objective, placed at a diametral distance D beyond it. Then if S is the vertical length of slit used, and f_c and f_t the focal lengths of the two objectives, respectively, it follows that the length $h = S$ is virtually illuminated. Hence,

$$\gamma = \frac{N\lambda}{2S\,(\cos\theta' - \cos i)} \qquad (22)$$

For since the angle γ, or a ratio, is in question, $N\delta e/h$ is constant and it makes no difference where the mirror M may be placed, *i.e.*, how great the absolute vertical height of the illumination h may be.

In case of this method (parallel light impinging on the slit) the illumination at each point of the image is received from but a single point (nearly) of the mirror, whereas if the light falling on the slit is convergent, the whole vertical extent of the mirror illumination contributes to each point of the image in the ocular. Hence in the latter case the fringes are only sharp when M and the grating are rigorously parallel, and they soon become blurred when this is increasingly less true. The same observation also accounts for the greater difficulty in adjustment when lamp-light is used. In any case, equation 22 furnishes N/S. N may be obtained with an ocular micrometer.

In the interest of greater precision the angle γ may be found by actually measuring the inclination to the vertical β of the fringes in the ocular. Here if the height of image s in the ocular corresponds to the vertical length of slit S,

$$\frac{s}{S}=\frac{f_t}{f_c}-2\left(1-\frac{D}{f_c}\right) \tag{23}$$

while

$$\beta=\frac{Nf_t}{s}\frac{d\theta'}{dn}$$

where $d\theta'/dn$ is given by equation 17. Hence s may be eliminated and

$$\beta=\frac{N}{S\left(\frac{1}{f_c}-\frac{2}{f_t}+\frac{2D}{f_cf_t}\right)}\frac{d\theta'}{dn} \tag{24}$$

If now we further eliminate N S in equation 22 by equation 24, we have finally

$$\gamma=\frac{\beta\lambda(f_t+2(D-f_c))}{2f_tf_t(\cos\theta'-\cos i)d\theta'/dn}$$

so that γ is given in terms of β, the observed inclination of fringes in the ocular. To measure β the ocular must be revolvable on its axis, so that the cross-hairs may be brought into coincidence with the fringes and the angles may be found. To measure M, the D lines as they remain vertical may often be used, if in focus, for reference in place of vertical cross-hairs.

Using the data of the above experiments, if $i=45°$—

$N=1$ $\quad f_c=f_t=D$(nearly) $=23$ cm., $\cos\theta'-\cos i=.2264$
$S=.9$ cm. $\quad \lambda=60\times10^{-6}$ $\quad d\theta'/dn=493\times10^{-6}$

whence $\gamma=146\times10^{-6}$ radians, or about a half-minute of arc per fringe, and $\beta=44'$ per fringe. Thus β is about 88 times as large as γ. At $i=22.5°$, $\gamma=1.5'$ per fringe, $\beta=45'$ per fringe. Naturally the sensitiveness increases with the angle of incidence i. When the fringes are large, one-tenth fringe is easily estimated, so that a horizontal angle γ of a few seconds between mirror and grating should be measurable. An ocular micrometer, as suggested, would carry the precision beyond this.

24. Summary.—It has been shown that the interferences here in question take place in accordance with the equations (6), (7), and (8) above. They therefore occur in triplicate, but not necessarily in the same focus. Their superposition gives rise to fluted interference patterns of which the coarse fringes (8) are less sensitive to micrometer displacements than the fine fringes (6) and (7), on the one hand, while they persist over a comparatively greater range of path difference, on the other. The eventual sensitiveness of both approaches the wave-length of light. The adjustment made is essentially self-compensating, in a way that excludes the wedge-angle of the plate; and the lines are rigorously straight and vertical, to the extent in which they may be regarded as parts of the periphery of ellipses, whose centers are infinitely distant on the same horizontal. As a whole, therefore, these interferences are special cases of the phenomenon described in chapters IV and V, where they may be made to pass through the zero of air-space.

The lines are inclined for a wedge-shaped air-space in a manner admitting of the measurement of very small angles.

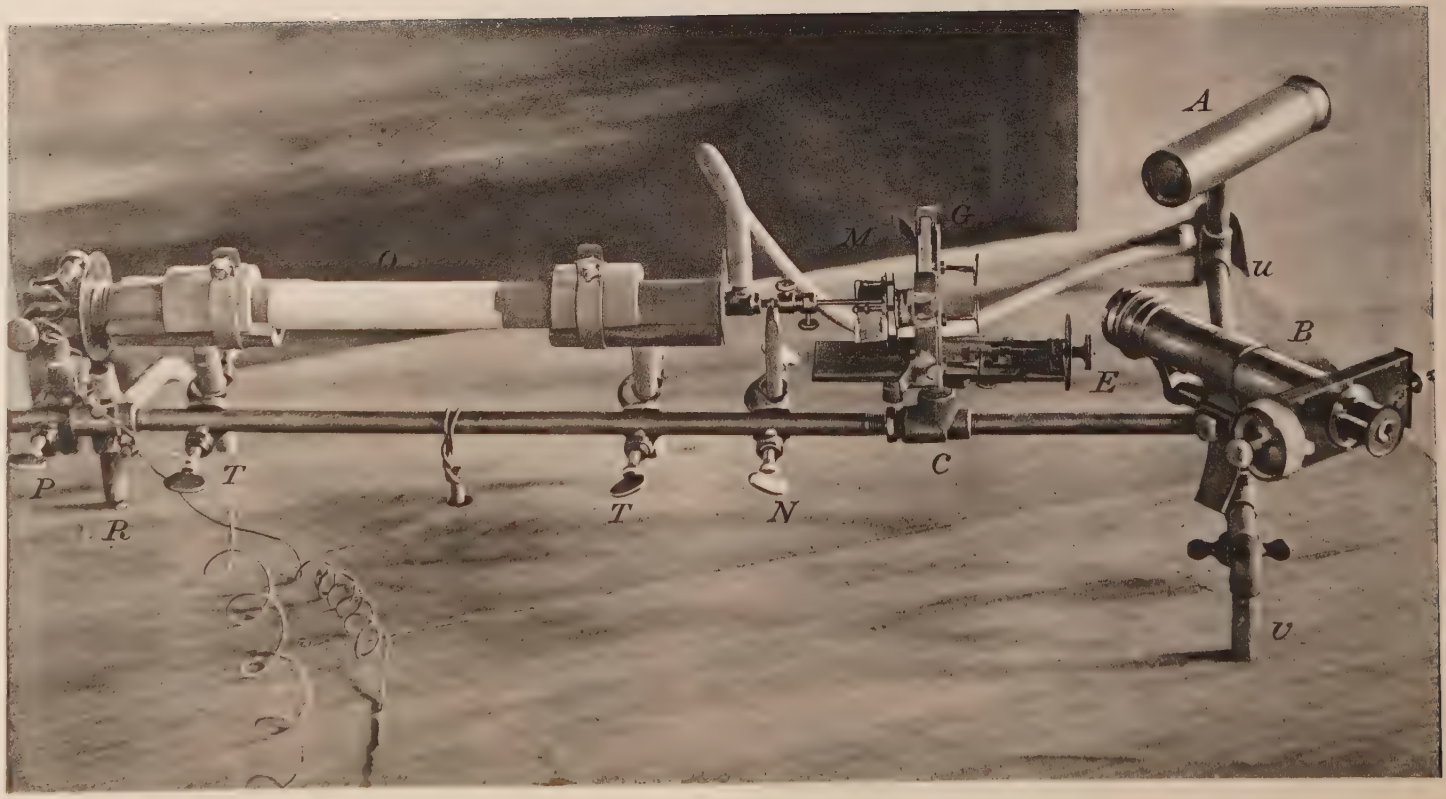

Fig. 10. Showing the Interferometer at *A*, *B*, *C*, and an attachment for Magnetostriction at *O*.

CHAPTER III.

THE GRATING INTERFEROMETER. By C. Barus and M. Barus.

25. Introductory.—In view of the perfection which has been attained in the construction of film gratings and of the simplicity of the instrumental equipment needed, we have been at some pains to put the type of interferometer recently described* into practical form. This is shown in the accompanying diagram, in which fig. 10 is a photographic view, the parts of which are easily recognized by aid of the simplified plan and elevation in fig. 11, A and B.

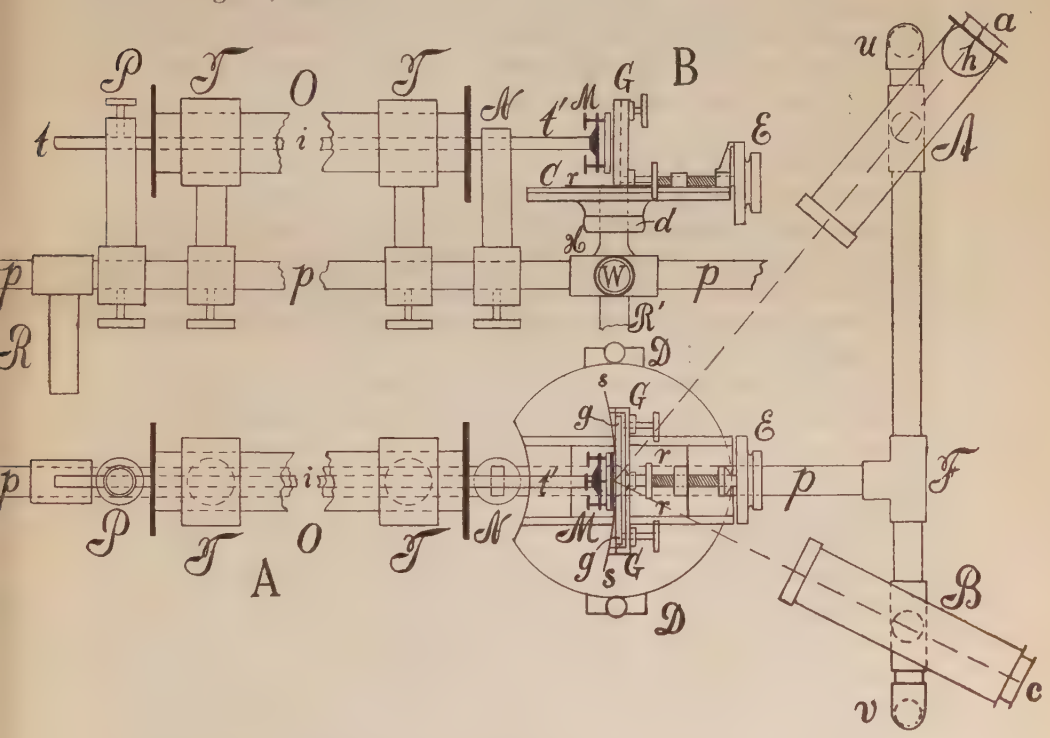

FIG. 11.—A. The same (fig. 10) in plan. B. The same in elevation.

The attachment for magneto-striction is purely incidental. The small increments of length in question were thought to offer an excellent test of the availability of the interferometer for micrometric length-measurements when these are of the sudden type and unlike the regular expansions.

* Science, xxxi, p. 394, 1910; Phil. Mag. (6), xx, p. 45, 1910; above chapter II.

26. Apparatus.—In fig. 11, *A* is the collimator, *B* the telescope for viewing the interference patterns reflected from the grating *gg* and mirror *M* over the revolvable table *CC*. These are the essential parts. The remainder is the incidental mounting just referred to, *O* being the helix containing an iron rod, soldered at its ends to brass or copper tubes, *t* and *t'*, the latter very light and movable in the V-groove *N*, the former *t* heavier and clamped in the upright *P*.

The whole is supported on a frame of quarter-inch gas piping and connections *uFvR*, the feet being at *uvR*, only the latter appearing in the figure. Under the grating is an attachment * with four or eight screw sockets, *W*, respectively at right angles to each other, into which a variety of apparatus may be screwed, in the absence of the removable pipe *pp*. When *p* is not used it is replaced by a foot.

Telescope *B* and collimator *A* are carried on T-pieces, with nipples at the same height (about 8 cm. or less) above the iron frame, and *B* may be slightly inclined about a horizontal axis. It may also be provided with a micrometer eyepiece, as shown in fig. 10.

The table, *CC*, carrying the grating, is revolvable on an upright *H* and may be clamped to fixed verniers, *D*, also carried at *d* by the upright *H*. The table is cut away on the further side so that vertical apparatus may approach closer to the grating in *GG*. It would even be an advantage to use (not much more than) a semicircular table with verniers *DD* alternately in use, set at an angle.

On the table two parallel brass guides determine the motion of the slide, *rr*, actuated by the micrometer screw *E*.

The grating is mounted with the film on a glass plate *gg*, and exposed on the side away from the observer, facing the mirror *M*. It is adjusted in a rectangular shallow brass case, *GG*, with the side toward *M* and the top open. The figure shows three adjustment screws actuating the rear of the glass plate, *gg*, and the springs *ss*, which push the plate to the rear, passing through slits in the sides of *GG*. There is one spring for the top and one for the bottom of the grating. The capsule *GG* is firmly attached to the slide *rr*, so that the grating may be moved fore and aft by the micrometer screw.

For some purposes the mirror *M*, similarly adjustable by three screws, may be attached to the plate *CC*, free from the slide *rr*. In the figure the mirror is on the light brass tube *t'*, which makes a prolongation of the iron rod, here to be tested for magneto-striction. The silvered face of *M* fronts the grating.

The coil, *O*, used is wound on a slender annular chamber or double tube, through which cold water may be kept in circulation (see fig. 10), to obviate changes of temperature of the rod. The uprights *P*, *T*, *T*, *N*, in figs. 10 and 11, moreover, are adjustable up and down as well as around the rod *pp*, by clamps shown in fig. 10, in which other unessential details may be seen, including the hose for supplying and removing water.

* In a later form a special base *R'* was provided below *W*.

27. Adjustments.—The micrometer screw controlled at E has a double purpose. In the first place it is an immediate check on all measurements of length increment made. It shows, moreover, whether the displacements are expansions or contractions, since it may compensate any motion of the mirror. In the second place, since the collimator A and telescope B are clamped at a fixed distance apart approximately, it enables the observer to put the part of the spectrum needed into the center of the field. For the angle aMc may here be considerably increased or decreased, and both telescopes are revolvable about the vertical. They may also be raised or lowered, moved right and left and rotated about the horizontal, being grasped by an ordinary clamp (not shown). The head E of the screw, moreover, as well as the adjustment screws of the grating, are at all times within easy reach of the observer. After an initial rough adjustment (the direct reflections from mirror and grating being put into coincidence), the adjustment screws on the grating are manipulated until the three spectra seen in the telescope B coincide both horizontally and vertically. For this purpose the D and E lines of the spectrum are useful and sunlight is preferable. In the absence of sunlight a small electric arc lamp with the rays issuing nearly parallel suffices equally well, supposing the apparatus is in adjustment. When telescope and collimator are fixed, motion at the micrometer screw naturally does not displace the spectrum line λ, on which the telescope has been focussed, so that the interferences recorded pass through a definite part of the spectrum.

The three sets of interferences available are subject to the equation

$$\delta e'' = \lambda/2 \cos i \qquad (1)$$

$$\delta e' = \lambda/2 \cos \theta \qquad (2)$$

$$\delta e = \lambda/2 (\cos \theta - \cos i) \qquad (3)$$

where λ is the wave-length of light used, i and θ the angles of incidence and of diffraction in air, and where δe, $\delta e'$, $\delta e''$, represent respectively the increment of air-space between mirror and grating per fringe passing the cross-hairs. It is therefore necessary to know the angles θ and i, and for this purpose the verniers D and the revolvable plate CC graduated on its edge are provided.

Let the mirror or grating plate be turned until the reflected image of the slit coincides with the slit itself. Here the observer must be able to look at the inner face of the slit in A through the hole h in the tube. Then let the angle be read off. Thereafter let the plate C be unclamped and turned until the slit is seen sharply on the cross wire of the telescope C and a second reading made. The angle so observed is $(i+\theta)/2 = a$. We may therefore write

$$\sin i - \sin \theta = 2 \cos (i+\theta)/2 \cdot \sin (i-\theta)/2 = \lambda/D$$

where D is the grating space. Thus

$$\sin (i-\theta)/2 = \lambda/D \cos a$$

from which $(i-\theta)/2=b$ may be found. Hence $i=a+b$; $\theta=a-b$. An eccentric position of the grating is of no consequence.

In the given apparatus the inner angle of diffraction has been utilized. This brings A and B closer together for a sufficiently large angle i to secure the best results.

In a later construction of the apparatus on an independent foot under W, uv is a long smooth rod and A and B are attached by clamps admitting of motion right and left, up and down, and rotation about the horizontal and vertical.

28. Angular extent of the fringes.—In chapter II the equations were worked out (*l.c.*) for the more complicated case of a medium of thickness e and refractive index μ. For the case of an air-space the equations become much simplified. Corresponding to equations 1, 2, 3, if $\theta<i$ and $\sin i-\sin\theta=\lambda/D$

$$\frac{d\theta'}{dn}=\frac{\lambda^2}{2eD}\,\frac{1}{\cos i\cos\theta} \tag{4}$$

$$\frac{d\theta''}{dn}=\frac{\lambda^2}{2eD}\,\frac{1}{1-\sin i\sin\theta} \tag{5}$$

$$\frac{d\theta}{dn}=\frac{\lambda^2}{2eD}\,\frac{1}{1-\cos(i-\theta)} \tag{6}$$

where $d\theta/dn$ is the angle subtended per fringe for the wave-length λ, the grating space D, the thickness of air-space e, at an angle of incidence i and of diffraction θ, in air.

These three sets need not be in focus at once. Equations 4 and 6 are usually easily put in focus together. Thus in the above case roughly,

$$i=50^\circ\ 24' \qquad \theta=24^\circ\ 44' \qquad \lambda/D=.352$$

whence for $\lambda=60\times10^{-6}$ cm. and $e=1$ cm.,

$$\frac{d\theta'}{dn}=.064' \qquad \frac{d\theta''}{dn}=.055' \qquad \frac{d\theta}{dn}=.378'$$

In case of the set of equations 4, 5, 6, therefore, there should be about 6 to 7 small fringes to one large fringe. This is about the order of values usually observed. When e is small the change of wave-length with $d\theta$ must be considered. To obtain a given ratio k of small and large fringe divergences, one may write for the cases 4 and 6, for instance,

$$k=2\,\frac{1-\cos(i-\theta)}{\cos(i-\theta)+\cos(i+\theta)} \tag{7}$$

Equation 7 is not easily treated. If, however, θ is computed in terms of i and expressed graphically, k may then also be expressed in terms of i; and thus the angle of incidence i for any ratio of size of fringes, k, in question, may be roughly adjusted. Table 7 shows these results.

TABLE 7.—Ratio of large and small fringes.

i	θ	$1/k$	$1/k'$	i	θ	$1/k$	$1/k'$
0°	−20° 1′	16.4	16.5	50°	24° 27′	6.0	7.0
10	−10 17	15.6	16.6	60	30 56	3.4	4.4
20	− 0 34	14.8	15.8	70	36 0	1.6	2.6
30	+ 8 31	12.3	13.3	80	39 15	.6	1.5
40	16 54	9.1	10.2	90	40 24	.0	1.0

Thus it appears that at $i=37°$ about there should be ten small fringes to one large fringe. In a general way, moreover, the ratio of small to large fringes gives an estimate of the value of i.

Similarly equations 5 and 6 give

$$k'=2\,\frac{1-\cos\,(i-\theta)}{2-(\cos\,(i-\theta)-\cos\,(i+\theta))}$$

from which the data also given in table 1, follow.

Here there will be ten small to one large fringe when i is 40.5° roughly.

The preceding equations 4, 5, and 6 are essentially approximate, inasmuch as the rates are taken for the finite quantities. If we return to the fundamental equations

$$2e\cos i=n\lambda \tag{8}$$

$$2e\cos\theta=n'\lambda \tag{9}$$

$$\sin\theta-\sin i=\lambda/D \tag{10}$$

for θ is greater than i, where n and n' are unequal distributive whole numbers; and if we put $e/D=a$, we find

$$\tan i=\frac{n^2-n'^2}{4an}-a \qquad \tan\theta=\frac{n^2-n'^2}{4an'}+a \tag{11}$$

which are free from λ, whereas $\sin i$ and $\sin\theta$ essentially contain λ. As the angular width of a fringe is

$$\theta=\int_n^{n+1}\frac{d\theta}{dn}\,dn$$

those corresponding to equations 4 and 5 may therefore be expressed as

$$\theta_1=2a\int_n^{n+1}\frac{-dn}{n\sqrt{n^2-4an\tan i-4a^2}} \tag{12}$$

$$\theta_2=2a\int_n^{n+1}\frac{-dn}{n(n-2a\tan i)} \tag{13}$$

for a given space e in $a=b/D$ and a given angle of incidence i in $\tan i$. These integrations are easily made, but the results are too diffuse to be

worth discussing here. Equation 12, moreover, is a restatement of the fact that in these interferences $n\lambda$ is constant throughout the spectrum.

Equations 8, 9, and 10, however, admit of the graphic treatment of the problem. For if we put $A = nD/2e$, they may be written according as $\theta > i$ or $\theta < i$

$$\sin\theta_1 = \pm\frac{\cos i}{A} + \sin i \tag{14}$$

$$\sin\theta_2 = \frac{A^2 \sin i \pm \sqrt{1 + A^2\cos^2 i}}{1 + A^2} \tag{15}$$

where the distributive number n in A takes the values of the successive whole numbers for a dark band in the respective spectra corresponding to equations 14 and 15. The coincidence of dark bands then determines the position of the coarse fringes.

If $i = 50^\circ\ 24'$

$$2e = .1 \text{ cm.} \qquad D = .000{,}169 \text{ cm.} \qquad \theta = 24^\circ\ 44'$$

then

$$A = .0017 \cdot n, \text{ nearly}$$

With these data table 8 was computed. Similar results might be computed for $\theta < i$, but I have abandoned it because, as is now evident, the practical demands are sufficiently met by the method of paragraph 28.

TABLE 8.—Showing θ_1 and n, θ_2 and n'. θ observed about 75°. $2e = 1$ cm., $i = 50.4°$, $\theta > i$. δe corresponds to the mean value $\bar{\theta}$.

n	θ_1	$10^3\delta e_1$	$\bar{\theta}_1$	n'	θ_2	$10^3\delta e_2$	$\bar{\theta}_2$
1650	86.1°	76	84.2°	300	83.4°	19	82.5°
1700	82.3	46	81.2	400	81.5	18	80.5
1750	80.0	36	79.1	500	79.6	17	78.8
1800	78.2	30	77.6	600	77.9	16	77.1
1840	77.0	23	76.7	700	76.2	15	75.5
1870	76.3	30	75.8	800	74.7	14	74.0
1900	75.4	22	75.0	900	73.3	12	72.7
1940	74.5	20	74.2	1000	72.1	..	..
1970	73.9	20	73.6	2000	64.0	..	....
2000	73.3	18	73.2	....	....	..	....
2020	73.0	20	72.8	..	..	..	....
2040	72.6	15	72.5	..	..	..	....
2060	72.3	..	....	..	..	..	....

29. Test made by magneto-striction. The very small elongation produced when iron is magnetized offers an excellent test of the above apparatus. The attached water-cooled helix has already been described. The rod of Swedish soft iron was quite within the helix, which surrounded it closely without contact, the rod being prolonged by light copper tubes soldered to its ends.

A large number of experiments were made for trial, brief examples of which are given in the following table and charts, where if the current is in amperes the magnetic field

$$H = 108i \text{ gauss}$$

and the elongation $\delta e = 105 \times 10^{-6}$ cm. per large fringe. Thus if n is the number of fringes and $l = 28$ cm. the effective length of the iron rod, the absolute elongation is $\delta a = 105n \times 10^{-6}$ cm. and the elongation per unit of length,

$$\delta\beta = 3.75n \times 10^{-6}$$

or if small fringes N are taken,

$$\delta\beta = .54N \times 10^{-6}$$

Elongations from 10^{-6} cm. to 10^{-4} cm. were measured without difficulty, though such measurement, without micrometer attachment, is essentially an estimate. Count was made of the number of small fringes between the large fringes.

TABLE 9.—Magneto-striction elongations. Coil* (separated by thin sheet of flowing water from rod) length 37 cm., 3200 turns, $H = 108i$ gauss (i in amperes). Swedish iron rod, diam., $2r = .64$ cm., length $l = 30.6$ cm., free length 28 cm. Elongations, $10^6\delta e = 105$ cm., $10^6\delta e_1 = 33$ cm., $10^6\delta e_2 = 47$ cm. Seven small fringes to one large fringe.

H	Fringes.	$\delta\beta \times 10^8$	H	Fringes.	$\delta\beta \times 10^8$
gauss	small	....	gauss	small	....
13	.0	0	98	6.0	320
22	1.5	79	56	7.0	370
36	4.0	210	36	5.0	310
44	6.0	320	23	2.0	110
62	7.0	370	9	.0	0
62	6.5	350	− 9	.5	26
44	5.5	300	−23	3.0	160
36	5.0	270	−36	5.5	300
13	.0	0	−56	6.0	320
−13	.5	26	−99	5.0	270
−22	3.5	190	+99	5.0	270
−62	7.0	370	69	6.0	320
+62	7.0	370	56	6.0	320
13	.5	26	19	1.2	64
6	.0	0	11	.0	0
			−11	.5	26

* A field of 150 gauss should more than practically saturate iron.

The data partake of the usual character of magnetic phenomena. There is marked hysteresis and irregularity due to residual magnetization. Table 9 has been inserted merely as an example of the results, which are otherwise given graphically. The maximum elongation corresponded to about 7 small fringes.

The curves bring out the following results consistently:

(1) The elongation apparently begins abruptly in small fields of 5 or 10 gauss, see fig. 12, etc., at *b*.

(2) In small fields, fig. 14, A, there is nevertheless a tendency of a very slow continual increase; but whether this is due to inevitable percussion during magnetization can not be stated. The case may be one of true magnetic elasticity.

(3) The maximum elongation is very rapidly reached in a field of 50 to 100 gauss. After this the elongation now due to strong fields decreases. In the case of strong fields, however, the rod as a whole is probably dis-

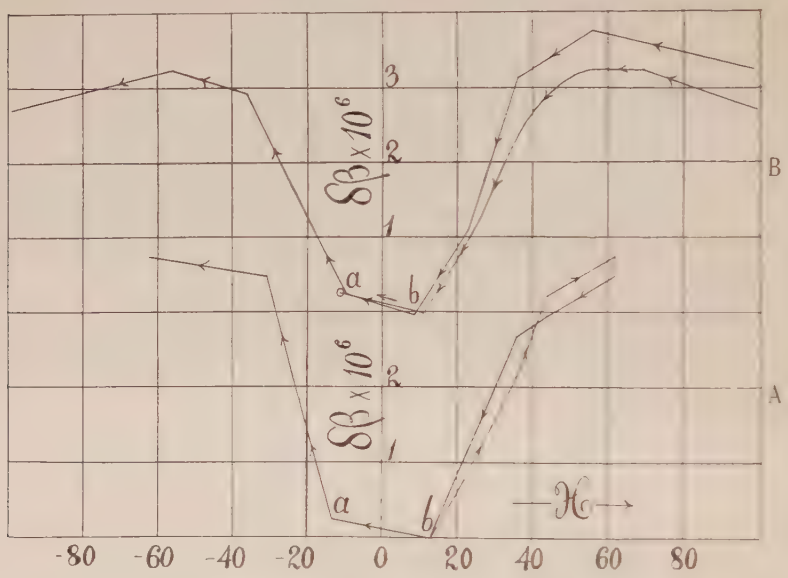

FIG. 12.—Charts showing the elongation of soft iron in millionths for different fields, positive and negative, in gauss. Field applied and removed for each observation.

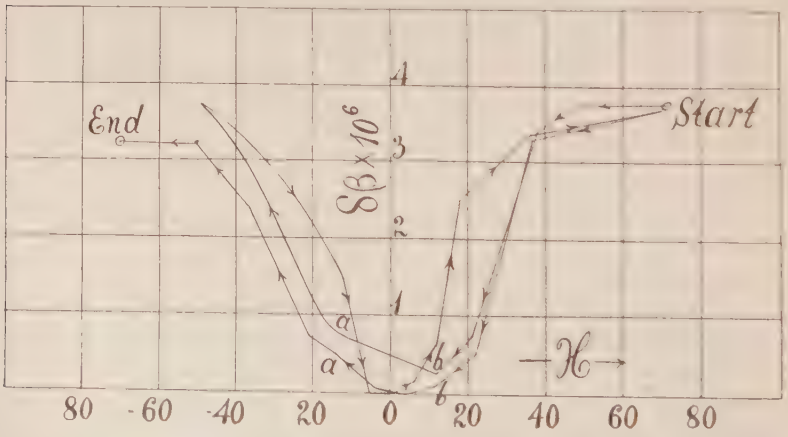

FIG. 13.—Chart showing the elongation of soft iron in millionths for different fields, positive and negative, in gauss. Field applied and removed for observation.

placed or warped. The results are less and less trustworthy and not suitable for exploration by the optic method in question (figs. 12, B, and 14, B and C).

(4) If the field is reversed the elongation is similar, but symmetrical with respect to a small positive field if the immediately preceding magnetization was positive, and symmetrical with respect to a small negative if the preceding magnetization was negative. See figs. 12, A, B, 13 (hysteresis). Thus in fig. 12, A and B, where a field of 13 gauss at *b* after a positive magnetization produces no elongation whatever, the reversal of the field to -13 gauss produces a very marked elongation of nearly 3×10^{-7} which

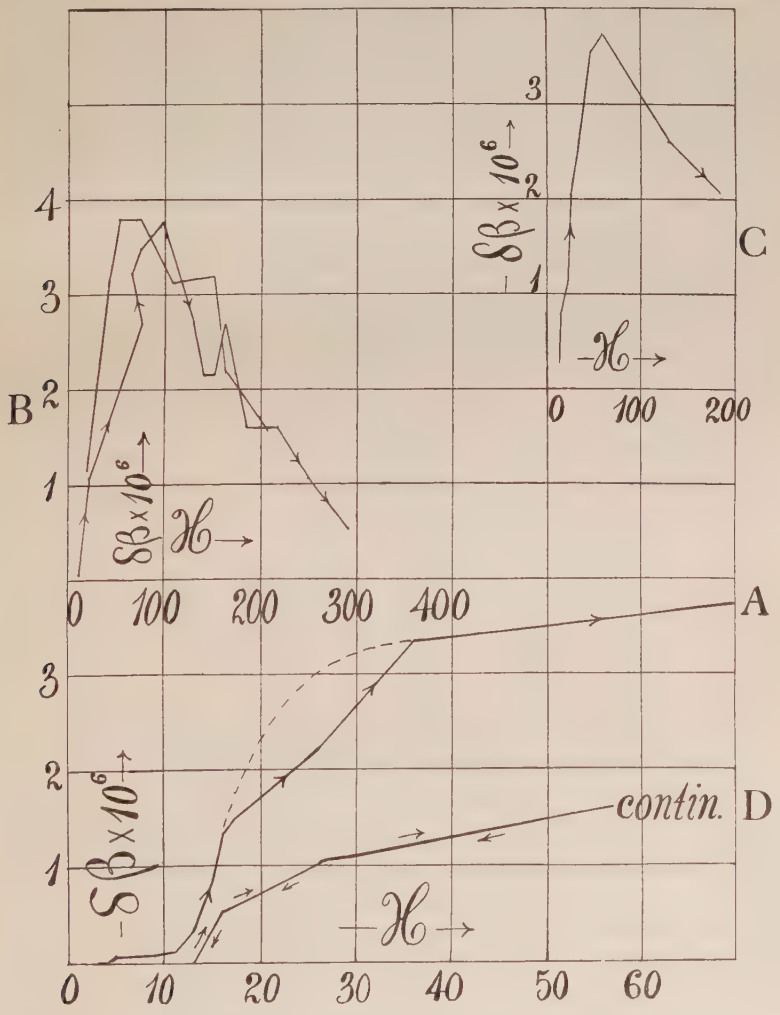

FIG. 14.—Charts showing the elongation of soft iron in millionths for different fields, positive and negative, in gauss. Field applied and removed for each observation except in fig. D.

may be repeated indefinitely. Hence there seems to be a definite magnetic elasticity with fields of less than 5 to 10 gauss. If this is exceeded the magnetic molecules are permanently set, even in soft iron.

(5) If the field varies continuously (liquid resistances) the elongations are much smaller in given fields (fig. 14, D).

The whole subject, which is here touched incidentally, is well summarized in Winkelmann's Handbuch, vol. 5, p. 307 *et seq.*, 1908, by Professor Auerbach. The above results agree closely with the elaborate experiments of Nagaoka and Honda,* who used a special type of contact lever. Recently Mr. Dorsey † has made a similar investigation, using an ingenious method of his own. The present method would not have been feasible but for the occurrence of large and small fringes in the field of the telescope.

30. Summary.—The present chapter has shown the ease with which the above phenomena may be adapted to the measurement of small displacements, has instanced their particular usefulness, inasmuch as fine and coarse adjustments are both available (recommending their use in the investigation of phenomena of sudden occurrence as in magneto-striction, etc.), and has given suggestions of practical forms of apparatus in addition to the usual spectrometric form.

* Nagaoka and Honda: Phil. Mag. (5), XXXVII, p. 131, 1894.
† Dorsey: Phys. Rev., XXX, p. 698, 1910.

CHAPTER IV.

THE USE OF THE GRATING IN INTERFEROMETRY; EXPERIMENTAL RESULTS.

31. Introductory.—In chapters II and III a method* was described of bringing reflected-diffracted and diffracted-reflected rays to interference, producing a series of phenomena which, in addition to their great beauty, promise to be useful. In fact, the interferometer so constructed needs but ordinary plate glass and replica gratings. It gives fringes rigorously straight, and their distance apart and inclination are thus measurable by ocular micrometry. Lengths and small angles are thus subject to micrometric measurement. Finally, the interferences are very easily produced and strong with white light, while the spectrum line used may be kept in the field.

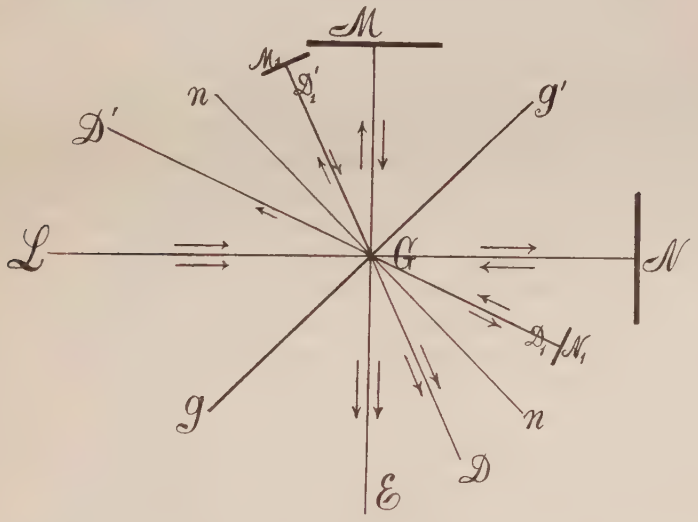

FIG. 15.—Diagram of grating interference adjustments adapted to Michelson's apparatus. *L*, source of white light (parallel rays), *gg'* grating, *M* and *N* opaque mirrors.

The same method is available as an adjunct to either Jamin's or Michelson's interferometers, except that here the transmitted-reflected-diffracted and reflected-transmitted-diffracted rays are brought to interfere. To take the example of the Michelson type, stripped of unnecessary details, let *gGg'* in fig. 15 be the grating or ruled surface, *n* its normal, *L* the source of white light, *M* and *N* the mirrors, and *E* the eye. In the usual way the rays from *L* interfere at *E*.

*Science, XXXII, p. 92, 1910; *cf.* Phil. Mag., July 1910, and chapters II and III above.

Now replace L by a slit and collimator, E by a telescope focussed for parallel rays. The eye at E now sees a sharp line of light. At D and D', however, there must be two diffraction spectra coinciding in all their parts and hence interfering rhythmically, if all adjustments are sufficiently perfected. The other two diffractions within MGg' and EGg are often lost at an incidence of 45°.

The attempt to produce these interferences at D, D' with replica gratings is liable to result in failure; for while the transmitted system NGD shows brilliant spectra, the reflected system MGE is dull and hazy. Both spectra are clearly in evidence and may be brought to overlap. The film, however, does not reflect in a degree adequate to the transmission. Attempts made to realize the conditions of interference eventually, however, resulted in complete success (chapter V).

What is strikingly feasible at once, with ordinary plate glass and a non-silvered grating, * is the production of interferences between pairs of diffracted spectra, D' and D, for instance, if returned by equidistant mirrors M and N to a telescope in the line D. Both of these spectra are very brilliant and not very unequally so and the coincidence of spectrum lines both horizontally and vertically brings out the phenomenon. This, for each of the cases specified, is of the ring type and not of the line type heretofore discussed; but it occupies the whole field of the spectrum from red to violet. One obtains brilliant large confocal ellipses with horizontal and vertical symmetry, and the spectrum lines, simultaneously in focus, may serve either as major or minor axes. The interferometer motion is twofold in character, consisting of radial motion, combined with a drift of the figure as a whole, in a horizontal direction. Naturally a fine slit is of advantage, but the experiment succeeds with quite a wide slit, especially in the red, much after spectrum lines vanish. Similarly the regular reflection from M and N (mirrors) will produce these phenomena along GD.

Such ellipses (I shall so call them, though they are probably ovals) as have their centers in the field, are clearly due to reflection from the same surface, as shown in fig. 15; curved lines or ellipses with remote centers are due to simultaneous reflections of the component rays from the opposite faces of the grating, since the angle of the wedge of glass can not be excluded. All owe their vertical and horizontal symmetry to the vertical slit and horizontal spectrum. The ellipses are identically present in the successive orders of spectra at once.

These elliptical fringes thus embody with the preceding linear set the common property of being duplex in character; only here the motion of dark rings to or from the centers of the ellipse, as a fine adjustment, is associated with a displacement of the fringes bodily through the spectrum (coarse adjustment).

* My thanks are due to Prof. J. S. Ames, of Johns Hopkins University, who was good enough to lend me this grating.

This displacement may be from red to violet or from violet to red, as the virtual air-space increases in thickness, depending upon the adjustment, as will presently appear. In other words, for a given small interferometer motion of mirror, there is in general less displacement of fringes bodily than radial motion of fringes to or from the center. Slight deflection of the grating, gg', is chiefly accompanied by radial motion of the fringes.* The effect thus produced is to give sharpness to the interference pattern, which soon vanishes for approximate adjustments of spectra.

Similarly the micrometer screw produces a rapid passage of the pattern through its maximum size, a play of the screw of 0.1 cm. being sufficient to pass from fringes of one extreme of small size, through the maximum size to the final extreme. One may note that in chapters II and III the admissible play for the coarse fringes was about 1 cm., ten times greater. On the other hand there are many regions of interference; in fact, different groups of interferences may sometimes be in the field at once, or more usually corresponding to slightly different angles between the mirrors and grating.

All admissible angles, provided that symmetry is maintained (the virtual plane of the grating bisecting the angle of the mirrors), bring out the phenomenon. This points to the fact that the earlier phenomenon referred to (*l.c.*), in which the center or normal ray was virtually at an infinite distance, is now produced near an accessible center, even if this is not actually in the field. However, in the earlier case, when the angle of incidence is zero, curved lines may also be obtainable. Such cases will be given in the next chapter.

Experiments with a silvered grating showed no advantage, whether the transparent film covered the grating or the plane face of the glass. In fact, in case of good adjustment the phenomenon is so strong as to need no accessory treatment; this is in fact one of its advantages. A great difficulty in adjustment is the occurrence of stationary fringes due to the rear face of the grating. These may even wipe out the spectrum lines; but usually they lie at a finite focus and are not seen with a sharp spectrum. Fortunately many positions are available for obtaining the ellipses, so that a satisfactory one is easily found. Unless all overlapping spectra show sharp lines the adjustment is very tedious.† The amount of grating space used is less than 1 sq. cm., though of course a larger size is convenient for experiment.

32. Special properties.—The motion of the ellipses bodily across the spectrum, corresponding to the increased or decreased virtual air-space (micrometer screw), shows that whereas the vertical dimension or axes (direction of fixed color) do not appreciably change,‡ the horizontal axes

* This changes the effective thickness of the grating.

† These difficulties are largely removed by the method of coincident white slit images given in chapter V.

‡ Probably referable to increased refraction and decreased diffraction from red to violet.

grow rapidly smaller; *i.e.*, the ellipse is more eccentric from red to violet. With the grating used, however (about 2800 lines per centimeter), the major axis remained vertical, *i.e.*, the circular form was not reached throughout the first order even in extreme red.

It follows from this that in the second order the major axis of the ellipses for 2800 lines to the centimeter will probably be horizontal, and this was found to be strikingly true. The figure, moreover, is necessarily coarser and the lights and shadows in greater contrast. In the third order the ellipses are drawn out horizontally to a correspondingly greater degree. Thus it is clear that with a more dispersive grating the circular or even the horizontally elongated form must occur in the first order. Indeed with 6000 lines to the centimeter, ellipses occur in the red having horizontal major axis while the figure in the green is circular. Spectrum lines are very distinct, particularly in the second order. In all orders of spectra the centers of the ellipses are simultaneously on the same spectrum line and their vertical dimensions are about the same. Hence the spectrum lines may be used instead of cross-hairs, as they are fixed landmarks among the moving ellipses.

With replica gratings the center of the ellipses is usually remote, *i.e.*, reflection does not easily take place at the free grating surface. Apart from this the curved lines are good and strong. Samples must be tried out, in which the lines are as clear as possible in all the overlapping spectra. Six gratings of this kind were examined with about the same results. The centers of the ellipses could only rarely be brought into the field. Centers may, however, be obtained for gratings cemented under pressure between unequally thick plates of glass.

It has been stated that considerable width of slit is admissible. Moreover, the focal plane of the collimator (convergent or divergent light) or the focus of the telescope makes little difference, though the condition of parallel rays is naturally preferable. An eye focussed for infinity sees the fringes very well without the telescope and they may be also caught on a screen; but coming through a slit they are liable to be dark and the advantage of the telescope is obvious. The second order is particularly accessible for naked-eye observation, and the light and black appearance is accentuated, but they are liable to be irregular. Inclining the collimator moves the spectrum across the fringes vertically, while inclination of the telescope moves both equally. In this way the centers may often be found. With strong tipping, however, the figure becomes distorted or open above and below, as would be expected. If the light is intensified for projection or naked-eye work, there is also distortion.

It is not necessary (and apparently of little advantage) to have the reflections from the mirrors M and N occur at normal incidence. In fact the patch of white light on the grating surface and the return patch of spectrum may be over an inch apart. Inasmuch as the spectra are rigorously coincident, it follows that (apart from the refraction of the thick

plate glass) the grating must be symmetrical with respect to the mirrors; *i.e.*, intersect the angle between them. Very little difference of size or shape is observable between extremes of such adjustment. Thus I rotated the grating about 10° (larger angles being unavailable) without appreciable effect, after one of the mirrors had been correspondingly adjusted.

On examination of the effective air-distances of the mirrors M and N from the grating, it is found that three positions are favorable to interference; in the first (case A), M is farther away than N from the corresponding faces of the glass plate; in the second (case B) they are about equidistant; finally, in the third (case C), N is further away, symmetrically with the first adjustment. For each case the admissible play of mirror (micrometer screw) does not much exceed 1 cm. for ordinary magnification. The second or equidistant adjustment brings out the lines or ellipses with distant centers, and there are usually three types easily found (after one has appeared), by slightly inclining either mirror around a horizontal axis by a tangent screw. Thus (see fig. 16) fine lines, say at 135° to the

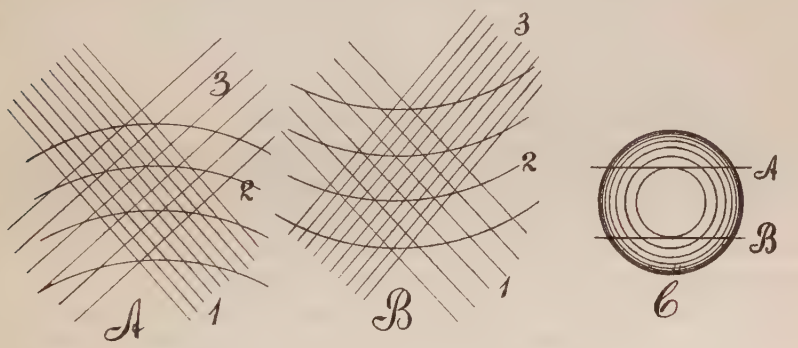

FIG. 16.—Interference patterns in case of self-compensation, B.

horizontal, coarse nearly circular lines, concave downward or upward as the case may be, and finally broad lines say 45° to the axis, may appear in succession. If the grating is rotated 180° around its normal, convexity upward (fig. 16, A) changesto concavity upward (fig. 16, B), showing the wedge angle of the glass plate to be effective. The micrometer-screw will pass any of these forms through a succession of inclinations corresponding to the eccentric intersection of a group of concentric circles by a straight line. This is also shown in fig. 16 at A and B, as observed for a fixed air-space and at C, on moving the micrometer in the A and B cases. These figures cover the coincident spectrum fields only. A solitary part of the field shows no interferences. For adjustment it is therefore necessary to cut off the spectra sharply above and below, by limiting the length of slit. Of the three or four spectra present the coincidence may then be secured with least difficulty. With each such coincidence there goes a definite position of the micrometer screw (interferometer), and this is the initial difficulty

of adjustment; *i.e.*, to coordinate the various spectrum coincidences with the three screw readings.

The non-equidistant case of mirrors and grating correspond to the ring types with the centers in the field. Hence both reflections take place from the *same* face of the grating. When the distance GM is shorter, $G'N$ longer, I have noticed two or even three ellipses successively in the field, obtained by slowly inclining the mirror N about the vertical (tangent screw), with their centers in turn in the yellow-green, the blue, and the green of the spectrum. They do not occur together. On turning the micrometer screw clockwise they move from red to violet, and vice versa.

When the distance GM is longer and $G'N$ shorter, rings also occur; but only a single set was found. The spectrum lines not being clear, finding them was a matter of discrimination. When the micrometer screw was turned clockwise, however, they marched from violet to red, *i.e.*, in *opposite* direction to the preceding. The drift of ellipses corresponds with the direction in which the violet fringes move horizontally.

It is at first an astonishing result that when the grating is reversed (front face put rearward, leaving the air space unchanged) the ring type is left in the field; though the solitary ring type changes to the multiple type. This is true for the case specified as A or case C. It is also true for the eccentric type, case B, where line types, single or multiple, reappear at slightly different mirror angles. Briefly, rotation has no effect on the march of ellipses through the spectrum; but in case B it changes convex lines downward to concave lines, and vice versa. Nor has reversal of grating any effect on the march. The position of the grating with respect to the mirrors (three places being available) alone determines this result, certainly in the extreme cases A and C, and probably in the intermediate case B.

The use of a compensator in either of the component rays is always accompanied by the two effects in question; *i.e.*, there is both relatively large radial motion of the fringes and relatively small displacement, within the field of the telescope. One may therefore be evaluated in terms of the other, the two having the stated relation of coarse and fine adjustments. In case B the fringes will rotate, expand, or contract.

33. Elementary theory.—The endeavor must now be made to explain these results more in detail. For this purpose fig. 17 may be consulted.

In the grating used at an incidence of about 45° the angle of diffraction in the first order was about 32° 30′ for the D_2 sodium line, there being about 2847 lines to the centimeter, corresponding to a grating space of $D = .0003512$ cm. Thus $\lambda\ D = 0.1077$. The index of refraction was assumed to be 1.53 for the same line.

The diagrams are drawn for an angle of incidence of 45° and for normal reflection from the mirrors M and N. In case of the grating given, the three positions of the grating at which interferences occur were about 0.6 cm. apart and are marked 124, 100, and 76 scale parts, on the micrometer

screw normal to the grating. In other words it was convenient to move the grating at the center of the spectrometer, rather than the mirrors M and N adjustably attached near the edge of the plate graduated in degrees.

In group A at 124 the short air-path is to M, the long path to N; in group C at 76 the reverse is true. In group B at 100, the system is self-compensating and the air-paths about equal.

In all cases the angle of diffraction, θ, is less than the angle of incidence, i. There are of course corresponding cases, $\theta > i$, which have not been drawn, because they merely duplicate the cases given, at a different angle. It is assumed that after more than one direct reflection or one diffraction the interferences are no longer observable.

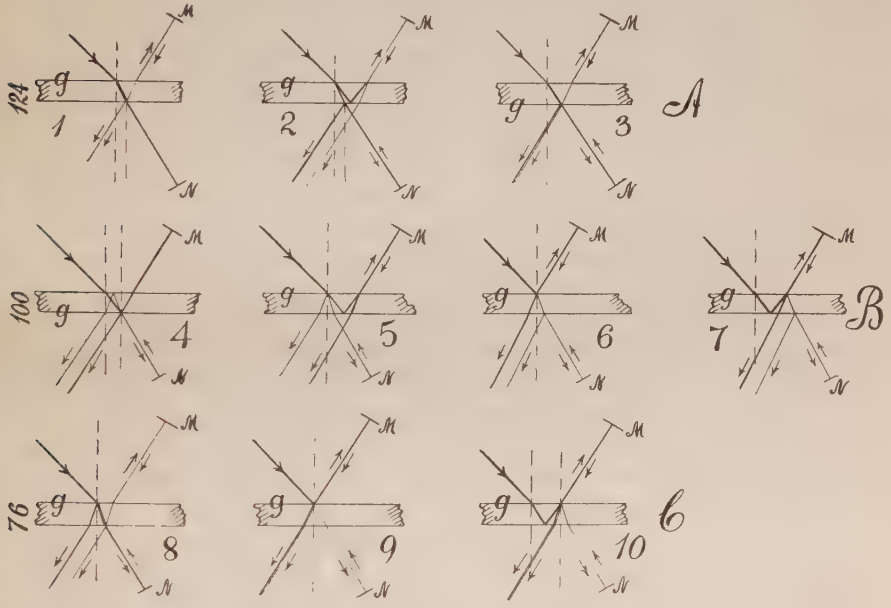

FIG. 17.—Chart of the three groups of interferences, A, B, C. Mirrors M and N return the spectrum. Grating face in position shown at g.

The diagrams 124 and 76 show that the two reflections of the component rays at the grating take place at the same surface; hence the occurrence of centered figures or rings. On the contrary the reflections in diagram 100 take place at the two different faces of the grating respectively; hence the angle of the grating is included and liable to produce eccentric ring systems. The center may be so far off that the dark lines are nearly straight, but they change their inclination as the vertical projection of the center moves horizontally through the field.

Some of these cases may coalesce in practice or they may destroy each other more or less. I have taken a single incident ray from which may come two parallel emergent rays, which are brought to interfere by the telescope. It would have been just as convenient to have taken the two

corresponding incident rays which interfere in a single emergent ray. From the position of the mirrors it is clear that the regularly refracted rays are not returned. Only rays *first diffracted* at the grating (where they may also be reflected) are returned by the mirrors.

As a whole we may distinguish two typical cases, those in which both component rays are diffracted as in No. 1 or refracted as in No. 2; and those in which one component ray is refracted and the other diffracted. If i and θ' are the angles of incidence and diffraction in air and r and θ the corresponding angles of refraction and diffraction in glass, the glass path differences, Δx, in the important cases are as follows:

No. 1.	$\Delta x = 2\mu e/\cos\theta = 2.2$ cm.	No. 7.	$\Delta x =$ Zero.
3.	$= 2\mu e/\cos\theta = 2.2$ cm.	8.	$=$ Zero.
4.	$=$ Zero.	9.	$= -2\mu e/\cos\theta = 2.2$ cm.
6.	$=$ Zero.	10.	$= -2\mu e/\cos\theta = 2.2$ cm.

Here μ is the index of refraction and e the thickness of the glass plate of the grating, and excess of path for the M ray is reckoned positive. These paths must be compensated by corresponding decrements and increments respectively of the air paths GM and GN. Ordinarily these path differences in glass being fixed for given angles θ' would fall away; but they vary essentially with color and hence the degree of compensation is never the same for all colors.

Furthermore, although the wave-fronts of the two rays are the same on emergence, this does not imply coincidence of phase even in such cases as Nos. 1 and 2, for instance; the absolute lengths of paths in glass are quite different, although their differences are the same. Consequently the cases 1 and 2 would again interfere if superimposed, one case being first diffracted and the other first refracted.

Thus it is not surprising that so many cases were identified. It is also apparent that the air compensations are very different and hence identification is facilitated. Finally, since a vertical slit and collimator are used, the section of a beam of light passing through the grating by a horizontal plane consists of parallel rays; the section by a vertical plane, however, is convergent.

It is interesting to find the numerical data for the above equations, assuming that

$$i = 45^\circ \qquad \theta' = 32^\circ 39' \qquad e = .68 \text{ cm.} \qquad \mu = 1.53 \text{ (estimated)} \qquad \lambda/D = .1677$$

for the sodium line of the spectrum. The results are given with the equations. Their value is about 2.2 cm., which is equivalent to a displacement of mirror actually found.

It follows, moreover, that the center of the ring system, order $n = 0$, must move from red to violet or the reverse, inasmuch as the compensation takes place successively, at each color, in the same way. Although the equations hold only for the center, and the symmetrically oblique rays

belonging to the rings have not been given consideration, an approximate computation of the motion of the ring centers may nevertheless be attempted.

From the equations qualitative interpretations of the above and the following data are obtainable; but quantitatively they are too crude, because they ignore the essential feature of oblique reflection from M and N.

Omitting these equations, to be fully discussed in the next chapter, an example of the displacement and radial motion in a given experiment may be adduced; the former was fully 16 times less sensitive per fringe than the latter. The displacement is thus a coarse adjustment in comparison with the usual radial motion of the fringes and this is the distinct advantage of the present method for many purposes. It is like a scale division into smaller and larger parts, where the enumeration of small parts alone would be confusing or impossible. The ratio of the micrometer value of displacement and radial motion per fringe may be given any value since $dz/d\lambda \propto e$ and the lateral displacement may actually be more sensitive than the radial motion, when the grating plate is thin.

The sodium lines here make admirable cross-hairs and the ocular itself need have none. The conditions are the same in the second order and the coarser rings and spectrum lines are often easier to count.

34. Compensator.—It is not necessary, however, to use thin glass, for if a compensator is provided, *i.e.*, if the grating is on the common plane between two thicknesses of identical plane-parallel glass plates, one of which carries the grating, the ideal plane in question is provided. The ellipses in this case would be infinite in size and their displacements infinitely large. By partial compensation (compensator thinner) ellipses of any convenient size and rate of displacement may therefore be provided at pleasure. The following table gives some rough experimental data where z is the advance of the micrometer screw normal to the grating, *i.e.*, the displacement of the grating to move the center of fringes from the D to

TABLE 10.—Displacement of ellipses from the D to the b line, by moving the grating Δz cm. normal to itself. $i = 45°$, nearly. Grating: $e = .68$ cm., $D = .000351$ cm., $\mu = 1.53$ (estimated). Compensation shown by negative sign. Position z taken while the sodium line was the major axis.

Compensator thickness* $e' \times 10^2$	Position of grating z	Micrometer displacement $\Delta z \times 10^4$	No. of fringes D to b	Displacement per fringe $10^4 \times dz/dn$	Ellipses.	Side of compensator.
cm.	*cm.*	*cm.*		*cm.*		
−48	.05	30	12	2.5	Very large....	N
−44	.08	35	...	...	Very large....	N
−29	.12	45	...	...	Large.....	N
−10	.20	65	...	...	Mean.....	N
+48	.38	115	44	2.6	Very small...	M
−65	.00	10	4.5	2.3	Enormous....	N
± 0	...	70	28	2.5	Mean.....	None

*Compensator parallel to mirror, M or N, respectively.

the b lines of the spectrum, e' the thickness of the compensator placed parallel to the mirror M or N as stated.

Rotation of the compensator offers the usual easy method of adjustment. In the second order the first rings, on compensation, usually more than fill the field. This is of course eventually the case in the first order also. With very perfect compensation the ellipses are quite eccentric and the lines under the limiting conditions nearly vertical and straight. Hence their motion, partaking of the twofold character specified, is complicated but usually opposite in direction on the two sides of the center for the same micrometer displacement. The whole phenomenon may vanish within a half millimeter of play of the grating, passing from fine lines through enormous ellipses back into reversed fine lines, all nearly vertical.

The displacement of the grating by the micrometer screw is of the same order per fringe, no matter whether the ellipses are large or small, and in the last table it was about .00025 cm. per fringe. The displacement at the mirror would exceed this. The radial motion per fringe is of the order of wave-length. Naturally the position z of the grating changes parallel to itself linearly with the thickness e' of the compensator, supposing other conditions the same, so that p, z, and ds/dn all vary linearly with e' the thickness of the compensator.

The full equations for the amounts of displacement, etc., require an evaluation of $d\theta/dn$, which in turn must take into consideration that reflection from the mirrors can not in general be normal except for the one color instanced above. This investigation will have to be reserved for the next chapter.

CHAPTER V.

INTERFEROMETRY WITH THE AID OF A GRATING; THEORETICAL RESULTS. By Carl Barus.

Part I. Introduction.

35. Remarks on the phenomena.—In the earlier papers* I described certain of the interferences obtained when the oblique plate *gg*, fig. 18, of Michelson's adjustment, is replaced by a plane diffraction grating on ordinary plate glass. Some explanation of these is necessary here. In the figure *L* is the source of white light from a collimator. Such light is therefore parallel relative to a horizontal plane, but convergent relatively to a vertical plane. *M* and *N* are the usual silver mirrors. A telescope adjusted for parallel rays in the line *GE* must therefore show sharp white images of the slit. As the grating is usually slightly wedge-shaped, there will be (normally) four such images, two returned by *M* after reflection from the front (white) and rear face (yellowish) of the plate *gg*, and two due to *N*. There will also be two other, not quite achromatic, slit images from *N* or *M*, respectively, due to *double* diffraction before and after reflection. These will be treated below. In the direction *GD* there will thus be a corresponding number of diffraction spectra, more or less coincident in all their parts, and therefore adapted to interfere in pairs throughout their extent. If the two white and the two yellow images of the slit be put in coincidence and the mirrors *M* and *N* are adjusted for the respective *reduced* or virtual path difference zero, the interferences obtained are usually eccentric; *i.e.*, the centers of the interference ellipses are not in the field of view. The effective reflection in each of these cases takes place from the front and rear face of the grating at the same time. Hence the interference pattern includes the prism angle of the grating plate and is not centered. The air-paths of the component rays are here practically equal. In addition to the ellipses, this position also shows revolving linear interferences and (as a rule) a double set is in the field at once, consisting of equidistant, symmetrically oblique crossed lines, passing through horizontality in opposite directions together, when either mirror *M* or *N* is slightly displaced.

If either pair of the white and yellowish images of the slit be placed in coincidence when looking along *EG*, the interference pattern along *DG* is ring-shaped, usually quasi-elliptic and centered. The light returned by *M* and *N* is in this case reflected from the *same* face of the grating, either from the face carrying the grating or the other (unruled) face. The corresponding air-paths of the rays are in this case quite unequal, because the

* Am. Journ. of Science, xxx, 1910, pp. 161–171; Science, July 15, 1910, p. 92; and Phil. Mag., July, 1910, pp. 45–59.

short air-path is compensated by the path of the rays within the glass plate. Hence these adjustments are very different, *GM* being the long path in one instance, *GN* in the other instance. For the same motion of the micrometer screw, the fringes are displaced in opposite directions. In one adjustment there may be a single family of ellipses; in the other there may be two or even three families nearly in the field at once.

If the grating were cut on optical plate glass, the adjustment for equal air-path would probably be best. But with the grating cut as usual on ordinary plate, or in case of replica gratings on collodion or celluloid films, the adjustment for unequal paths is preferable. Here again one of the positions is much to be preferred to the other, owing to the occurrence of multiple slit images from one of the mirrors, as above specified. In fig. 19, for instance, where the grating face is to the rear, there are but two images, 1 and 2 from *M*, if the plate is slightly wedge-shaped; but from *N*, in

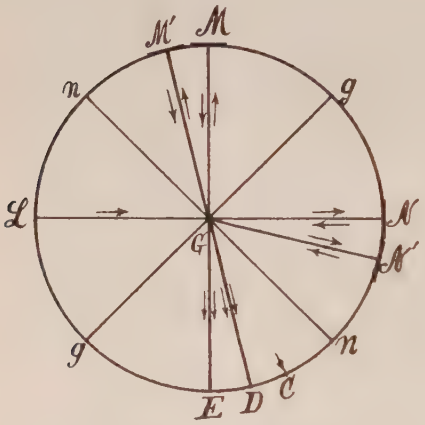

FIG. 18.—Diagram showing adjustments for interference.

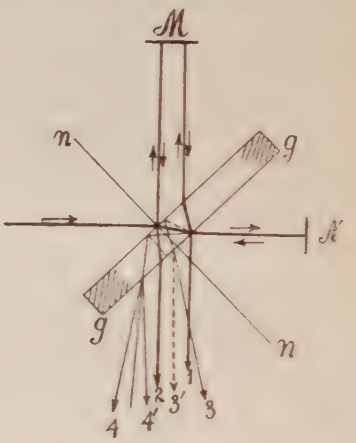

FIG. 19.—Diagram showing double diffraction.

addition to these two normal cases (not necessarily coinciding with 1 and 2), there are two other images 3′ and 4′ (3 and 4 are spectrum rays), resulting from double diffraction, with a deviation θ and angle of incidence I, respectively $\theta < I$ and $\theta > I$, in succession; or the reverse. As the compensation for color can not here be perfect, the two slit images obtained are very narrow, practically linear spectra, but they are strong enough to produce interferences like the normal images of the slits, with which they nearly agree in position. Other very faint slit images also occur, but they may be disregarded. The doubly-diffracted slit images are often useful in the adjustments for interference.

Among the normal slit images there are two, respectively white and yellowish, which are remote from secondary images. If these be placed in coincidence both horizontally and vertically along *EG*, fig. 18, the observation along *DG* through the telescope will show a magnificent display of black

apparently confocal ellipses, with their axes respectively horizontal and vertical, extending through the whole width of the spectrum, from red to violet, with the Fraunhofer lines simultaneously in focus. The vertical axes are not primarily dependent on diffraction and are therefore of about the same angular length throughout; the horizontal axes, however, increase with the magnitude of the diffraction, and hence these axes increase from violet to red, from the first to the second and higher orders of spectra, and in general as the grating space is smaller. It is not unusual to obtain circles in some parts of the spectrum, since ellipses which in one extreme case have long axes vertically, in the other extreme case have long axes horizontally. The interference figure occurs simultaneously in all orders of spectra, and it is interesting to note that, even in the chromatic slit images shown in fig. 19, needle-shaped vertical ellipses are quite apparent.

It is surprising that all these interferences may be obtained with replica or film gratings, though not of course so sharply as with ruled gratings, the ideal being an optical plate. With thin films two sets of interferences are liable to be in the field at once and I have yet to study these features from the practical point of view. If the film is mounted between two identical plates of glass, rigorously linear, vertical and movable interference fringes, as described* by my son and myself, may be obtained.

36. Cause of ellipses.—The slit at *L*, fig. 18, furnishes a divergent pencil of light due (at least) to its diffraction, the rays becoming parallel in a horizontal section after passing the strong lens of the collimator. But the vertical section of the issuing pencil is essentially convergent. Hence if such a pencil passes the grating the oblique rays relatively to the vertical plane pass through a greater thickness of glass than the horizontal rays. The interference pattern, if it occurs, is thus subject to a cause for contraction in the former case that is absent in the latter. Hence also the vertical axes of the ellipses are about the same in all orders of spectra. They tend to conform in their vertical symmetry to the regular type of circular ring-shaped figure as studied by Michelson and his associates and more recently by Feussner,† but in view of the slit the symmetry is cylindric.

On the other hand the obliquity in the horizontal direction, which is essential to successive interferences of rays, is furnished by the diffraction of the grating itself, as the deviation here increases from violet to red. In other words the interference which is latent or condensed in the normal white linear image of the slit is drawn out horizontally and displayed in the successive orders of spectra to right and left of it. The vertical and horizontal symmetry of ellipses thus follows totally different laws, the former of which have been thoroughly studied The present paper will therefore be devoted to phenomena in the horizontal direction only.

* Phil. Mag., *l.c.*

† See Professor Feussner's excellent summary in Winkelmann's Handbuch der Physik, vol. 6, 1906, p. 958 *et seq.*

At the center of ellipses the *reduced* path difference is zero; but it can not increase quite at the same rate toward red and violet. Neither does the refractive index of the glass admit of this symmetry. Hence the so-called ellipses are necessarily complicated ovals, but their resemblance to confocal ellipses is nevertheless so close that the term is admissible. This will appear in the data.

If either the mirror or the grating is displaced parallel to itself by the micrometer screw the interference figure *drifts* as a whole to the right or to the left, while the rings partake of the customary motion toward or from a center. The horizontal motion in such a case is of the nature of a coarse adjustment as compared with the radial motion, a state of things which is often advantageous—in other words, the large divisions of the scale are not lost; moreover the displacements may be used independently.

The two motions are coordinated, inasmuch as violet travels toward the center faster in a horizontal direction, *i.e.*, at a greater angular rate, than red. Hence the ellipses drift horizontally but not vertically. Naturally in the two positions specified above for ellipses, the fringes travel in opposite directions for the same motion of the micrometer screw. As the thickness of the grating is less the ellipses will tend to open into vertical curved lines, while their displacement is correspondingly increased. With the grating on a plate of glass about $e = .68$ cm. thick and having a grating space of about $D = .000351$ cm., at an angle of incidence of about $45°$, the displacement of the center of ellipses from the D to the E line of the spectrum corresponded to a displacement of the grating parallel to itself of about .006 cm. It makes no difference whether the grating side or the plane side of the plate is toward the light or which side of the grating is made the top. If the grating in question is stationary and the mirror N alone moves parallel to itself along the micrometer screw, a displacement of $N = .01$ cm. roughly moves the center of ellipses from D to E, as before. This displacement varies primarily with the thickness of the grating and its refraction. It does not depend on the grating constant. Thus the following data were obtained with film gratings on different thicknesses e of glass and different grating spaces D for the displacements N of the mirror at N, to move the ellipses from the D to the E line, as specified.

Glass grating, ruled.	$e = .68$ cm.	$\lambda/D = .168$	$N = .010$ cm.
Film on glass plate	$e = .57$	.352	.008
Film on glass plate	$e = .24$	.352	.003
Film between glass plates.	$\left\{ \begin{matrix} e = .48 \\ e' = .24 \end{matrix} \right\}$	.352	.003

Reduced linearly to $e = .68$ cm., the latter data would be $N' = .010$ and $N' = .009$, which are of the same order and as close as the diffuse interference patterns of film gratings permit. The large difference in dispersion, together with some differences in the glass, has produced no discernible effect.

An interesting case is the film grating between two *equally* thick plates of glass. With this, in addition to the elliptical interferences above described, a pattern of vertical interferences identical with those discussed in a preceding paper* was obtained. These are linear, persistently vertical fringes extending throughout the spectrum and within the field of view, nearly equidistant and of all colors. Their distances apart, however, may now be passed *through* infinity when the virtual air-space passes through zero; and for micrometer displacements of mirror in a given direction, the motion of fringes is in opposite directions on different sides of the null position of the mirror. I have not been able, however, to make them as strong and sharp as they were obtained in the paper specified.

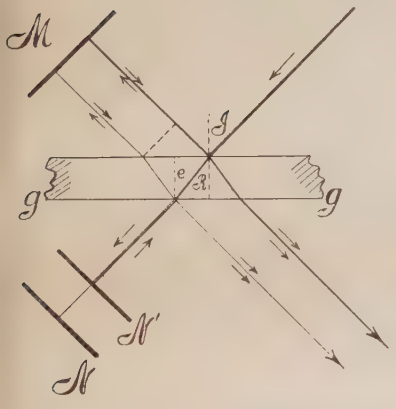

FIG. 20.—Diagram showing displacement of mirror N.

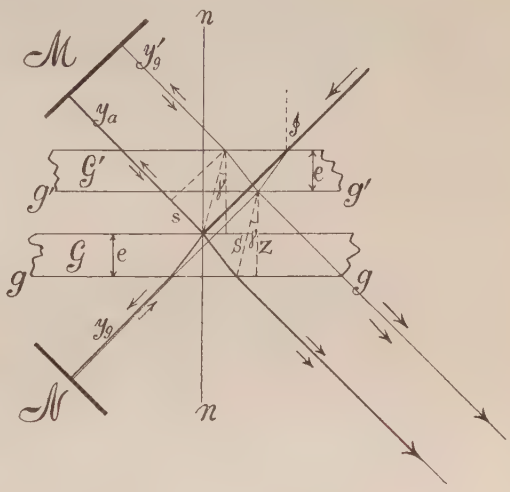

FIG. 21.—Diagram showing displacement of grating G.

37. The three principal adjustments for interference.—To compute the extreme adjustments of the grating when the mirror N is moved, fig. 20 may be consulted. Let y_g be the air-path on the glass side, whereas y_a is the air-path on the other, e the thickness of the grating and μ its index of refraction for a given color. Then for the simplest case of interferences, in the first position N of the mirror, if I is the normal angle of incidence and R the normal angle of refraction for a given color,

$$y_g + e\mu/\cos R = y_a$$

for equal paths. Similarly in the second position of the mirror

$$y_a' = y_g' + e\mu/\cos R$$

Hence if the displacement at the mirror N be N,

$$N = y_a - y_g = 2e\mu/\cos R + y_g' - y_a$$

The figure shows

$$y_a - y_g' = 2e \tan R \sin I$$

whence

$$N = 2e\mu \cos R$$

* Phil. Mag., *l.c.*

The measurement of this quantity showed about 1.88 cm. The computed value would be $2\times.68\times1.53\times.71=1.84$ cm. The difference is due to the wedge-shaped glass which requires a readjustment of the grating for the two positions.

The corresponding extreme adjustments, when the grating gg instead of a mirror N is moved over a distance z, are given in fig. 21. The mirrors M and N are stationary. It is first necessary to compute γ, the angle between the displacement z and the side S in the figure, or

$$\tan\gamma=\tan I-2e\tan R/z$$

so that the semi-air-path difference of rays to the mirror M becomes

$$s=y_a-y_g'=z(\cos I-\sin I\tan\gamma)$$

We may now write, with the same notation as before, for the extreme position of the grating, G and G', respectively,

$$y_g+e\mu/\cos R=y_a \qquad y_a'=y_g'+e\mu/\cos R$$

or

$$z/\cos I=2e\mu/\cos R-z(\cos I-\sin I\tan\gamma)$$

whence

$$z(1/\cos I+\cos I-\sin I\tan\gamma)=2e\mu/\cos R$$

If $e=0$, it follows that $z=0$, or $\gamma=I$, since the parenthesis by the above equation is not zero. There is only one position. The angle γ may now be eliminated by inserting $\tan\gamma$, whence

$$z=\frac{e\mu}{\cos I\cos R}-e\tan I\tan R$$

The observed value of z for the two positions was about 1.3 cm. The computed value for $I=45°$ is the same.

On the other hand, when reflection takes place from the same face of the grating, while the latter is displaced z cm. parallel to itself, the relations of y and z for normal incidence at an angle I are obviously

$$y\cos I=z$$

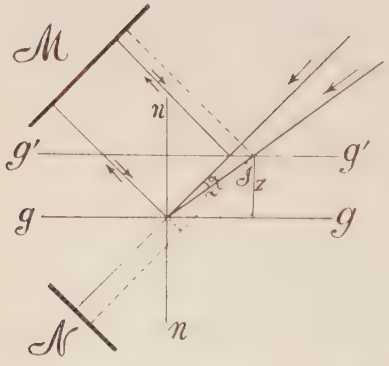

FIG. 22.—Diagram showing displacement of grating for deviated rays.

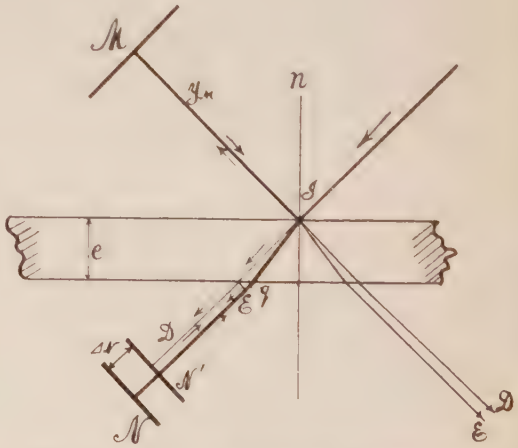

FIG. 23.—Diagram showing displacement of mirror N for different colors.

For an oblique incidence i, where $i-I=\alpha$, a small angle, the equation is more complicated. Fig. 22, for $e=0$, g and g' being the planes of the grating, shows that in this case

$$y=z(1+2\frac{\sin\alpha}{\cos i}\sin I)/\cos I$$

or, approximately for small α

$$y=z(1+2\sin\alpha\tan I)/\cos I$$

This equation is also true for a grating of thickness e, whose faces are plane parallel, for the direction of the air-rays in this case remains unchanged.

Finally, a distinction is necessary between the path difference $2y$ and the motion of the opaque mirror $2N$, which is equivalent to it, since the light is not monochromatic. This motion $2N$ is oblique to the grating and if the rays *differ in color* further consideration is needed. In fig. 23 for the simplest type of interferences, in which the glass-path difference is $e\mu/\cos R$ and for normal incidence at an angle I, let the upper ray y_M and the grating be fixed. The mirror moving over the distance ΔN changes the zero of path difference from any color of index of refraction μ_D to another of index μ_E, while y_{ND} passes to y_{NE}. Then

$$y_M=y_{ND}+e\mu_D/\cos R_D=y_{ND}+e\mu_E/\cos R_E+\Delta N$$

Hence

$$\Delta N=-e\sin I\,(\tan R_D-\tan R_E)+e\left(\frac{\mu_D}{\cos R_D}-\frac{\mu_E}{\cos R_E}\right)$$

or

$$\Delta N=e(\mu_D\cos R_D-\mu_E\cos R_E)$$

This difference belongs to all rays of the same color difference, or for two interpenetrating pencils.

If reflection takes place from the lower face the rays are somewhat different, but the result is the same. If the plate of the grating is a wedge of small angle φ, the normal rays will leave it on one side at an angle $I+\delta$ where δ is the deviation

$$\delta=(\mu-1)\varphi$$

The mirror N will also be inclined at an angle $I+\delta$, to return these rays normally. We may disregard $d\delta=\varphi d\mu$, if φ is small.

Part II. Direct Cases of Interference. Diffraction Antecedent.

38. Diffraction before reflection.—If in fig. 18 the diffracted beams (spectra) be returned by the mirrors M' and N' to be reflected at the grating, interference must also be producible along GD. Again there will be three primary cases: if reflection takes place from both faces of the grating at once, the air-paths must be nearly equal, the grating itself acting as a compensator. The interference pattern is ring-shaped, but as usual very eccentric. If the reflection of both component beams takes place from the

same face of the grating, the interference pattern is elliptical and centered and the air-paths are unequal. The case is then similar to the preceding §§1, 2; but there is no direct or normal image of the slit, as M and N are absent. In its place there may be *chromatic* images of the slit (linear spectra) at C due to the *double* diffraction of each component beam in a positive and negative direction successively. But these chromatic images are nevertheless sharp enough to complete the adjustments for interference by placing the slit images in coincidence. It is not usually necessary to put the spectrum lines into coincidence separately (both horizontally and vertically), as was originally done, both spectra being observed. Again along GE, fig. 18, approximately, there must be two successive positive diffractions of each component beam, which would correspond closely to the second order of diffraction. The advantage of this adjustment lies in the fact that there are but two slit images effectively returned by M' and N', and hence these interferences were at first believed to be stronger and more isolated. As a consequence I used this method in most of my early experiments, before finding the equally good adjustment described in the preceding section.

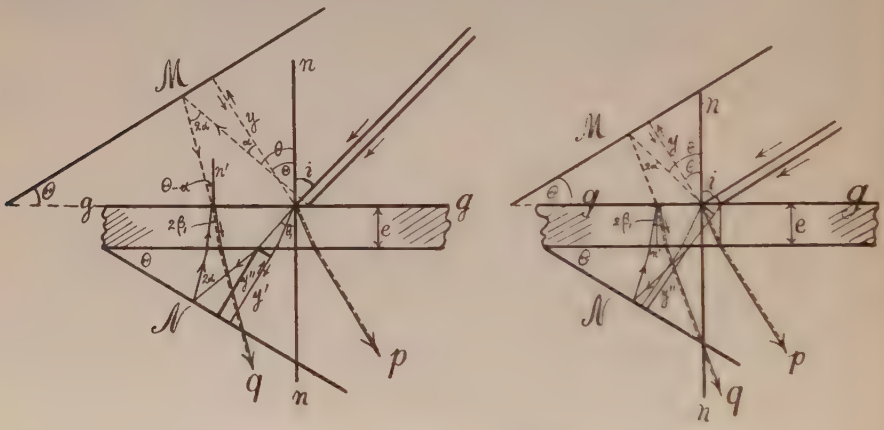

FIG. 24.—Diagrams showing interferences of diffracted rays, case θ normal to mirrors M and N; case θ oblique to mirrors. Double incidence.

39. Elementary theory.—To find the path differences figs. 24 and 25 may be consulted. In both the grating face is shown at gg, the glass plate being e cm. in thickness below it, and n is the normal to the grating. M and N are the two opaque mirrors, each at an angle Θ to the face of the grating. Light is incident on the right at an angle i nearly 45°. In both figures the rays y_m and y_n (air-paths) diffracted at an angle θ in air, are reflected normally from the mirrors M and N respectively and issue toward p for interference. The rays y_n (primed in figure) pass through glass. Both figures also contain two component rays diffracted at an angle θ in air, where $\theta - \Theta = \alpha$, and reflected obliquely at the mirrors M and N, thus inclosing an angle 2α in air and $2\beta_1$ in glass, and issuing toward q. These

component rays are drawn in full and dotted, respectively. In fig. 24 there are two incident rays for a single emergent ray, in fig. 25 a single incident ray for two emergent rays interfering in the telescope. The treatment of the two cases is different in detail; but as the results must be the same, they corroborate each other.

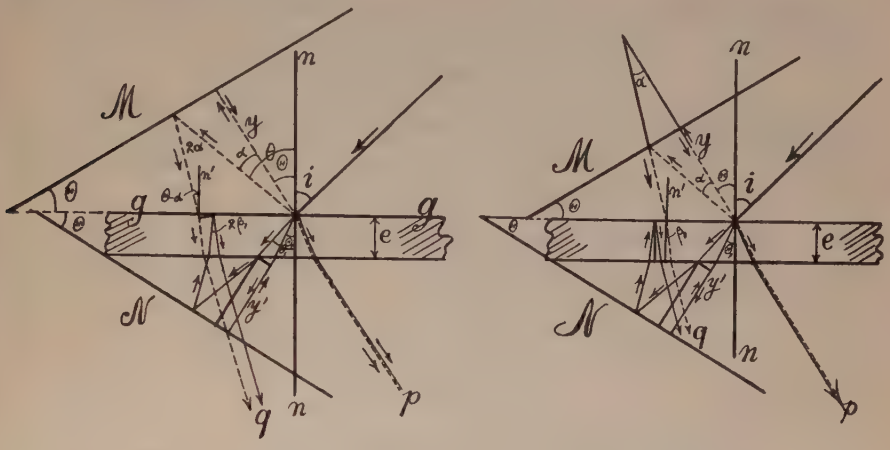

FIG. 25.—Diagrams showing interferences of diffracted rays, case θ normal to mirrors M and N; case θ oblique to mirrors. Single incidence.

The notation used is as follows: Let e be the normal thickness of the grating, e' the effective thickness of the compensator when used. Let distance measured normal to the mirror be termed y, y_n and y_m being the component air-paths passing on the glass and on the air side of the grating gg, so that $y_m > y_n$. Let $y = y_m - y_n$ be the air-path difference. Similarly let distances z be measured normal to the grating, so that z may refer to displacements of the grating.

Let i be the angle of incidence, r the angle of refraction, and μ_r the index of refraction for the given color, whence $\sin i = \mu_r \sin r$. Similarly if θ is the angle of diffraction in air of the y rays and θ_1 the corresponding angle in glass,

$$\sin \theta = \mu_\Theta \sin \theta_1 \qquad (1)$$

and if θ is the angle of diffraction of any oblique ray in air and θ_1 the corresponding angle in glass

$$\sin \theta = \sin (\theta + \alpha) = \mu_\theta \sin \theta_1 \qquad (2)$$

I have here supposed that $\theta > \Theta$, so that $\alpha = \theta - \Theta$ is the deviation of the oblique ray from the normal ray in air. Finally, the second reflection of the oblique ray necessarily introduces the angle of refraction within the glass such that

$$\sin (\theta - \alpha) = \mu_\theta \sin \beta_1 \qquad (3)$$

If D is the grating space we have, moreover,

$$\sin i - \sin \theta = \lambda_\theta / D \quad \text{and} \quad \sin i - \sin \Theta = \lambda_\Theta / D \qquad (4)$$

For a displacement, z, of the grating, or an equivalent displacement, y, of either mirror, the path difference produced in case of the oblique ray will be

$$2y/\cos\alpha = 2z\,(\cos(i-\theta)+\sin(i-\theta))/\cos\alpha\cos i \qquad (5)$$

For normal rays $\cos\alpha = 1$. If as in paragraph 1 the reflection is antecedent

$$i=\theta \qquad 2y/\cos\alpha = 2z/\cos\alpha\cos i$$

40. Equations for the present case.—From a solution of the triangles, preferably in the case for single incidence, as in fig. 25, the air-path of the upper oblique component ray at a deviation α is

$$2y_m\cos\theta/\cos(\theta-\alpha)$$

The air-path of the lower component ray is

$$2\cos\theta\,(y_n - e\sin\theta(\tan\theta_1-\tan\theta_1))/\cos(\theta-\alpha)$$

The optic path of this (lower) ray in glass as far as the final wave front in glass at β_1 is

$$\mu_\theta e(1/\cos\theta_1+1/\cos\beta_1)$$

The optic path of the upper ray as far as the same wave front in glass is

$$\mu_\theta\sin\beta_1\left\{2\frac{\sin\alpha}{\cos(\theta-\alpha)}(y_m-y_n-e\sin\theta(\tan\theta_1-\tan\theta_1))-\right.$$
$$\left.e(\tan\theta_1-\tan\beta_1)\right\} \qquad (6)$$

Hence the path difference between the lower and the upper ray as far as the final wave front is, on collecting similar terms,

$$2(y_n-y_m)\left(\frac{\cos\theta}{\cos(\theta-\alpha)}+\frac{\sin\alpha\sin(\theta-\alpha)}{\cos(\theta-\alpha)}\right)+\mu_\theta e\left(\frac{1}{\cos\theta_1}+\frac{1}{\cos\beta_1}\right)$$
$$+e\sin(\theta-\alpha)(\tan\theta_1-\tan\beta_1)-\frac{2e}{\cos(\theta-\alpha)}(\tan\theta_1-\tan\theta_1)$$
$$(\sin\theta\cos\theta+\sin\alpha\sin\theta\sin(\theta-\alpha)) \qquad (7)$$

Before reducing further, one may remark that if incident and emergent rays were coincident, the quantity given under (6) would be zero. Hence if this particular $y_n-y_m=y_1$, it follows that

$$2y_1 = 2e\sin\theta(\tan\theta_1-\tan\theta_1)-\frac{e\cos(\theta-\alpha)}{\sin\alpha}(\tan\theta_1-\tan\beta_1)$$

Hence the particular path difference for this case would be

$$\mu_\theta e(1/\cos\theta_1+1/\cos\beta_1)-e\cos\theta(\tan\theta_1-\tan\beta_1)/\cos\alpha$$

which becomes indeterminate when $\alpha=0$.

To return to path differences, equation (7), the coefficients of $y_m-y_n=y$ (where y is positive) and of e may now be brought together, as far as

possible. If the path difference corresponds to n wave-lengths λ_θ we may write after final reduction

$$n\lambda_\theta = -2y\cos\alpha + 2e\mu_\Theta\cos\alpha(1/\cos\theta_1 - \cos(\theta_1-\theta_1)/\cos\theta_1) + e\mu_\theta(1+\cos(\theta_1-\beta_1))/\cos\theta_1 \qquad (8)$$

which is the full equation in question for a dark fringe. It is unfortunately very cumbersome and for this reason fails to answer many questions perspicuously. It will be used below in another form.

The equation refers primarily to the horizontal axes of the ellipses only, as e increases vertically above and below this line. The equation may be abbreviated

$$n\lambda_\theta = -2y\cos\alpha + eZ_\Theta + eZ_\theta$$

where Z_Θ and Z_θ are the coefficients of e in the equation. In case of a parallel compensator of thickness e' we may therefore write, y being the path difference in air,

$$n\lambda_\theta = -2y\cos\alpha + (e-e')(Z_\Theta - Z_\theta) \qquad (9)$$

If $e=e'$, *i.e.*, for an infinitely thin plate $e=0$,

$$n\lambda_\theta = 2y\cos\alpha \qquad (10)$$

Again for normal rays y_m and y_n, $\alpha=0$ and $\theta_1=\theta_1=\beta_1$. Hence

$$n\lambda_\Theta = -2y + 2e\mu_\Theta/\cos\theta_1 \qquad (11)$$

and for a parallel compensator of thickness e'

$$n\lambda_\Theta = -2y + 2(e-e')\mu_\Theta/\cos\theta_1 \qquad (12)$$

If $\mu_\Theta = 1 = \mu_\theta$, equation (8) reduces to

$$n\lambda = 2\cos\alpha(y + e/\cos\theta),$$

clearly identical with the case $e=0$ for a different y.

TABLE 11.—Table for path difference, $-2(y_m - y_n)\cos\alpha + eZ_\Theta + eZ_\theta = -2y\cos\alpha + eZ$. Light crown glass. E rays normal to mirrors. Grating space, D, = .000 351 2 cm. $I=45°$. $\theta=33°\ 51'$.

Spectrum lines =	B	D	E	F	G
$\lambda\times10^8$ =	68.7	58.93	52.70	48.61	43.08 cm.
μ_θ =	1.5118	1.5153	1.5186	1.5214	1.5267
θ =	30° 46′	32° 38′	33° 51′	34° 40′	35° 46′
θ_1 =	19° 47′	20° 51′	21° 31′	21° 57′	22° 30′
α =	− 3° 5′	− 1° 13′	0° 0′	0° 49′	1° 55′
$\theta_1-\theta_1$ =	− 1° 44′	− 0° 40′	0° 0′	0° 26′	0° 59′
β_1 =	23° 25′	22° 17′	21° 30′	21° 13′	20° 49′
$\theta_1-\beta_1$ =	− 3° 38′	− 1° 26′	0° 0′	0° 44′	1° 41′
$2\cos\alpha$ =	1.9970	1.9996	2.0000	1.9998	1.9996 cm.
Z_Θ =	.0383	.0176	.0000	− .0095	− .0219 cm.
Z_θ =	3.2100	3.2404	3.2648	3.2805	3.3038 cm.
Path difference,* $n\lambda$ =	−1.9970y − 1.9996y − 2.0000y − 1.9998y − 1.9996y +3.2483e + 3.2580e + 3.2648e + 3.2710e + 3.2819e				cm.
Path difference $2y=3.2648$ cm. $e=1$ cm. $2\Delta y_0$ =	− .0116	− .0062	± .0000	+ .0059	+ .0177 cm.
The same for $e=.68$ cm. $2\Delta y_0$ =	− .0079	− .0042	± .0	+ .0040	+ .0120 cm.
$2\Delta N_0$ =	− .0107	− .0056	± .0	+ .0049	+ .0156 cm.

* The purpose of these data is merely to elucidate the equations. ΔN refers to the displacement of either opaque mirror, M or N.

In view of the complicated nature of equation (8), I have computed path differences for a typical case of light crown glass,* as shown in table 11, for the Fraunhofer lines B, D, E, F, G, supposing the E ray to be normal ($\alpha = 0$). The table is particularly drawn up to indicate the relative value of the functions Z_Θ and Z_θ. It will be seen that $Z = Z_\Theta + Z_\theta$ in terms of λ, is a curve of regular decrease having no tendency to assume maximum or minimum values within the range of λ, whereas $y \cos \alpha$ passes through a flat maximum for $\alpha = 0$. This is shown in the curves of fig. 26.

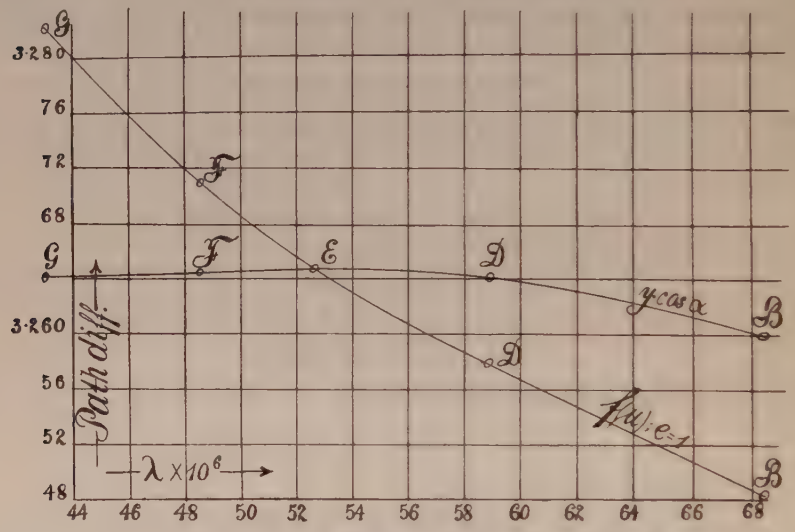

FIG. 26.—Chart showing path difference in centimeters (to be annulled at E line), in terms of wave-length.

The path difference, which is the difference of the ordinates of these curves, thus passes through zero for a definite value of e and y, and this would at first sight seem to correspond to the center of ellipses. That it *does not* so correspond will be particularly brought out in the next section, but here this tentative surmise may be temporarily admitted to simplify the descriptions. It is obvious that for a given e the value of y (air-path difference) which makes the total path difference zero, varies with the wave-length, hence on increasing y continuously the ellipses must pass through the spectrum. It is also obvious that, if the grating is reversed, the path difference will change sign, *caet. par.*, and the ellipses will move in a contrary direction, for the same displacements y of the micrometer screw, at the mirror M or N, respectively.

If $e = 1$ cm. and $y = 3.2648$ cm., the path difference will be zero for the E ray and (barring further investigation as just stated) one is inclined to place the center of ellipses there. The table shows the residual path differences in the red and blue parts of the spectrum. Fig. 27 has been constructed for

* Taken from Kohlrausch's Practical Physics, 11th edition, 1910, p. 712.

the same condition. It follows, therefore, that in proportion as e is smaller y will be smaller for extinction at the E line. Hence their differences will be smaller and the number of wave-lengths corresponding to the path difference of the Fraunhofer lines will be smaller. In other words, the major axes of the ellipses will be larger. Thus the ellipses will be larger as e is smaller, the limit of enormous ellipses being reached for $e=0$ or $e=e'$ of the compensator.

This result may be obtained to better advantage by reconstructing equation (8), and making the path difference equal to zero for the normal ray. This determines

$$y=e\mu_\Theta/\cos\theta \tag{13}$$

in terms of e, and the path difference now becomes

$$n\lambda_\theta=e\{-\mu_\Theta\cos\alpha\cos(\theta_1-\theta_1)+\mu_\theta(1+\cos(\theta_1-\beta_1))\}/\cos\theta_1 \tag{14}$$

This is zero for $\alpha=0$, $\theta_1=\beta_1=\theta_1$ at the E line. The other values are given in the table in centimeters and in wave-lengths. Path difference diminishes as e; the horizontal axes of the ellipses increase with e. If observations are made very near the E line (normal ray) the following approximate form may be used:

$$n\lambda_\theta=(e\mu_\Theta/\cos\theta_1)\{2(\mu_\theta/\mu_\Theta-1)+\alpha^2+(\theta_1-\theta_1)^2-\mu_\theta(\theta_1-\beta_1)^2/2\mu_\Theta\} \tag{15}$$

but this rapidly becomes insufficient unless $\theta_1-\theta_1$ and $\theta_1-\beta_1$ are very small.

41. Interferometer.—If in equation (8), y alone is variable with the order of fringe n while α, θ, θ, θ_1, θ_1, β_1, e, λ, μ, are all constant (*i.e.*, if the number of fringes n cross a given fixed spectrum line like the D line, when the mirror is displaced over a distance y) it appears that

$$\frac{dy}{dn}=\frac{\lambda_\theta}{2\cos\alpha} \tag{16}$$

where α refers to the deviation of λ_θ from λ_Θ normal to the mirror. If $\alpha=0$, $dy/dn=0$, the limiting sensitiveness of the apparatus, which appears for the case of normal rays.

If the grating is displaced along z

$$\frac{dz}{dn}=\frac{\lambda_\theta}{2\cos\alpha}\,\frac{\cos i}{\cos(i-\theta)+\sin(i-\theta)} \tag{17}$$

where $\cos\alpha=1$ for normal rays. In both cases the displacement per fringe dy/dn and dz/dn vary with the wave-length. Hence if the ellipses are nearly symmetrical on both sides of the center, *i.e.*, if the red and violet sides of the periphery are nearly the same, or the fringes nearly equidistant, the smaller wave-length will move faster than the larger for a given displacement of mirror. In other words, the violet side will pass over a whole fringe before the red and consequently the ellipses, as a whole, must drift in

the direction in which violet moves. It is at first quite puzzling to observe the motion of ellipses as a whole in a direction opposed to the motion of the more reddish fringes when these are alone in the field.

42. Discrepancy of the table.—The data of table 1 are computed supposing that the path difference zero corresponds to the center of ellipses. This assumption has been admitted for discussion only and the inferences drawn are qualitatively correct. Quantitatively, however, the displacement of about $\Delta N = .003$ cm. should move the center of ellipses from the D to the E line of the spectrum, whereas observations show that a displacement of either opaque mirror of about $\Delta N = .01$ cm. is necessary for this purpose; *i.e.*, over three times as much displacement as has been computed. The equation can not be incorrect; hence the assumption that the center of ellipses corresponds to the path difference zero is not vouched for and must be particularly examined. This may be done to greater advantage in connection with the next section, where the conditions are throughout simpler, but the data are of the same order of value.

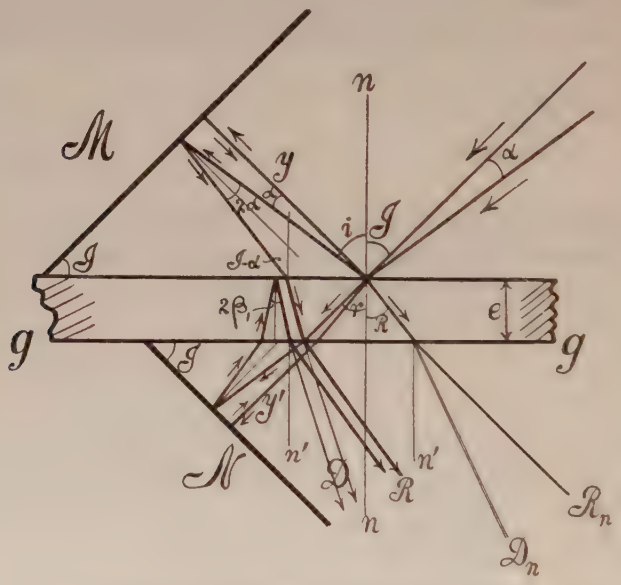

FIG. 27.—Diagram showing interferences of reflected rays, subsequently diffracted. Case I, normal to mirrors; case $i = I + \alpha$ oblique to mirrors. Rays R refracted, D diffracted.

PART III. DIRECT CASE; REFLECTION ANTECEDENT.

43. Equations for this case.—If reflection at the opaque mirrors takes place before diffraction at the grating, the form of the equations and their mode of derivation are similar to the case of paragraph 40, but the variables contained are essentially different. In this case the deviation from the

normal ray is due not to diffraction but to the angle of incidence, and the equations are derived for homogeneous light of wave-length λ and index of refraction μ.

In fig. 27 let $y_n = y'$ and $y_m = y$ be the air-paths of the component rays, the former first passing through the glass plate of thickness e. Let the angle of incidence of the ray be I, so that y_m and y_n are returned normally from the mirrors M and N, respectively, these being also at an angle I to the plane of the grating. Let i be the angle of incidence of an oblique ray, whose deviation from the normal is $i - I = a$. Let R, r, and β_1 be angles of refraction such that

$$\sin i = \sin (I+a) = \mu \sin r \qquad \sin I = \mu \sin R \qquad \sin (I-a) = \mu \sin \beta_1 \quad (18)$$

The face of the grating is here supposed to be away from the incident ray, as shown at gg in the figure.

TABLE 12.—Path difference, $-2(y_m - y_n)\cos a + eZ_1 - eZ_2 + eZ_3$. Light crown glass. $a = 3°$ throughout. Grating space .000351 cm. $I = 45°$. $e = 1$ cm.

Spectrum lines	B	D	E	F	G
$\lambda \times 10^6 =$	68.7	58.93	52.70	48.61	43.08 cm.
$\mu =$	1.5118	1.5153	1.5186	1.5214	1.5267
$R =$	27° 53′	27° 49′	27° 45′	27° 42′	27° 35′
$r =$	29° 26′	29° 22′	29° 18′	29° 14′	29° 8′
$\beta_1 =$	26° 16′	26° 12′	26° 8′	26° 5′	26° 0′
$a =$	3° 0′	3° 0′	3° 0′	3° 0′	3° 0′
$r - R =$	1° 33′	1° 33′	1° 33′	1° 33′	1° 33′
$r - \beta_1 =$	3° 10′	3° 10′	3° 10′	3° 9′	3° 8′
$Z_1 =$	3.4160	3.4218	3.4272	3.4318	3.4403 cm.
$Z_2 =$	656	714	767	808	896 cm.
$Z_3 =$	689	647	799	841	928 cm.
Path difference, $a = 3°$, $e = 1$ cm., $y = 1$ cm. $n\lambda =$	−1.9992	−1.9992	−1.9992	−1.9992	−1.9992
	+3.4193	+3.4252	+3.4304	+3.4352	+3.4436
If path difference is annulled at E line, $a = 3°$, $e = 1$ cm. $2\Delta y_0 =$	− .0111	− .0052	±.0	+ .0048	+ .0132
The same, if $a = 0°$, $e = 1$ cm. $2\Delta y_0 =$	− .0111	− .0052	±.0	+ .0048	+ .0132

The data are merely intended to elucidate the equations.
The values Z are nearly equal. So also the cases for $a = 3°$ and $a = 0°$.

Fig. 28 has been added to accentuate the symmetrical conditions when a compensator parallel to the grating and of the same thickness is employed.

Then it follows as in paragraph 40, *mutatis mutandis*, that the path difference is (if $y = y_m - y_n$)

$$n\lambda = -2y\cos a + \mu e \left\{ \frac{2\cos a}{\cos R} - \frac{2\cos a \cos (r-R)}{\cos r} + \frac{1+\cos (r-\beta_1)}{\cos r} \right\} \quad (19)$$
$$= -2y\cos a + e(Z_1 - Z_2 + Z_3)$$

where n is the order of interference (whole number). This equation is intrinsically simpler than equation (8) since $\mu_r = \mu_R$, as already stated, and since α is constant for all colors, or all values of μ and λ, in question. R and r replace θ_1 and θ_1.

In most respects the discussion of equation (19) is similar to equation (8) and may be omitted in favor of the special interpretations presently to be given. If $\mu = 1$, equation (19) like equation (8) reduces to the case corresponding to $e = 0$, with a different y normal to the grating.

All the colors are superposed in the direct image of the slit, R_n and R in fig. 27, seen in the telescope, and the slit is therefore white. This shows

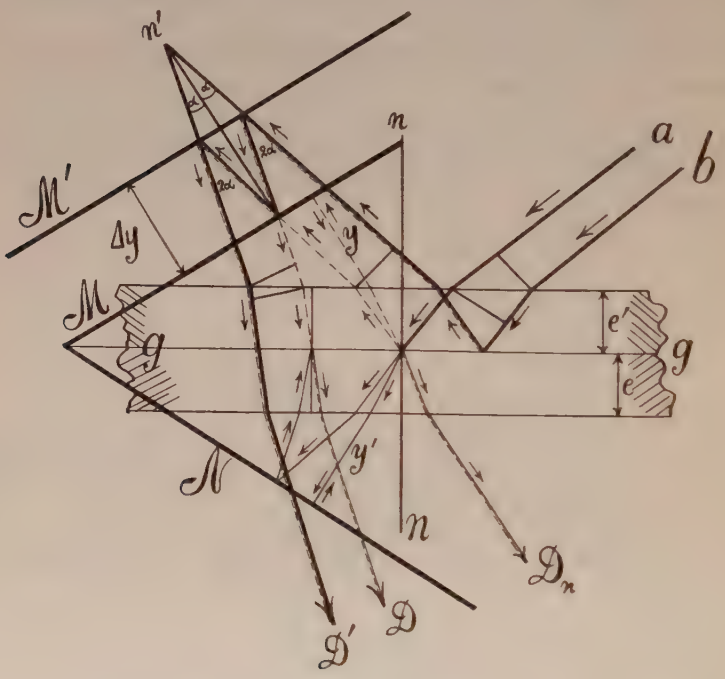

FIG. 28.—Diagram showing symmetrical interference for compensated grating, *gg*. Rays oblique to mirror.

also that prismatic deviation due to the plate of the grating (wedge) is inappreciable. The colors appear, however, when the light of the slit is analyzed by the grating in the successive diffraction spectra, D_n or D, respectively. In equation (19) μ is a function of λ and hence of the deviation θ produced by the grating, since $\sin(I-\alpha) - \sin\theta = \lambda/D$.

The values of equation (19) for successive Fraunhofer lines and for $\alpha = 3°$, have been computed in table 12 for the same glass treated in table 11, the data being similar and in fact of about the same order of value. The feature of this table is the occurrence of nearly constant values $\alpha = i - I$,

$r-R$ and $r-\beta_1$, throughout the visible spectrum. Hence if the following abbreviations be used

$$A=\cos\alpha=.9986 \qquad B=\cos(r-R)=.9996 \qquad C=1+\cos(r-\beta_1)=1.9984$$

A, B, C are practically functions of α only and do not vary with color or λ. Furthermore, if the path difference is annulled, at the E line for instance, for the normal ray, since $r=\beta_1=R$, $\alpha=0$, so that $R=R_E$ is the normal angle of refraction,

$$0=-y+2\mu e/\cos R_E$$

and equation (19) reduces to

$$n\lambda=2eA(\mu/\cos R-\mu\cos R_E)+e(C-2AB)\mu/\cos r \qquad (20)$$

where $2eA$ and $e(C-2AB)$ are nearly independent of λ and the last quantity is relatively small. The two terms of this equation for $e=1$ cm. show about the following variation:

TABLE 13.

B	D	E	F	G
−.0111	−.0052	.0	+.0048	.0132
−.000009	−.000004	.0	+.000005	.000013

Hence for deviations even larger than $\alpha=3°$, the path difference does not differ practically from the path difference for the normal ray. Thus it follows that the equation

$$n\lambda=-2y+2e\mu/\cos R \qquad (21)$$

is a sufficient approximation for such purposes as are here in view.

Finally, for $e=.68$ cm. (the actual thickness of the plate of the grating), y and N, the semi-path difference and the displacement of the opaque mirror, will be

TABLE 14.

	B	D	E	F	G
y_0 =	1.1630	1.1650	1.1668	1.1686	1.1730
Δy_0 =	−.0038	−.0018	.0	+.0016	+.0045
δN_0 =	+.0014	+.0007	.0	−.0005	−.0018
ΔN_0 =	−.0052	−.0025	.0	+.0021	+.0063

where δN_0 is the color correction of Δy_0 and $\Delta N_0=\Delta y_0-\delta N_0$ determines the corresponding displacements of the opaque mirror; or more briefly

$$N_0=y_0-e\mu\tan R\sin R=2e\mu\cos R \qquad (22)$$

The data actually found were

	C	D	E	F
ΔN_0 =	−.0148	−.0093	.0	+.0057

These results are again from 2 to 4 times larger than the computed values. True the glass on which the grating was cut is not identical with the light crown glass of the tables; but nevertheless a discrepancy so large and irregular is out of the question. It is necessary to conclude therefore that here, as in paragraph 42, the assumption of a total path difference zero for the center of ellipses is not true. In other words the equality of air-path difference and glass-path does not correspond to the centers in question. It is now in place to examine this result in detail.

44. Divergence per fringe.—The approximate sufficiency of the equation

$$n\lambda = 2e\mu/\cos R - 2y = 2e\mu \cos R - 2N \tag{23}$$

makes it easy to obtain certain important derivatives among which $d\theta/dn$, where θ is the angle of diffraction corresponding to the angle of incidence I and n the order of interference, is prominent.

If e and y are constant and if n, λ, μ and R are variable, the differential coefficients may be reduced successively by the following fundamental equation, D being the grating space, μ and r corresponding to wave-length λ and angle of diffraction θ.

$$dR = -\tan R\, d\mu/\mu \tag{24}$$

$$d\lambda = -D \cos\theta \cdot d\theta \tag{25}$$

$$d\mu/\mu = -ad\lambda/\lambda \tag{26}$$

where, as a first approximation, $a = .015$, is an experimental correction, interpolated for the given glass. Incorporating these equations it is found that

$$\frac{d\theta}{dn} = \frac{\lambda^2}{2D\cos\theta} \cdot \frac{\cos R}{e\mu - y\cos R + ae\mu(1-\tan^2 R)} \tag{27}$$

If the path difference $n\lambda$ is annulled

$$\frac{d\theta_0}{dn} = \frac{\lambda^2}{2D\cos\theta} \cdot \frac{\cos R}{ae\mu(1-\tan^2 R)} \tag{28}$$

which is the deviation per fringe, *supposedly* referred to the center of ellipses.

These equations indicate the nature of the dependence of the horizontal axes of ellipses on $1/D$ (hence also on the order of the spectrum), $1/e$, $1/\mu$, and $1/a$, where the meaning of a, here apparently an important variable, is given in equation (26). If instead of the path difference y the displacement N of either opaque mirror is primarily considered (necessarily the case in practice), the factor $(1-\tan^2 R)$ vanishes.

Table 15 contains a survey of data for equations (27) and (28). The results for $d\theta_0/dn$ would be plausible, as to order of values. The data for $d\theta/dn$, however, are again necessarily in error, as already instanced above, paragraph 42. They do not show the maximum at e and the $\lambda-$ effect is overwhelmingly large.

TABLE 15.—Values of $d\theta/dn$ and displacements N. $e = .68$ cm. N_0 and y_0, etc. refer to centers of ellipses.

Spectrum line	B	D	E	F	G
Equation 28.....$d\theta_0/dn =$	1′ 27″	1′ 5″	53″	46″	35″
27.....$d\theta/dn =$	3′ 4″	1′ 52″	1′ 20″	59″	38″
31.....$d\theta/dn =$	−6′ 53″	−10′ 38″	∞	+8′ 47″	+3′ 51″
$-\frac{d\mu}{d\lambda} =$	281	445	622	793	1140
33.....$d\theta/dn =$	−1′ 54″	−1′ 50″	∞	+2′ 21″	+ 40″
34.....$d\theta/dn =$	−1′ 44″	−1′ 44″	∞	+2′ 11″	+ 36″
35.....$y_0 =$	1.1779	1.1811	1.1921	1.1981	1.2090
$\Delta y_0 =$	−.0142	−.0110	±.0	+.0060	+.0169
$N_0 =$	.9235	.9274	.9391	.9456	.9578
$\Delta N_0 =$	−.0156	−.0117	±.0	+.0065	+.0187
(observed) $\Delta N_0 =$	−.0153	−.0098	±.0	+.0057	....
34*.....$d\theta/dn =$	....	−1′ 54″	∞	2′ 21″	48″

Since equation (27) is clearly inapplicable, giving neither maxima nor counting the fringes, it follows that in this equation $y > e\mu/\cos R$; *i.e.*, the centers of ellipses are not in correspondence with the path difference zero. In other words the air-path difference is larger than the glass-path difference

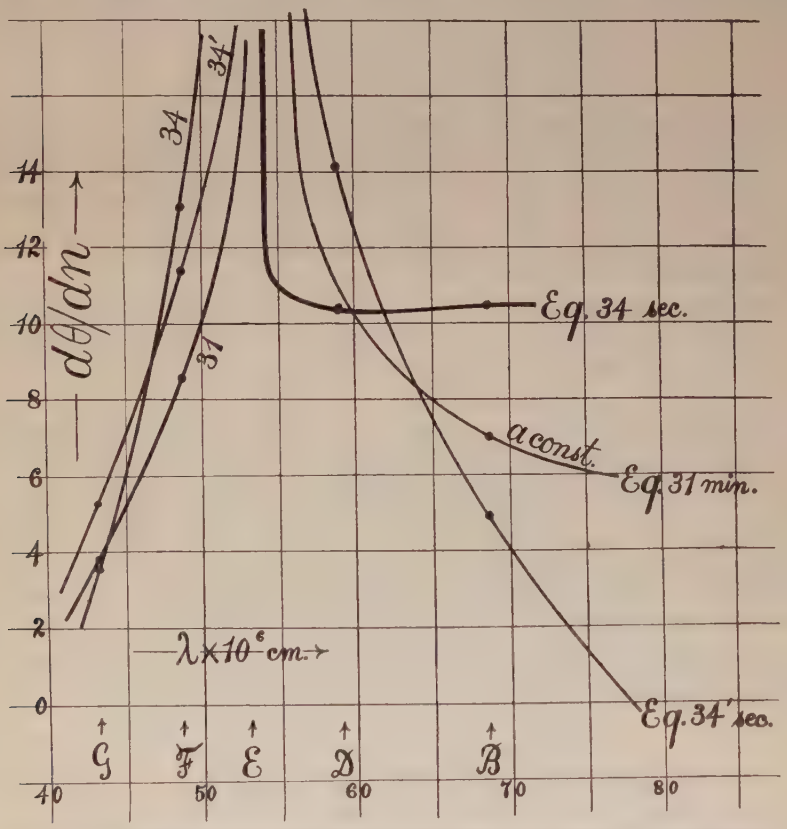

FIG. 29.—Chart showing dispersion per fringe in terms of wave-length.

*Interpolated between D and G by $\mu = a + b\lambda + c\lambda^2$ where $b = -.00273$, $c = .0000197$.

in such a way that $d\theta/dn$ is equal to ∞ for centers (here at the E line), but falls off rapidly toward both sides of the spectrum.

There is another feature of importance which must now be accentuated. In case of different colors, and stationary mirrors and grating, y is not constant from color to color, whereas

$$2N = 2y - 2e\mu \sin R \tan R$$

is constant for all colors, as has been shown above. Thus the equation to be differentiated for constancy of adjustment but variable color loses the variable y and becomes

$$n\lambda = 2e\mu \cos R - 2N \tag{29}$$

N here is the difference of perpendicular distances to the mirrors, M and N, from the ends of the normal in the glass plate, at the point of incidence of the white ray. Performing the operations

$$\frac{d\lambda}{dn} = \frac{\lambda^2 \cos R}{2(y \cos R - e\mu(1+a))} \tag{30}$$

$$\frac{d\theta}{dn} = \frac{\lambda^2}{2D \cos\theta} \quad \frac{\cos R}{e\mu(1+a) - y \cos R} \tag{31}$$

Hence maximum $d\theta/dn = \infty$ at the centers of ellipses which occur for

$$y = \frac{e\mu(1+a)}{\cos R} \tag{32}$$

The value of $d\theta/dn$ for the different Fraunhofer lines above, if $a = .015$ is still considered constant and $e = .68$, is given in table 15.

These results show that the distance apart of fringes on the two sides of the center of ellipses is not very different, though they are somewhat closer together in the blue than in the red end of the spectrum, as observed. There is thus an approximate symmetry of ovals, and $d\theta\, dn$ falls off very fast on both sides of the infinite value at the center. This is shown in fig. 29.

The observed angle between the Fraunhofer lines D and E for the given grating was 4,380″. The number of fringes between D and E would thus be even less than 4,380″, 638″ = 6.7 only, which is itself about 4 times too small. The cause of this is then finally to be ascribed to the assumed constancy of $-a = (d\mu/\mu), (d\lambda, \lambda)$, and a discrepancy is still to be remedied. We may note that a does not now enter as directly as appeared in equation (27).

By replacing a by its equivalent, equation (31) takes the form

$$\frac{d\theta}{dn} = \frac{\lambda^2}{2D \cos\theta} \quad \frac{1}{\frac{e}{\cos R}\left(\mu - \lambda \frac{d\mu}{d\lambda}\right) - y} \tag{33}$$

and a definite series of values may be obtained by computing $d\mu/d\lambda$; but as all experimental reference here is, practically, not to path differences

but to displacements of the movable opaque mirror N, the form of the equation applicable is

$$\frac{d\theta}{dn}=\frac{\lambda^2}{2D\cos\theta}\cdot\frac{1}{e\left(\mu\cos R-\frac{\lambda}{\cos R}\frac{d\mu}{d\lambda}\right)-N} \tag{34}$$

To make the final reduction, I have supposed that for the present purposes a quadratic interpolation of μ, between the B and the G lines of the spectrum, would suffice. Taking the E line as fiducial, I have therefore assumed an equation for short ranges, corresponding to Cauchy's in simplified form

$$\mu-\mu_E=b/(1/\lambda^2-1/\lambda^2_E)$$

in preference to the more complicated dispersion equations. From the above data for light crown glass we may then put, roughly,

$$b=.456\times10^{-20} \qquad d\mu/d\lambda=-2b/\lambda^3$$

Thus I found the remaining data of table 15. The results for $d\theta/dn$ agree as well with observations as may be expected. The ovals resemble ellipses, but are somewhat coarser on the red side, as is the case.

TABLE 16.—Values of $d\lambda/dy$, $d\theta/dy$, etc. $e=.68$ cm.

			B	D	E	F	G	
Equation	36	$d\lambda_0/dy=$	.00372	.00318	.00283	.00260	.00229	cm.
	38	$d\lambda_0/dN=$	269	229	205	189	167	cm.
	39	$d\lambda/dN=$	−.017	−.031	∞	+.030	+.015	cm.
	42*	$d\lambda/dN=$	....	−.0055	∞	+.0081	+.0031	cm.
	42	$d\lambda/dN=$	−.0044	−.0050	∞	+.0075	+.0023	cm.
	42	$d\theta/dN=$	−14.6	−17.0	∞	+26.0	+8.1	radians

The centers of ellipses are thus defined by the semi-air-path equation

$$y_c=\frac{e}{\cos R}\left(\mu-\lambda\frac{d\mu}{d\lambda}\right)=\frac{e}{\cos R}(\mu+2b/\lambda^2) \text{ nearly,} \tag{35}$$

or the corresponding equation in terms of N_c. The trend data for ΔN_c agree fairly well with observation, except at the D line, which difference is very probably referable to the properties of the glass, since the grating was not cut on light crown.

The number of fringes between the D and E lines now comes out plausibly, being *less* than $4{,}380''/104''=42$. It is difficult to count these fringes without special methods of experiment; but the number computed is a reasonable order of values, about 25 to 30 lines being observed.

Some estimate may finally be attempted as to the mean displacement of mirror δN per fringe, between the D and E lines. As their deviation is $\theta=1^\circ\,13'$ and the displacement from D to E, ΔN_c,

$$\delta N=\frac{\Delta N_c}{\theta/(d\theta/dn)}=\frac{d\theta}{dn}\frac{\Delta N_c}{\theta}>\frac{\lambda^2}{2D\cos\theta}\cdot\frac{1}{\Delta N_c}\cdot\frac{\Delta N_c}{\theta}$$

* Constants interpolated between D and G by $\mu=a+b\lambda+c\lambda^2$ when $b=-.00273$. $c=.0000197$.

if the value of $d\theta/dn$ for the D line be taken. Thus

$$\delta N > \lambda^2/(2D\theta \cos \theta) = \lambda^2/D \sin 2\theta, \text{ nearly}$$

Hence δN is independent of the thickness, e, of the plate of the grating, as I showed* by using a variety of different thicknesses of compensator.

Since $\lambda = .000059$ cm., $D = .000351$ cm.

$$\delta N > .00031 \text{ cm.}$$

The values found were between .00033 and .00039, naturally difficult to measure, but of the order required.

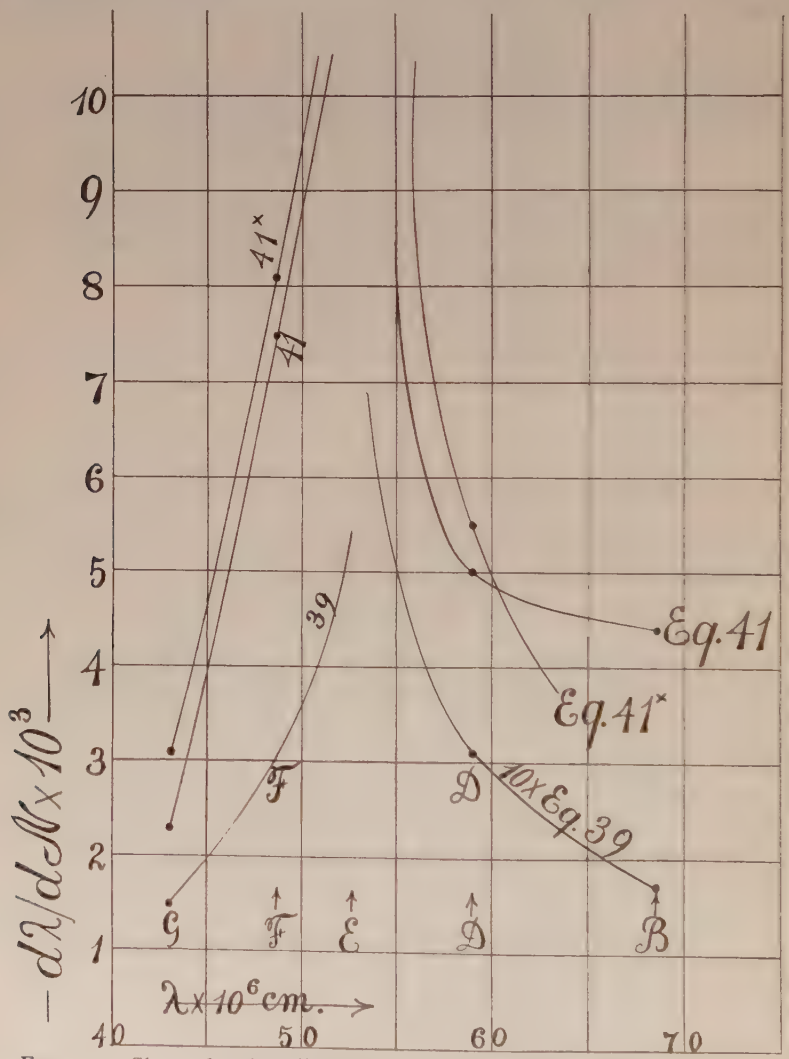

FIG. 30.—Chart showing dispersion ($d\lambda/dN$), per cm. of displacement of mirror in terms of wave-length.

*American Journal of Science, XXX, 1910, p. 170.

45. Case of $d\lambda/dy$, and $d\theta/dy$, etc.—If in equation (23) e and n are constant while μ, R, y, and λ vary, the micrometer equivalent of the displacement of fringes may be found. Here

$$d\mu/dy=(d\mu/d\lambda)\cdot(d\lambda/dy) \text{ and } dR/dy=(dR/d\mu)\cdot(d\mu/d\lambda)\cdot(d\lambda/dy)$$

which coefficients are given by equations (24), (25), and (26). In this way

$$\frac{d\lambda}{dy}=-\frac{\lambda\cos R}{e\mu(1+a(1-\tan^2 R))-y\cos R} \tag{36}$$

and

$$d\theta/dy=-(d\lambda/dy)/D\cos\theta$$

If $y=e\mu/\cos R$, where y is variable, the motion is supposedly referred to the centers of ellipses. Thus

$$\frac{d\theta_0}{dy}=\frac{\lambda}{D\cos\theta}\,\frac{\cos R}{ae\mu(1-\tan^2 R)} \tag{37}$$

Values are given in table 4 and hold for the glass of tables 11–15. These results are, as usual, many times too large and they contain no suggestion of opposed motion on the two sides of the center.

If we consider the displacement of the mirror N instead of the path difference and for a given color write

$$N=y-e\,\sin I\tan R$$

then

$$\frac{dN}{dy}=\frac{e\mu(1+a)-y\cos R}{e\mu(1+a(1-\tan^2 R))-y\cos R}$$

and hence in

$$\frac{d\lambda_0}{dN}=-\frac{\lambda\cos R}{ae\mu} \tag{38}$$

the factor $(1-\tan^2 R)$ is removed from the equation. But the data are not much improved.

The equation $n\lambda=2e\mu\cos R-N$ gives, on differentiation and reduction,

$$\frac{d\lambda}{dN}=\frac{\lambda}{y-e\mu(1+a)/\cos R} \tag{39}$$

To be consistent with the preceding paragraphs, it is therefore necessary to put $y-e\mu(1+a)/\cos R=0$, for centers of ellipses, so that $(d\lambda/dN)_0=\infty$. If a is constant this supposition leads to results which are throughout out of the question. The values of $d\lambda/dN$ may, however, be found by inserting the data for $d\mu/d\lambda$ given in the preceding paragraph.

Centers thus correspond to

$$N=e\mu\cos R-\frac{e\lambda}{\cos R}\,\frac{d\mu}{d\lambda} \tag{40}$$

or

$$\frac{d\lambda}{dN}=\frac{\lambda}{N-e\mu\cos R+e\lambda(d\mu/d\lambda)/\cos R} \tag{41}$$

so that if $d\lambda/dN = \infty$, the maximum at the centers of ellipses, the simultaneous effect at λ' will be (as the mirror has not moved)

$$\frac{d\lambda'}{dN} = \frac{\lambda'}{e(\mu \cos R - \mu' \cos R') - e\left(\frac{\lambda}{\cos R}\frac{d\mu}{d\lambda} - \frac{\lambda'}{\cos R'}\frac{d\mu'}{d\lambda'}\right)} \qquad (42)$$

If the center of ellipses is at the E line the values of table 4 hold. The motion on the blue side of the E line is thus larger than the simultaneous motion on the yellow side, conformably with observation.

All the results are given graphically in fig. 30.

46. Interferometry in terms of radial motion.—Either by direct observation or combining the equations (34) and (41) for $d\lambda\ dn$ and $d\lambda\ dN$ the usual equation for radial motion again results

$$\frac{dN}{dn} = \frac{\lambda}{2}$$

where N is the displacement of mirror per fringe. This equation is best tested on an ordinary spectrometer, by aid of a thin compensator of microscope glass revolvable about its axis and placed parallel to the mirror M. The change of virtual thickness e' for a given small angle of incidence i may then be written.

$$de' = e' \frac{\sin R dR}{\cos^2 R} = \frac{e'}{2} \frac{dI^2/\mu^2}{1 - I^2/\mu^2}$$

nearly. If $I = 0$, $dI^2 = (dI)^2$. Therefore $2de' = dI^2\ \mu^2$. In a rough trial for $e' = .0226$ cm., $dI = .053$ radians, $\mu = 1.53$, one fringe reappeared. Hence

$$dN/dn = \mu de' = \tfrac{1}{2} \times 1.53 \times 27 \times 10^{-6} = 21 \times 10^{-6} \text{cm.}$$

which is of the order of half the wave-length used.

47. Interferometry by displacement.—In a similar experiment the displacement of ellipses due to the insertion of the above glass, $e' = .0226$ cm., was from the D line to about the G line. If ΔN is the displacement of the mirror N, to bring the center of ellipses back to the same line, D or E, we may write $\mu = 1 + \Delta N/e'$. I found at the E line $\mu = 1.53$, at the D line $\mu = 1.53$; special precautions would have to be taken to further determine these indices.

Thus there are two methods for measuring μ, either in terms of the radial motion of the fringes or, second, in terms of the displacement of the fringes as a whole. Moreover, paragraph 44 may be looked upon reciprocally, as a method for measuring $d\mu/d\lambda$, directly.

Part IV. Interferences in General, and Summary.

48. The individual interferences.—In figs. 31, 32, 33, *gg* is the face of the grating, *M* and *N* the opaque mirrors, and *I* the incident ray.

As the result of reflection from the top face, the available air-path being y_m and y_m', there must be two images of the slit seen in the telescope directly, *viz*, *a* and *c*, fig. 31. Of these *c* will be more intense than *a*, which is tinged by the long path in the glass. These two rays together, on diffraction, will produce stationary interferences whose path corresponds to the equation

$$n\lambda = 2e\mu \cos R$$

The optical paths of the two rays are

reflected-refracted, I′, $2y_m + e\mu(2 \cos R - \sec R)$

refracted-reflected, II′, $2y_m' + 3e\mu \sec R = 2y_m + e\mu(3 \sec R - 4 \sin R \tan R)$

If the plate of the grating were perfectly plane parallel, the slit images *a* and *c* would obviously coincide.

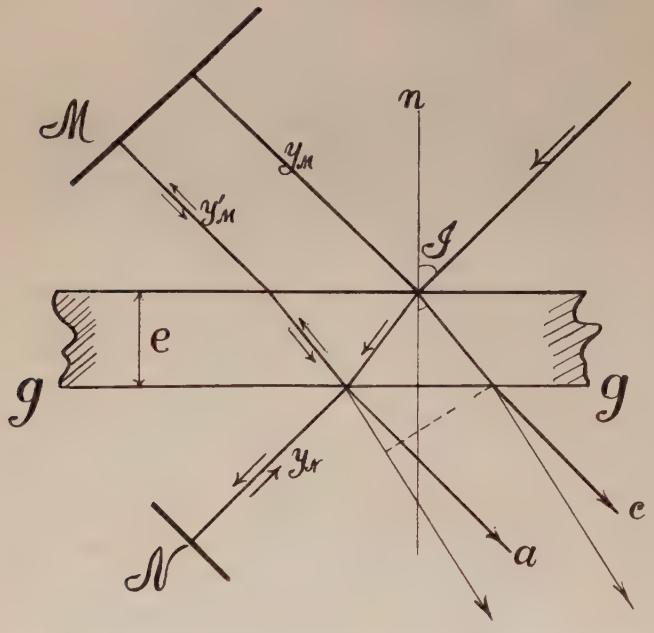

Fig. 31.—Diagram of interferences reflected from same face of grating plate. Non-compensated.

The directly transmitted rays, however, after reflection from *N* give rise to four images of the slit—in case of a slightly wedge-shaped plate, the one at *a*, fig. 31, being white, that at *c* yellowish, the distances apart being the same as in the preceding case. Besides this there are two images of the slit at *b*, figs. 32 and 33, which result from double diffraction at the lower face, the

case shown corresponding to $\theta<i$ first with $\theta>i$ thereafter, while the other image corresponds to $\theta>i$ and $\theta<i$ in the two successive diffractions. These slits show strong chromatic aberration but are nevertheless linear and useful. The optical paths for the three lower rays are

$$\text{transmitted, I. } 2y_n+e\mu/\cos R$$

$$\text{transmitted-refracted, II. } 2y_n+e\mu/\cos R+2e\mu\cos R$$

$$\text{transmitted-diffracted, III. } 2y_n+e\mu/\cos R+2e\mu\cos\theta_1$$

These three equations determine the three stationary interferences

$$n\lambda=2e\mu\cos R \qquad n\lambda=2e\mu\cos\theta_1 \qquad n\lambda=2e\mu(\cos\theta_1-\cos R)$$

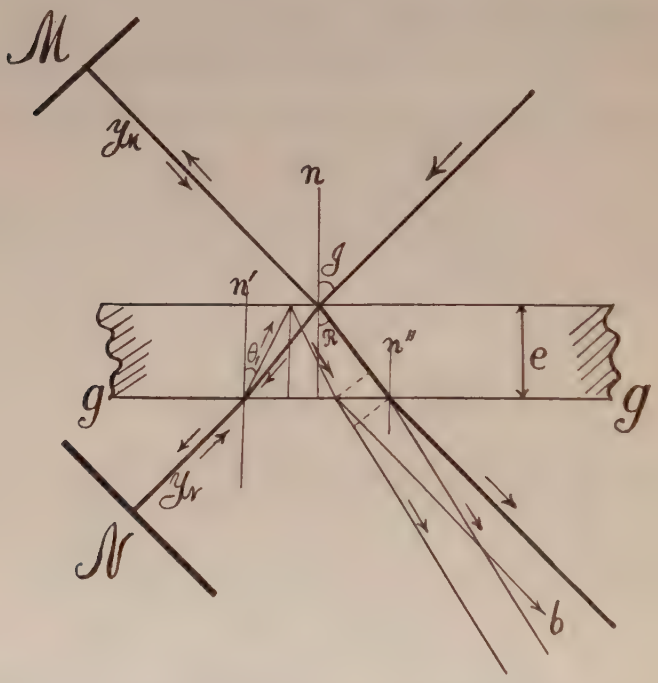

FIG. 32.—Diagram of interferences reflected from both faces of grating *gg*. Excess of glass path on *N* side. Self-compensated.

discussed in the preceding paper*. If the grating is between two identical plates of glass, these stationary fringes may become movable; for, inasmuch as there is complete symmetry between the rays to be reflected from the mirrors *M* and *N*, the stationary fringes become identical for both plates of glass, from either of which they may be reflected, before or after diffraction. Hence the motion of either opaque mirror changes the phase and moves the fringes, which are now linear, vertical, and nearly equidistant.

*C. and M. Barus.

They may also be regarded as confocal ellipses of infinite size, the visible parts of their peripheries lying close together in the field of view. They pass through infinity in this field, when the virtual path difference is zero.

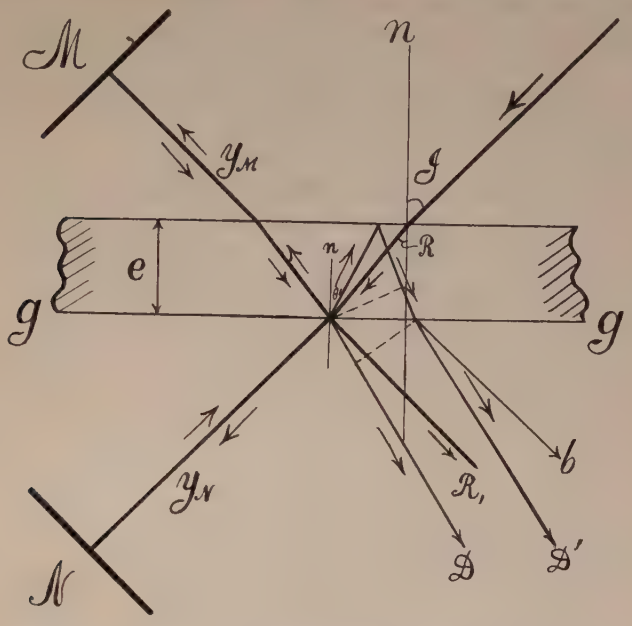

FIG. 33.—Diagram of interferences reflected from both faces of grating plate. Excess of glass path on *M* side. Self-compensated.

49. The combined interferences.—The five equations given by the first group I′ and II′ when combined with the second group, I, II, III, lead to six other interferences, all of them of the movable type and useful for interferometry. If for simplicity the path difference is zero, they may be written, if $y = y_n - y_m$ and $y' = y_n - y_m'$ and y_o corresponds to the glass-path difference, N as usual referring to the displacement of the opaque mirror:

IV, Reflection at bottom, equation I–II′, $y_o' = e\mu/\cos R$, $N = e\mu \cos R$

V, Reflection at bottom, equation II–I′, $-y_o = e\mu/\cos R$, $N = e\mu \cos R$

VI, Reflection at top, equation III–I′, $-y_o = e\mu(\cos \theta_1 + \sin R \tan R)$, $N = e\mu \cos \theta_1$

VII, Reflection at top and bottom, eq. II–II′, $y_o' = e\mu \sin R \tan R$, $N = 0$

VIII, Reflection at top and bottom, eq. III–II′, $y_o' = e\mu(\sec R - \cos \theta_1)$, $N = e\mu(\cos R - \cos \theta_1)$

IX, Reflection at bottom and top, eq. I–I′, $-y_o = e\mu \sin R \tan R$, $N = 0$

Hence the fringes of the interference VII and IX are identical throughout the spectrum, when the mirror N moves. The remaining fringes are elliptic and eccentric, because reflected from two faces of the thin wedge.

Nos. VII and IX are parallel lines which pass symmetrically from negative to positive obliquity, or the reverse, respectively, through horizontality, in opposed directions.

The results of these equations have been computed for light crown glass and the Fraunhofer lines *B*, *D*, *E*, *F*, *G* above and in the following table 17.

TABLE 17.—Diffracted-reflected and reflected-diffracted rays. $e=.68$ cm. $D=.000351$ cm. $I=45°$, nearly. Light crown glass. $y=y_N-y_M$. Change of faces: $y-N$.

Line of Spectrum	B	D	E	F	G
$10^6\lambda=$	68.7	58.93	52.70	48.61	43.08
$\mu=$	1.5118	1.5153	1.5186	1.5214	1.5267
$R=$	27° 53′	27° 49′	27° 45′	27° 42′	27° 35′
$\theta_1=$	19° 47′	20° 51′	21° 31′	21° 57′	22° 30′
(correction) $2N=$	.5088	.5074	.5059	.5050	.5023
I. Reflection from a single face. $y_0=e\mu\cos(R-\theta_1)/\cos R$:					
$n\lambda=0;-\ 2y_0=$	2.3030	2.3128	2.3199	2.3252	2.3334
$E=0;-\ 2\Delta y_0=$	− .0169	− .0071	± .0	+ .0053	+ .0135
correction $-2\delta N_0=$	+ .0028	+ .0014	± .0	− .0009	− .0036
$-2\Delta N_0=$	− .0197	− .0085	± .0	+ .0062	+ .00171
II. Reflection from one face. $y_0=e\mu/\cos R$:					
$+\ 2y_0=$	2.3261	2.3301	2.3337	2.3369	2.3426
$+\ 2\Delta y_0=$	− .0076	− .0036	± .0	+ .0032	+ .0089
$+2\Delta N_0=$	− .0104	− .0050	± .0	+ .0043	+ .0126
III. Reflection from both faces. $y_0=e\mu\ (\sec R-\cos\theta_1)$:					
$+\ 2y_0=$	.3913	.4043	.4124	.4177	.4242
$+\ 2\Delta y_0=$	− .0211	− .0081	± .0	+ .0053	+ .0118
$+2\Delta N_0=$	− .0239	− .0095	± .0	+ .0062	+ .0154
IV. Reflection from both faces. $y_0=e\mu\sin\theta_1\tan R$:					
$+\ 2y_0=$	.3682	.3870	.3985	.4061	.4151
$+\ 2\Delta y_0=$	− .0303	− .0115	.0	+ .0075	+ .0166
$+2\Delta N_0=$	− .0332	− .0130	.0	+ .0084	+ .0202
V. Same as II, but reflection from top face :					
$-\ 2y_0=$	2.3261	2.3301	2.3337	2.3369	2.3426
$-\ 2\Delta y_0=$	− .0076	− .0036	± .0	+ .0032	+ .0089
$-2\Delta N_0=$	− .0104	− .0050	± .0	+ .0043	+ .0126

50. Special results.—The table shows the following positions for the successive interferences, *i.e.*, for $2y-N$ when the reflection changes from the lower to the upper face. $N=2e\mu\tan R\sin R$.

Reflection from bottom, $y_m<y_n$	Cases I–II′,	$y_0=1.1650$,	Equation IV,	Position, 1.1650
	II–II′,	.2537,	VII,	.2537
	III–II′,	.2021,	VIII,	.2021
Reflection from top, $y_m>y_n$	I– I′,	− .2537,	IX,	.2537
	II– I′,	−1.1650,	V,	− .6576
	III– I′,	−1.2166,	VI,	− .7092

Hence the total play of the mirror *N* should be $1.1650-(-.7092)=1.8742$ cm., with which the observed datum 1.88 agrees as nearly as the experiment warrants. Again the fringes of equations VII and IX are simultaneously in the field, which is true, these being a series of lines which change their obliquity in opposite directions symmetrically. The two ellipses of equations V and VI, however, were found nearer together than the com-

puted value. Thus their distance apart in the D region corresponded to $\Delta y = .0075$ cm.; in the E region it corresponded to $\Delta y = .0050$ cm., whereas the above data require .0516 cm. Here, however, there is some confusion. For instance, the spectra may coincide, whereas the doubly diffracted white and colored images of the slit do not. Moreover, there are three ellipses in this region of y, since the double diffraction for $\theta > i$ also gives an ellipse, not included, because not belonging to the above enumeration. The motion of ellipses from the D to the E line has different values. The set toward the violet corresponds to $\Delta N = .0090$ cm.; the set toward the red to $\Delta N = .0070$ cm. There is thus a different speed of fringes relative to N, and closer contact in the violet than in the red. The latter are also more nearly circular than the former. Equation IV gives the strong solitary interferences useful in practice and treated in detail in the earlier parts of this paper. The treatment of the other cases, being less important, may be omitted here.

My thanks are due to Prof. Joseph S. Ames, of Johns Hopkins University, for his kindness in lending me the glass-diffraction grating by which the above equations were tested. I hope at some other opportunity to work with a grating whose refraction is known throughout the spectrum and also to endeavor to obtain the phenomenon as clearly from film gratings (replicas) as has been possible for the linear series in the preceding paper (*l.c.*). Thus far the above phenomena as obtained from film gratings were not strong and sharp enough for measurements of precision but in a series of experiments which has since been completed I will show how this desideratum may be realized.

THE PRODUCTION OF ELLIPTIC INTERFERENCES IN RELATION TO INTERFEROMETRY

PART II

By CARL BARUS

Hazard Professor of Physics and Dean of the Graduate Department in Brown University

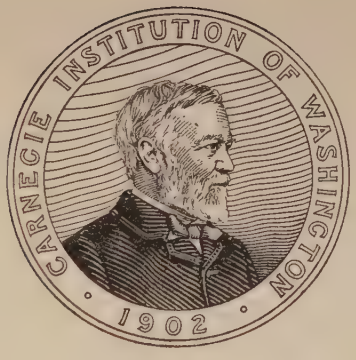

WASHINGTON, D. C.
Published by the Carnegie Institution of Washington
1912

CARNEGIE INSTITUTION OF WASHINGTON
Publication No. 149, Part II

PRESS OF J. B. LIPPINCOTT COMPANY
PHILADELPHIA, PA.

PREFACE.

The present report is, in the main, an extension of my work on the displacement interferometer described in the preceding investigation (Publication No. 149 of the Carnegie Institution of Washington); but beyond this, it is a contribution to the theory of coronas and their practical application for the measurement of sizes of fog-particles in cloudy condensation. In other words, if the source of light is not simple, but a doublet of two interfering beams as in chapter VI, indistinguishable from a simple source in case of white light, the coronas must show concentric dark interference rings, for the same reason that the spectra in case of the grating show elliptic loci of interference. It is therefore from rings of this general character that measurements of precision with coronas may be obtained. In its practical aspects chapter VI deals with the production of elliptic interferences with plane reflecting gratings instead of transparent glass gratings, as the former are much easier to rule. Again, the special type of linear fringes, produced by identical halves of a reflecting grating with their rulings parallel to the slit and nearly in the same plane, probably has a direct bearing on the theory of coronas, as in both cases an interference phenomenon is superimposed on the diffractions.

In chapters VII, VIII, and IX I have included certain incidental experiments on fog-particles made by aid of the coronas of cloudy condensation. The first investigation shows that the angular aperture of coronas is independent of the thickness of the layer of fog, single and triple layers, each about 6 inches thick, giving the same (continuous) corona. The next investigation adduces the curious result that when the diameter and size of the fog-chamber diminish indefinitely relative to the size of the exhaust pipe, its efficiency does not uniformly increase, but that it is rather more efficient for the (virtually) larger nuclei and less efficient for the smaller groups. Certain allied results on the rate of decay of nuclei of different sizes produced by mild X-radiation in dust-free wet air are added. These show the remarkable result that the coefficient of decay increases from less than one-tenth of the usual value for ions in dry air, to even 50 times the normal value, as the nuclei range in dimensions from very large to very small sizes. Hence if these nuclei be regarded as water-drops, they evaporate more and more rapidly to a persistent limiting small diameter, in proportion as they are larger. In the last investigation (chapter IX), I have returned to the moot subject of the regular persistent nuclei produced by strong X-rays, through earthed metallic aluminum screens and a fog-chamber of wood, with the endeavor to find the lower limit of the density of ionization which must be reached before these typical persistent nuclei (*i.e.*, those requiring little or no supersaturation to precipitate con-

densation) are formed. This chapter deals with large persistent nuclei produced by X-rays and is thus in a measure supplementary to the preceding. From both I conclude that the decay of ions as such beyond the scope of easy determination by the electrometer with the production of neutral pairs and multiples finds its counterpart in the growth of persistent nuclei, as the result of such coalescence. These nuclei now fall specially within the scope of detection by the fog-chamber. The number of persistent nuclei produced by the X-rays (*caet. par.*) will increase with the time of exposure at an accelerated rate, inasmuch as the nuclei or ions present themselves take part in the production, and these are present in continually greater number, as the lower limit of size decreases.

In chapter X the equation derived in the preceding report (No. 149, chapter V) for the displacement of the center of ellipses produced by the opaque mirror on the micrometer is tested throughout the spectrum and for all angles of incidence. This requires a knowledge of the indices of refraction of the glass of the grating for all wave-lengths. A method of total reflection suitable to the case, where only a flat spicule of glass is at hand, was therefore developed and applied.

In conclusion, a displacement interferometer is described, combining the desiderata of rigidity, lightness, and portability, and provided with long arms of invariable length and with sufficiently high mirrors to admit of the introduction of bulky apparatus, like a fog-chamber, between them. The apparatus is peculiarly adapted for the measurement of the refraction of gases at high temperatures, and conversely for the measurement of high temperatures by means of the refraction of a gas, as well as for the measurement of the adiabatic transformations of a gas, either dry or wet, and at all temperatures. It is hoped that the researches may develop fruitfully in this direction, and some promising work has already been completed.

Chapter XI, with a special view to an application of the interference method, endeavors to measure the degree of adiabatic expansion encountered in fog-chambers of such dimensions as I have used. To actually measure the ratio of specific heats much more voluminous apparatus will be necessary, and the present form of the interferometer is not adapted for air-chambers large in their vertical dimensions. An interesting result of the investigation is the marked difference of the heat ratio for wet and dry air, data from which it should be possible to compute the amount of water precipitated per cubic centimeter.

My thanks are due to Miss Ada I. Burton, who assisted me with rare efficiency both in the editorial part of the work and in the preparation of diagrams, as well as in the experimental parts and in the extended computations which a research of the present kind demands.

CARL BARUS.

BROWN UNIVERSITY, *December* 1911.

CONTENTS.

CHAPTER VI.—*Elliptic Interferences with Reflecting Gratings.*

PAGE

51. First method. Fig. 34 79
52. Inversion of the method 80
53. Second method. Resolution of the slit image 81
54. Third method. Parallel gratings. Figs. 35, 36 81
55. Nature of the evanescence. Fig. 37 83
56. Data. Table 18 85
57. Equations. Fig. 38 85
58. Differential equations. Displacement per fringe, de/dn 87
59. Deviation per fringe, $d\theta/dn$, $d\theta/de$ 88
60. Colored slit images and disk colors of coronas 89

CHAPTER VII.—*Independence of Coronas of Thickness of the Fog Layer.*

61. Introductory 91
62. Effect of thickness. Apparatus. Fig. 39 91
63. Results and summary 92

CHAPTER VIII.—*Experiments with a very Small Fog-Chamber, together with Data on the Decay of Large and Small Nuclei.*

64. Small fog-chamber. Figs. 40, 41, 42, 43; tables 19, 20 93
65. Decay of different sizes of ions. Fig. 44; tables 21, 22, 23 96

CHAPTER IX.—*On the Persistent Nuclei Produced by the X-rays.*

66. Introductory 101
67. Older series of experiments 103
68. Recent experiments. Table 24 104
69. Initial fogs 107
70. Amount of ionization needed to produce persistent nuclei 107

CHAPTER X.—*The Rectification of the Spectrum by the Aid of Total Reflection, together with a Computation of the Shift of Ellipses in Elliptic Interferometry.*

71. Introductory 111
72. Apparatus. Fig. 45 111
73. Methods 113
74. Examples. Liquids. Figs. 46, 47; tables 25, 26 114
75. Examples. Solids. Figs. 48, 49; tables 27, 28 116
76. Independent measurements 119
77. Prism (liquid CS_2) and submerged grating. Fig. 50; table 29 119
78. The dispersion constants of the glass of the grating. Table 30 121
79. Computation of the shift of centers in elliptic interferometry. Fig. 51; tables 31, 32 122
80. Continued. Case of $I=0°$. Figs. 52, 53; tables 33, 34 126
81. Case of $I=90°$, nearly. Tables 35, 36 128
82. Summary 129
83. Apparatus. Figs. 54, 55, 56 129
84. Other interferences. Fig. 57 134
85. Other measurements; high temperature, adiabatic transformations, etc. Fig. 58; table 37 135

CHAPTER XI.—*The Degree of Adiabatic Expansion in Gases Rapidly Cooled, as Observed by Displacement Interferometry.*

PAGE

86. Introduction. Apparatus. Fig. 59 141
87. Equations 143
88. Small brass fog-chamber, dry and wet. Fig. 60; tables 38, 39, 40, 41, 42 ... 148
89. Larger (wood) fog-chamber. Dry air. Fig. 61; tables 43, 44, 45, 46 151
90. The same. Wet air. Tables 47, 48, 49 154
91. Copper fog-chamber. Exhaustion. Dry air. Tables 50, 51 155
92. The same. Compression. One-inch stop-cock. Tables 52, 53 157
93. The same. Compression. Two and one-half inch stop-cock. Tables 54, 55 157
94. Clement and Desormes's apparatus. Fig. 62; tables 56, 57, 58, 59, 60 158
95. Large wood fog-chamber. Figs. 63, 64; tables 61, 62, 63, 64, 65, 66 161
96. Air-chamber of vanishing thickness. Tables 67, 68 165
97. Conclusion 166

CHAPTER VI.

ELLIPTIC INTERFERENCES WITH REFLECTING GRATINGS.

51. First method.—There are two or three typical cases in the use of reflecting gratings for the production of interferences in the spectrum, each of which shows peculiarly interesting features. The first of these is given in fig. 34 and corresponds closely to the method described for transmission gratings in a preceding paper. If L is the source of light and M a glass plate grating, it was shown that plane mirrors in the positions G_m and G_n, each reflecting a spectrum from M, produce elliptical interferences whenever the rays returned after passing M by transmission and reflection, respectively, are made to overlap in the spectrum, under suitable conditions.

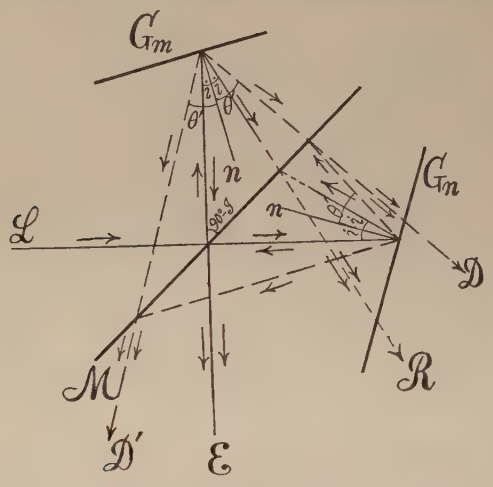

FIG. 34.—Diagram showing production of elliptic interferences from mirror M and reflecting gratings G_m and G_n.

The present method is the converse of this, since the gratings and the opaque mirrors change places. Parallel rays from L strike the plate of glass M and the component rays reach identical reflecting gratings G_m and G_n, placed symmetrically with respect to M at an angle i to the E and L directions. The undeviated rays pass off eccentrically at R and are not seen in the telescope at E. They may, however, be seen in an auxiliary telescope pointed in the line R and they then facilitate the adjustments. Rays diffracted at the angle $2i$, however, are respectively transmitted and reflected by M and interfere in the telescope in the line E. Similarly rays diffracted at an angle $\theta' > i$ interfere in the line D.

To make the adjustment it is sufficient to bring the Fraunhofer lines in the two spectra seen at E into complete coincidence, horizontally and vertically. Coincidence of slit images at R (at least vertically) aids in the same result. It is also necessary that the rulings on G_m and G_n and the slit shall be parallel, or that the images of slit and spectra shall lie between the same horizontals. One of the gratings, G_n, may now be moved parallel to itself by the micrometer screw until the elliptic interferences appear. If the plate M is not half-silvered there are three groups of these, as described in the preceding paper. Each group passes from the initial degree of extreme fineness, through maximum size, to a final degree, for a play of the screw of about 1 mm. There is the usual radial motion of the fringes, together with the drift through the spectrum as a whole. To bring out the set of solitary ellipses, the silvered surface of M should be toward the light and remote from the eye. As a rule the adjustment is difficult, as an extra condition is imposed in the parallelism of the slit and the rulings of the gratings. The ellipses are liable to be coarse, with their axes oblique, clearer in some parts of the spectrum than in others, unless means are provided for placing the rulings accurately parallel. Even when well adjusted they are rather polygonal than rounded in their contours. They are about as strong with non-silvered glass M as with half-silvered glass; but in view of the multiple spectra the adjustment is much more difficult in the former case.

It has been suggested that the white slit image must appear eccentrically in the direction R. Hence if a special telescope is directed in this line, the final adjustment is reached on coincidence of the proper slit images, provided the rulings of the gratings and the slit are parallel.

For $\theta' > i$ the second series of interference spectra occurring at D eccentrically is broader, but only on perfect adjustment does it occur simultaneously with the other set. In fact, since for the preceding case $i = \theta$, or

$$2 \sin i = \lambda/D$$

and in the present case,

$$\sin \theta' - \sin i = \lambda/D$$

therefore

$$\sin \theta' = 3 \sin i = 3 \sin \theta$$

There is also an available set in the second order to the left of E. In the gratings used above D lies in front of G_n, being nearer the E than the L direction.

52. Inversion of the method.—The occurrence of the undeviated ray R suggests another method; for if the white ray R is reversed, *i.e.*, comes from an eccentric collimator, slit images will be seen in telescopes at L and E, whereas overlapping spectra will appear in the direction D' eccentrically and in the lines R and R'. One of the latter may be lost in the collimator. The former occurs for the same angle θ', so that

$$\sin \theta' = 3 \sin i$$

Moreover, if $I = 45°$ is the angle of incidence of L upon M when sodium light is taken, so that $\theta' = 26° 14'$, $i = 8° 28'$, the R, D, D' rays make angles $2i$, $\theta' + i$, $\theta' - i$, respectively, with the E direction; or the sum of the angles at D and D' with the E line is $2\theta'$, their difference $2i$, and the rays D, R, D' intersect at a common center on G_m. Hence if we place the plane of G_m at the center of the spherometer and arrange M and G_n eccentrically, the angles may be measured as before.

53. Second method. Resolution of the slit image.—If the sharp white images of the slit in a Michelson apparatus for the case in which the incident light consists of parallel white rays from a collimator be accurately superimposed and the opaque mirrors be set at the proper distances from the semi-transparent mirror by the micrometer, the slit image may itself be viewed through a grating and will then show elliptic interferences in all the spectra. The apparatus is here eccentric, while the grating (either transmitting or reflecting) must be at the center of the spectrometer, if angles are to be measured. The same is true for any of the other superimposed white slit images in the above or the earlier experiments and may even be repeated with successive transmitting gratings. It is interesting to note that the position of the center of ellipses is at the same wavelength in all the spectra, though the form of ellipses may differ enormously. The same phenomenon may thus be seen by a number of observers at the same time, each looking through his own telescope.

It is this phenomenon which may be repeated with the fog-particles of cloudy condensation instead of with the grating and must then give rise to concentric black interference rings symmetrical with the colored field. Measurements of precision in case of the coronas are thus feasible, in view of the varying distances apart of these rings, increasing in size as they do with diminishing sizes of fog-particles.

54. Third method. Parallel gratings.—In this case the two halves of the grating are treated displaced parallel to themselves from their original coplanar position in the grating from which they are cut. Their mounting is thus something like the case of the two black plates of Fresnel's mirror apparatus, one of the plates being adapted for displacement parallel to itself.

In fig. 35, g and g' show the two halves of the grating cut along the plane S, normal to the plates and parallel to the rulings. The half g' is provided with a micrometer screw, so that it may be successively moved from the position g' in fig. 35 to the position g' in fig. 36, through all intermediate positions, while the half g remains stationary. Each of the halves g and g' is controlled by three adjustment screws (horizontal and vertical axes of rotation), to secure complete parallelism of the faces of the grating. Each, moreover, may be rotated around a horizontal axis to place the lines parallel to the slit of the collimator. The duplex grating is mounted on a

spectrometer, as is usual for reflection. Finally, each half may be raised and lowered and moved horizontally to and fro, parallel to itself, so that the half gratings when coplanar may approximately reproduce the original grating.

After each of the spectra is clear as to Fraunhofer lines, the interferences here in question are produced by bringing these lines (the D lines, for instance) into perfect coincidence, horizontally and vertically. Under these circumstances if the distance apart, e, is suitably chosen, the interference fringes will appear throughout the spectrum. These consist of an approximately equidistant series of lines parallel to the slit, *i.e.*, vertical lines, which are finer, *cæt. par.*, as the breadth of the crack at S between the gratings is larger. They may be increased from the extreme fineness as they enter the range of visibility, to a maximum coarseness (in the above

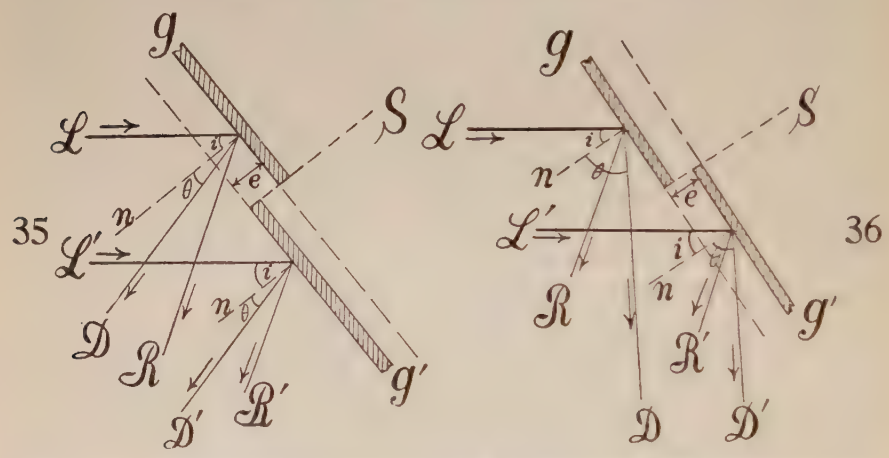

FIGS. 35 AND 36.—Diagram showing production of interferences from identical gratings, nearly in same plane, with their rulings parallel to the slit.

experiments) of about 3 to 5 minutes per fringe, after which they vanish. They can not, in practice, be passed through infinite size; neither can they be produced symmetrically on the two sides of the adjustment for infinite size. They can not, in other words, be changed from the positive to the negative condition of appearance.

The occurrences are in fact as follows: If as in fig. 35, $i > \theta$ (parallel white rays coming from L and L', R and R' being reflected, D and D' diffracted rays for the normal n), the grating g' must be in advance or forward of g. If now the air-space e is reduced micrometrically, g' retreating, the lines travel in a given direction (from left to right) through the spectrum, while at the same time they grow continually larger until for a minimum value of e still positive they vanish as a whole. The period of indistinctness before evanescence is not marked.

On the other hand, if $\theta' > i$, as in fig. 36, the grating g' must be to the rear of g and the air-space e is throughout negative. If this is now decreased

numerically the lines travel through the spectrum in the opposite direction to the preceding case, while at the same time they coarsen until they vanish as a whole as before. The grating g' is still behind g when this occurs.

Finally, if for any suitable value of e the grating g' is moved in its own plane without rotation away from g, so as to widen the crack at S between them, the fringes grow continually finer until they pass beyond visibility, and *vice versa; i.e.*, as the crack at S is made smaller the lines continually coarsen.

55. Nature of the evanescence.—The fact that the lines vanish as a whole and almost suddenly after reaching their maximum distance apart is very peculiar, as is also the fact that they can not be passed through infinite size or made to appear symmetrically on both sides of this adjustment. To investigate this case I provided both the collimator and the telescope with slits, so that the parts of the grating g and g' from which the interfering pencils come might be investigated.

If a single vertical slit about 1 mm. wide is passed from right to left toward the objective of the telescope, a black line passes across the field of the spectrum, which line is merely the image of the crack at S. In the diagram (fig. 37) the G rays, for instance, come from the edge of both gratings g and g', whereas the R rays and the V rays come from but a single grating. Now, when the space e is diminished, the black band at G gradually vanishes and in its place appear the coarsest fringes producible. When the slit F is removed these coarse fringes disappear. The fringes visible through the slit have, however, both an inferior and superior limit of angular size. When e is diminished to zero they vanish and when e is sufficiently increased they again vanish, though they now appear when the slit is either removed or widened. From this it follows that the coarsest fringes come from the edges of the crack S of the gratings, and that the remainder of the grating will not produce coarse fringes. By moving the slit the fringes may be made to appear in any other part of the spectrum.

The same fact may be proved by putting the vertical slit F over the lens of the collimator and allowing the white light L to fall on the edges of the grating at S. Coarse fringes limited as to range and size are then seen throughout the spectrum at g.

Whenever the slit or vertical stop is used, the fringes are exceptionally sharp and easily controlled for micrometry. It is not even necessary to adjust the two spectra horizontally with the same care as when no slit is used, but the vertical coincidence of spectrum lines must be sharp. Naturally the use of the slit has one drawback, as the resolving power of the grating is decreased and the spectrum lines are only just visible. The adjustment, however, may be made before the slit is added. A few examples may be given. For a slit 1 mm. wide over the telescope or collimator, only the immediate edges at the crack S, about 0.5 mm. each in

breadth, are active. A narrow range of large fringes is seen in the field, easily controlled by the micrometer screw. With a slit 3 mm. in width the lower limit is much increased, the upper diminished, to a size of about 3 inches per fringe. In the absence of the slit the field is free from fringes. With a slit 6 mm. wide, the upper limit is again decreased, the lower much increased; nevertheless the finest fringes appear only after the slit is removed. Using double slits over the collimator, each 1 mm. wide and 3 mm. apart, fringes of medium size limited at both ends appear; 3 mm. slits 6 mm. apart show only the very fine fringes, but both sizes are still limited. Finally, when all but about 0.5 mm. of the edge of the crack of the grating g' is screened off, whereas the whole grating g (about one-half inch square) is without a screen, all the fringes from the maximum size to

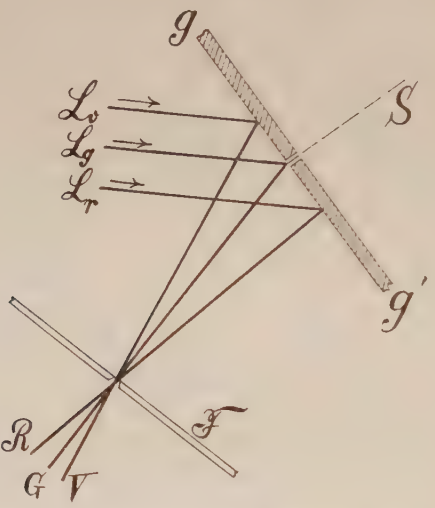

FIG. 37.—Diagram showing effect of a slit in front of telescope.

complete evanescence beyond the range of visibility are producible. Naturally if the edge of g' is quite dark everything vanishes.

It follows, therefore, that pairs of corresponding rays are always in question. These corresponding rays are at a definite ND apart, where D is the grating space and N the number of lines per centimeter of the grating in question. This distance ND is greater as the fringes are smaller and may be of the order of a centimeter when the fringes pass beyond the range of visibility. Again ND is equal to the width of the crack when the largest fringes vanish. Finally, when ND is zero, as is the original unbroken grating, the size of the fringes is infinite.

It has been stated that the use of the slit or a laterally limited objective is advantageous because all the lines are much sharper. Inert or harmful illumination is cut off. If the slit is over the objective of the telescope only a small part of the field of view shows the lines; if placed over the

objective of the collimator, the fringes are of extreme clearness throughout the spectrum. It may be ultimately of advantage to use the edge near the crack g' only, together with the whole of g; for if a small strip of g' at the crack S is used with the whole of g, the smaller fringes are weakened or wiped out. Thus the inner edge of the nearer grating with successive parts of the further grating is chiefly effective in the production of these interferences.

To bring the two edges quite together was not possible in my work, as they were rough and the apparatus improvised.

56. Data.—Some measurements were attempted with the view only of checking the equations presently to be deduced. The adjustment on an ordinary spectrometer is not firm enough and the fringes being very fine (a few minutes of arc) are difficult to follow unless quite stationary.

Table 18, however, gives both the values of de/dn, displacement per fringe, for different angles of incidence i and of diffraction θ, and $d\theta/dn$, the angular deviation per fringe at the D line. In measuring the latter it was necessary to count the fringes between the C and D lines and divide their angular distance apart by these numbers. As e can not be measured, its successive increments Δe from the first position are given. These are presently to be associated with the corresponding increments of $dn/d\theta$.

TABLE 18.—Values of $d\theta/dn$, etc. $i = 53° 15'$. $D = 200 \times 10^{-6}$ cm.

Observed.						Computed.			
No. of fringes	θ and θ'	$d\theta/dn$	$dn/d\theta$	$\Delta dn/d\theta$	Δe	At θ $\Delta dn/d\theta$	At θ' $\Delta dn/d\theta$	Mean $\Delta dn/d\theta$	Region.
120	30° 27′	1′ 17″	3080	1130	0.025	1260	1028	1140	Between C and D lines.
75	28 14	1 46	1950						
	Diff. 2° 13′								
90	29° 09′								
71	28 14	46	4438	1000	.025	1116	1027	1072	Near C line
55	Diff.	1 0	3438	1188	.050	....	....	....	
36	55′	1 32	2250		.075	....	....	....	
24	30° 27′	1 50	1875	1328	.025	1259	1196	1228	Near D line
41	29 43	1 4	3203						
	Diff. 44′								

57. Equations.—In fig. 38, L and L' represent a pair of corresponding white rays, reflected into R and R' and diffracted into D and D' at angles i and θ, respectively. The half gratings g and g' are separated along the crack S, and g' is movable parallel to itself by a micrometer screw normal to g'. Let the normal distance apart of the gratings be e. The incident rays L, L' strike the originally coplanar grating at points N rulings apart,

or ND cm. apart, if D is the grating space. In the separated grating let these points be at a distance c apart. Let d (the broken line ia) be the incident wave-front and h the corresponding diffracted wave-front and call the angle between c and d, γ.

When there is reinforcement the path difference of the rays L and L' from the incident (d) to the diffracted (h) wave-front, may be

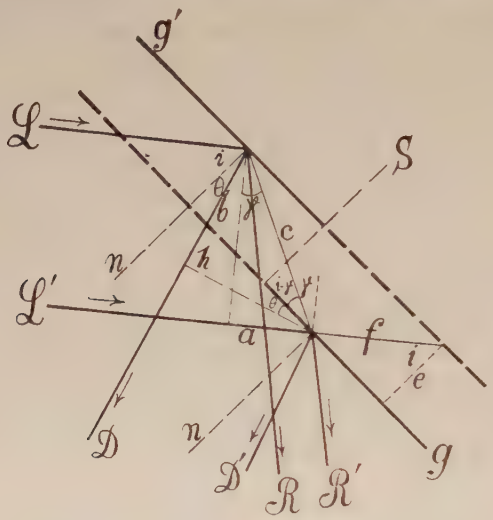

FIG. 38.—Diagram showing production of interferences from two identical nearly coplanar gratings, with rulings parallel to slit. Details.

written $n\lambda = b - a$, where b and a are the distances of h and d from the points of incidence of L and L' on the grating g and g' respectively. If, finally, f is the length of the prolongation of L' between the gratings we may write in succession

(1) $$d = ND \cos i$$

(2) $$f = e \sec i$$

(3) $$a = ND \sin i - e \sec i$$

(4) $$\tan \gamma = a/d$$

(5) $$C = ND \cos i \sec \gamma$$

(6) $$b = c \sin (i + \theta - \gamma)$$

To these should be added

(7) $$dN/de = \tan i/D$$

Hence after removing γ and arranging

$$n\lambda = ND \left\{ \cos i \sin (i+\theta) - \sin i \cos (i+\theta) - \sin i \right\} + e \sec i \,(1 + \cos (i+\theta))$$

which reduces to

$$n\lambda = ND(\sin\theta - \sin i) + e\sec i\,(1+\cos(i+\theta)),$$

or since

$$\sin i - \sin\theta = \lambda/D$$

finally

$$(8)\qquad (n+N)\lambda = e\frac{1+\cos(i+\theta)}{\cos i} = \frac{2e\cos^2(i+\theta)/2}{\cos i}$$

This must therefore be regarded as the fundamental equation of the phenomenon. Equation (7), however, leads on integration to

$$(9)\qquad N = e\tan i/D + N_0,$$

where $N_0 D$ is the width of the crack.

If the value of N from (9) be put into (8), together with the equivalent of λ/D, it appears after reduction that

$$(n+N_0)\,\lambda = e(\cos i + \cos\theta) = 2e\cos\frac{i+\theta}{2}\cos\frac{i-\theta}{2}$$

The case of $N=0$, $e>0$ would correspond to the equation

$$(10)\qquad n\lambda = e\,(1+\cos(i+\theta))/\cos i = 2e\cos^2\frac{i+\theta}{2}/\cos i$$

which is only a part of the complete equation (8). For $i>\theta$, one active half, kh, is necessarily partly behind the other half, $k'h'$, and therefore not adapted to bring out the phenomenon as explained, unless $e=0$.

58. Differential equations. Displacement per fringe, de/dn.—To test equation (8) or (10) increments must be compared. The latter gives at once, since N is constant relative to e like i, θ, and λ,

$$(11)\qquad \frac{de}{dn} = \frac{\lambda}{\cos i + \cos\theta} = \frac{\lambda}{2\cos\frac{i+\theta}{2}\cos\frac{i-\theta}{2}}$$

which is the interferometer equation when the fringes pass a given spectrum line, like either D line, which is sharp and stationary in the field. Equations (7) and (11), moreover, give after reduction

$$(12)\qquad dN/dn = \tan i\tan\frac{i-\theta}{2}$$

Table 18 contains values of de/dn computed from (11), made under widely different conditions ($i>\theta$, $i<\theta$, first and second order). The agreement is as good as the small fringes and the difficulty of getting the grating normal to the micrometer screw in my improvised apparatus admit. If this adjustment is not perfect N_0 changes with e. From equation (12), moreover,

$$(12')\qquad \frac{dN}{dn} = \frac{dN}{d\theta}\frac{d\theta}{dn} = \frac{dN_0}{d\theta}\frac{d\theta}{dn} = \frac{dN_0}{dn}$$

since N_0 is constant only relative to e when θ varies.

59. Deviation per fringe, etc., $d\theta/dn$, $d\theta/de$.—These measurements are still more difficult in the absence of special apparatus, since e is not determinable and the counting of fine flickering fringes is unsatisfactory; but the order of results may be corroborated by observing the number of fringes between two Fraunhofer lines, like the C, D, and other lines used. Differentiating equations (8) and (10) for variable n, λ, θ, and N (since $dN/d\theta$ is equal to $dN_0/d\theta$, equation (12′)) and inserting $-D\cos\theta\, d\theta/dn = d\lambda/dn$, it follows after arranging that

$$\frac{d\theta}{dn} = \frac{\lambda^2}{eD}\frac{1+dN/dn}{1+\cos(i+\theta)} = \frac{\lambda^2}{eD}\frac{1}{\cos i\,(\cos i+\cos\theta)} \tag{13}$$

or

$$\frac{d\theta}{dn} = \frac{\lambda}{e\cos i}\tan\frac{i-\theta}{2}$$

Combining this with (11)

$$\frac{d\theta}{dn} = \frac{\lambda}{eD\cos i} = \frac{\sin i-\sin\theta}{e\cos i} \tag{14}$$

Since, in equation (13), e is not determinable, it is necessary to compare increments $\Delta dn/d\theta$ in terms of the corresponding increments Δe, whence

$$\Delta(dn/d\theta) = \left(\cos i/\lambda\tan\frac{i-\theta}{2}\right)\Delta e \tag{15}$$

Table 18 also contains data of this kind computed separately for the Fraunhofer lines, D, C, etc., employed and their mean values. To find the mean width of fringes between these lines, their angular deviations were divided by the number of fringes counted between them at different values of e. The results agree as closely as the difficulty of the observations warrants. One may note that without removing N, the corresponding coefficients would be $\Delta d(n+N)/d\theta$, and these are much more in error, here and in the preceding cases. If from $d\theta/dn$, e is eliminated in terms of $(n+N)$ the equation is

$$\frac{d\theta}{dn} = \frac{\lambda}{D}\frac{1}{(n+N_0)\cos i} \tag{16}$$

so that for a given value of i, θ, N_0, they decrease in size with n. If $n=0$, they reach the limiting size

$$\frac{d\theta}{dn} = \frac{\lambda}{DN_0\cos i}$$

If the crack N_0D should be made infinitely small, they would be infinitely large. To pass through infinity, N_0 must be negative, which has no meaning for $i>\theta$, or would place one effective edge of the crack S behind the other. These inferences agree with the observations as above detailed. If, however, $i<\theta$, a negative value of N_0 restores equation (16) for $n=0$ to equation (17), as was actually observed (figs. 35 and 36).

Finally, equation (14) might be used for observation in the incremented form

$$\Delta(de/d\theta) = \frac{D \cos i}{\lambda} \Delta e \tag{17}$$

but I did not succeed with it. One loses track of the run of a fringe with *de*.

60. Colored slit images and disk colors of coronas.—In the above experiment the fringes were but a few minutes apart. It is obvious, however, that if N_0 is sufficiently small the fringes will grow with decreasing n, in angular magnitude, until there are but a few black bands in the spectrum. Under these circumstances, the undeviated image of the superimposed slits must appear colored, particularly so if an effect equivalent to N_0 is present throughout the grating. This phenomenon of colored slits is apparently of interest in its bearing on the theory of coronas, where there is also an interference phenomenon superimposed upon a diffraction phenomenon, as is evidenced by the brilliant disk colors. For instance, suppose a corona were produced by a sufficient number of fog-particles distributed throughout a plane normal to the undeviated rays. Now let the alternate particles be moved *in the same way* slightly to the rear of their original position and let the distance between the two planes be small relatively to the wave-length of light. In such a case there should be two identical coronas, superimposed in all their parts, and they should therefore interfere. Inasmuch, however, as even small fog-particles are of the order of size of 0.0001 cm. and their mean distance apart 50 times larger, *i.e.*, 0.005 cm., it remains to be proved whether such an effect can be looked to as an explanation of the disk colors of coronas.

CHAPTER VII.

INDEPENDENCE OF CORONAS OF THICKNESS OF THE FOG-LAYER.

61. Introductory.—As an adequate theory of coronas is yet to be given, experiments with a definite bearing on the various features of the phenomenon are desirable. In earlier work* I endeavored to elucidate the character of the interference phenomenon superimposed on the diffraction phenomenon, whereby the disks of coronas with white light eventually show a rhythmic succession of colors. A theory was suggested corresponding to that given by Verdet for the lamellar grating. Inferences so deduced were quantitatively in accord with facts. I showed that the reappearance of the same type of corona corresponds to a succession of diameters of fog-particles in the order of the natural numbers $n = 1, 2, 3, 4$, etc. Further, in a survey of coronas obtained with monochromatic light (mercury), it appeared that the disk and the first ring are alternately luminous in a way corresponding to the interference phenomenon in question. Finally, that in case of even the largest true coronas fog-particles of an order of size greater than 10^{-4} cm. were in question, beyond which the corona degenerates into a mere fog.

In a preceding paper† I touched upon the question of the interference of coronas due separately to two successive layers of fog-particles normal to the line of sight, with each other, but the quantitative relations did not seem to be as promising as interferences inferred from the mere thickness of fog-particles, already alluded to in comparison with the lamellar grating.

62. Effect of thickness. Apparatus.—From the point of view of the elementary theory the effect of the thickness of the fog-layer should be negligible; but it does not by any means follow that this is actually the case. In very many experiments with coronas the thickness of the fog-layer is not at the observer's disposal or cases of different thicknesses have to be compared. Hence the following experiment was devised with the object of definitely testing the question:

In fig. 39 FF' is a cross-section of the fog-chamber, a long rectangular trough of wood, cloth-lined and provided with two glass plates g and g' on the broad sides of the trough. The pool of water is seen at w. Two mirrors M and M', of plate glass, horizontally hinged at h and h' and capable of being displaced parallel to their own plane by virtue of the screw-extension

* See Publication No. 96, Carnegie Institution of Washington, Part I, 1908; Part II, 1910. American Journal of Science, XXIV, pp. 309–312, 1907 (cycles of coronas); *ibid.*, XXV, p. 224, 1908 (axial colors); *ibid.*, XXVII, pp. 73–81, 1909 (mercury light).

†*Cf.* Proc. Am. Phil. Soc., April, 1911.

adjustment s and s', are attached parallel to each other. The lower margin of M is somewhat above the upper margin of M'. Hence the observer on the left of the apparatus (in front) sees the direct rays $A\ A'$ from the source as well as the reflected rays $B\ M\ M'\ B'$. By properly adjusting the angle α, the small round distant source of white light and its image in the mirrors (A' and B' respectively) may be made to coincide at the upper edge of M'. In such a case the corona due to the direct rays produced by a single thickness, $d = 15.5$ cm., of fog-layer, should exactly coincide with, *i.e.*, be the complement of, the coronas due to the reflected rays and produced by a triple thickness, $d' = 46.5$ cm., of fog-layer, if the variation of thickness in question is without effect. Otherwise the coronas should be dislocated at the margin of the mirrors.

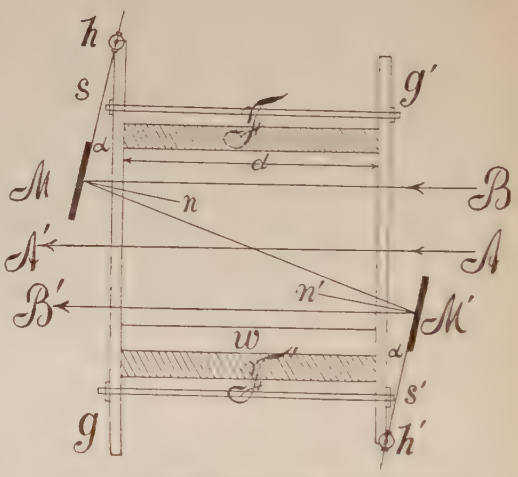

FIG. 39.—Cross-section of fog-chamber, showing path of direct and reflected rays.

63. Results and summary.—These experiments were carried through in regular series, for the dust nuclei of ordinary air as well as for an artificial nucleation due to phosphorus. The exhaustions were made systematically every 2 minutes. The coronas due both to the A rays (direct) and the B rays (reflected) were read off as quickly as possible, after which filtered air was introduced to dispel the coronas by evaporating the fog-particles. In this way about 20 coronas were successively compared, from the largest easily observable, having an aperture of about 34°, to the small ones of vanishing size, the nucleation ranging from about 10^6 to zero (particles per cubic centimeter) and the fog-particles from a diameter of about 2×10^{-4} cm. to 10^{-3} cm.

In no case was there any dislocation of coronas, or of color, detected, though naturally the coronas in case of reflection from the mirrors were somewhat more yellowish in color (due to the reflecting surfaces) and less vivid (due to the reflections and greater thickness of fog-layer; for it is hardly probable that the fog-particles are quite of a size). The continuity of corresponding colored rings, however, was exact within the limits of observation. Hence thicknesses of 15 cm. and over 46 cm. produce identical coronas identical in aperture; or the thickness of the cloud-layer is without influence on the coronas.

CHAPTER VIII.

EXPERIMENTS WITH A VERY SMALL FOG-CHAMBER, TOGETHER WITH DATA ON THE DECAY OF LARGE AND SMALL NUCLEI.

64. Small fog-chamber.—Tables 19 and 20 contain results with exceptionally small fog-chambers in relation to the size of the vacuum-chamber and the diameter of the connecting tube. They are compared with the data of the smallest of the fog-chambers recently* observed. The dimensions of the cylindrical chambers of glass were, respectively, length 20 cm., diameter 6.5 cm. for the pint chamber and length 16 cm., diameter 11 cm. for the quart chamber, both attached to a 2-inch brass exhaustion pipe 15 cm. long.

TABLE 19.—Small (quart) fog-chamber. $l = 16$ cm.; $r = 5.5$ cm.; cleaned with 8 exhaustions; vapor nuclei and x-ray effect; barometer 76.40 cm. at 24.5°; n in the exhausted F. C.

	$\frac{\delta p}{p}$	cor. s	$n \times 10^{-3}$		$\frac{\delta p}{p}$	cor. s	$n \times 10^{-3}$
Vapor nuclei	0.203	0.0	0.0	Vapor nuclei	0.383	*y o* 15	773
	0.220	0.0	0.0		0.357	6.1	50
	0.249	0.0	0.0		0.343	4.3	18.3
	0.275	0.0	0.0		0.327	2.9	5.0
	0.291	2.0	1.4		0.304	2.4	2.9
	0.307	2.5	2.9		0.290	2.0	1.5
	0.327	3.5	8.5	Ions (x-rays)	0.210	0.0	0.0
	0.333	4.0	14.2		0.250	1.0	0.2
	0.345	4.4	19.7		0.275	*y o* 13.0	425
	0.356	5.8	41.2		0.301	*g* 17	825
	0.367	8.5	136		0.321	*v* 19	1310
	0.380	12.2	417		0.334	*r* 20	1620
	0.393	*g* 16.7	1087		0.304	*v* 19	1260
	0.393	*g* 17.5	1290		0.268	*r* 10.2	186
	0.410	*v* 18.5	1570		0.253	2.3	2.1
	0.415	*v* 18	2180		0.244	1.0	0.2
	0.435	*r*	2740				
	0.487	*r o* 21	3760				

The results computed in the usual way are given above, $s/30$ denoting the approximate angular diameter of the coronas, δp the drop of pressure, n the number of nuclei per cubic centimeter in the exhausted fog-chamber. The goniometer in this case was a special contrivance shown in fig. 40, in which the eye was at the near wall of the fog-chamber and the needles for measuring angles beyond the far wall. This makes it possible to use small fog-chambers and yet measure large apertures.

* *Cf.* Publication No. 96, Carnegie Institution of Washington, Part II, §27 *et seq.*, 1910.

The results contained in these tables show curiously enough that for smaller exhaustions the small fog-chamber is more efficient than the larger fog-chamber (fig. 41), but at larger exhaustions (δp) the reverse is the case (figs. 42 and 43). Similarly, or compatibly with this result, ions are more easily caught by the small fog-chamber than by the large chamber, whereas the finer vapor nuclei are more easily caught by the larger chamber. In both cases the number caught increases with the exhaustion (δp), continually. The upper coronas of the pint chamber, however, are not brilliant in color and they are diffuse in character. The goniometer measurement nevertheless shows very definite increase of aperture for increased exhaustion, even throughout the same color or type of corona. It follows, then, that increased exhaustion must continually bring down more water, even at the highest exhaustion used. The number of nuclei eventually caught approaches 5 million per cubic centimeter.

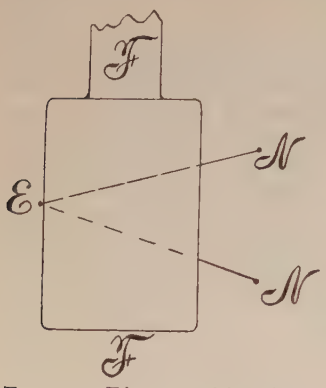

FIG. 40.—Diagram of fog-chamber and straddling goniometer.

The above results are difficult to discuss. It is, however, probable that

TABLE 20.—Pint bottle fog-chamber; length 20 cm. (glass*) and 15 cm. brass, radius 6.5 cm.; cleaned with 17 exhaustions. Vapor nuclei found in ascending and descending exhaustions; barometer, 75.87 cm. at 27.5°; new (straddling) goniometer, n in exhausted F. C.

	$\frac{\delta p}{p}$	cor. s	$n \times 10^{-3}$		$\frac{\delta p}{p}$	cor s	$n \times 10^{-3}$
Vapor nuclei	0.257	?	0.0	Ions (x-rays)	0.230	0.0	
	0.278	?	0.0		0.248	0.0	0.0
	0.299	1.5	.5		0.270	*c* 12	325
	0.328	3.0	5.4		0.290	*c* 18	1100
	0.353	*g* 7.0	76.8		0.311	*r* 20	155
	0.360	*vb* 10.0	217		0.373	*r* 24	3210
	0.369	*g* 14	600		0.443	*y'* 26	450
	0.385	*g'* 16	980		0.305	*r* 20	1520
	0.401	*c* 18	1310		0.276	*g*	708
	0.414	*c* 18.5	1570		0.261	*r* 9	123
	0.432	*r'* 19	1771		0.250	4.0	11.4
	0.457	*r'* 20	2140		0.244	.0	
	0.490	*r'* 22	2910	Vapor nuclei	0.263	faint 1.0	.2
	0.540	*r'* 24†	3990		0.296	2.0	1.5
	0.418	*c* 17	1335		0.346	5.0	27.1
	0.390	*g*	876		0.361	10.0	214
	0.373	*o* 14	603				
	0.343	*r* 6.2	51				
	0.325	3.5	9.0				
	0.303	3.0	5.2				
	0.282	.0	.0				

*Brass pipe not included.
†Aperture of r' continually increasing, coronas diffuse.

as the fog-chamber becomes smaller, the rapidity of radiation from without inward increases conformably with the smaller bulk of air adiabatically

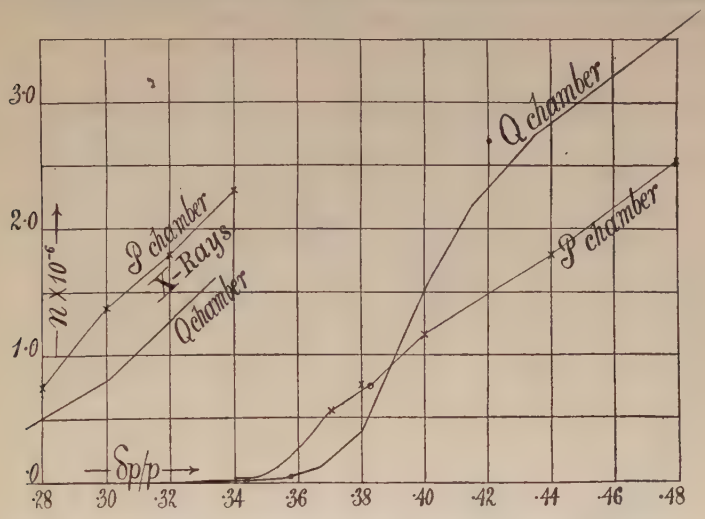

FIG. 41.—Number, n, of nuclei per cubic centimeter, caught at different exhaustions, in case of pint and quart fog-chambers.

cooled by sudden exhaustion; or, other things being equal, that conditions favorable to the attainment of a high degree of adiabatic cooling are more

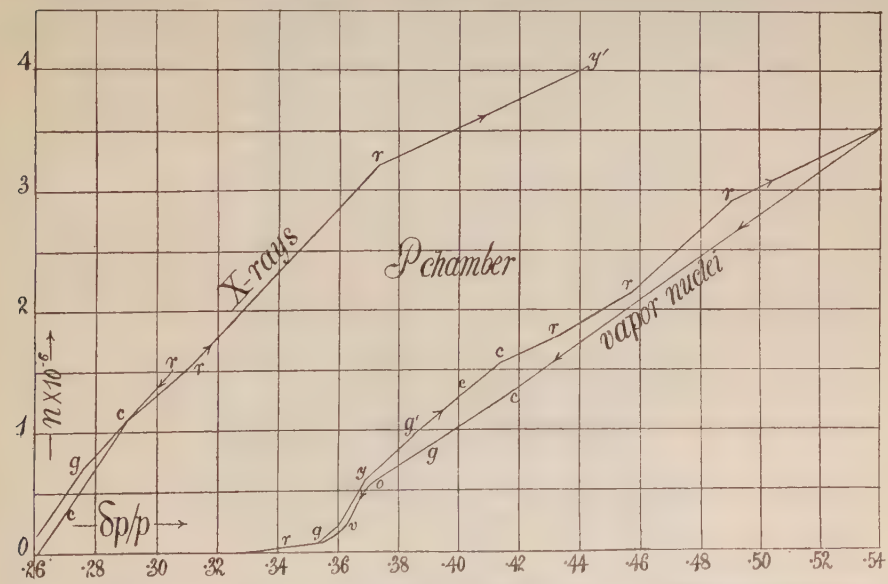

FIG. 42.—Number, n, of nuclei per cubic centimeter, caught at different exhaustions, in cases of pint and quart fog-chambers.

easily met, in proportion as a larger bulk of air is cooled. On the other hand, however, the increased bulk is more difficult to exhaust with ade-

quate rapidity. In case of the quart fog-chamber in comparison with the pint fog-chamber, each with an identical 2-inch exhaustion pipe, these transitional relations seem to be manifest in the experiments made.

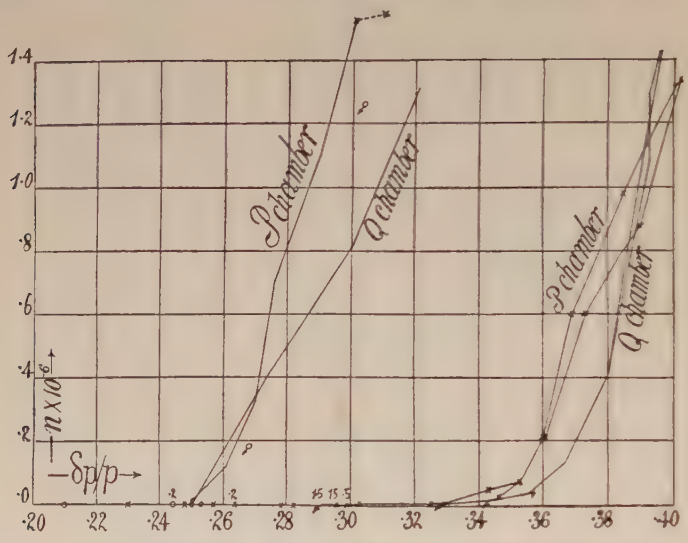

FIG. 43.—Sudden drop of pressure δp from total pressure p.

65. Decay of different sizes of ions.—A second series of experiments into which I entered at some length and which, though from the nature of the experiment they can not lay claim to a high order of precision,

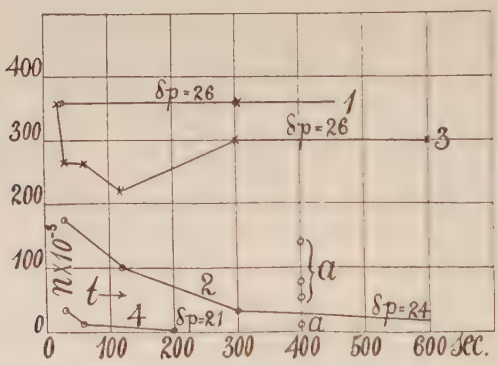

FIG. 44.—Number of nuclei per cubic centimeter in the lapse of time, after cut-off of X-radiation, for different drops of pressure δp; a, vapor nuclei belonging to series 1 and 3.

nevertheless lead to very definite results, is contained in tables 21, 22, and 23. These ions were produced by X-rays (of moderate intensity) in an aluminum-covered fog-chamber with short exposures to an X-ray bulb and a glass fog-chamber. The data show that no persistent nuclei of the

usual large type are appreciably produced, since if present they require almost no supersaturation of moist air for condensation. Moreover, the vapor nuclei of dust-free wet air are not caught in the presence of ions, or else their number is specially determined and smaller in comparison

TABLE 21.—Rate of decay for different sizes of ions. Aluminum-covered fog-chamber.

$\delta p/p$	t Lapse sec.	$n \times 10^{-3}$	$b \times 10^{6}$	$r \times 10^{7}$
0.35	D. f. air	77		0.43
	30	360		
	300	360		
	D. f. air	140		
0.32	D. f. air	9.5	0.10	0.48
	30	175		
	120	100		
	300	31		
0.35	30	360		0.43
	D. f. air	54		
	30	265		
	60	265		
	120	220		
	300	300		
	600	300		
	D. f. air	140		
0.28	30	33	2.0	0.60
	60	12		
	60	12		
	200	2.3		

TABLE 22.—Decay of different sizes of ions.

$\delta p/p$	t Lapse sec.	$n \times 10^{-3}$	$b \times 10^{6}$	$r \times 10^{7}$
0.26	0	73.8	43	0.66
	30	0.9		
	15	1.3		
0.28	0	484	2	0.61
	30	15.7		
0.30	15	32.8	3	0.54
	60	6.4		
0.33	15	36.8	0.4	0.48
	60	29.7		
	30	29.7		
	120	21.8		
	240	6.2		
	D. f. air	4.4		
0.35	15	55.0	0.1	0.43
	30	113.5		
	60	86.7		
	120	55.0		
	240	38.8		
	D. f. air	31.3		

with the ions obtained by the X-rays. This premised, the tables give the relative drop of pressure $\delta p/p$ from p, and the lapse of time t between the instant the X-radiation is cut off and the instant of the exhaustion made to catch ions, together with the number of nuclei, n per cubic centimeter, caught. The column r is an estimate of the size of nuclei obtained from the drop of pressure δp and b is the rate of decay.

In table 21, reproduced in fig. 44, the nucleation discovered in dust-free wet air at any $\delta p/p$ in the absence of X-radiation is always relatively small, even at the highest exhaustions made (see points a in figure).

TABLE 23.—Decay of different sizes of ions.

$\delta p/p$	t Lapse sec.	$n \times 10^{-3}$	$b \times 10^{6}$	$r \times 10^{7}$
0.26	0	39.6	30	0.66
	30	1.1		
0.28	0	378	3	0.61
	30	12.4		
0.30	30	16.8	4	0.54
	60	6.4		
	120	2.4		
	0	630		
0.33	30	24.8	0.5	0.48
	60	57.6		
	120	26.1		
	240	9.1		
	30	24.8		
	D. f. air	5.5		
	60	47.0		
	*30	34.8		
0.35	30	109.2	0.1	0.44
	60	79.7		
	120	51.7		
	240	46.1		
	D. f. air	34.7		

* Aluminum screen on.

Nevertheless, in the first and third series the persistence of ions surviving as much as 10 minutes after exposure is remarkably large, as if all nuclei (vapor nuclei and ions) were eventually caught together. Series 3 passes erratically through a minimum, but nevertheless points to an almost indefinite persistence throughout. On the other hand, at the lower exhaustion, series 2 and 4, the number of nuclei soon vanishes. The rates of decay determined by the usual equation

$$\Delta \frac{1}{n} = b\Delta t \text{ or } dn/dt = -bn^2$$

in series 2, however, are usually less than $b = 10^{-7}$. In series 4 the rate would be about $b = 2 \times 10^{-6}$, but too few nuclei are present for certainty of measurement. The chief interest lies in series 1 and 3, showing that at

a sufficiently high drop in pressure, $\delta p/p = 0.35$, the ions produced in dust-free moist air by the X-rays decay at phenomenally small rates, or are almost indefinitely persistent, whereas larger nuclei decay faster in proportion to their size.

Similar facts are brought out by tables 22 and 23, constructed on the same plan and showing the drop of pressure δp from the total pressure p, from which the radius r of the drop is estimated. The nucleation n is given after the lapse of seconds t since the X-radiation ceased. From this the coefficient of decay b is computed. Both tables show that as $\delta p/p$ decreases or r increases, b increases at a rapidly accelerated rate, from very small values $b = 10^{-7}$, to enormous values. The small coefficient b is less than one-tenth the normal value obtained for ions with the electrometer (of the order of 10^{-6}), while the large values are nearly 50 times the normal value.

The interpretation of these results is made difficult by the variability of the X-ray bulb. It is safe to assert, however, that the large ions or nuclei produced by the X-rays in dust-free wet air vanish with relatively enormous rapidity, whereas the very small nuclei are almost indefinitely persistent, and that there is a definite relation between the rate of decay and the size of nucleus. If, therefore, we regard these nuclei as water droplets of different sizes, evaporation is rapid until a limiting diameter depending on the intensity of radiation is reached, after which evaporation nearly ceases. It is also probable, and will be further brought out in the next chapter, that the limiting diameter increases with the intensity of radiation. If, therefore, as has been supposed, the X-rays produce any chemical body which may go into solution, the greater or less abundance of this body, supplied by greater or less intensity of X-radiation, would account for larger or smaller persistent nuclei. The next chapter is a further contribution to this question.

CHAPTER IX.

ON THE PERSISTENT NUCLEI PRODUCED BY THE X-RAYS.

66. Introductory.—Throughout many of my experiments on condensation* and particularly during the earlier work,† I made use of a fog-chamber impregnated, when hot, with a mixture of wax and Burgundy pitch. These chambers were usually of an elongated rectangular form, with plates of glass on the opposed broad sides, cemented on, while hot, with an intervening layer of flat cotton wick saturated with the same molten mixture, and allowed to cool under pressure. Wooden clamps on the outside are a safeguard against any yielding due to the viscosity of the cement. Such fog-chambers may be made rigorously tight and they last for years, even when charged with water. The coronas are strong (the fog-layers being thick), visible without distortion and measurable throughout their extent, even when approaching 50° of aperture with a 6-inch stratum of fog-particles, or more.

These fog-chambers have the additional advantage of being exceedingly pervious to soft X-rays, and hence throughout my work I encountered the phenomenon of persistent nucleation, produced in dust-free wet air by the X-rays, when acting continuously for a period of minutes. I can not but think that the occurrence of persistent nuclei, as an accompaniment of an adequately strong and adequately prolonged X-radiation, are an important property of these rays. It would ally them in quality with ultra-violet light, with which C. T. R. Wilson‡ and others obtained similar results. The present observations would, therefore, have some bearing on the probability of the pulse theory, which has recently been put seriously on the defensive by Prof. H. Bragg.§

Again, if it is true that beyond a certain density of ionization (a sufficient number of ions per cubic centimeter) the ions invariably react on each other, or on the wet dust-free medium, to produce permanent nuclei of enormous size by any method whatsoever, this fact is itself a result of importance.

Nevertheless, these effects of X-light have not always been taken seriously. Thus, for instance. Mr. C. T. R. Wilson‖ states: " . . . . results, obtained with a chamber of wood impregnated with resinous cement and not rigorously shielded from all possible direct electrical effects from an

* Publication No. 62, Carnegie Institution of Washington, pp. 18–21, 1907.
† Am. Journ. of Sci., XIX, pp. 175–184, 1905; Publication No. 40, Carnegie Institution of Washington, pp. 1–16, 1906.
‡ C. T. R. Wilson, Phil. Trans., A, vol. 192, pp. 412 *et seq.*
§ Nature, vol. 85, p. 491, 1911.
‖ C. T. R. Wilson, Nature, vol. 74, p. 620, 1906.

X-ray bulb placed a few centimeters from it, are not free from ambiguity." Criticism of this kind, it seems to me, is quite gratuitous; for it is the first thing anybody under such circumstances would try for himself, viz, to see whether discrepancies due to electro-static or other induction or to resonance are really absent. To do this it is merely necessary to place a tin plate before the bulb, whereupon no persistent nuclei are obtained at all comparable with the yield of nuclei through an identical aluminum plate. Naturally I repeatedly shielded the whole apparatus; but apart from this Wilson knows, for he made this experiment, as I also did, that a fog-chamber damp within shields itself. I doubt whether it need even be cloth-lined, as mine always were. Here I would also like to add a word in defence of the above type of fog-chamber. If there were within any source of nuclei whatsoever, that fact could not escape detection; for the chamber must be rigorously and permanently dust-free before any experiments can be tried with it.

Again, in a controversy with G. C. Simpson,* Wilson† remarks:

> It is quite true that spark discharges in air, as well as other ionizing processes which are accompanied by chemical effects, do produce large persistent nuclei in addition to the ordinary ions; a lightning-flash would, therefore, almost certainly produce such nuclei.

As to spark discharge Wilson says (Phil. Trans., *l.c.*, p. 439): "No condensation nuclei were produced except when the point of wire was luminous when viewed in the dark." Wilson's evidence is, therefore, in turn ambiguous as to large nuclei produced from ions, for to draw such an inference he should first sift out the metallic particles transferred. Furthermore, the action of ultra-violet light, which produces persistent nucleation similar in character to that in question, is not a normal ionizing process, even if slow-moving ions are produced. So far as I can see, the only unambiguous ionizing process productive of persistent nuclei is given by my experiments with X-rays which Wilson has not only not acknowledged, but done his best to discredit. It is true that in the meantime E. Barkow,‡ in Professor Richarz's laboratory, succeeded in corroborating the fact that persistent nuclei are produced by X-light, but as he worked with an aluminum screened glass fog-chamber, he was obliged to use X-radiation pushed to the limit of intensity.

In view of this unsatisfactory state of the case, I have on two occasions incidentally resumed the experiments for persistent nuclei, once about a year ago, and again quite recently. I used an ordinary 4-inch spark coil energized by 6 or 7 storage cells and a Foucault interrupter. The common X-ray bulbs 4 inches in diameter, or even the smaller bulb 3 inches in diameter, functioned equally well. They were placed above or at the end of the long rectangular fog-chamber, the conventional earthed screen of tin plate, with a hole in it 4 inches in diameter, covered with aluminum foil,

* G. C. Simpson, Phil. Mag., XVII, p. 619, 1909.
† C. T. R. Wilson, Phil. Mag., XVII, pp. 634–641, 1909; *cf.* 640.
‡ E. Barkow, Inaugural Dissertation, Marburg, 1906.

being interposed for safety. To close this hole with a tin plate, or even a glass plate in the case of the coil specified, is to cut off all effects so far as the production of persistent nuclei is concerned. Ions, of course, are still produced in abundance. The time of exposure was usually about 2 minutes and the lapse of time prior to exhaustion thereafter usually 1 minute. As a rule, the exhaustion was such as would not catch ions, so that exhaustion could be made if necessary even during exposure.

67. Older series of experiments.—A brief digest may be given of the work of last year. The endeavor to further identify the persistent nuclei was begun with the normal cylindrical glass fog-chamber and the old X-ray bulbs Nos. 0 to 4 heretofore described (*l.c.*). The chamber may be cleaned with a rubber probang and the cap is to be earthed. Aluminum jackets were provided for the body. No effect was obtainable for exposures of 2 minutes and longer. The chamber was then tested with the walls dry, with an absence of earth connection, with aluminum tubes and brass tubes within, with long exposures up to 5 minutes, all to no effect. Persistent nuclei were not producible. Only once, in a first experiment, with the vibrator not quite normal in action, I obtained about 25,000 nuclei per cubic centimeter through glass. The experiment could not be repeated. Cold bulbs were as inefficient as warm bulbs. The X-ray bulbs were then softened till the anodal light appeared and then successively sparked to hardness. No effect was observable. Meanwhile all the bulbs showed good shadows on a fluorescent screen.

The small glass fog-chamber was now installed, but no further success was obtainable. The failure to obtain persistent nuclei through glass contrasts strangely with the marked results obtained on an earlier occasion.* The difference may be due either to a more efficient bulb, or to a thinner fog-chamber used in the latter case. But a full explanation is yet to be found.

Persistent nuclei were not again detected until the wood fog-chamber described (45 by 15 by 15 cubic centimeters) was installed, with the X-ray bulb at a distance of about $D = 10$ cm. above it. Here bulb No. 4, for a two-minute exposure and a thirty-second lapse, gave at once 89,000 nuclei per cubic centimeter, repeatedly and strong. The wood fog-chamber was now encased in aluminum above and with tin plates on the sides and end, with an apparently even greater advantage in the production of persistent nuclei. Thus, for instance, 165,000 nuclei per cubic centimeter were obtained, after a lapse of 1 minute succeeding an exposure of 2 minutes; while a tin plate on top (completing the tin case) absolutely removed all action. The persistent nuclei are thus due to X-radiation and not to induced or Herzian effects. The coronas are characteristic, being heavy with much rain, and the second exhaustion, for cleaning, frequently shows larger

* Publication No. 62, Carnegie Institution of Washington, p. 18, 1907.

coronas than the first. Spontaneous generation of nuclei during long exposure could not be detected. A trial of the available bulbs under like circumstances, for efficiency, showed (n nuclei per cubic centimeter)

No. 0, $n=0$	No. 2, ——	No. 4, $n=90{,}000$–$165{,}000$
No. 1, $n=26{,}000$	No. 3, $n=1{,}600$	

so that only bulbs No. 1 and No. 4 were good producers of persistent nuclei, at a distance of 10 cm. from the fog-chamber.

Next day, however, the effect of No. 4, for the same distance, $D=10$ cm., had materially weakened, as if the dampness had penetrated the wood until it became all but impervious. The results, for an exposure of 3 minutes, were, for instance,

No. 0, $n=0$	No. 2, $n=14{,}000$	No. 4, $n=6{,}000$
No. 1, $n=20{,}000$	No. 3, $n=0$	

No. 1 with longer exposures, 5 minutes, gave 35,000 nuclei for all lapses of time. The further trial to soften No. 3 was ineffectual, and continued so after sparking to hardness. In the pursuit of this group of experiments, bulbs Nos. 1, 3, and 4 gradually became inefficient. Cooling with water, variations at the interrupter, etc., did not improve the results. The fog-chamber seemed to gradually shut off radiation coming from a distance of 10 cm., and the bulbs deteriorated.

The top of the fog-chamber was now covered with thin aluminum 0.05 cm. thick and the X-ray bulbs were placed close to it, so that the distance, D, was now reduced to zero. The production of persistent nuclei was again strong, No. 4 after an exposure of 2 minutes, for instance, showing 46,000 nuclei, in many successive experiments. Secondary radiation from lead, etc., produced no result.

Summarizing the above experiments, it appears that all bulbs lose the power of producing persistent nuclei after continued use. They soon cease to penetrate glass or even wood from a distance. Close up to the wood walls, however, the effect (through an aluminum screen for safety) is always marked. A wood fog-chamber aging in damp air seems to grow continually less pervious, or dry wood is superior to damp wood. The test showing that an aluminum-covered chamber is pervious, whereas a tin-covered chamber is not so, is sufficient to guarantee the radiation effect, as compared with possible discrepancies due to induction and resonance. So also is the difference in the efficiency of bulbs. Secondary radiation is powerless to produce persistent nuclei. Spontaneous generation could not be detected in these experiments.

68. Recent experiments.—The two fog-chambers used were of wood. No. 1 had just been charged with water; the wood fiber, therefore, was dry within, whereas No. 2 had held a charge of water for about a year and the fiber was probably wet. As a result, No. 1 was found to be much more pervious than No. 2.

Table 24 gives an exhibit of the results, showing the fog-chamber and bulb used, the time of exposure, the time of observation (lapse) after exposure, the distance, D, between the outside of the bulb and the fog-chamber, the apertures of coronas, s, in the first and second exhaustions, and n, the corresponding nucleation. The corona of the first exhaustion was usually distorted and not measurable. The fog was allowed to subside completely, which it did almost at once, after which filtered air was introduced and a second identical exhaustion made. These second coronas are uniform, and in systematic work the first nucleation may, in a measure, be inferred from them. The column marked ions shows the number present under a sufficiently high exhaustion to catch them all. In this case the exhaustion is made during exposure, because of the rapid decay. The remarks refer to the presence or absence of the tin screen placed over the aluminum cover between bulb and fog-chamber to cut off radiation, to the character of the bulb used, etc. Some comparative experiments are made with radium, the available strength of which did not produce persistent nuclei. In the following paragraphs I shall give a brief description of the features of the phenomenon.

TABLE 24.—Results of experiments with persistent nuclei. Wood fog-chambers. $\delta p = 17$ cm. Fog-chamber within metal screen with Al below bulb. Coil with 6–7 storage cells.

I, BULBS (4″) OVER FOG-CHAMBER.*

Bulb No.	Exposure.	Lapse.	$n_1 \times 10^{-3}$	$n_2 \times 10^{-3}$	$n \times 10^{-3}$ (ions)	D	Remarks.
	min.	*min.*					
N	1	1	Fog.	17	....	0	
N	1.5	..	Fog. 64	37	....	0	
N	1.5	1	0	..	....	0	Tin shield on.
N	1.5	1	Fog.	59	....	0	Off.
N	1.5	2	Fog.	35	....	0	
7″ spark							
u	1	1	0	..	....	0	Very hard.
o	1.5	1	Fog.	12	....	0	
N	2	1	Fog.	10	....	0	
3	2	1	Fog.	37	....	0	
N	2	1	Fog.	17	....	0	
No evidence of soaking. Difference due to bulb and sparker. Fog-chamber changed. Soaked a year and more impervious. Quite tight.							
N	2	1	0.5	....	....	0	
U	4	1	2.6	....	....	0	Softened.
	4	1	9.5	....	....	0	
	10	1	39	....	....	0	
	10	1	39	....	....	0	
All the preceding facts brought out on smaller scale. Time of exposure important.							

*Fog-chamber not quite tight. Short exposure has no effect; acceleration on increase of time. All bulbs active unless too hard for energizing. First fog a whirlwind. Disk or strip of tin as large as bulb cuts off all effect.

TABLE 24—Continued.

II. BULB (4″) AT END OF FOG-CHAMBER.

First fog decreases to nothing from bulb to free end of chamber.

Bulb No.	Exposure.	Lapse.	$n_1 \times 10^{-3}$	$n_2 \times 10^{-3}$	$n \times 10^{-3}$ (ions)	D	Remarks.
	min.	*min.*					
N	2	1	Fog. 12	4	....	1	
N	2	1	Fog.	9	....	1	Tin jacket on.
N	2–3	1	Fog elliptic	10	....	1	
N	5	1	Fog. end to end	35	....	1	
N	5	1	0	....	....	1	Tin screen before bulb.
N	5	1	Fog. end to end	29	....	1	
N	5	1	Fog.	7	....	1	1½″ hole in screen
N	5	1	3	.6	....	1	¾″ hole in screen
N	5	1	0	....	....	1	½″ hole in screen
Tests made for persistent nuclei and ions at different distances, successively. Also with radium.							
N	5	1	10.8	16	670	1	
	5	1	20	1.6	530	4	X-rays
	5	1	1.2	....	400	10	X-rays
	5	1	.4	....	330	24	X-rays
I–V	....	....	....	....	130	..	Radium on side.
I–V	3 hours	....	....	....	270	..	Radium within.
Time effect (exposures).							
N	5	1	59	....	....	1	
	2	1	23	....	....	1	
	1	1	.3	....	....	1	
	5	1	0	....	....	1	Tin screen.
Time lapse after exposure.							
N	5	1	7	2.0 / 1.6	....	1	
	5	2	11	....	....	1	
	5	4	14	....	....	1	
	5	1	7	....	....	1	

III. SMALL BULB (3″) No. 2, AT END OF FOG-CHAMBER.

N	5	1	21	3	....	1	
2	5	1	Fog. 130	25	....	1	
2	5	1	0	....	....	1	Glass screen 15 cm. thick.
N	5	1	0	....	....	1	Do.

69. Initial fogs.—These are as a rule distorted as heretofore described,* and in a long fog-chamber with the bulb near one end they decrease in size from this to the other end, which is liable to be free from nuclei. Frequently, therefore, the nucleation must be estimated from the second corona, the cloud being precipitated on the nuclei not caught in the first exhaustion. The first nucleation may be three or more times larger.

But it is the whirlwind character of this first fog to which I wish chiefly to refer. It is quite dissipated in a relatively short time, precisely as if it were under the influence of a point discharge. True, the X-ray tube, if in action, is liable to make the surrounding atmosphere strongly negative; but that any electrification should exist on the fog-chamber, 2 or 4 minutes after exposure, is out of the question. In my apparatus the whole is kept permanently earthed through the metallic vacuum-chamber. Nevertheless, I most carefully jacketed the fog-chamber with tin during exposure, though the effect was obviously *nil*. I also supposed that the fog-particles precipitated on persistent nuclei might carry charge; but no evidence of this could be obtained. The whirlwind is, therefore, probably due to gravitational readjustment of very heavy fog-particles, precipitated on large persistent nuclei.

Another characteristic feature observed in the production of persistent nuclei is this, that the number per cubic centimeter increases at an accelerated rate with the time of exposure, for a fixed ionization. In other words, the number produced per second by exposure to X-rays increases with the number present. The condition is thus an inversion of the case of the decay of ions, and it is probable that a similar quadratic law, but with positive coefficients, will be applicable. Again, the accelerated production specified is sufficient evidence of generation of nuclei within the medium and not at the walls of the vessel.

Compatibly with this result, the number of the persistent nuclei caught increases, within certain limits, with the time elapsed after the given X-radiation ceases. Thus more are liable to be caught 2 minutes after exposure than 1 minute after exposure; and more 4 minutes than 2 minutes after. Observations of this kind were extremely difficult to make in a way quite trustworthy, because of the variability of the X-ray bulb, and I adduce the mean results of a large number of trials.

70. Amount of ionization needed to produce persistent nuclei.—The ionization, n per cubic centimeter, may be varied by placing the X-ray bulb at different distances, D, from the outside of the fog-chamber, and estimated at a sufficiently high exhaustion to catch them all, by aid of the coronas. The persistent nuclei (n per cubic centimeter) produced in a given time (5 minutes) under the same conditions are determined, in turn, by a correspondingly low exhaustion, after the lapse of 1 minute after exposure to the rays.

* Am. Journ., XIX, pp. 185–194, 1905.

The ionization thus must exceed at least 300,000 per cubic centimeter if a crop of persistent nuclei requiring scarcely any supersaturation to condense water-vapor is to be observable, within a few minutes of exposure. The number of these nuclei found, in view of the distorted coronas, etc., is, of course, an estimate; but it is none the less clear that here again the rate of production of large persistent nuclei increases at an accelerated rate with the ionization.

One may note that in no case was it possible to obtain persistent nuclei on exposure through a glass plate 0.15 cm. thick. This glass plate, in case of the coil used, cuts off all influence almost as effectually as tin plate. I am at a loss to account for this result, as on an earlier occasion persistent nuclei were obtained in abundance through glass. The frequency of similar results might in fact lead one to suggest the possibility of a special kind of X-radiation as the cause of persistent nuclei.

The radium used was sealed in aluminum tubes, so that chiefly the γ rays are in question. The available amount of radium in my possession, compatibly with the ionization produced, is insufficient to generate persistent nuclei in any time. It is none the less important to actually demonstrate that if the ionization produced by radium is sufficient in amount, it will really produce persistent nuclei. Wilson.* indeed, assents to this, referring again to the point discharge.

Radiation.	D	Ions $n \times 10^{-3}$	Persistent nuclei, first exhaustion $n \times 10^{-3}$	Persistent nuclei, second exhaustion $n \times 10^{-3}$
	cm.			
X-rays.....	1	700	108	16.0
	4	500	20	1.6
	10	400	1.2	....
	24	330	.4	....
Radium, just outside....	....	130	.0	....
within, exposure 3 min....	....	270	.0	....

Since there is no evidence that persistent nuclei of the present type are associated with some specific kind of mild radiation, the conclusion of the last chapter, *viz*, that these nuclei are ultimately solutional nuclei and that the solute is produced spontaneously in dust-free wet air by the X-rays, is plausible. It is merely necessary to admit that the difference in size of the nuclei of the preceding and the present cases is due to the greater penetration of X-radiation in the latter; *i.e.*, to the greater abundance of the soluble body in question for the case of larger nuclei.

* ". . . that such nuclei should, under appropriate conditions (the occurrence of chemical action giving rise to soluble products) grow into larger bodies is what might be expected; such a growth has for example been observed in the case of the ions arising from a point discharge." (Nature, vol. 74, p. 620, 1906.)

This explanation fails to account, however, for one essential point: it does not easily suggest why the number of persistent nuclei produced per cubic centimeter increases at an *accelerated rate* with the time of exposure to X-radiation, *caet. par.*, a fact long since conclusively brought out in my earlier reports.* The rate at which persistent nuclei are produced increases with the number present, which means that the nuclei or the ions present *must take part* in the production. If, however, it is granted (as I have also shown at length) that the number of nuclei or ions increases in marked degree as the lower limit of size diminishes, and (for simplicity) that the growth of any nucleus increases directly with the time of exposure to the X-rays, then an accelerated increase of persistent nuclei in the same time may be predicted. For nuclei in continually increasing number must fall within the scope of the low exhaustion with which the persistent nuclei in question are to be caught. The coarseness and whirlwind character of the first corona are evidently pointed in the same direction.

* *Cf.* Presidential address, Phys. Review, XXII, pp. 82–110, 1906.

CHAPTER X.

THE RECTIFICATION OF THE SPECTRUM BY THE AID OF TOTAL REFLECTION, TOGETHER WITH A COMPUTATION OF THE SHIFT OF ELLIPSES IN ELLIPTIC INTERFEROMETRY.

71. Introductory.—In my work of last year,* the quantity $\mu - \lambda \frac{d\mu}{d\lambda}$ (μ index of refraction of glass, λ wave-length) occurred in the reductions and in the absence of direct data I temporarily made use of the corresponding quantity computed from standard data for a somewhat similar glass. In this way the amount of displacement of the centers of ellipses per centimeter of displacement of the micrometer was determined. It must, however, frequently be necessary to find $d\mu/d\lambda$ from a small piece of glass, and I have therefore tested the following method in which a Kohlrausch total reflectometer slides along the graduated rail of Rowland's adjustment for the grating, as modified for the plate grating by M. Barus and myself.†

The method is then further modified, in a way that is applicable when a glass grating is given for investigation, as in the immediate problem, but not otherwise. It admits of some interesting applications, as, for instance, to the refraction of the material of film gratings.

In all cases of solids, the refraction of the more strongly refracting liquid in which the solid is submerged must of course be known for all wave-lengths; but this is true for carbon disulphide. If the liquid indices are not known throughout, in terms of wave-length, they may be determined by aid of an air-plate, using virtually the same apparatus and method. I shall give examples of all these measurements below.

72. Apparatus.—In figure 45, AA and BB are the two fixed rails of Rowland's adjustment at right angles to each other. R, joining the vertical axes at a and p, is the cross-rail, stretching from the slide D, which carries the grating g, to the slide C which carries the total reflectometer T. Slides C and D move at right angles to each other and the position x of C is measured along the brass millimeter scale ss by aid of the vernier v.

The rail BB is further provided with a slide F for the plane mirror m, by which white light is thrown upon the slit c on the slide S, through the condensing lens L'. L'' is the achromatic collimating objective and the rod k (which may be grasped in front at h when necessary) is adapted for clamping S and L'' together at the principal focal distance of the latter. The collimator SL'' does not move with D. The grating g, fixed to a hori-

* Publication No. 149, Carnegie Institution of Washington, Part I, 1911. The Production of Elliptic Interferences in Relation to Interferometry.

† American Journal of Science, XXXI, 1911, pp. 85–95.

zontal disk with a spring and three leveling screws, is securely fastened to the table t, which here preferably rotates with the end a of the rod R. The grating, in other words, is kept normal to R, so that the angle of diffraction is zero, while the angle of incidence alone varies when C passes from end to end of AA. If x_1 and x_2 measured on s be the positions of C for identical lines of the spectrum,

$$\lambda/D = (x_2 - x_1)/2R$$

where D is the grating space and R the length ap.

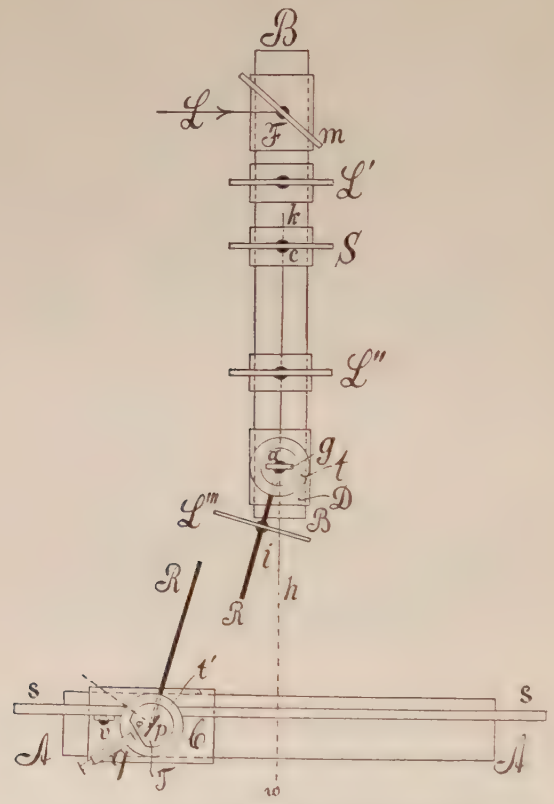

FIG. 45.—Plan of Rowland mounting, adapted for a plate film grating and used for rectification of the spectrum of glass, by total reflection.

The lens L''' on R is the objective of a telescope which focusses the colored image of the slit at the slide C, so that it may there be viewed by an ocular preliminarily. The latter is held in a standard placed on the table t' revolving on a common axis p with this end of R. When the ocular is replaced by the total reflectometer T, of which p is the plate of glass (properly centered) to be examined and q the telescope, the weak lens L''' is superfluous; but as a rule it need not be removed and is rather advantageous in condensing light when sunlight is not used.

When sunlight is used, the lens L''' may be moved a trifle backward so as to put the colored images of the slit slightly in front of the cylindrical glass vessel T of the total reflectometer. If the adjustment is properly made the lines are adequately visible in the telescope q and the index may be found for a given Fraunhofer line without reference to the scale ss. Without sunlight the scale ss is essential. Naturally the images seen in the telescope are not sharp, inasmuch as the cylindrical mantle of the bottle acts as one of the lenses; but they are clear enough for the purpose. It is usually more satisfactory, however, to ignore the lines and to determine the index of refraction for successive positions x of the carriage C on the rail AA, given by the scale ss.

With the total reflectometer revolvable, as a whole, on its axis, the two symmetrical positions of q relative to R give the double angle of total reflection, or 2φ, for the given liquid (usually carbon disulphide) in which the glass plate p is submerged. The graduated circle of the instrument with which the telescope q is rigidly connected is available for the measurement of angles.

73. Methods.—When the air-plate is used for the measurements of the indices of refraction of the liquid, the telescope q is directed along the rail R and $2\varphi_t$ found by rotating the plate p until the two limits or ends of the visible part of the spectrum successively coincide with the cross-hairs. The spectrum is usually nearly homogeneous in color; but the ends are liable to show interference fringes. Simultaneously the position x of the slide C and the temperature t of the liquid are read off. Thus if

$$N_t = 1/\sin \varphi_t$$

be the index * of the liquid at t,

$$N_{20} = N_t(1+\alpha(t-20)) = (1+\alpha(t-20))/\sin \varphi_t$$

is the index at 20°. For carbon disulphide, at mean temperatures, $\alpha = .0008$, nearly.

Again, if the glass-plate is now introduced and similar measurements $\varphi_{t'}$, t' be made at x, the index of the plate will be

$$n = N_{t'} \sin \varphi_{t'} = N_{20} \sin \varphi_{t'}/(1+\alpha(t'-20))$$

or

$$n = \sin \varphi_{t'}(1+\alpha(t-t'))/\sin \varphi_t$$

Two symmetrical sets of values are thus obtained, one for each of the two first orders of spectra at x_1 and x_2 on opposed sides of the undeviated white ray w. This method does not usually succeed very well, for it presupposes that in case of the air-plate and glass-plate, which are successively inserted, the total reflection occurs at identical parts of the spectrum for identical positions x along the scale s. But supposing the adjustment trustworthy,

* In conformity with Kohlrausch's notation, N and n are here used as symbols for index of refraction. They are replaced by μ, below.

the wave-length corresponding to any given n is found from the two positions x_1 and x_2 at which the same n occurs, from the equation

$$\lambda = D(x_2 - x_1)/2R$$

In general it is preferable to use the air-plate first to find the indices of refraction of the liquid, if these are not known throughout the spectrum. There will thus be given two symmetrical curves for the two first orders of spectra, separately. Their distance apart $x_2 - x_1$ for the given values of N determines the wave-length λ sought; *i.e.*, if N is plotted in terms of x, the horizontal distance apart of the two curves is the $x_2 - x_1$ which determines the wave-length for the index N selected. Hence N is given in terms of λ and should be reduced to 20°. In case of many liquids, in particular carbon disulphide, N is well known in terms of wave-length at the outset, so that the air-plate is superfluous.

The observations with the glass-plate are made in the same way. The symmetrical curves for $\sin \varphi_t$ at t', reduced to $\sin \varphi'$ at 20°, as found from the two first orders of spectra, are first plotted in terms of x. Hence their distance apart for two equal values of $\sin \varphi'$ is $x_2 - x_1$, from which the wave-length λ is computed. This datum in turn gives the appropriate (known) value N of the index of the liquid, all at 20°, so that finally

$$n = N \sin \varphi'$$

74. Examples. Liquids.—The circle of the Kohlrausch total reflectometer is only a little over 3 inches in diameter and the reading is just within 0.1 degree of arc. The index of carbon disulphide, moreover, varies, relatively speaking, in marked degree with temperature; *i.e.*, 0.0008 per degree centigrade. Unless unusual precautions are taken, therefore, one can not expect the units of the third place to be quite trustworthy, as it corresponds to about 0.07° of arc. The apparatus in my possession was an old instrument, and a high order of precision was of secondary interest and not attempted.

TABLE 25.—Air-plate between thin plates of glass in CS_2. Temp. $t = 22.2°$. $N_{20} = (1 + .00176)/\sin \varphi_t$.

x	Mean φ_t	N_{20}	N_{20}	x_2	x_1	$\lambda \times 10^6$
cm.						
66.15	38.14°	1.6220	1.6230	193.30	67.20	62.82
70	37.98	1.6278	1.6290	189.00	70.40	59.08
75	37.69	1.6385	1.6340	185.60	73.10	56.04
80	37.24	1.6553	1.6390	183.10	75.30	53.70
85	36.69	1.6766	1.6450	181.00	77.20	51.71
175	36.99	1.6649	1.6500	179.10	78.80	49.96
180	37.46	1.6471	1.6560	177.40	80.10	48.47
185	37.79	1.6347	1.6610	176.00	81.30	47.17
190	37.99	1.6275	1.6670	174.50	82.60	45.78
195	38.16	1.6215	1.6720	173.40	83.90	44.58
			1.6780	172.50	85.30	43.44

I will first take the case of an air-plate with carbon disulphide. A film of air was inclosed between two small plates of microscope cover-glass by cementing them at their edges with glue. In another case, plates of glass 0.3 centimeter thick were similarly prepared. Examples of the results

TABLE 26.—Air-plate between thick plates of glass in CS_2. Temp., $t=18.3°$.

x	Mean φ_t	N_{20}	N_{20}	x_2	x_1	$\lambda\times10^6$
cm.						
66.15	38.00°	1.6220	1.6180	193.10	64.30	64.16
70	37.73	1.6318	1.6230	189.70	66.80	61.22
75	37.40	1.6441	1.6290	186.70	69.00	58.63
80	36.93	1.6620	1.6340	184.00	71.20	56.19
85	36.15	1.6928	1.6390	181.50	73.30	53.90
172	36.66	1.6726	1.6450	179.50	75.10	52.01
175	36.98	1.6601	1.6500	177.80	76.90	50.26
180	37.43	1.6430	1.6560	176.30	78.50	49.71
185	37.73	1.6318	1.6610	174.80	79.80	47.32
190	37.94	1.6241	1.6670	173.40	81.20	45.93
195	38.18	1.6155	1.6720	172.10	82.30	44.73
			1.6780	170.90	83.20	43.69
			1.6840	170.00	84.00	42.84
			1.6890	169.30	84.60	42.19

are given in tables 25 and 26. In each table the position x of the total reflectometer on the rail AA is given, together with the corresponding angle of total reflection φ_t, of the air-plate and the value of N_{20} reduced to 20°.

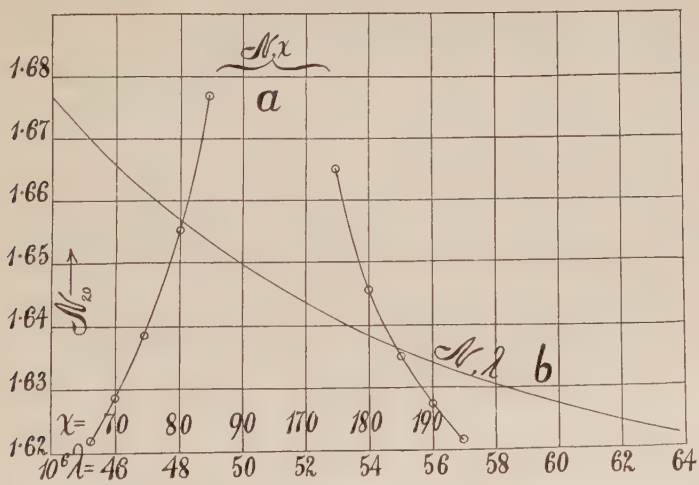

FIG. 46.—Graphs showing index of refraction of CS_2 for (a) different positions, x, of air-plate on graduated rail, and (b) different wave-lengths.

The curves, figs. 46(a) and 47(a), show the value of N_{20} in terms of x. These curves should be quite symmetrical to the vertical, so that for any height N_{20}, $(x_1+x_2)/2$ is constant.

Similarly a given horizontal N_{20} determines the values $x_2 - x_1$ for the computation of the wave-length λ. The film of the grating had nominally 15,050 lines to the inch and the oblique rail R was 169.4 cm. long. Hence

$$\lambda = \frac{x_2 - x_1}{15{,}050 \times .3937 \times 2 \times 169.4} = 4.98 \times 10^{-7} (x_2 - x_1)$$

These values x_2, x_1, λ, and N_{20} are also given in tables 25 and 26, for the successive values of N_{20} used, and figs. 46(*b*) and 47(*b*) show the corresponding dispersion curves for carbon disulphide at 20°, resulting.

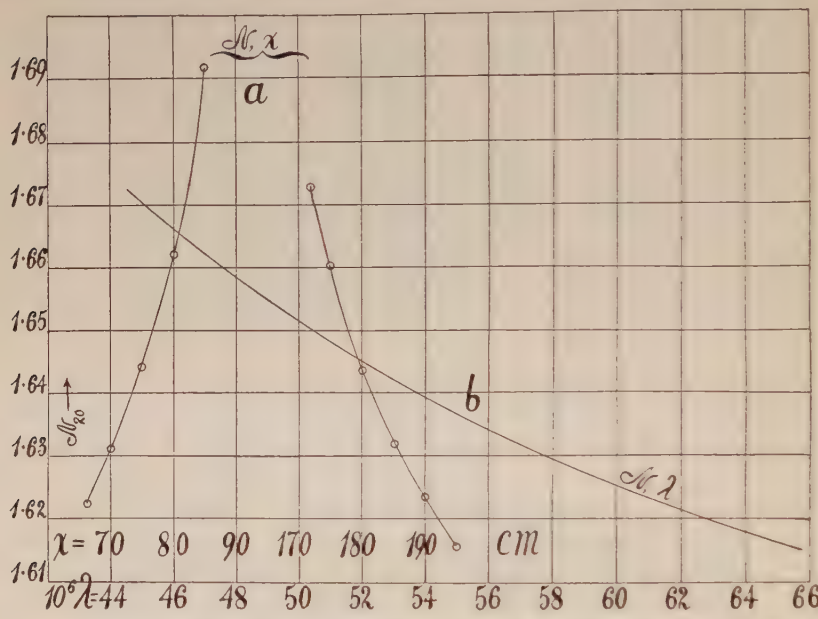

FIG. 47.—Graphs showing index of refraction of CS_2 for (*a*) different positions, x, of air-plate on graduated rail, and (*b*) different wave-lengths.

The curves for N_{20} in terms of λ, both for thick and for thin glass-plates holding the air-plate between them, are systematically above the standard values given by Kohlrausch.* The difference is 2 to 3 units in the third place, which would be equivalent to 2.5° in temperature, or about 0.06° of angle at the vernier, or else to some systematic error or to an actual difference in composition of the liquid. I did not consider it worth while to seek for the cause of this constant systematic difference of absolute results, seeing that the differential coefficients of the curves figs. 46(*b*) and 47(*b*) would be correctly given, and these are chiefly in question.

75. Examples. Solids.—The treatment of a solid medium is similar, except that the total reflections are observed by reflected light. If the data for carbon disulphide be taken at 20°

$$n = N_{20} (1 - a(t - 20)) \sin \varphi$$

* Kohlrausch, Lehrbuch der Praktischen Physik, p. 712, 1910.

Tables 27 and 28 contain the data for x, φ, and $(1-a(t-20))\sin\varphi$, which refers the case to 20°. Figures 48(a) and 49(a) show the values of the corrected $\sin\varphi$ in terms of x. The curves, as they should be, are nearly symmetrical to the vertical or $(x_1+x_2)/2$ is nearly constant for the same sine.

TABLE 27.—Refraction of the glass of the grating. Temp., 21.8°.
$n = N_{20}\sin\varphi\ (1-.00144)$.

x	Mean φ	Sin φ	Sin φ	x_2	x_1	$\lambda\times10^6$	N_{20}	n
cm.								
66.15	70.00°	0.93834	0.9360	191.70	69.90	60.67	1.6245	1.5206
70	69.60	.93592	.9340	187.80	72.70	57.34	1.6292	1.5217
75	68.96	.93199	.9320	185.50	75.00	55.04	1.6335	1.5224
80	68.16	.92688	.9300	183.40	77.30	52.85	1.6391	1.5244
85	67.03	.91937	.9280	181.40	79.10	50.96	1.6441	1.5258
172	65.70	.91008	.9260	179.70	80.60	49.37	1.6489	1.5269
175	66.80	.91781	.9240	178.40	82.20	47.92	1.6538	1.5281
180	68.08	.92637	.9220	177.20	83.50	46.68	1.6588	1.5294
185	68.89	.93153	.9200	176.10	84.60	45.58	1.6634	1.5303
190	69.54	.93556	.9180	175.00	85.60	44.53	1.6682	1.5314
195	70.03	.93850	.9160	174.10	86.50	43.64	1.6728	1.5323

TABLE 28.—Refraction of the glass of the grating. Temp., 19.2°.
$n = N_{20}\sin\varphi\ (1+.00064)$.

x	Mean φ	Sin φ	Sin φ	x_2	x_1	$\lambda\times10^6$	N_{20}	n
cm.								
66.15	69.56°	0.93760	0.9360	189.20	69.20	59.78	1.6254	1.5214
70	69.19	.93534	.9340	186.10	71.80	56.94	1.6298	1.5223
75	68.54	.93124	.9320	183.50	74.20	54.45	1.6350	1.5239
80	67.55	.92476	.9300	181.30	76.20	52.35	1.6404	1.5255
85	66.28	.91608	.9280	179.60	77.80	50.71	1.6447	1.5263
172	66.29	.91615	.9260	177.60	79.40	49.08	1.6499	1.5278
175	67.11	.92182	.9240	176.40	80.50	47.77	1.6540	1.5283
180	68.11	.92847	.9220	175.10	81.50	46.63	1.6588	1.5294
185	68.84	.93316	.9200	173.80	82.70	45.38	1.6641	1.5310
190	69.38	.93650	.9180	172.80	83.80	44.33	1.6691	1.5323
195	69.81	.93913	.9160	171.90	85.00	43.29	1.6747	1.5340

If now the distance apart of equal values of the reduced $\sin\varphi$ be taken, *i.e.*, if x_2-x_1 be found for nearly equal increments of $\sin\varphi$, the former values determine λ, from which the corresponding N_{20} for carbon disulphide is found in turn.

In this way the data for the values of n to be computed are found, and n may now be expressed in terms of the λ used. Tables 27 and 28 also contain x_2-x_1, λ, N_{20}, for carbon disulphide, taken from Kohlrausch's tables, and n for the glass. Figs. 48(b) and 49(b) show the final dispersion curves, index of refraction n varying with wave-length λ for the glass of the grating. The constants of these curves will be computed below and their character will then appear.

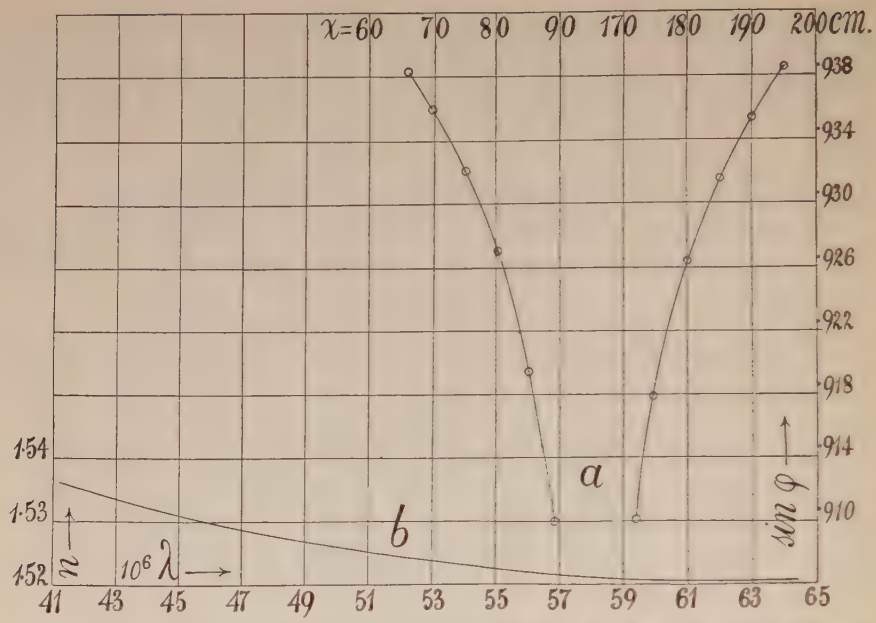

FIG. 48.—*a*, graphs showing refraction of glass submerged in CS_2 for different positions of totally reflecting plate on graduated rail; *b*, dispersion curves for glass plate of grating.

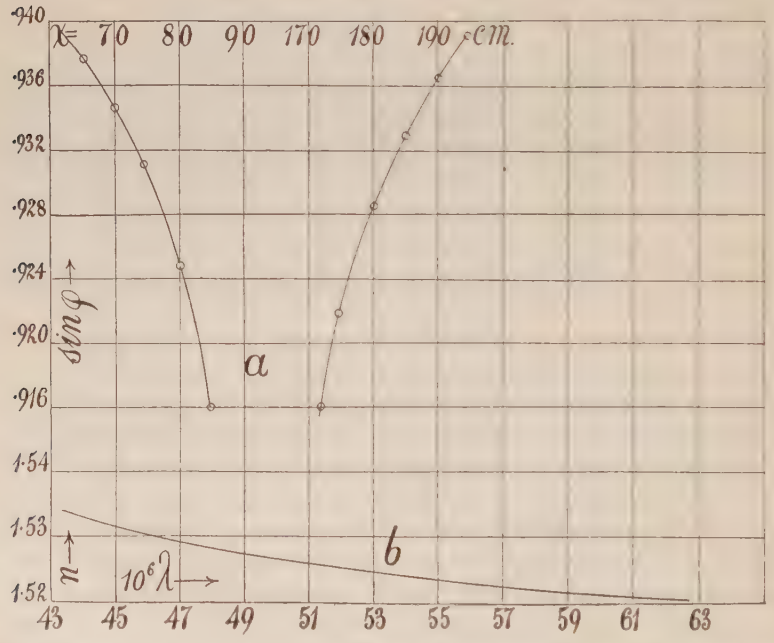

FIG. 49.—*a*, graphs showing refraction of glass submerged in CS_2 for different positions of totally reflecting plate on graduated rail; *b*, dispersion curves for glass plate of grating.

76. Independent measurements.—As an example of coördinated work, in which the index of the liquid and of the solid are simultaneously found, the following experiment may be cited. The air-plate was inclosed between two thin plates of microscope cover-glass. In such a case the limits of total reflection are determinable both for the reflected rays and for the transmitted rays. The angle φ in the former case gives the index of refraction n of the glass, in relation to the liquid (carbon disulphide), since

$$n = N \sin \varphi$$

whereas the angle φ_0 in the latter case gives the index of the liquid alone, or

$$N = 1/\sin \varphi_0$$

Hence

$$n = \sin \varphi / \sin \varphi_0$$

needing no correction for temperature.

In an experiment made at 18.3° with the plate of microscope glass in question inclosing the air-film, $\varphi = 68.90°$ and $\varphi_0 = 38.02°$, whence $n = 1.5198$. Using $\varphi = 68.90°$ as found and the tabulated data for carbon disulphide from Kohlrausch, $N = 1.6291$, $n = 1.5199$, which happens to agree accurately with the preceding n.

77. Prism (liquid CS_2) and submerged grating.—The present method for the above purpose makes use of the grating directly. This is inclosed in a suitable closed trough, preferably triangular in form, with windows of plate-glass and filled with carbon disulphide. If the grating is mounted with its ruled face coinciding with the axis of rotation, as in Kohlrausch's total reflectometer, the angle of total reflection may be measured in all parts of the spectrum. The Fraunhofer lines which are simultaneously in focus are used for reference in succession. Parallel rays of sunlight from a collimator are thrown into one face of the liquid prism, normally to its plane. They emerge at the other face. The undeviated rays are ignored, while the telescope is directed toward the first order of diffraction spectra, this emergence also being not far from normal. Like the first order of spectra, the second and third orders may often be used with advantage, the limit of total reflection being identical in all spectra on the same side of the undeviated ray. Fig. 50 shows the details of the apparatus. *ABC* is an equilateral hollow prism of wood, closed above and below, but provided with the plate-glass windows *a*, *b*, *c*. The whole interior, except the plate, is thoroughly coated with a thin layer of glue, which renders it impervious to carbon disulphide. The windows also are glued into place, while the top is merely screwed down and therefore removable. This is, moreover, centrally perforated, to receive a brass tube 1.25 inches in diameter, which carries the graduated circle *ee*, the alidade, and the axial clutches of the total reflectometer. The telescope *T* is fixed to *ee* by an arm (not shown), so that *T*, *ee*, *ABC* make a rigid

system. To introduce large objects like the grating, the whole top is removed. Small objects may be introduced through the tube, as in Kohlrausch's instrument.

Figure 50 shows an adjustment made under conditions of total reflection. L is a beam of white sunlight, entering nearly normally to a, totally reflected at d from the plate-glass grating p, ruled on the front face, and emerging obliquely at R. This is the undeviated beam. The first order of spectrum emerges at D, also nearly normal to the plate c, and is seen in the telescope T. The second and third orders of spectra appear to the

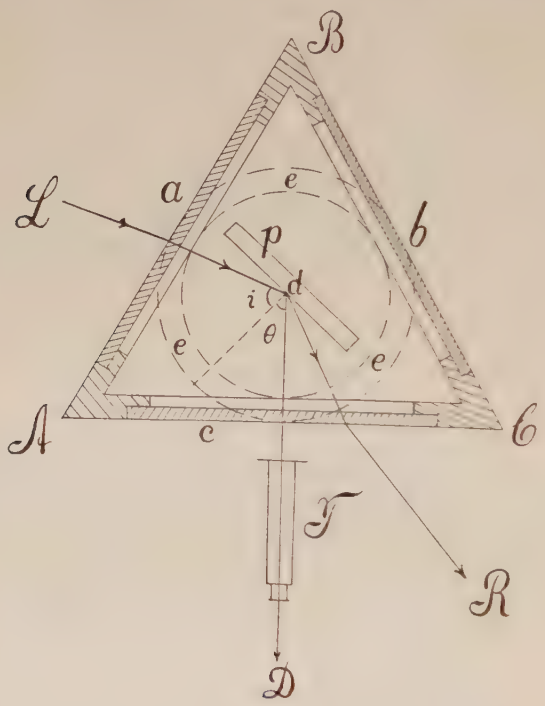

FIG. 50.—Hollow prism of wood with glass sides, containing CS_2, in which plate of grating is submerged for total reflection.

left of D, in succession. The spectra on the other side of R are not usually available. Moreover, the reading of these would be different than the reading for the case where the angle of diffraction θ is smaller than the angle of incidence i.

The limit of total reflection moves through the spectrum both with the rotation of the prism as a whole (which must therefore be on an axle) and with the independent rotation of the plate p, actuated by the alidade rotating within ee. In the definite adjustment this limit must coincide both with the spectrum line λ for which n is to be found, and with the cross-hairs of the telescope T. Three lines, in other words, are to be brought

into coincidence; but after a little practice this succeeds fairly well, unless the limit of total reflection is too faint. As a rule, since T rotates with the prism, if the limit of total reflection is put on the cross-hairs in any part of the spectrum, it will remain there on rotating the alidade till the spectrum line selected is brought to the same coincidence by turning the alidade. The adjustment is then repeated in succession for greater precision.

After taking the reading for the position in figure, the light is introduced through b and the symmetrical position of p found. The difference in angular reading is the double angle of total reflection, 2φ. The adjustment in the first spectrum holds equally for the second and third orders, and it is in the latter that the phenomenon is liable to be particularly clear and the adjustment correspondingly precise. The beam of white light should illuminate the whole grating whose ruled face is very nearly on the axis of rotation d of the alidade. Sunlight is essential for these measurements, since the spectrum lines are to be used. This was not of course necessary in the preceding paragraph.

The following example of results obtained in this way may be given:

TABLE 29.

Line.	2φ	t	n	n from figs. 48(b) and 49(b)
D	138.28°	19.0°	1.5210	{ 1.5215 1.5206
E	136.53°	18.7°	1.5244	{ 1.5240 1.5250

which is practical coincidence within the errors of observation and thus verifies the above work as a whole.

78. The dispersion constants of the glass of the grating.—To reduce these data for practical purposes it will be sufficient within the range and relatively to the precision of observations to assume the simplified form of Cauchy's equation,

$$n = A + B/\lambda^2$$

if n_E is the index for the E line and λ_E its wave-length

$$n - n_E = B\left(\frac{1}{\lambda^2} - \frac{1}{\lambda^2_E}\right)$$

from which B may be computed for each pair of values of n and λ. The results are given in table 30. B was found separately from each of the curves (figs. 48(b) and 49(b)). The values of $n - n_E$ and λ are chosen as near the observations as possible.

The results for $n-n_E$ agree as well with the observed data as the small instrument used can warrant. The two groups show a displacement with reference to each other which is probably due to temperature. A few outstanding larger differences are errors, since they occur irregularly.

TABLE 30.—Index of refraction of glass n in terms of wave-length, λ. $n-n_E=B(1/\lambda^2-1/\lambda^2_E)$. Mean $B=48\times10^{-12}$.

Observed $n-n_E$	$\lambda\times10^6$	Mean $B\times10^{12}$	Computed $n-n_E$	Observed $n-n_E$	$\lambda\times10^6$	Mean $B\times10^{12}$	Computed $n-n_E$
−.0035	58.880	48.9	−.0035	−.0046	60.076	47.5	−.0040
+.0032	48.319	....	+.0033	+.0014	50.013	....	+.0019
.0090	43.338	....	.0084	.0113	41.296	....	.0107
.0011	51.109	....	.0011	.0019	49.614	....	.0022
−.0041	60.573	....	−.0043	−.0043	59.528	....	−.0037

From table 30 the value of the differential coefficient

$$\frac{d\mu}{d\lambda}=-\frac{2B}{\lambda^3}$$

may also be obtained for any wave-length λ. This and the corresponding value* of

$$\mu-\lambda\frac{d\mu}{d\lambda}=\mu+\frac{2B}{\lambda^2}$$

needed in the reduction of the observations of the earlier paper† will be computed by accepting the mean value $B\times10^{10}=0.48$.

79. Computation of the shift of centers in elliptic interferometry.—In the preceding report,‡ I showed that the path difference, y, corresponding to the centers of ellipses throughout the spectrum is

$$y=\frac{e}{\cos R}\left(\mu-\lambda\frac{d\mu}{d\lambda}\right) \qquad (1)$$

where e is the thickness of the glass and μ its index of refraction, for any given color of wave-length λ. R is the corresponding angle of refraction for light incidence at an angle I, or $\sin I=\mu\sin R$. In the former experiment $I=45°$. In view of the oblique position of the grating, however, the micrometer motion N of the opaque mirror introduces an additional displacement. Let N be the coördinate for this mirror. Then

$$N=y-e\,\mu\sin R\tan R. \qquad (2)$$

Hence the readings of the micrometer are determined by (subscripts c referring to centers of ellipses)

$$N_c=\frac{e}{\cos R}\left(\mu\cos^2R-\lambda\frac{d\mu}{d\lambda}\right) \qquad (3)$$

* The symbol μ for index of refraction is resumed throughout the following paragraphs.
† Publication No. 149, Carnegie Institution of Washington, 1911, p. 69.
‡ Publication No. 149, Carnegie Institution of Washington, §44, p. 66 *et seq.*, 1911.

For the present purpose it is sufficient to assume

$$\mu = A + B/\lambda^2$$

and to take the E line as a standard of reference, whence

$$\mu - \mu_E = B\left(\frac{1}{\lambda^2} - \frac{1}{\lambda^2_E}\right)$$

Table 31, then, gives an exhibition of the quantities here in question, computed both for light crown glass, $10^{10}B = 0.456$, in accordance with the data for μ and λ given in Kohlrausch's tables, and for the glass of the grating actually used, $10^{10}B = 0.48$, as measured in the above paragraphs. Δy_c and ΔN_c refer to distances from the value corresponding to the E line. N_c, y_c, and λ are in centimeters and the angle of incidence is 45°.

TABLE 31.—Light crown glass. $10^8\lambda_E = 52.70$. $10^{10}B = 0.456$. Computed values of y and N.

Lines.	B	C	D	E	b	F	G
$10^8 \times \lambda$ . . .	68.70	65.63	58.93	52.70	51.80	48.61	43.08
μ	1.5118	1.5128	1.5152	1.5186	1.5192	1.5214	1.5267
R	27° 53′	27° 52′	27° 49′	27° 45′	27° 44′	27° 42′	27° 35′
$d\mu/d\lambda$ . . .	281.26	322.62	445.62	623.10	656.14	793.96	1140.64
y_c	1.1779	1.1799	1.1853	1.1920	1.1941	1.1981	1.2091
Δy_c	−.0141	−.0121	−.0067	.0	+.0021	+.0061	+.0171
N_c	.9235	.9257	.9315	.9390	.9412	.9456	.9578
ΔN_c	−.0155	−.0133	−.0075	.0	+.0022	+.0066	+.0188
Plate glass of the grating. $10^8\lambda_E = 52.70$. $10^{10}B = 0.48$.							
$10^8 \times \lambda$ . . .	68.70	65.63	58.93	52.70	51.80	48.61	43.08
μ	1.5179	1.5179	1.5205	1.5240	1.5252	1.5270	1.5326
R	27° 46′	27° 46′	27° 41.7′	27° 37.5′	27° 37′	27° 34′	27° 27.3′
$d\mu/d\lambda$ . . .	296.07	339.60	469.08	655.90	690.68	835.76	1200.70
y_c	1.1820	1.1841	1.1890	1.1962	1.1980	1.2025	1.2140
Δy_c	−.0142	−.0121	−.0072	.0	+.0018	+.0063	+.0178
N_c	.9288	.9309	.9367	.9447	.9464	.9516	.9643
ΔN_c	−.0159	−.0138	−.0080	.0	+.0017	+.0069	+.0196

Measurements of N_c were now made with the aid of a Fraunhofer micrometer reading to a few ten thousandths of a centimeter. The opaque mirror was adjustably mounted on a slide and moved normally to itself, in order to put the centers of ellipses successively in coincidence with the B, C, D, etc., lines of the spectrum. At each coincidence a reading was made, care being taken to proceed in one direction only. As there are four spectra more or less in coincidence, it is easily possible to select the wrong line. By temporarily screening off the reflection from one mirror, however, and then marking the line desired of the remaining pair by the cross-hairs of the telescope, mistakes are usually avoidable. In the extreme blue and red it is often difficult to see the lines clearly in the superimposed spectra, so that the data for the B and G lines are not quite so trustworthy.

In fact, the ellipses come out sharpest when but a narrow strip of the grating is used; whereas the resolving power of the grating or general sharpness of lines increases with the breadth of the grating. If the whole grating is used (an intense spot of sunlight focussed on the slit) the adjustment must be very perfect and the surfaces quite true to bring out the ellipses; this is not the case if parallel rays fall on the slit and the whole divergence in the collimator is due to the diffraction of the slit. With optical plate-glass none of these difficulties would appear.

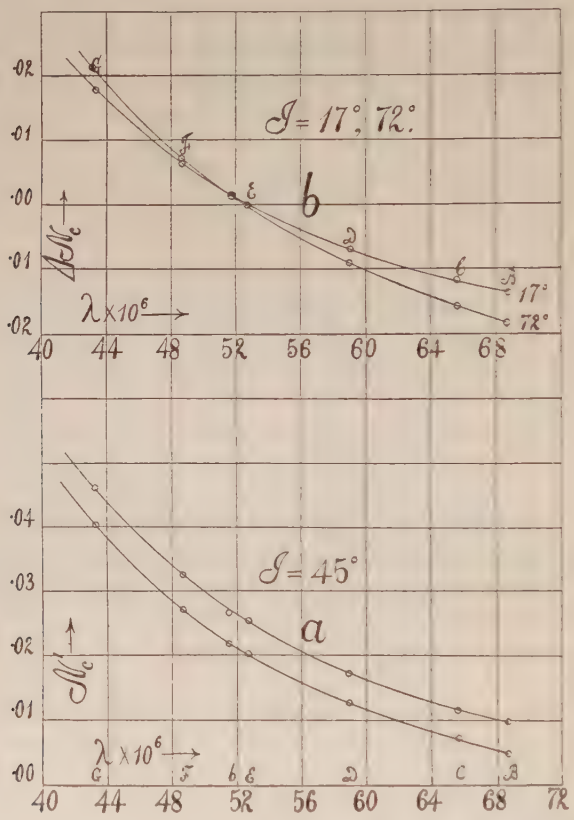

FIG. 51.—Graphs showing displacement of opaque mirror (micrometer motion) to place center of ellipses in different parts of spectrum, for case of different angles of incidence, I.

Apart from drawbacks of this nature, which require patience for their removal, the measurements are quite satisfactory as a whole, as may be seen in fig. 51(a).

In table 32 I have given the observed results, N'_c being the arbitrary drum-reading of the micrometer and its equivalent in centimeters, from which $\Delta N_c = N'_c - (N'_c)_E$ is deduced, relatively to the position $(N'_c)_E$ corresponding to the E line. Different values of $(N'_c)_E$ in the two series of fig.

51(*a*) are due to the backlash in the micrometer, as the mirror traveled in opposed directions in these cases.

In the last two columns of table 32 the observed mean data are compared with the computed data for ΔN_c in table 31. The results are practically

TABLE 32.—Observed values of the shift of ellipses compared with the computed values of table 31 ($B \times 10^{10} = 0.48$).

Line.	$10^6\lambda$	N'_c Drum	N'_c cm.	ΔN_c	N'_c Drum	N'_c cm.	ΔN_c	Mean ΔN_c obs.	Mean ΔN_c comp.
B....	68.70	18.6	0.0093	−0.0162	9.6	0.0048	−0.0157	−0.0160	−0.0159
C....	65.63	23.0	.0115	− .0140	14.4	.0072	− .0133	− .0137	− .0138
D....	58.93	34.6	.0173	− .0082	25.5	.0127	− .0078	− .0080	− .0080
E....	52.70	....	.0255	.0	....	.0205	.0	.0	.0
b....	51.80	53.3	.0267	+ .0012	43.6	.0218	+ .0013	+ .0012	+ .0017
F....	48.61	65.0	.0325	+ .0070	54.4	.0272	+ .0067	+ .0069	+ .0069
G....	43.08	92.4	.0462	+ .0207	80.7	.0404	+ .0199	+ .0203	+ .0196

coincident, except at the *G* line, where the ellipses were too dark to be seen distinctly. Hence equation (3) for N_c may be accepted as correct. If we write it

$$N_c = \frac{e}{\sqrt{\mu^2 - \sin^2 I}} \left((\mu^2 - \sin^2 I) - \mu\lambda \frac{d\mu}{d\lambda} \right) \tag{4}$$

and put $m^2 = \mu^2 - \sin^2 I$, $x = \log \mu$, the equation becomes

$$N_c = e\left(m - \frac{dm}{dx}\right) \tag{5}$$

On integration and reduction this may be written

$$e\mu \cos R = \lambda \left(C - \int N_c d\lambda/\lambda^2\right) \tag{6}$$

where C is a constant of integration. Unfortunately equation (6) is too complicated for the computation of μ when N_c is observed in terms of λ throughout the spectrum; for the reference to the standard *E* line gives (sin I = constant)

$$\sqrt{\mu^2 - \sin^2 I}/\lambda - \sqrt{\mu^2_E - \sin^2 I}/\lambda_E = -\frac{1}{e}\int_E \Delta N_c \frac{d\lambda}{\lambda} \tag{7}$$

If, however, I is very small, or $R = 0$,

$$\frac{\mu}{\lambda} - \frac{\mu_E}{\lambda_E} = -\frac{1}{e}\int \Delta N_c \frac{d\lambda}{\lambda} \tag{8}$$

Let $\mu = B(1/\lambda^2 - 1/\lambda^2_E)$ as above. Then either equation (3) or equation (8) for $I = 0$, leads to

$$(\Delta N_c)_0 = (N_c - N_E)_0 = 3eB\,(1/\lambda^2 - 1/\lambda^2_E) \tag{9}$$

This equation is to be tested in the following paragraph.

In conclusion, the effect of a change of the angle of incidence I on N_c may be added. Since

$$N_c = e\mu \cos R + 2e\, B/\lambda^2 \cos R$$

$$dN_c/dI = (dN_c/dR)\,(dR/dI) = N_c \sin 2I/2\,(\mu^2 - \sin^2 I)$$

whence

$$dN_c/dI$$

is zero when $I = 0°$ and $I = 90°$ while at 45°

$$(dN_c/dI)_{45} = N_c/(2\mu^2 - 1)$$

or the intermediate values are significant. The effect of R is thus marked for intermediate angles between 0° and 90°.

80. Continued. Case of I = 0°.—The limiting values of I in equation (7) are interesting. They correspond to the form of interferometer approached in figure 52, where gg is the face of the grating, I the incident ray, M and N the two opaque mirrors symmetrically inclined relatively to the grating. Rays R are refracted and rays D are diffracted. In figure 52 the spectra on the left of R are also available; but they are often complicated with the orders of spectra of the undeviated ray before it has

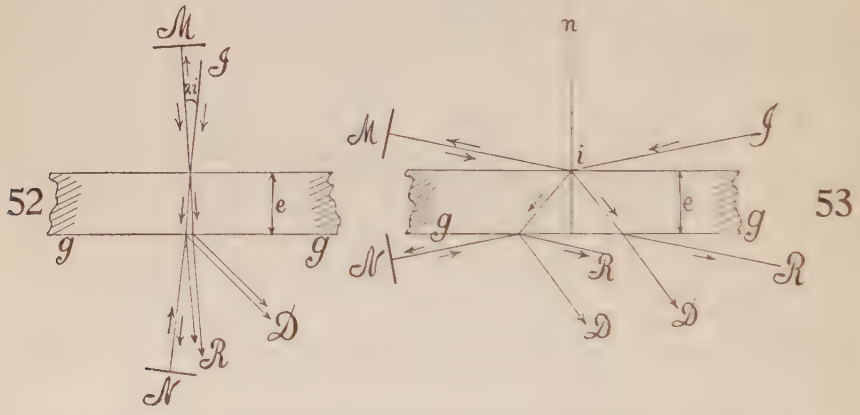

FIG. 52.—Adjustment for elliptic interference, in case of small angles of incidence, I.
FIG. 53.—Adjustment for elliptic interference, in case of large angles of incidence, I.

been reflected. To avoid these, one should observe between the spectra of the non-reflected ray, or else in the region of non-reflected spectra of the third or higher orders, as these are too faint to interfere with the reflected spectra. They often advantageously supply fixed lines in the spectrum when arc light is used.

To realize the condition of small angle, a collimator I and the mirror N (micrometer movable parallel to itself) were fixed on the edge of the spectrometer plate, diametrically opposite to each other. The mirror M, the grating gg, and the telescope at R or D were revolvable around the axis

of the spectrometer. Grating and mirrors could be clamped. With such an adjustment all values of I, in fact, may be tested between about 10° and 80°, smaller and larger angles being excluded, because of the lateral dimensions of the apparatus and mounting.

The present method of interference is often exceedingly convenient, inasmuch as the telescope at R is almost in contact with the micrometer at N, which may therefore be manipulated with ease by the observer. A typical form of instrument will be described below in § 83.

The endeavor may now be made to compute B from the shift of ellipses as suggested in the preceding equation (9) or

$$\Delta N_c = 3eB\,(1/\lambda^2 - 1/\lambda^2_E)$$

If we compute β in

$$\Delta N_c = \beta\,(1/\lambda^2 - 1/\lambda^2_E)$$

from the observed value of ΔN_c, the mean value for the B, C, D, F, G lines is found to be $\beta = 0.975 \times 10^{-10}$. Since $e = 0.68$ cm. and $B = 0.48 \times 10^{-10}$ in table 30, $3eB = 10^{-10} \times 0.979$, which agrees very nicely with the computed value of β just stated, particularly in view of the fact that I is not yet quite zero.

Table 33 contains data computed for y_c and N_c, etc., in case of $I = 17°$ and the glass of the grating ($B \times 10^{10} = 0.48$)

TABLE 33.—Computed values of y_c and N_c when $I = 17°$. $B \times 10^{10} = 0.48$.

Lines.	B	C	D	E	b	F	G
$\lambda \times 10^6$...	68.70	65.63	58.93	52.70	51.80	48.61	43.08
μ.....	1.5179	1.5179	1.5205	1.5240	1.5252	1.5270	1.5326
R.....	11° 6′	11° 6′	11° 5′	11° 4′	11° 3′	11° 2′	11°
$d\mu/d\lambda$....	296.07	339.60	469.08	655.90	690.68	835.76	1200.70
y_c.....	1.0660	1.0677	1.0728	1.0799	1.0815	1.0860	1.0975
Δy_c.....	−.0139	−.0122	−.0071	.0	+.0016	+.0061	+.0176
N_c.....	1.0269	1.0287	1.0338	1.0410	1.0427	1.0472	1.0589
ΔN_c.....	−.0141	−.0123	−.0072	.0	+.0017	+.0062	+.0179

TABLE 34.—Observed values of ΔN_c. $I = 17°$.

Lines.	B	C	D	E	b	F	G
$\lambda \times 10^6$...	68.70	65.63	58.93	52.70	51.80	48.61	43.08
N'_c drum.	41.9	46.3	6.2	....	22.3	31.9	5.0
N'_c cm...	.0210	.0232	.0281	.0348	.0362	.0410	.0525
ΔN_c.....	−.0138	−.0116	−.0067	.0	+.0014	+.0062	+.0177
N'_c drum.	33.6	39.4	49.2	....	15.8	25.1	48.0
N'_c cm...	.0168	.0197	.0246	.0315	.0329	.0376	.0490
ΔN_c.....	−.0147	−.0118	−.0069	.0	+.0014	+.0061	+.0175
N'_c drum.	39.3	44.3	4.3	....	20.2	30.0	1.8
N'_c cm...	.0197	.0222	.0272	.0337	.0351	.0400	.0509
ΔN_c.....	−.0140	−.0115	−.0065	.0	+.0014	+.0063	+.0172
Mean:							
ΔN_c obs..	−.0142	−.0116	−.0067	.0	+.0014	+.0062	+.0175
ΔN_c comp.	−.0142	−.0123	−.0073	.0	+.0016	+.0063	+.0178

Table 34 shows the observed results. Fig. 51(*b*) (upper curve, marked 17°) distributes the observations on the computed curve for ΔN_c, when ΔN_c for the E line is zero. Table 34 also contains the mean of the observed results, compared with the computed results for the same $I = 17°$, in table 33. The agreement is not quite as good as in table 32, the impression being that some of the lines (C, D) have been mistaken in the observed work or located in the wrong spectrum. But the general order of values for the small value of R is well brought out.

81. Case of I = 90° nearly.—The further case of interest corresponds to fig. 53, where the angle $I = 72°$ and as large as it could be made in the given spectrometer. The observations for N'_c are given in table 35, N'_c being taken from an arbitrary zero on the drum of the micrometer and (owing to backlash as before) the zero changes by a fixed amount with the direction of the rotation. The spectra were very fine and sharp, but too dark at the violet end and red end.

TABLE 35.—Observed values of ΔN_c. $I = 72°$.

Lines.	B	C	D	E	b	F	G
$10^6\lambda$.....	68.70	65.63	58.93	52.70	51.80	48.61	43.08
N'_c drum.	82.2	75.6	62.4	44.4	41.5	30.4	1.4
N'_c cm...	.0411	.0378	.0312	.0222	.0208	.0152	.0007
ΔN_c.....	−.0189	−.0156	−.0090	.0	+.0014	+.0070	+.0215
N'_c drum.	89.2	83.8	70.4	52.5	49.5	36.2	5.4
N'_c cm...	.0446	.0419	.0352	.0263	.0248	.0181	.0027
ΔN_c.....	−.0183	−.0156	−.0089	.0	+.0015	+.0082	+.0236
Mean:							
ΔN_c obs..	−.0186	−.0156	−.0090	.0	+.0015	+.0076	+.0225
ΔN_c comp.	−.0177	−.0161	−.0091	.0	+.0020	+.0077	+.0222

TABLE 36.—Computed values of y_c and N_c, when $I = 72°$. $B \times 10^{10} = 0.48$.

Lines.	B	C	D	E	b	F	G
$\lambda \times 10^6$...	68.70	65.63	58.93	52.70	51.80	48.61	43.08
μ.....	1.5179	1.5179	1.5205	1.5240	1.5252	1.5270	1.5326
R.....	38° 48′	38° 48′	38° 43′	38° 37′	38° 34′	38° 31′	38° 21′
$d\mu/d\lambda$....	296.07	339.60	469.08	655.90	690.68	835.76	1200.70
y_c.....	1.3421	1.3444	1.3493	1.3562	1.3578	1.3625	1.3738
Δy_c.....	−.0141	−.0118	−.0069	.0	+.0016	+.0063	+.0176
N_c.....	.8222	.8238	.8308	.8399	.8419	.8476	.8621
ΔN_c.....	−.0177	−.0161	−.0091	.0	+.0020	+.0077	+.0222

The computed values of y_c and N_c are given in full in table 36 and ΔN_c computed is also inserted in the last line of table 35. The agreement of observed and computed is satisfactory so far as the observations as a whole are concerned. Certain lines are more discrepant than others, but the errors are irregular.

The computed graph with the observations located with reference to it is given in fig. 51(*b*) on the curve marked 72°. The two curves together

indicate the change of sensitiveness on passing from a very small to a very large angle, the slope of the curve, fig. 53, where $I=45°$ being intermediate. The method of interference given in figure 53 is very useful when observations are made with polarized light (as in the examination of doubly refracting media) and the observer finds it convenient to be near the polarizer at the slit.

82. Summary.—I conclude, therefore, that the observations made at angles of incidence $I=45°$, 17°, 72°, have verified the equation

$$N_c=e\cos R\left(\mu-\frac{\lambda}{\cos^2 R}\frac{d\mu}{d\lambda}\right)=e\cos R\left(\mu+\frac{2B}{\lambda^2\cos^2 R}\right)$$

for the shift of the centers of the ellipses satisfactorily. To restore the ellipses from one spectrum line to another is equivalent to a motion of the micrometer over $N_c-N'_c=\Delta N_c$. This constitutes a second method of interferometry of relatively low sensitiveness, *i.e.*, a coarse adjustment on the number of fringes which pass a given spectrum line. Per fringe or per vanishing ring, obviously, the displacement of the mirror on the micrometer will be a half wave-length of the part of the spectrum in question.

83. Apparatus.—Interferometry by displacement has an advantage, inasmuch as the observer never loses the ellipses, even when the displacement is sudden. Their center may always be brought back again to a given spectrum line by the micrometer. Moreover, since

$$N_c=e\mu\cos R-\frac{e\lambda}{\cos R}\frac{d\mu}{d\lambda}=e\cos R\,(\mu+2B/\cos^2 R)$$

where N_c is the reduced micrometer reading, e the thickness, μ the index of refraction of the glass-plate of the grating for the wave-length λ, R the angle of refraction, and where $\mu=A+B/\lambda^2$, the sensitiveness may be regulated by decreasing the thickness of the grating, e, by aid of a compensator of thickness e'. For the virtual thickness is now $e-e'$. Hence, since for radial motion the sensitiveness per fringe across any given Fraunhofer line is

$$dN/dn=\lambda/2$$

this may be combined with the shift of ellipses controlled by N_c, in any ratio. The limit of this procedure is conditioned by the size of the ellipses or the available size of the field of the telescope, since when $e-e'$ approaches zero the ellipses become enormous.

Furthermore, it has been shown in the report cited* that the quantity $d\mu/d\lambda$ occurring in the value of N_c may be computed preliminarily from observations of $\Delta N_c=N_c-N'_c$, between definite Fraunhofer lines, particularly when the angles of incidence I and of refraction R are small. In such a case the constant $3eB=\beta$ nearly, where $(I=0)$

$$\Delta\mu=B(1/\lambda^2-1/\lambda^2_E),\ \Delta N_c=\beta(1/\lambda^2-1/\lambda^2_E)$$

* Publication No. 149, Carnegie Institution of Washington, §44, 1911.

Finally, if ΔN is the motion of the micrometer to bring the center of ellipses back to a given line

$$\Delta N = (\mu - 1)e'$$

where e' is the thickness of the compensator. If e' is large one may expect to distinguish between the indices of refraction of a birefringent crystal, when the source of light is polarized. Again, when the arms or the interfering beams of light are long, the index of refraction of a gas and its relation to pressure and temperature are accurately determinable.

In view of these advantages among others I have constructed a definite form of apparatus for elliptic interferometry, specially adapted for general observations, such for instance as I have in view with fog-particles. The

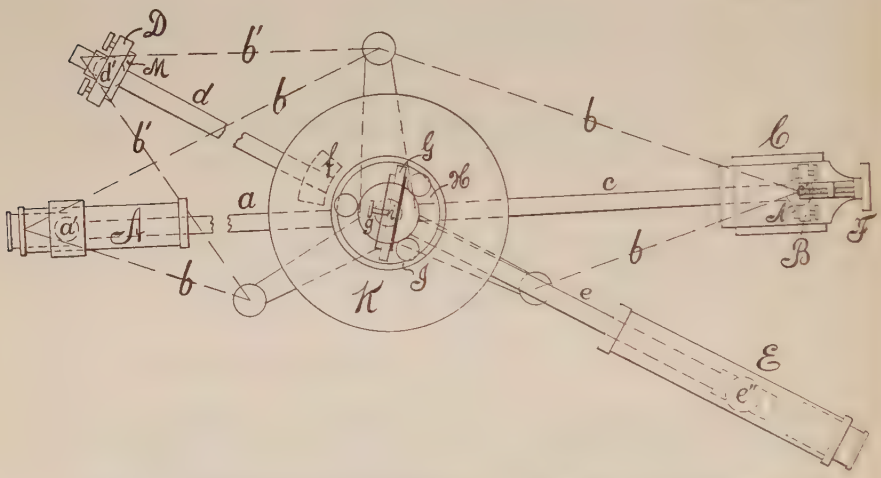

FIG. 54.—Plan of displacement interferometer; A, collimator; M, N, opaque mirrors; G, grating; E, telescope.

apparatus is to be light, portable, rigid, with relatively long distance between the opaque orthogonal mirrors M and N and the oblique mirror or grating, as well as height of mirrors above the arms, and with an easy adjustment for different angles of incidence I, large and small. As shown in figs. 54, 55, and 56, the distance between the center and either remote mirror is about 35 cm. It may easily be enlarged many times beyond this. The angles of incidence $I = 15°$, $45°$, and $75°$, are available at once for the given braces, though of course other angles may be used.

The long arms and feet of the apparatus, which in general form is naturally much like a spectrometer, are made of ¼-inch gas-pipe, and the braces are heavy strips of tin-plate, bent so as to be U-shaped in cross-section, much like umbrella steel, with the ends bolted down. In the drawing (of which fig. 54 is the plan and fig. 55 the elevation) the axles are cylindric or slightly conical. In my own apparatus sufficient rotation, 180°, of the parts was secured by ordinary well-cut gas-pipe screws.

The tripod (figs. 54 and 55) carries a standard Q of ⅜-inch gas-pipe, which is secured snugly by the cross-coupling R. From this the horizontal rigid arms a and c lead respectively to the collimator A and to the slide micrometer C and they are screwed into R parallel to the plane of fig. 55. The arm e which carries the telescope E must be revolvable around Q, a wide axle PP' and braces b'' *diverging* as they approach Q sufficing for the purpose. The telescope is used for reading only and need not be clamped. It must, however, be quite firm so as not to shake the instrument.

The long arms of gas-pipe (a, c, d, e) are not only convenient for the attachment, by ordinary clamps, of objects to be examined, but they admit of a circulation of cold water (constant temperature), entering or leaving at the feet, so that the lengths of arms are invariable, whatever be the temperature of the environment of air.

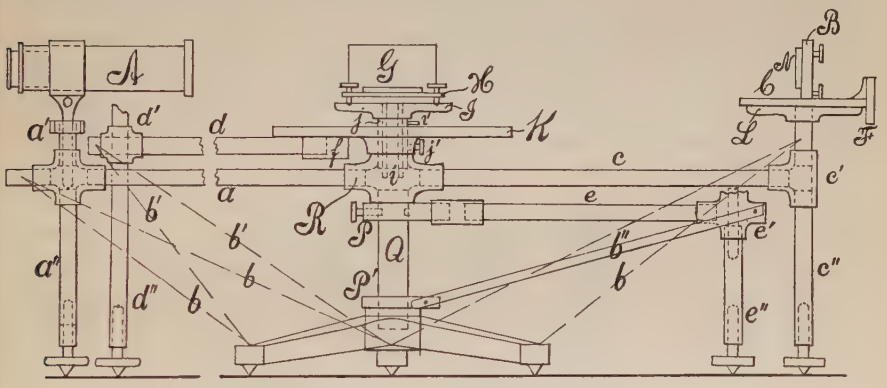

FIG. 55.—Elevation of displacement interferometer.

The standard Q is prolonged above the cross-coupling R as shown at j and the graduated plate at K (for measuring the angle of incidence I) rotates around Q prolonged. The plate may be clamped by the set-screw j'. Radially to K, the lateral arm d is bolted below the plate at f. D carries the opaque mirror N, which thus rotates around Q with K.

The adjustment chosen is such that the parts M, N, the grating G, the telescope E, and the collimator A may be displaced upward several inches, in the clear. It is thus possible, for instance, to place the fog-chamber between MG or NG.

The inside of j or Q prolonged is ground and receives the hollow cylindrical plug i of the table I and this may be clamped by the set-screws i'.

Upon I stands the grating G secured by the screw g to the ring-shaped support H which reposes in an annular gutter in I on three leveling screws. Moreover, a spiral spring (not shown) in the inside of the hollow conical tube i pulls down the ring H firmly upon I, so that nothing is liable to fall on transportation. The ruled surface of the grating G is toward the light or collimator A and in the axis of rotation. The adjustment need not be very accurate. The rulings are parallel to the slit.

Certain details of the parts of the apparatus may now be pointed out. The collimator A may be raised or lowered on its vertical stem or clamped in any position by aid of the wing-nut, a', on a longitudinally split tube. It may also be slightly inclined to the horizontal, either by the hinge indicated in the figure or by the special device shown in fig. 56, where the telescope or collimator reposes on Y's made of strips of elastic brass aa. These are so adjusted that the end of T at a' is naturally higher than at a. The ring b and the thumbscrew c then lower this end against the upward pressure of all the springs. Reading telescopes so mounted are firm and the device is very convenient if a slight inclination is to be imparted. They are removed by loosening c.

The tube a ends on the left in the cross-coupling, which also admits the adjustable standard a'' and affords an attachment for the braces bb (U-shaped in section), the other ends of which are bolted down to the nearer feet of the tripod. Thus A is held sufficiently rigid by the braced system aa'' bb. An inch or a ¾-inch objective and a 6-inch focus is sufficient and by reason of its lightness perhaps preferable to a larger and heavier tube. The slit may usually be opened about 0.5 mm.

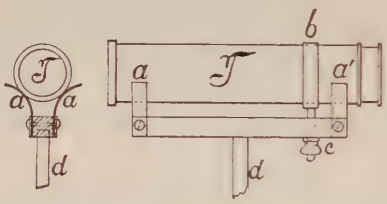

FIG. 56.—Details showing mounting of collimator and telescope.

In a similar way steadiness, elevation, and inclination of the telescope E are secured, the tubes e and e'' (adjustable foot) and the braces b'' terminating in the cross-coupling e' as has been suggested. An inch objective and a 6-inch focus is adequate. Cross-hairs are convenient but not necessary, as the spectrum lines are available when sunlight is used. If the arc light is used, strong sodium lines are usually in the field with the spectrum.

The opaque mirror M is controlled by three leveling screws (horizontal and vertical axes) and a suitable spring in the capsule D. It is adjusted vertically like the telescope and kept firm by the tubes d and d'' (adjustable foot) and braces $b'b'$, all parts meeting at the cross-coupling d'. The braces $b'b'$ are of equal length. Hence they may be bolted down to two of the feet of the tripod in succession, while the tube d together with the plate K take the three positions at 30°, 90°, and 150° to the rod a. The grating G does not turn with K, but must be specially adjusted to corresponding angles of 15°, 45°, and 75°, as easily determined by the reflected rays.

Finally, the slide micrometer is sustained by the tubes c and c'' (adjustable foot) and the braces bb, all parts meeting in the cross-coupling c'.

The latter carries the table L, to which the slide micrometer C with its drum at F is bolted down. N is the opaque mirror adjusted by three leveling screws and a spring (horizontal and vertical axes) within the capsule B. The slide should have from 1 inch to 2 inches of clear play and its displacements should be determinable to about 0.0001 cm. The opaque mirrors M and N may both be silvered on the back. They thus last indefinitely.

Since the telescope E rotates both around its own axis e'' and around the standard Q, elaborate centering of the grating G is not usually necessary. The latter is mounted between strips of cardboard or wood and secured by the screw g, the brass clutches being about twice as far apart as the thickness of the grating. In other words, the grating may be slightly moved in a direction normal to itself.

To adjust the parts, sunlight (preferably) is passed into the widened slit of the collimator, in a dark room, so that the spots falling on the mirrors M and N (the grating being suitably turned) and on the objective of the telescope E are seen and the different reflected images brought nearly into coincidence. A further adjustment is then made through the telescope E, two of the usual four images of the slit (now narrowed) being placed in coincidence horizontally and vertically by manipulating the leveling screws on B. Specks of dust, or nicks in the slit, greatly facilitate this adjustment. The telescope is then turned to the diffraction spectrum, preferably of the first order, and the drum actuated till the interferences appear. Naturally the distances GN and GM are to be approximately equal to begin with. The solitary ellipses are best for general purposes, and they usually correspond to undeviated yellowish and bluish single-slit images. The multiple-slit image is to be avoided. If the rings are not quite centered in the spectrum, they may be made so by cautiously adjusting the screws at B, which tip the mirror about a horizontal axis. The telescope should be moved with its foot sliding on a plane. The three possible positions of the mirror N (positive uncompensated, self-compensated, negatively uncompensated) are about 1 cm. apart on the micrometer, for a plate of glass 0.68 cm. thick. When the arc lamp is used the accentuated sodium lines in the spectrum may be used in place of the white undeviated images of the slit, both for adjustment of the two spectra for coincidence and as a fiducial mark, in place of the cross-hairs in the telescope. For a small angle of incidence the sodium lines of higher orders of spectra are also liable to be available.

To measure the angle of incidence I the table I is turned in its socket until the reflected image of the slit coincides with the slit itself. A hole is cut in the top or side of the collimator tube near the slit (not shown) for this purpose. Thereupon the table I is turned back again until the images coincide in the telescope. The angle read off on the graduated plate K is I, the reflected ray traveling over $2I$. The table I is provided with an index and vernier (also omitted in the diagram).

The apparatus described, being made virtually of hollow parts, is light enough to be carried about with convenience. In the case of the figure where the angle of incidence I is small, the distance from M to N is about 70 centimeters. It may easily be increased to several times this, by inserting longer gas-pipes at c and d with appropriate braces. The fringes are very stable even when the instrument stands on a table fastened to a wall-bracket. They naturally quiver when the observer is manipulating the micrometer screw, but they return at once to quiescence when the hands are removed. To obviate the quiver, *i.e.*, to follow the motion of individual rings, the usual tangent screw method may be employed.

I may add in conclusion that in order to make the rings sharply black and color, a slit about a millimeter wide, placed vertically in front of the objective of the telescope E, may be employed. This may be supported by an ordinary clamp on the arm e, the clamp giving opportunity for the lateral motion needed in adjustment.

84. Other interferences.—The same apparatus may be adapted for observing the linear diffraction-reflection interferences described by Mr. M. Barus and myself.* The equations here available are

$$\delta e = \lambda/2 \cos i \qquad \delta e' = \lambda/2 \cos \theta \qquad \delta e'' = \lambda/2 (\cos \theta - \cos i)$$

where δe, $\delta e'$, and $\delta e''$ are the respective increments of the air-spaces between the face (rulings) of the grating and the parallel opaque mirror in front of it, per fringe passing the cross-hairs of the telescope or a given spectrum line, λ the wave-length of light, and i and θ the angles of incidence and diffraction in air. For the measurement of δe, λ, i, θ should be known or determinable.

For these observations let the micrometer C be removed from its plate and now bolted down on the graduated plate K (fig. 57), the tube I and appurtenances being discarded. This must be so done that the face of the opaque mirror N and the rulings of the grating g are in the axis of rotation with the lines of the grating parallel to it and the slit. Hence the mirror must be adjustable by aid of a capsule B with set-screws (horizontal and vertical axes of rotation) and springs. The grating g has its independent mounting with three similar set-screws and springs. In the figure the mirror N is stationary, *i.e.*, fixed to the rigid part C of the micrometer, while the grating is movable to and fro, *i.e.*, fixed to the slide D and actuated by the micrometer screw s and graduated head F. Usually N will be attached to some apparatus whose linear excursions are to be found, and for this purpose of attachment the cross-coupling R in fig. 55 is abundantly supplied with screw sockets (front and rear, not shown), so that such parts may be here attached. In fig. 57 the counterpoise H, for instance, has been added.

* The grating interferometer, Science, XXXI, 394, 1910; Phil. Mag. (6), XX, p. 45, 1910; Publication No. 149, Carnegie Institution of Washington, chap. 2, 1911.

To prepare for observation the plate K and the telescope E are turned until a suitable angle of incidence $i = ANs$ and of diffraction $\theta = sNE$ are obtained. The fringes are seen when g and N are sufficiently near together (the distance apart may be as much as 1 centimeter), on condition that the direct images of the slit from the front face of N and the rear face of g are in coincidence horizontally and vertically. E may be revolved for this preliminary adjustment. To find i, the angle of incidence, the graduated plate K is turned from the given position of coincidence until the image of the slit falls upon the slit itself at the end of the collimator A, a hole (not shown) being left in the collimator tube near the slit for this purpose, as explained above. If the fringes are not sharp, they may be made so by

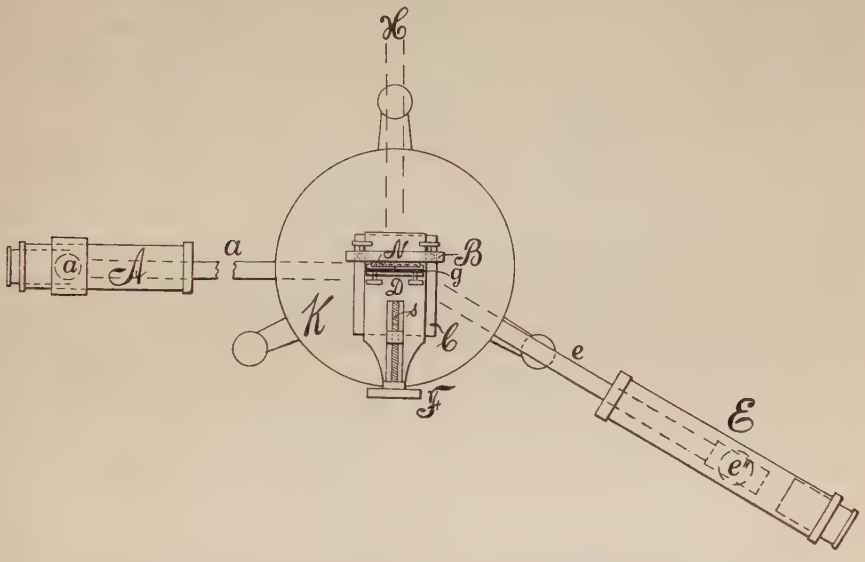

FIG. 57.—Modification of apparatus for diffraction-reflection interferometer.

further adjusting the set screws of N or g by trial. This usually succeeds easily, remembering that the fringes move about a horizontal axis normal to the mirror when the mirror moves about a horizontal axis parallel to its face. For other details the earlier paper should be consulted.

85. Other measurements: high temperature, adiabatic transformations, etc.—The displacement interferometer constructed with its arms made of gas-pipe is adapted for high-temperature investigation. For if a current of cold water at constant temperature be passed through the arms in question they will be kept at invariable length, however much the atmosphere about them may change in temperature. Furthermore, since the distance between the central grating and the opaque mirror may easily be increased to a meter or more, tubes of considerable length may be inserted in the

interfering beams of light. The displacement interferometer should be used with the angle of incidence nearly zero, in which case this angle is without effect on the micrometer reading and the observing telescope lies in a particularly convenient position side by side with the opaque mirror on the micrometer. This is thus immediately at hand.

It seemed to me, therefore, that a particularly interesting subject for investigation would be the relation of temperature and pressure of the index of refraction μ of air. According to Lorentz* the $\mu-1$ for air follows the equation

$$p=C\,(\mu-1)\,\vartheta$$

(p pressure, C constant, ϑ absolute temperature), coinciding in form to the intrinsic equation of a gas, since the temperature coefficient of $\mu-1$ for air is very nearly equal to its coefficient of expansion. Mascart finds this not quite true. Pressures are to be corrected by $(1+\beta p)$ where β is equal to 0.0000072 relative to centimeters of mercury and the temperature coefficient is $\alpha=0.00382$.

At all events, the temperature coefficient α is so large that a method of high-temperature measurement is not out of the question on the one hand, while on the other the variation of α throughout long ranges of temperature is of considerable interest. I have, therefore, made a few tentative measurements at low temperatures to test the apparatus and have found it trustworthy throughout. In table 37 the apparatus is adjusted with an angle of incidence of $I=15°$. The index of refraction is determined from the displacement of ellipses when the air contained in a longitudinal sealed tube in one of the component beams of light which interfere is alternately filled with air at pressure p and exhausted at a given temperature t. This tube was 23.8 centimeters long and of brass surrounded with a close-fitting tubular temperature bath.

The first column of table 37 shows the barometric height and degree of exhaustion (residual pressure). The second the micrometer displacement of the opaque mirror which brings the centers of ellipses back to their original position with reference to a given spectrum line. This reading is taken on the drum of the micrometer, the scale parts being 0.0005 centimeters. When electric arc light is used the accentuated sodium line is always in presence in the spectrum and makes an excellent fiducial line for the centers of the ellipses. A single exhaustion is sufficient for two readings, as the displacement occurs on exhaustion (from red to green, for instance) and is measured by the turn of the micrometer to bring the ellipses back; while on readmitting air the displacement is in the opposed direction and is again measured by restoring the center of ellipses to the position of the sodium line. If this displacement of the opaque mirror on the micrometer is ΔN centimeters the index required is

$$\mu=1+\Delta N/c$$

* See the admirable summary in Landolt and Boernstein's Tables.

if e is the length of the tube. ΔN must be given in centimeters, as shown in the third column of the table, and from this the μ of the fourth is found at the temperature t in the last column. They refer to the wave-length of the D line, as this was taken as the fiducial mark. The absolute values of μ are good, but here of relatively little interest, as no attempt was made to standardize the screw, etc., of the measuring apparatus, and the water circulation had not yet been installed. The temperature coefficient may be found without this. If, therefore, $(\mu-1)$ is expressed in terms of t the result is $\alpha=0.0036$, or of the order expected.

TABLE 37.—Index of refraction of air from shifts ΔN of ellipses. $e=23.8$ cm. Angle of incidence, $I=15°$.

Barometer. vacuum.	Shift* drum.	Mean shift ΔN	$\mu=\frac{\Delta N}{e}+1$	t
		cm.		
76.95 : 19°	13.3	0.00663	1.000279	30°(?)
	13.3			
0.5 cm.	13.3			
	13.2			
	13.5			
	13.0			
	13.6			
76.98 : 24°	13.4	.00674	1.000283	23°
	13.6			
0.4 cm.	13.3			
	13.7 ccl			
77.15 : 21°	13.4 cl	.00677	1.000284	21°
	13.8			
0.4 cm.	13.3			
	14.5 cl			
77.15 : 21°	14.5 ccl	.00727	1.000306	2°
	14.1			
0.4 cm.	15.0			
	14.4			
	14.9			
	14.1			
	14.8			

* These fluctuations are due to the absence of water circulation.

From this datum the working conditions of the apparatus may be specified. For a tube 23.8 centimeters long the micrometer displacement per degree centigrade is 0.051 scale parts or 0.0005 centimeter each; *i.e.*, the micrometer displacement is about 0.000025 centimeter per degree centigrade, or about 10^{-6} centimeter per degree centigrade per centimeter of length of tube. Thus a minimum of about 2° C. is directly appreciable in the given case, or for a tube about half a meter long a minimum of 1° C. should be appreciable at all temperatures. This, moreover, would correspond to the evanescence of two rings in succession, whereas in the above

apparatus a little less than one ring vanishes per degree centigrade, at all temperatures. The displacement of ellipses for an atmosphere of pressure is roughly from the D nearly to the E line.

In this method the arms need not be of invariable length except during the short period of exhaustion, as the data are obtained by differences.

To turn to the second method for obtaining the same results: the displacement of ellipses is accompanied by the radial motion of rings to and from the center, and the number vanishing may be counted. If λ is the mean wave-length between the initial and final positions of the rings and n is the number of rings vanishing, then the equivalent micrometer displacement would be

$$\Delta N = n\lambda/2$$

so that the micrometer reading ΔN need not be taken. Hence

$$\mu = 1 + n\lambda/2e$$

To make use of the method, a fine screw stop-cock is to be inserted through which dry air may be admitted at any rate into the exhausted tube. In this way the motion of the rings toward the center may be controlled perfectly and their evanescence counted. The experiment is very interesting. Clearly the arms must be kept at invariable length while the rings are being counted, *i.e.*, until they cease to move, when the pressure is again normal. Fig. 58 contains an example of many results of this kind. Here the abscissas denote the number of rings which have vanished and the ordinates the corresponding pressure, the latter increasing from a few millimeters to an atmosphere. The line of observations happens to be nearly continuous. An interruption of the count is, however, of no serious consequence, as the slope of the line is alone in question when the initial pressure and final pressure are known. It is surprising to note how closely these observations lie on a straight line. They do so quite within the errors of observation.

The slope of the line is

$$\frac{70.0 - 2.8}{210} = .320$$

i.e., 0.32 centimeter of mercury at 0° C. per ring vanishing, or a little over three rings (3.125) per centimeter of mercury. The mean wave-length in question (between the D and E lines) is about $\lambda = 55.8 \times 10^{-6}$. Hence, as the effective barometer was $76.95 - .500 = 76.45$ centimeters and the tube length 23.8 centimeters,

$$\mu = 1 + \frac{76.45 \times 27.9 \times 10^{-6}}{.32 \times 23.8} = 1.0002806$$

The datum obtained from the displacement of ellipses at the same temperature (unfortunately not taken) was 1.000279. Inasmuch as the water circulation was omitted during the ring measurements and the exact

value of λ was not specially found, the agreement is as close as may be expected.

The two data selected from many similar results show how easily both methods may be used for mutual corroboration. Clearly the ring method, since it involves the evanescence of about 236 rings, is more sensitive, but also less expeditious.[1] It is not, however, necessary to observe all the rings; the disappearance of a reasonable number, say 25 or 50, establishes the rate of evanescence per centimeter of mercury, or more conveniently the number of centimeters of mercury per vanishing ring. If this is determined at the beginning and end of exhaustion the mean result is adequate.

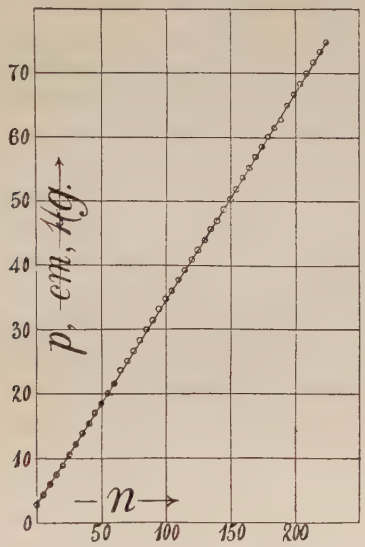

FIG. 58.—Graphs showing number of interference rings, vanishing in case of increasing pressure of imprisoned air, kept at constant temperature.

If the air-tube of the apparatus is so modified that the air may be heated electrically the ring method should be equally available for temperature measurements. The results could be compared with a thermo-couple having its fine junction inserted in the tube and read simultaneously.

As a method of pressure measurement, since for a tube 23.8 centimeters long, 3.12 rings vanish per centimeter of mercury, *i.e.*, about 0.1313 ring per centimeter of tube-length per centimeter of mercury pressure, the method is not very sensitive unless a long tube be used. A tube 1 meter long would, for instance, give 13 rings per centimeter of mercury, admitting of the measurement of pressure to 0.08 centimeter per ring. One might estimate to 0.5 millimeter.

The method of pressure measurement has the rare advantage, however, of being absolutely instantaneous, as reproducing, immediately, the state

of the gas. It is, therefore, remarkably well adapted for the study of adiabatic phenomena. Many questions relative to such transformation of gases are thus open to investigation. Since $(\mu-1)=\Delta N/e=n\lambda/2e$ and $p=C(\mu-1)\vartheta$

$$\frac{p}{\vartheta}=C\cdot\Delta N/e=C\lambda n/2e$$

the variations of p/ϑ are directly given by the number, n, of rings vanishing. But the relation of p and ϑ is also given either by the intrinsic equation of the gas or by its adiabatic equation, according to the transformation which has been imposed on the gas, so that p and ϑ are each determinable.

CHAPTER XI.

THE DEGREE OF ADIABATIC EXPANSION IN GASES RAPIDLY COOLED, AS OBSERVED BY DISPLACEMENT INTERFEROMETRY.

86. Introduction. Apparatus.—In the present paper I shall make a first application of the displacement interferometer described in the preceding chapter of this report. The investigation is purely tentative, the endeavor being both to exhibit the interference method for a case in which it is put to a test lying near the limit of its sensitiveness and at the same time to measure the degree of adiabatic expansion attainable in fog-chambers of regularly increasing size. The paper is, therefore, not to be construed as purposing to actually measure the ratio γ of the specific heats of a gas, but rather to determine the degree of adiabatic expansion in any given apparatus in terms of the value of γ found for that apparatus. From this point of view γ will increase from 1 to 1.41 in proportion as the expansion in question is more truly adiabatic.

The adjustment adopted is shown in fig. 59, the angle of incidence I being as small as possible (about 15°), in which case the equation for the position coördinate, N_c, of the movable opaque mirror (micrometer), when the center of ellipses is at the wave-length λ, *viz*,

$$(1) \qquad N_c = e'\left(\mu \cos R - \frac{\lambda}{\cos R}\frac{d\mu}{d\lambda}\right) = e'\left(\mu \cos R + \frac{2b}{\lambda^2 \cos R}\right)$$

takes its simplest form, since the angle of refraction R approaches zero. In the equation e' is the thickness of the grating, μ its index of refraction for the wave-length λ, and b the coefficient of Cauchy's equation. If, as in the present paper, the centers of ellipses after displacement are brought back to the *same spectrum line* (D line for instance) again, immediate reference to change of μ with λ is excluded and the equation for the displacement of the opaque mirror on the micrometer is then apparently

$$(2) \qquad \Delta N_c = e\,(\mu - 1)$$

where e is the thickness of the object placed in one of the interfering beams, μ its index of refraction relative to air for the given wave-length λ.

This simple theory, however, is only approximately true, inasmuch as the ellipses change in size with the amount of compensation introduced by the object. The conditions reëstablished at the D line are thus not quite identical in the presence and the absence of the object. In fact, the grating as in equation (1) is alternately reinforced by a column of dense and rare air through which the beam travels at normal incidence. If ΔN be the difference of the micrometer readings for the two positions, equa-

tion (2), in which the dispersion of air is neglected, is to be modified in the way suggested for equation (1), so that for the D line of the spectrum as fiducial

$$(2') \qquad \Delta N/e = \mu_0 - \mu - \frac{\lambda}{e}\left(\frac{d\mu_0}{d\lambda} - \frac{d\mu}{d\lambda}\right) = \mu_0 - \mu + \frac{2}{e\lambda^2}(b_0 - b)$$

Here e is the length, μ_0 and μ the respective indices of refraction for the high and low densities of the column of air. Equation (2') is, however, apparently too cumbersome for use at the outset, so that equation (2) has been preferably admitted for experimental purposes, the dispersion of air being disregarded. The values of ΔN so found are too large and the consequent values of γ all too small. They will be corrected, however, in § 97, in which the theory is to be developed in full. It will then be found that the data of the interference method agree with the data of the mechanical method as nearly as may be expected.

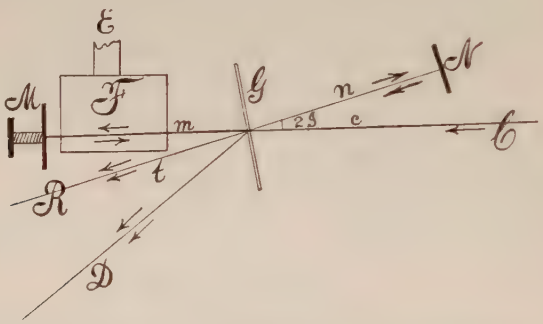

FIG. 59.—Diagram of displacement interferometer, $C\ G\ M\ N\ D$, and the air-chamber F.

If ΔN_c is equivalent to n interference rings of the *mean* wave-length λ,

$$(3) \qquad \Delta N_c = n\frac{\lambda}{2}$$

In fig. 59 the pencil of light c enters from a collimator at C and encounters the grating G at a small angle of incidence I. The reflected undeviated beam n is returned by the stationary opaque mirror N, the transmitted beam m by the movable opaque mirror M on the micrometer, after which both enter the telescope R. The arms m and n of the interferometer are of gas-pipe and provided with a circulation of cold water at constant temperature, though in the present chapter this is not needed. The micrometer at M is graduated to 0.0005 cm. on the drum and easily read off by estimation or vernier to 0.00005, *i.e.*, to the mean wave-length of light. The tests below show that the center of ellipses may be placed on a given spectrum line with about the same precision. Hence the displacement method is not much less sensitive than the ring method.

The object F to be examined for change of index of refraction, *i.e.*, the air within a closed chamber, dry or wet, at any temperature, is conveniently

placed in the beam *m*. If its lateral extent is wide, the angle *I* must be increased; but it is obviously desirable, apart from the other reasons given above, to have the telescope as near the micrometer *M* as possible, in order that the micrometer may be manipulated with ease and expedition. Though the telescope at *R* is needed for adjustment, the position at *D* is used for observation. Hence if the adjustment is made once for all, a much larger angle is available than for the undeviated beam. Incidental adjustment may be made after the fog-chamber *F* is inserted, by placing the two diffracted images of the sodium line used in coincidence, together with a simultaneous coincidence of the pairs of sharp shadows (horizontal black line) of dust-specks or a cross-wire at the slit. Finally, in the method used below the pencils *m*, *R*, *D*, etc., may all be made to pass through the plate-glass sides of the fog-chamber (see fig. 63).

To obtain ellipses quite sharp (alternating black and colored bands), a part of the objective of the telescope should be cut off by a small adjustable vertical screen about 1 inch square, or by a wide slit. More than one-fourth of the ¾-inch objective is rarely needed in the horizontal direction. When this is done, undesirable beams of light are excluded and the stationary interferences are also liable to vanish, whereupon in the case of sunlight the Fraunhofer lines (to be used as fiducial lines) become unmistakably sharp and clear. In case of electric arc light, the sodium line from the silicate in the carbons is always strong and a number of them are usually available in the different orders of spectra. The ellipses, too, remain in the field, in spite of rough usage of the apparatus near at hand (air-pump, sudden exhaustion, etc.). The electric arc should be used *directly*, *i.e.*, without lenses or condensation, the arc being adjusted in height, etc., and at a distance of about one foot or less from the slit. The present method depends essentially on the use of *narrow* pencils. The sodium line is apt to be much higher than the spectrum band in the telescope. It is intersected by interference bands even in dark parts of the field of view. With the motion of the rings these move up and down the line.

The use of the coincident sodium lines for reference reduces all the measurements to the wave-length of this line, as the centers of ellipses are invariably brought back to it.

The fog-chamber in the present experiments is much too short for accurate measurements; but it is admitted (as suggested above) to test the details of the method. In definite experiments the component pencils of light should be made to pass (by reflection between mirrors) many times through the fog-chamber, in which case not only would the sensitiveness be increased proportionally but mean increments would be reached for all parts of the air-chamber.

87. Equations.—It is convenient to test the present method of observation by a determination of the ratio γ of the specific heats of constant pressure and of constant volume, as has been suggested. This offers a

serviceable method of arranging results, even if an absolute measurement of γ is not directly aimed at. The degree of adiabatic expansion reached in vessels of different sizes, by sudden exhaustion into a vacuum-chamber by the plug-cock method, is the chief point at issue, both when the exhausted chamber is dry and when it is wet. In proportion as the exhaustion is less adiabatic and more isothermal the value of γ found will decrease from about 1.4 to 1.0.

The normal equation of the transformation impressed on the gas is thus

$$p v^{\gamma} = \frac{p}{\rho^{\gamma}} = \frac{p_0}{\rho_0^{\gamma}} \tag{4}$$

for approximately adiabatic expansion, in case of pressure p, specific volume v, and density ρ, for two different states. Similarly the intrinsic equation of a gas and the Lorentz equation (afterwards to be corrected) for the change of index of refraction of air with temperature and pressure (the temperature coefficient being approximately identical with the coefficient of expansion), are

$$p = R\rho\vartheta \tag{5}$$

$$p = C(\mu - 1)\vartheta \tag{6}$$

Here R is the gas constant and ϑ the absolute temperature. C for refraction thus corresponds to R and $(\mu - 1)$ to ρ. To determine C, since

$$C = \frac{p_0}{\vartheta_0(\mu_0 - 1)}$$

the data in Landolt and Boernstein's tables are available. If Mascart's or Kaiser and Runge's data be taken

$$C = \frac{76}{273} \quad \frac{1}{.000292} = 952.6$$

Mascart's equation differs from equation (6) by the appearance of two corrective members and may be written, if t is temperature in degrees centigrade and the pressure p is expressed in centimeters of mercury,

$$p = C(\mu - 1)\vartheta \frac{1 + .00015\, t}{1 + .0000072\, p}$$

which is nearly equivalent to replacing C in equation (6) by

$$C\,(1 + 10^{-6} \times 150\, t - 10^{-6} \times 7.2\, p)$$

The difference is usually within 0.3 per cent and thus easily allowed for. The full equation will be considered below.

Returning to equations (5) and (6), we obtain by division

$$\rho = \frac{C}{R}(\mu - 1)$$

which in (4) gives

$$\frac{p}{(\mu - 1)^{\gamma}} = \frac{p_0}{(\mu_0 - 1)^{\gamma}} \tag{7}$$

If the air in the chamber F is partially exhausted from p_0 to p, changing the index of refraction of air from μ_0 to μ and ΔN, the displacement of the opaque mirror at the micrometer, is needed to return the center of ellipses to its original position on the sodium line

$$\mu_0 e = \mu e + \mu_0 \Delta N$$

where e is the length, *i.e.*, the thickness of the exhaustion-chamber in the direction of the transmitted beam of light. Hence

$$\mu - 1 = \mu_0 - 1 - \frac{\Delta N}{e}$$

since μ_0 is practically equal to 1 in association with ΔN. This together with (5) and (6) inserted in equation (7) gives

$$\frac{p}{p_0} = \left(1 - \frac{C\vartheta_0}{ep_0}\Delta N\right)^{\gamma} \tag{8}$$

From (8)

$$\gamma = \frac{\lg (p/p_0)}{\lg\left(1 - \frac{C\vartheta_0}{ep_0}\Delta N\right)} \tag{9}$$

where p_0 and ϑ_0 are the initial pressure and temperature in the air-chamber just before exhaustion.

Furthermore, whenever the evanescence of n rings is observed

$$\Delta N = n(\lambda/2)$$

for a mean wave-length λ over which the center of rings passes. Equation (9), which may now be written

$$\Delta N = \frac{e}{C}\left(\frac{p_0}{\vartheta_0} - \frac{p}{\vartheta}\right) \tag{10}$$

shows that ΔN depends simply on the change of density of the gas and not on its temperature and pressure separately. Hence ΔN does not change after exhaustion while the air in the chamber, with rise of temperature and of pressure, gets back to atmospheric temperature. For if the chamber is tight, ρ remains constant. This is true to the extent in which C is constant. Nevertheless in practice, during the short period of apparently stationary minimum temperature and pressure subsequent to exhaustion, it is easy to observe the evanescence of a number of rings in a sense equivalent to an increase of ΔN. This phenomenon will be discussed at length below.

If in equation (8) corrected with reference to Mascart's results the correction factor is placed within the parenthesis and $\delta t = t_0 - t$ and $\delta p = p_0 - p$, the value of γ is very nearly

$$\gamma = \frac{\lg (p/p_0)}{\lg\left(1 - \alpha''\delta\vartheta + \beta\delta p - \frac{C\vartheta_0\Delta N}{ep_0}(1 + \alpha''t - \beta p)\right)} \tag{11}$$

where $\alpha = 0.00015$ and $\beta = 0.0000072$ relative to centimeters of mercury. Thus γ is not quite independent of the individual pressures and tempera-

tures, but it is difficult to state at the outset what will happen. If an expansion in series is to be made from equation (11) to include the correction, δp must be very small and the equation becomes

$$\gamma = \frac{e\delta p}{C\vartheta_0 \Delta N + a''(C\vartheta_0 t \Delta N + ep_0 t_0) - \beta(C\vartheta_0 \Delta N p + ep^2_0)} \tag{12}$$

which shows that γ without the correction is too large.

For the case in which δp and ΔN are small, equation (9), if expanded, thus leads simply to

$$\gamma = \frac{e\delta p}{C\vartheta_0 \Delta N} \tag{13}$$

where δp is the drop of pressure on adiabatic expansion. Here γ depends on the percentage accuracy of δp, e, C, ϑ_0, and ΔN, while p_0 does not enter the equation. The sensitiveness is thus directly increased by elongating the chamber in the direction of the beam of light as suggested above. A similar approximation is obvious when $\gamma = 1$, very nearly. In such a case (13) also applies, or ΔN and δp are here proportional quantities.

In general, if $\gamma a = \log_{10}(p/p_0)$

$$\Delta N = \frac{1 - 10^a}{C\vartheta_0 / ep_0}$$

When use is made of the combined air-chamber and vacuum-chamber (the latter having been taken as infinite in size in the above equations) and sudden expansion takes place from one to the other, the initial temperature and pressure p_0 and ϑ_0 in the air-chamber and the initial pressure p of the vacuum-chamber are observed; but the final common pressure, p', when the chambers are in communication, can not as a rule be found by observation. The pressure p' may, however, be computed from the initial pressure p of the vacuum-chamber before exhaustion as follows: Let v be the (small) volume of the air-chamber where γ is observed and which contains a plenum of air and V the (large) volume of the vacuum-chamber. The functions of these chambers may, of course, be reversed, so that low pressure exists in the air-chamber and a plenum in the vacuum-chamber. Since the increase and diminution of volume v' are identical for the two chambers

$$p_0 v^\gamma = p'(v + v')^\gamma; \quad p V^\gamma = p'(V - v')^\gamma$$

and v' may be eliminated; whence

$$\left(\frac{p'}{p_0}\right)^{1/\gamma} = \left(\frac{p}{p_0}\right)^{1/\gamma} \frac{V}{V+v} + \frac{v}{V+v} = 1 - \frac{C\vartheta_0 \Delta N}{ep_0} \tag{15}$$

and finally

$$\gamma = \frac{\lg(p/p_0)}{\lg\left(1 - \frac{V+v}{V}\,\frac{C\vartheta_0 \Delta N}{ep_0}\right)} \tag{16}$$

so that the initial pressure, p_0, of the air-chamber and p of the vacuum chamber need only be observed, if the relative volumes v/V are known.

If $v/V=0$, the above equation (9) is reproduced. From equation (16) the values of ΔN for $\gamma=1$ and $\gamma=1.41$ may be computed, *viz*,

$$\Delta N_{\gamma=1}=\frac{ep_0}{C\vartheta_0}\left(1-\frac{p}{p_0}\right)\frac{V}{V+v} \tag{17}$$

and

$$\Delta N_{\gamma=1.41}=\frac{ep_0}{C\vartheta_0}\left(1-\frac{p}{p_0}\right)^{.71}\frac{V}{V+v} \tag{18}$$

where $1/\gamma=.71$.

Finally, the fall of temperature appears as

$$\lg\vartheta'=\lg\vartheta_0+(\gamma-1)\lg\left\{\left(\frac{p}{p_0}\right)^{1/\gamma}\frac{V}{V+v}+\frac{v}{V+v}\right\} \tag{19}$$

where ϑ_0 is the initial and ϑ' the final temperature in the air-chamber immediately after exhaustion.

If the rôles of the air-chamber and the vacuum-chamber are exchanged, *i.e.*, if the vacuum-chamber now contains a plenum of air, ΔN becomes negative, so that arithmetically $p>p_0$,

$$\gamma=\frac{\lg\,(p/p_0)}{\lg\left(1+\frac{V+v}{V}\frac{C\vartheta_0\Delta N}{ep_0}\right)} \tag{20}$$

which, if $v/V=0$, or the atmospheric pressure, B, becomes the common adiabatic pressure, reduces to

$$\gamma=\frac{\lg\,(B/(B-\delta p))}{\lg\left(1+\frac{C\vartheta_0\Delta N}{e(B-\delta p)}\right)} \tag{21}$$

All the quantities needed in equation (9) are easily measured except ΔN, the micrometer displacement for so small a value of e as has entered into these experiments. The error made in ΔN due to the mere placing of the center of ellipses on the fiducial sodium line is not larger than .00005 cm. But there may be further discrepancy owing to the flexure of glass windows or to their displacement. To compute it, the equation ($v/V=0$)

$$\frac{\partial\gamma/\gamma}{\partial(\Delta N)}=\frac{C\vartheta_0/ep_0}{\left(\lg\,(1-\frac{C\vartheta_0\Delta N}{ep_0})\right)\left(1-\frac{C\vartheta_0\Delta N}{ep_0}\right)} \tag{22}$$

may be used.

Finally, we may add to these equations the value of the actual expansion v' which the volume v of the air-chamber undergoes on sudden change of pressure from p_0 to p', when p is the pressure of the vacuum-chamber of volume V. From equation (15) on reduction

$$\frac{v'}{v}=\frac{p_0^{1/\gamma}-p^{1/\gamma}}{p^{1/\gamma}+\frac{v}{V}p_0^{1/\gamma}} \tag{23}$$

if $V=\infty$

$$v'/v=(p_0/p)^{1/\gamma}-1$$

which is identical with the adiabatic equation.

88. Small brass fog-chamber dry and wet.—The first experiments were tried with a small air-chamber of brass (fig. 60), flanged at both ends and provided with an exhaust-pipe E leading by way of a 1½-inch rubber hose to a large vacuum-chamber. This was kept at a definite low pressure by an air-pump. A cock (not shown) was available for influx of dry air into F. The ends of F are closed with glass plates g g', secured by a ring and bolts which press the plates against the rubber gaskets r r' with complete freedom from leakage. The dimensions of the chamber F were: length, 17 cm., diameter, 3.7 cm. The exhaust-pipe was 2.7 cm. in diameter and somewhat over 50 cm. long. The volumes of the air (v) and vacuum (V) chambers were thus

$$v = 183 + 442 = 625 \text{ cu. cm.}$$
$$V = 12770 + 97 = 12867 \text{ cu. cm.}$$

respectively, whence $v/V = .049$. Unavoidably the pipe comprised a greater volume than the air-chamber. The latter was lined with thick dry blotting-paper to be moistened with water at the end of the experiment.

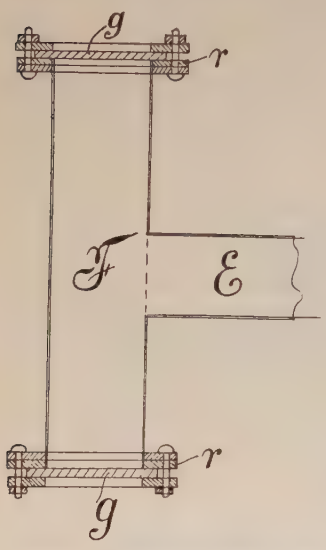

FIG. 60.—Longitudinal section of tubular air-chamber, 17 cm. long.

The measurements were made with this by placing the center of ellipses on the sodium line and noting the micrometer reading, then suddenly exhausting by opening the 1-inch stop-cock into the vacuum-chamber and closing it again by a single sweep of 180°. The ellipses were now brought back to the sodium line by moving the micrometer over the measured distance ΔN from the first position. Table 38 gives an example of the mean results for drops of pressure between 20 and 60 cm. At each of these stages many measurements were made and the mean of the results taken. ΔN, so far as mere measurement is concerned, is correct to 0.00005 cm. in a single reading.

TABLE 38.—Experiments made with the small brass air-chamber attached to the arm m, fig. 59. Method by exhaustion into vacuum-chamber. Barometer, $p_0 = 76.13$ cm.; temperature, $t_0 = 20.7°$, $\theta_0 = 293.7°$; length, $e = 17$ cm.; $C = 952.6$; $v/V = .049$.

p	$10^6 \Delta N$	γ
56.13	1250	0.97
36.13	2500	.96
16.13	3900	.84

Here γ is so nearly 1 that the expansion takes place under virtually sothermal conditions, in view of the small air-chamber and in spite of

the rapidity of exhaustion. That this is not quite the case, however, is shown by the distorted ellipses immediately after exhaustion, indicating that the rays corresponding to different parts of the ellipses have passed through air at different temperatures; but the uniformity is soon again restored. It is also to be borne in mind that γ for the case of equation (2) is inherently too small.

It is not impossible, however, that these low values of γ which imply an excessive ΔN may in a measure be owing to some distortion of the arm m to which the chamber was attached during exhaustion. Strains introduced here are necessarily very serious and they would be largest at the highest exhaustion.

The air-chamber was therefore detached from the arm m and supported on an *independent* standard, screwed to the same table on which the interferometer stood. The results are given in table 39, which again is a mean of many observations.

TABLE 39.—Experiments made with a small brass fog-chamber attached to independent standard on table. Exhaustion into vacuum-chamber. Barometer, $p_0 = 74.57$; temperature, $t_0 = 21.2°$, $\theta_0 = 294.2°$; constants as in table 38.

p	$10^6 \Delta N$	γ
54.57	1250	0.97
34.57	2750	.82
14.57	4150	.66

These data for γ are actually worse than the preceding, showing that distortion during exhaustion has been effectively increased. It is disconcerting to find that the individual observations, corresponding to any given drop of pressure, are definite and consistent, *i.e.*, apparently quite trustworthy; but this merely shows the subtle character of the strain error involved when transmitted through the table. If special tests are made they again prove that some adiabatic expansion does occur; for when the cock is left open, the rings continue to move outward, indicating a current from the air-chamber to the vacuum-chamber. This is nearly absent when the cock is rapidly closed. Moreover, by warping the table the effect observed is quite significant, being in part elastic and in part viscous.

Hence the small brass fog-chamber was now detached and *suspended from the wall* on an *independent* bracket and clamp, so as to be entirely free from the interferometer and table. The data are given in table 40.

These values of γ are probably correct, subject to the final correction, for the conditions involved, *i.e.*, for the degree of adiabatic expansion which can be reached in so small a chamber with the given means of exhaustion and so large a drop of pressure. The inadequacy of the small tube for the present purposes is shown (as instanced above) by the distortion of rings immediately after exhaustion, while their figures gradually become symmetrical again as the uniform temperature is regained, and

by the continuous exhaustion if the exhaust cock is left open instead of being swept rapidly from closed to closed over an arc of 180°. If the conditions had been isothermal, $\gamma = 1$, or quite adiabatic, $\gamma = 1.41$, the data

TABLE 40.—Experiments with air-chamber suspended from wall on independent bracket. Dry air. Exhaustion into vacuum-chamber. Barometer, $p_0 = 75.80$; mean absolute temperature, $\theta_0 = 291.8°$; constants as in table 38.

p	$10^6 \Delta N$	γ	$10^6 \Delta N$ for $\gamma = 1$	$10^6 \Delta N$ for $\gamma = 1.41$	γ corrected
55.80	1100	1.08	1170	868	1.12
35.80	2250	1.06	2330	1834	1.11
15.80	3450	1.05	3500	2985	1.13

of ΔN computed in the table should have been found. The error of mere measurement, being not much larger than $\Delta N = 5 \times 10^{-5}$ cm., can not explain any of these discrepancies, though it does account for the irregularities.

TABLE 41.—Small brass fog-chamber remounted. Brass-tube connection. Fog-chamber exhausted. Barometer, $p = 75.26$, $\theta = 290°$ to 290.8°; $v/V = .014$; $e = 17$ cm.

p_0	$10^6 \Delta N$	γ	Comp. $10^6 \Delta N$ $\gamma = 1$	Comp. $10^6 \Delta N$ $\gamma = 1.41$	γ corrected
65.22	575	1.056	607	426	1.090
55.17	1050	1.138	1214	826	1.172
45.13	1650	1.082	1816	1196	1.112
35.08	2225	1.065	2421	1527	1.091
25.04	2633	1.068	3036	1795	1.116
15.00	3300	1.052	3632	1946	1.070
4.95	4000	1.021	4237	1769	1.034

Some time later experiments were repeated with the same chamber, using, however, a 2-inch brass exhaust-pipe (with the exception of the 1-inch mouth at the chamber), a $2\frac{1}{2}$-inch stop-cock, and a very large vacuum-chamber, $v/V = .014$. The new results are given in table 41.

TABLE 42.—Experiments with fog-chamber suspended from an independent wall-bracket. Wet air. Barometer, $p_0 = 76.00$ cm.; absolute temperature, $\theta_0 = 297.3°$; constants as in table 38.

p	$10^6 \Delta N$	γ	Comp. $10^6 \Delta N$ $\gamma = 1$	Comp. $10^6 \Delta N$ $\gamma = 1.41$
56.00	1050	1.11	1140	852
36.00	2100	1.14	2290	1799
16.00	3400	1.03	3430	2927

The improvements have made little difference in the results for γ. They are still of the same low order as in the preceding case. It is probable, moreover, that the transformation in the large exhaust-pipe unavoidably attached is more nearly adiabatic than in the small fog-chamber.

Additional experiments with dry air did not seem to promise new returns. The air-chamber was therefore converted into a fog-chamber by thoroughly wetting the blotting-paper within. The results obtained with air saturated with moisture are shown in table 42.

These data are virtually the same as for dry air. The computed values of ΔN for $\gamma=1$ and $\gamma=1.41$, compared with the observed ΔN, together with the values of γ found, indicate the degree of imperfect adiabatic cooling. The glass faces at the ends of the chamber at first remained quite clear. Later they were apt to become cloudy, making observation exceedingly difficult. The film of moisture may be removed by heating the glass slightly, but this is not a trustworthy procedure, even if time is allowed before the next observation.

89. Larger (wood) fog-chamber. Dry air.—The next experiments were made with an air-chamber, F, fig. 59, of wood with walls about 0.25 inch thick, covered while hot, within and without, with an adhesive coating of resin and beeswax. The ends were perforated with holes about

TABLE 43.—Experiments with small rectangular wood fog-chamber, with wax and resin, suspended from independent wall-bracket, probably too loose. Exhaustion into vacuum-chamber. Dimensions $14\times10.7\times7.8=1155$ c. c. Barometer, $p_0=77.08$ cm.; absolute temperature, $\theta_0=296.5°$; $C=952.6$; effective length, $e=15.32$ cm.; $v/V=.124$. Fog-chamber slightly leaking.

p	$10^6\Delta N$	γ	Comp. $10^6\Delta N$ $\gamma=1$	Comp. $10^6\Delta N$ $\gamma=1.41$	t
57.08	650	1.57	970	718	1.51°
37.08	1550	1.37	1930	1515	−26.40
17.08	2500	1.37	2900	2459	−66.81

1½ inches in diameter and closed with glass plates cemented to the wood. The inside as before was lined with thick dry blotting-paper, subsequently to be moistened. The dimensions of the chamber (within) were: length, 14 cm., breadth, 10.7 cm., thickness, 7.8 cm.; and the exhaust-pipe was over 3 cm. in diameter. Thus the volume of the chamber with its pipe as far as the stop-cock was $v=1155+442=1597$ c. c., while the corresponding volume of the vacuum-chamber and pipe was $V=12771+96=12867$ c. c. Hence $v/V=.124$. With a chamber of this size a reasonable degree of adiabatic expansion may be expected and the results obtained in table 43 show the improvement.

We here encounter the curious result of a value of γ larger than the normal value for air. From the above equations it therefore follows that ΔN is too small or γ too large [equations (10) and (13)]. The values of ΔN computed for $\gamma=1.41$ or $\gamma=1$ are given in the table. The large result might therefore occur in consequence of leakage, but in view of the low drop of pressure it is probably to be referred to some residual distortion. If we consider the equation (9) for γ, it will be seen that for a given δp,

γ would decrease from $\propto$ to zero, while ΔN varies from zero to $ep_0/C\theta_0$, the maximum value (about 0.004 in the given work) consistent with a real value of γ, in the absence of all leakage. ΔN must therefore be greater for isothermal than for adiabatic expansion.

TABLE 44.—Experiments with wood-chamber as in table 43. Exhaustion into vacuum-chamber. Barometer, $p_0 = 76.65$; absolute temperature, $\theta_0 = 296.1°$.

p	$10^6\Delta N$	γ	Comp. $10^6\Delta N$ $\gamma = 1$	Comp. $10^6\Delta N$ $\gamma = 1.41$	t
56.65	800	1.248	970	720	1.05°
36.65	1750	1.16	1930	1520	−27.05
16.65	2800	1.09	2900	2470	−67.93

It is probable, as suggested, that the excessive γ in question is due to some sort of distortion in the apparatus. Seeing that the efficient length of ray used is relatively small (15.3 cm.), a slight change of the inclination or of the optical properties of the glass plate through which the ray passes during the occurrence of exhaustion might be the cause of it. However, in table 44 the results were repeated with care (5 to 10 observations for ΔN, the means of which were taken), with the apparatus practically free from leakage. The table as before contains the values for ΔN which would obtain when $\gamma = 1$ and $\gamma = 1.41$, as well as the reduction of temperature in degrees centigrade, due to adiabatic cooling, when $\gamma = 1.41$.

TABLE 45.—Experiments with wood fog-chamber as in table 43. Suspension laterally braced. Exhaustion into vacuum-chamber. Barometer, $p_0 = 76.14$; absolute temperature $\theta_0 = 295.5°$.

p	$10^6\Delta N$	γ	Comp. $10^6\Delta N$ $\gamma = 1$	Comp. $10^6\Delta N$ $\gamma = 1.41$	t
66.14	400	1.23	480	350	+11.99°
56.14	810	1.23	970	720	.31
46.14	1260	1.23	1450	1110	−12.86
36.14	1690	1.22	1940	1520	28.03
26.14	2290	1.11	2420	1970	46.18
16.14	2760	1.14	2910	2480	69.46
6.14	3315	1.12	3390	3090	102.96

The adjustment was now further improved by additionally bracing the wall-bracket from which the fog-chamber was suspended. This resulted in a much more definite fiducial reading at the micrometer. The results are given on the same plan as above, in table 45. Readings were taken systematically in series, the drop of pressure δp varying in succession by intervals of 10 cm.

These results are throughout as near the true value as may be anticipated for the case of so short an apparatus.

Another more detailed series of experiments was now made, with the drop of pressure δp increasing in steps of 10 cm. as far as 70 cm., and then decreasing again. These results as a whole are about the same as in the preceding table, except that γ at the beginning is relatively high. The

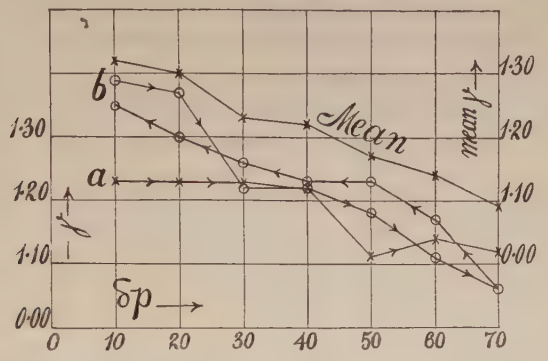

FIG. 61.—Charts showing relation of γ to $\delta p = p_0 - p$ (approximately the drop of pressure) in case of small wood fog-chamber. Curve *a* corresponds to table 45 and curve *b* to table 46. Mean result shown above these curves.

two series of table 46 together give a good account of the actual degree of adiabatic expansion reached. The mean results are shown graphically in fig. 61. A few other experiments were incidentally made, showing values of about the same order, and may therefore be withdrawn here.

TABLE 46.—Experiments with wood fog-chamber as in table 43, well braced. Exhaustion into vacuum-chamber. Barometer, $p_0 = 75.75$; absolute temperature, $\theta_0 = 291.7°$ to 292.3°.

p	$10^6 \Delta N$	γ	Comp. $10^6 \Delta N$ $\gamma = 1$	Comp. $10^6 \Delta N$ $\gamma = 1.41$	t
I. Pressure drop δp increasing.					
65.75	360	1.39	490	360	+8.27
55.75	750	1.37	980	730	−3.26
45.75	1280	1.20	1470	1120	16.25
35.75	1710	1.22	1960	1540	31.27
25.75	2230	1.18	2450	2000	49.31
15.75	2820	1.11	2940	2510	72.57
5.75	3400	1.06	3430	3140	108.07
II. Pressure drop δp decreasing.					
5.75	3400	1.06	3430	3140	−108.02
15.75	2750	1.17	2940	2510	72.43
25.75	2170	1.23	2450	1990	49.01
35.75	1700	1.23	1960	1540	30.85
45.75	1230	1.26	1470	1120	15.71
55.75	780	1.30	980	730	2.61
65.75	370	1.35	490	360	+ 9.24

90. The same. Wet air.—The endeavor was now made to obtain the corresponding data for the same (wood) fog-chamber respectively dry and wet in succession. Tables 47 and 48 contain the results given on the same plan as in the preceding tables. Neither of these series, either the dry or the wet set, is satisfactory. In the latter case, in particular, the clouding over of the window, which occurs in the lapse of time, is a constant

TABLE 47.—Experiments with wood fog-chamber as in table 43, well braced. Exhaustion into vacuum-chamber. Barometer, $p_0 = 76.90$; absolute temperature, $\theta_0 = 293.2°$. Dry air.

p	$10^6 \Delta N$	γ	t	p	$10^6 \Delta N$	γ	t
66.86	450	1.10	+12.97°	26.68	2090	1.30	−20.15°
56.81	800	1.26	5.57	16.64	2700	1.20	20.27
46.77	1150	1.36	− 6.07	6.59	3200	1.28	33.51
36.72	1750	1.18	10.25				

TABLE 48.—Experiments with wood fog-chamber as in table 43, well braced. Exhaustion into vacuum-chamber. Barometer, $p_0 = 76.90$; absolute temperature, $\theta_0 = 293.3°$. Wet air.

p	$10^6 \Delta N$	γ	p	$10^6 \Delta N$	γ
66.86	350	1.43	26.68	2330	1.09
56.81	830	1.21	16.64	2840	1.08
46.77	1280	1.19	6.59	3450	.97
36.72	1680	1.24			

annoyance. On the other hand, it is curious to note the essential transparency of the fog produced. The observer at the telescope scarcely notices any difference in the sharpness of the ellipses so long as the windows remain clear. If the wet data are compared with the mean results of tables 45 and 46 above, they show about the same order of behavior, though the wet values for γ are as a rule below those for dry air, as they should be. In

TABLE 49.—Experiments with wet air as in table 48. Barometer, $p_0 = 74.64$; absolute temperature, $\theta_0 = 291.5°$.

p	$10^6 \Delta N$	γ	t
54.55	1000	.98	− 3.90°
34.46	1850	1.10	32.66
14.38	2720	1.21	75.53

general, however, no very marked difference in character has been detected, and it was a disappointment to note that the presence of fog-particles contributed almost nothing to the experiment. The further trials of the wet chamber became more unsatisfactory, owing both to the lack of transparency of the glass and the gradual development of leakage in the chamber. The values in table 49 are of the same order as the preceding and lead to no new conclusions.

In some of the experiments radium was placed on top of the chamber to increase the density of the fog at low exhaustions, but no definite effect was detected.

91. Copper fog-chamber. Exhaustion. Dry air.—A larger vessel of thin copper well braced within, with large glass windows, was now constructed with a special view to an increase of the size of the efflux-pipe and stop-cock. The dimensions of this chamber were $20.4 \times 15.6 \times 18.7 = 5937$ c. c. In the first experiments the inch exhaust-cock with the wide

TABLE 50.—Adiabatic expansion in copper air-chamber, $20.4 \times 15.6 \times 18.7$ cm., well-braced. Exhaustion into vacuum-chamber. $v/V = .496$; barometer, $p_0 = 76.55$; absolute temperature, $\theta_0 = 291°$; $e = 20.89$.

p	Obs. $10^6 \Delta N$	γ	$10^6 \Delta N$ comp. $\gamma = 1$	$10^6 \Delta N$ comp. $\gamma = 1.41$	t $\gamma = 1.41$	t obs. γ
66.51	400	1.29	500	370	+10.3°	+11.99°
56.46	775	1.36	1010	750	1.9	3.22
46.42	1200	1.34	1510	1150	− 7.4	− 4.32
36.37	1650	1.33	2020	1580	17.9	12.61
26.33	2280	1.19	2520	2050	29.9	8.56

rubber tubing was directly attached, increasing the volume by 442 c. c. Hence the total volume was $v = 6379$, while that of the vacuum-chamber (as above) amounted to $V = 12867$ c. c.; hence $v/V = .50$ to be used in the reduction of initial pressure p_0 and temperature θ_0 of the air-chamber and the initial pressure p and temperature θ_0 of the vacuum-chamber to the values when momentarily in communication. A very careful series of

TABLE 51.—Adiabatic expansion in copper air-chamber as in table 50. Exhaustion into vacuum-chamber. Barometer, $p_0 = 74.60$; absolute temperature, $\theta_0 = 294.5°$.

p	Obs. $10^6 \Delta N$	γ	$10^6 \Delta N$ comp. $\gamma = 1$	$10^6 \Delta N$ comp. $\gamma = 1.41$	t $\gamma = 1.41$	t γ obs.
64.56	380	1.34	498	362	+13.5°	+14.5°
54.51	800	1.29	996	742	4.7	8.6
44.47	1316	1.18	1490	1140	− 5.0	7.4
34.42	1738	1.23	1990	1570	16.0	− 2.9
24.38	2125	1.32	2490	2040	28.8	20.6

experiments was now made with dry air, the vacuum increasing in steps of pressure of 10 cm. each as far as $\delta p = 50$ cm. Exhaustion, as above, took place from the air-chamber to the vacuum-chamber. The results are summarized in table 50, experiments being made both for increasing and decreasing exhaustion.

A comparison of the observed ΔN which should be correct to 5×10^{-5} cm. and the computed ΔN both for $\gamma = 1$ and $\gamma = 1.41$, shows the degree

to which the observations may be trusted. The difficulties are naturally most serious at the low and the high values of δp. Neglecting these, the values of γ are as a whole higher than in the mean case of tables 45 and 46, for the small wood fog-chamber. The table, moreover, contains the fall of temperature both for the case of $\gamma = 1.41$ and the actual fall, as computed for the mean values of γ observed. The experiments were now repeated, using an uncompensated interferometer with smaller ellipses. The results are given in table 51, the method being the same as in the preceding case.

These data are lower in general value and correspond to tables 45 and 46. The three causes of discrepancy are (as before) the relatively long interval of communication of the chambers, the distortion of the air-chamber and its effect on interference, and the same in its effect on the volume and density of the gas contained. The mean result of these two tables may be compiled for reference.

δp =	10	20	30	40	50 cm.
γ (mean) =	1.31	1.32	1.26	1.28	1.25

Curiously enough the mean curves so obtained are similar (see fig. 62), showing that the larger chamber is more favorable to adiabatic expansion, as would be anticipated.

If in table 51 instead of equation (16) the corresponding equation (12) correcting the temperature and pressure coefficients is taken, the values of γ are scarcely changed.

$\alpha'' = .00015$; $\beta = .0000072$; $\delta t = t_0 - t$; $\delta p = p_0 - p$

δp =	10	20	30	40	50
γ =	1.32	1.28	1.17	1.21	1.30
δt =	7°	13°	14°	24°	42°
$(\alpha''t - \beta p) \times 10^6$ =	1710	898	+798	−683	−3270
$(\alpha''\delta t - \beta\delta p) \times 10^6$ =	978	1790	1884	3370	5950

In the present experiments, therefore, this correction may be neglected.

In view of the evanescence of two or more rings after adiabatic expansion or compression, always in the same sense as the expansion or compression, *i.e.*, corresponding to an increase of ΔN, it is worth while to compute the possible effect of the Mascart correction on a gas kept at constant volume or density, while p and θ change subject to the intrinsic equation of a gas. If the latter passes from t and p through t_0 and p_0 and ΔN is the corresponding displacement of the micrometer, we may write very nearly

$$-\delta N = \frac{e p_0}{C \vartheta_0}(\alpha''(t_0 - t) + \beta(p_0 - p))$$

Hence in table 51, where $e/_0\, C\theta_0 = .00555$, the following values would hold, $\delta p = p_0 - p$,

δp =	10	20	30	40	50 cm.
$\delta N \times 10^6$ =	5.4	9.9	10.4	18.7	33.0

quantities too small to be measured, and even in the latter extreme case equivalent to the evanescence of only a single ring in the sense *opposite* to the motion of those observed. Thus the observed phenomenon is not due to the present correction. It might be due to slight leakage through the 2½-inch stop-cock, from the initially colder to the initially hotter vessels, as these regain atmospheric temperature. In such a case, however, it would not stop with a few rings while the pressure difference remained.

92. The same. Compression. One-inch stop-cock.—An inversion of the method was now made, in which the air-chamber was exhausted, while the former vacuum-chamber contained a plenum of air. The latter may therefore be removed with advantage, and the atmosphere used directly, in which case $v/V=0$ and equation (9) is applicable in the form (21). The results are given in tables 52 and 53. These data for γ are surprisingly small, much below the mean results for the preceding tables. The reason for this will presently appear.

TABLE 52.—Adiabatic compression of air in copper fog-chamber (as in table 50). Dry air. Interference method. $p_0<B$. One-inch stop-cock and pipe. Barometer, $p=76.74$; absolute temperature, $\theta_0=296.5°$.

p_0	Obs. $10^6\Delta N$	γ	Comp. $10^6\Delta N$ $\gamma=1$	Comp. $10^6\Delta N$ $\gamma=1.41$	t $\gamma=1.41$	t γ obs.
46.61	1868	1.15	2220	1465	69.80°	53.78°
36.56	2553	1.11	2960	1874	94.88	69.36

TABLE 53.—The same. Barometer, $p=75.40$; absolute temperature, $\theta_0=298.3°$.

p_0	Obs. $10^6\Delta N$	γ	Comp. $10^6\Delta N$ $\gamma=1$	Comp. $10^6\Delta N$ $\gamma=1.41$	t $\gamma=1.41$	t γ obs.
45.27	1781	1.19	2210	1455	72.59°	50.2°
35.22	2481	1.13	2940	1853	99.75	53.0

93. The same. Compression. Two and one-half inch stop-cock.—The endeavor was now made to raise the value of γ by replacing the rubber tube and inch stop-cock previously used with a 2½-inch brass stop-cock and a 2-inch brass tube. It was necessary, however, to make use of the very large vacuum-chamber to which the cock was attached, so that a small ratio of volume enters, as in equation (20) above. The volumes were $v=5937+1374=7311$ c. c., $V=103,908+393=104,301$ c. c., whence $v/V=.070$. The experiments are given in tables 54 and 55. These data are virtually identical with the preceding set by the same method, in spite of the larger stop-cock used. Supposing that the inevitable leak in the large stop-cock is practically negligible, a sufficient explanation for the low results in the compression method is the inrush of relatively cold air which

at high exhaustion introduces an additional and very serious error, to which the exhaustion method is obviously not subject.

TABLE 54.—Adiabatic compression of dry air in copper fog-chamber (as in table 50). Interference method. $p_0 < B$. Two and one-half inch stop-cock; 2-inch pipe. $v/V = .07$. Barometer, $p = 76.44$; absolute temperature, $\theta_0 = 297°$.

p_0	Obs. $10^6\Delta N$	γ	Comp. $10^6\Delta N$ $\gamma = 1$	Comp. $10^6\Delta N$ $\gamma = 1.41$	t $\gamma = 1.41$	t γ obs.
46.31	1786	1.13	2070	1366	67.88°	40.8°
36.26	2400	1.11	2760	1747	91.89	45.6

TABLE 55.—The same. Barometer, $p = 75.43$; absolute temperature, $\theta_0 = 294.7°$.

p_0	Obs. $10^6\Delta N$	γ	Comp. $10^6\Delta N$ $\gamma = 1$	Comp. $10^6\Delta N$ $\gamma = 1.41$	t $\gamma = 1.41$	t γ obs.
65.39	595	1.16	694	486	33.4°	27.2°
45.30	1783	1.14	2081	1374	66.1	39.8
35.25	2407	1.11	2775	1755	90.6	43.6
25.21	3050	1.09	3469	2064	126.5	48.5

94. Clement and Desormes's apparatus.—It now seemed desirable to compare the above results for the copper air-chamber with the value of γ directly determinable by the classic method of Clement and Desormes. For this purpose the vacuum-chamber was completely removed, so that the partially exhausted air-chamber instantaneously communicated with the air at barometric pressure. To determine the adiabatic temperature an accessory mercury column, h, was considered sufficient, as no great accuracy was aimed at. Thus if p_0 and θ_0 be the initial pressure and temperature of the air-chamber and p and θ_0 those of the atmosphere, while θ is the adiabatic temperature,

$$\frac{\vartheta_0}{\vartheta} = 1 - h/p$$

or no temperature measurement is necessary. Thus if B be the height of the barometer

$$\gamma = \frac{\lg (p_0/p)}{\lg(p_0/(B-h))} \tag{24}$$

quite generally, if p_0 and p are the pressures in the air-chamber and the vacuum-chamber, if at hand. The results are given in tables 56 and 57.

It was not possible to quite overcome the slight leakage of the large 2½-inch plug stop-cock. Hence the final h is too small. In general these results are of the same order of value, though somewhat larger than the corresponding results (air-chamber exhausted) by the interference method.

It is difficult to suggest any reason for this, since any leakage in consequence of the long waiting for h necessary, in the present method, should decrease γ.

TABLE 56.—Clement and Desormes's method for γ. Copper fog-chamber. Exhaustion into air-chamber. Barometer, $p=76.12$; absolute temperature, $\theta=293.8°$.

p_0	h	γ
66.12	2.16	1.257
56.12	4.28	1.234
46.12	6.07	1.199
36.12	7.79	1.169
26.12	9.33	1.139

TABLE 57.—The same. Barometer, $p=75.89$; absolute temperature, $\theta=295°$.

p_0	h	γ
55.89	4.28	1.234
45.89	6.08	1.199
35.89	7.63	1.165
25.89	9.18	1.136

Hence the experiments were repeated with the large vacuum-chamber attached, so that both the reciprocal cases of an exhausted air-chamber

TABLE 58.—Clement and Desormes's method. Copper fog-chamber. Air-chamber exhausted. $v/V=.070$. Barometer, $p=75.08$; absolute temperature, $\theta=290.8°$.

p_0	p' approximate	h	γ
65.04	74.28	3.03	1.315
54.99	73.58	5.59	1.253
44.95	72.93	8.05	1.215
34.90	72.33	10.10	1.172
24.86	71.53	11.95	1.135

TABLE 59.—Clement and Desormes's method. $v/V=.070$. Vacuum-chamber exhausted. Barometer, $p_0=\left\{\begin{matrix}75.08\\75.22*\end{matrix}\right\}$; absolute temperature, $\theta=\left\{\begin{matrix}290.8°\\296.0*\end{matrix}\right\}$.

p	p' approximate	h	γ
64.95	65.59	7.19	1.367
55.05	53.36	14.32	1.359
45.03	47.08	22.20	1.344

* First observation, $\delta p=10$.

$p_0<B=p$ and a full chamber $p<B=p_0$ might be compared. The data are given in tables 58 and 59, where p' is the approximate adiabatic expansion as read off on the gauge of the *large* vacuum-chamber.

To compute these results, equation (24), if p' is the adiabatic pressure in question,

$$\gamma = \frac{\lg (p'/p_0)}{\lg ((B-h)/p_0)}$$

may be modified to read

$$\gamma = \frac{\lg (p/p_0)}{\lg \left\{ \frac{B-h}{p_0} \frac{V+v}{V} - \frac{v}{V} \right\}} \tag{25}$$

where p_0 and p are the initial pressures of air and vacuum chambers and v/V the volume ratio of their contents, respectively. If equation (24) be differentiated with respect to h,

$$\frac{\partial \gamma}{\partial h} = \gamma \frac{1}{(B-h)\left(\lg \frac{B-h}{p_0}\right)}$$

Hence γ increases with h, if $B-h > p_0$ or when the air-chamber is exhausted, and *vice versa*. In the former case h is followed to a maximum and in the case of leakage is too small; hence γ is too small. If the vacuum-chamber is exhausted, h continually decreases and is liable to be observed too large; hence γ is again too small.

The results of table 58 are slightly larger than the similar case of tables 56 and 57, and they show a definite tendency to reach $\gamma = 1.41$ when δp_0 the exhaustion of the fog-chamber vanishes. Possibly the leakage of the large stop-cock was under better control and the diminution of γ with the exhaustion δp is probably a trustworthy exhibit of the actual state of things.

TABLE 60.—Clement and Desormes's method. Copper fog-chamber. Vacuum-chamber exhausted, $v/V = .070$. Barometer, $p_0 = 75.58$; absolute temperature, $\theta = 295°$ (about).

p	p' approximate	h corrected	γ
64.58	64.98	8.2	1.316
55.03	56.18	14.7	1.371
45.08	47.08	21.6	1.406

Since h reaches a definite maximum γ can not be too large. The results of table 59 have not the same certainty, since h must continually decrease, and the expansion after adiabatic exhaustion is indistinguishable finally from the small permanent leak into which it eventually passes. Hence h is too small and the results for γ are thus probably too large in proportion as δp increases.

The data of this method (vacuum-chamber exhausted) tend to approach the order of values of the corresponding interference data, though the latter are again small since equation (2) enters. In all cases, therefore, a full air-chamber shows large nearly normal values of γ, whereas the ex-

hausted air-chamber shows the reverse or small values of γ. True, this is in the same sense as the discrepancy of the leak in the large stop-cock, but it is not probably due to it. The actual value of the error in question per centimeter of h is shown in each table and its magnitude proves that the discrepancy can not be due to the leak.

Nevertheless it was thought advisable to actually evaluate the leak of the stop-cock in case of the latter method. The results so found are given in table 60, which may be regarded as free from the effects of leakage.

These results curiously enough show an increase of γ with the drop of pressure, the value for $\delta p = 40$ cm. being actually excessive. It is extremely difficult to account for this erratic behavior. The experiments were throughout made with great care. In the latter table in particular γ is reduced to the lowest value possible. Under these circumstances the mean values of γ for each method may be taken for reference. They are compared with the corresponding data for the interference method in fig. 62.

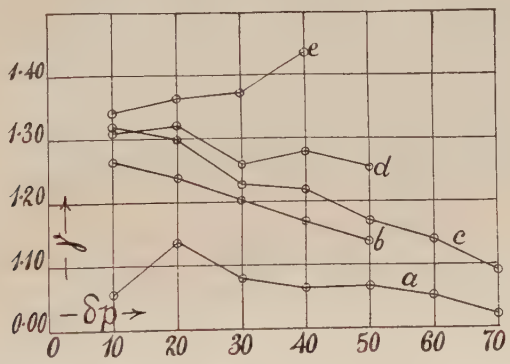

FIG. 62.—Charts showing relation of γ to $\delta p = p_0 - p$, for different fog-chambers and methods. Mean results.

95. Large wood fog-chamber.—The experiments were concluded with the aid of a large wood fog-chamber coated while hot with the mixture of wax and resin. The dimensions in centimeters were $15.6 \times 11.5 \times 45$, being those usually used in my experiments with coronas. This chamber was quite dry at the outset and throughout free from leakage. The volumes, including the 2-inch pipe for exhaustion and the 2½-inch stop-cock (the vacuum-chamber being the same as before), were

$$v = 8073 + 1374 \text{ c.c.} \qquad V = 104300 \text{ c.c.}$$

so that $v/V = .091$. Allowance was made for the very slight leakage of air from the fog-chamber to the vacuum-chamber through the stop-cock (as above), for each observation. In the chief experiments the plenum of air was in the fog-chamber. Table 61 shows the results obtained with dry air by Clement and Desormes's method. They are reproduced in fig. 64.

These results appear to be more trustworthy. The value of γ decreases but slightly up to the highest exhaustion, $\delta p = 40$ cm., which it was safe to apply.

The same chamber was now used for the measurement of γ by the interference method. The adjustments differed slightly from the above, as shown in fig. 63, where C is the light from the collimator incident on the grating G at an angle I, M and N the opaque mirrors, the latter on the micrometer. Both the component beams m and n and the reflected and diffracted R and D pass through the fog-chamber FF, the front and rear

TABLE 61.—Experiments with Clement and Desormes's method. Large wood fog-chamber, $v/V = .091$. Vacuum-chamber exhausted. Barometer, $p_0 = 76.22$; absolute temperature, $\theta_0 = 296°$ (about).

p	h	γ
66.09	6.89	1.374
56.22	13.63	1.403
46.69	21.14	1.361
36.02	29.60	1.361

sides of which are thick plate-glass. E is the 2-inch exhaust-pipe leading through the 2½-inch stop-cock to the vacuum-chamber. Other cocks (not shown in the figure) are at hand for influx of air, etc., together with a large hole for cleaning. The thermometer dipped into the fog-chamber. In the adjustment chosen not only the diffracted beam D (angle of diffraction, $\theta > I$), but another on the inner side of R ($\theta < I$), was available for measure-

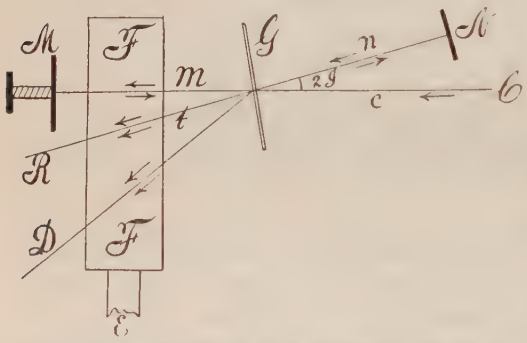

FIG. 63.—Diagram of displacement interferometer, $C\,G\,M\,N$, and large wood fog-chamber, FF, with 2-inch exhaust at E.

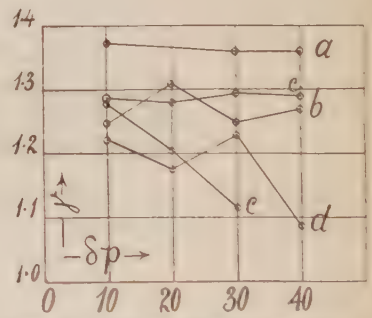

FIG. 64.—Charts showing relation of γ and $\delta p = p_0 - p$ in case of large wood fog-chamber.

ment. In the latter case θ was nearly zero, but though this is more luminous there seemed to be no advantage of one over the other. In view of the thick glass sides of the fog-chamber, it is preferable to put compensator plates in the component beam n to counterbalance those of the beam m. Otherwise the ellipses are too small and move too slowly. The method throughout worked admirably. Even when the inside is wet and a thick phosphorus fog is produced, measurement is still possible *through the fog*, a very unexpected result. In the course of time the glass becomes cloudy and must be rubbed clean. In such a case the observations are much

more difficult, unless the glass plates are very slightly heated by a moving Bunsen burner to evaporate the film of moisture. This procedure would not, however, be favorable to the occurrence of the nearest approach to adiabatic expansion which the chamber affords. From the different beams of spectrum light which pass through the fog-chamber, a number of sodium lines are available as fiducial lines, to which the center of ellipses is to be brought back. But the coincident ones for which the interference is adjusted are necessarily the most convenient. The construction of the interferometer did not permit the beam m to pass near the middle of the apparatus as would have been desirable. The results for γ are given in tables 62 and 63 and in fig. 63. They are as usual below the data of table 61 in case of Clement and Desormes's method for the same chamber. The reason for this has frequently been stated and is due to the assumption of the approximate equation (2) for experimental purposes.

TABLE 62.—Wood fog-chamber. Interference method. $v/V=.091$. Vacuum-chamber exhausted. Barometer, $p_0=75.92$; absolute temperature, $\theta=299.0°$ to $298.6°$; $e=15.6$.

p	$10^6\Delta N$	γ	γ corrected
65.52	425	1.247	1.2919
55.87	813	1.280	1.3292
45.94	1338	1.164	1.2139

TABLE 63.—The same. Barometer, $p_0=75.52$; absolute temperature, $\theta=293.4°$ to $293.1°$. Vacuum-chamber exhausted.

p	$10^6\Delta N$	γ	γ corrected
55.92	775	1.344	1.3950
45.92	1200	1.339	1.3953
35.52	1733	1.270	1.3289

An inverse series of experiments was now made by compressing the air in the exhausted air-chamber, but it was not completed, owing to an accident to the chamber. The data so far as available are shown in table 64 and figure 63. The tendency here is to fall below the data for the exhaustion method, consistently with the earlier experiments.

TABLE 64.—Wood fog-chamber. Interference method. Fog-chamber exhausted. Barometer, $p=75.62$; absolute temperature, $\theta=287.4°$ to $290.6°$.

p_0	$10^6\Delta N$	γ	γ corrected
65.68	400	1.278	1.3195
55.43	833	1.205	1.2415
45.41	1300	1.157	1.1888

Finally, water was introduced into the fog-chamber so as to provide saturated air and the value of γ was redetermined under these conditions. In the first measurements, as stated, no difficulties were encountered, even in the case of a very dense phosphorus fog. Later the glass became permanently cloudy and could only be cleared by slight heating. The data are given in table 65 and figure 63. As a whole these results lie somewhat below the data for the dry chamber, but they are not sufficiently regular to admit of very definite statement.

TABLE 65.—Wood fog-chamber. Interference method. Air saturated with water-vapor. Vacuum-chamber exhausted. Barometer, $p_0 = 76.17$; absolute temperature, $\theta = 291.5°$.

p	$10^6 \Delta N$	γ	γ corrected
65.92	438	1.221	1.2653
56.09	900	1.175	1.2204
45.92	1325	1.229	1.2803
36.09	1950	1.087	1.1406

At $\delta p = 30$ certain tests were made by precipitating a very dense fog with phosphorus with results as follows:

Without phosphorus: $10^6 \times \Delta N = 1350, 1350, 1300$.
With phosphorus; dense fog: $10^6 \times \Delta N = 1300, 1250$.

Thus no effect of the very dense fog could be detected.

The phenomenon of rings vanishing jerkily in the same sense as an increase of ΔN was apparent in all the experiments, immediately after exhaustion. Three or four such rings were counted. The observation is referable as before to some sort of strain in the solid parts of the apparatus, and probably not due to any thermo-dynamic transformation of the gas. The behavior of these rings suggests the properties of a solid under strain and not those of a gas.

In general it is curious to note that whenever any part of the interferometer is strained a succession of rings gradually vanishes, *after* the strain has been imparted. They vanish too soon to be referable to solid viscosity in the ordinary sense. They rather show that full strain does not follow the stress instantaneously.

The same chamber was now used in order to find γ by Clement and Desormes's method, using all the precautions to guard against leaks, etc. The data are given in table 66. Owing to precipitation of fog, these results are as usual distinctly below the results for dry air and the same chamber (table 61). In both tables the value of γ is constant for drops of pressure between $\delta p = 20$ and 40 cm., a very unexpected result, as one would fancy that the data for γ would be more trustworthy (apart from measurement) as δp is smaller and there is less adiabatic cooling. The constancy of these values makes it possible to state a mean value of γ for each individual case apart from δp.

It is clear, moreover, that the difference of values for γ in wet and dry air suggests a practical method of determining the amount of water precipitated per cubic centimeter, seeing that $\gamma_{dry} - \gamma_{wet}$ is sufficiently large for such a purpose. The equation, however, is yet to be deduced.

TABLE 66.—Wood fog-chamber and saturated air as in table 65. Clement and Desormes's method. Vacuum-chamber exhausted. Barometer, $p_0 = 76.81$; absolute temperature, $\theta_0 = 297°$; $v/V = .09$.

p	h	γ
66.45	7.5	1.29
56.61	14.93	1.28
46.81	22.4	1.29
36.81	30.6	1.29

96. Air-chamber of vanishing thickness.—To test the adequacy of the interference method it is necessary, in conclusion, to construct a cell of plate-glass, in which the thickness of the layer of air in the direction of the component beam of light shall be negligible. ΔN in this case would therefore reveal the discrepancy due to the chamber itself, and γ, from the small volume of air contained, should be nearly 1. The cell constructed was $e = 2$ cm. thick (within), in the direction of the interfering ray m, fig. 63. It could not be made thinner, seeing that an exhaust-pipe had to be introduced. Its volume was $2 \times 12 \times 9.5$ cm^3. Thus $v = 228 + 245 = 473$ and $V = 12867$, so that $v/V = .03676$. The glass walls were of the same plate-glass used in the preceding wood fog-chamber, being 0.870 and 0.854 cm. thick, respectively.

The results are given in table 67. The drop of pressure was eventually as high as 70 cm. Below $\delta p = 40$ cm., no effect could be determined, as the ellipses scarcely moved.

TABLE 67.—Flat fog-chamber, $e = 2$ cm. in direction of beam of light. Dimensions, $2 \times 12 \times 9.5 = 228$ c.c. Dry air. Exhaustion method. $v/V = .03676$. Glass plates .870 and .854 cm. thick. Barometer, $p_0 = 76.58$; absolute temperature, $\theta = 293.5°$.

δp	$\Delta N \times 10^6$	γ	δp	$\Delta N \times 10^6$	γ
10	0	....	50	400	0.75
20	0	....	60	450	.81
30	0	....	70	550	.78
40	0	....	..	...	....

The value of ΔN for a column of air only 2 cm. long is near the limit of measurement, and the results for γ, to be interpreted, are necessarily crude. ΔN is again distinctly excessive, even in this limiting case, and the data for γ (which can not be less than 1) are deficient in the same manner as above. Something has therefore entered consistently into all these interference experiments in virtue of which ΔN is too large and γ too small

throughout. The value of this discrepancy, the real nature of which is inherent in the use of equation (2), may be considered as given in table 67. It will be seen that it is sufficiently large to increase the mean data for γ found by the interference method to the values obtained by the Clement and Desormes method for identical methods of expansion and air-chambers. As in the case of tubes, the expansion in this thin chamber is practically isothermal.

TABLE 68.—Interpolated data for the dispersion of air. Practical table, $\mu - 1 = B\,\lambda^x$ $B = .0002101$, $x = .0341$.

Line.	B.	C.	D.	E.	F.
$10^6\lambda$.....	68.70	65.63	58.93	52.70	48.61
Observed $10^6(\mu-1)$...	291.4	291.8	292.7	293.9	295.0
Computed $10^6(\mu-1)$...	291.4	291.8	292.9	293.9	294.8
Difference.....	.0	.0	− .2	.0	+ .2

97. Conclusion.—As a whole the results of this long and laborious series of experiments, made with a view to determine the actual value of γ in such particular apparatus as was described, have been unsatisfactory, in spite of the care which was taken with the individual measurements. This is not, however, to be ascribed to the interference method applied; for, in so far as the method is concerned, its sensitiveness could be increased at pleasure by passing the component beams between mirrors and one of them many times through the fog-chamber. The difficulty is rather due to the shortcomings of the fog-chamber itself, which even in the final case was not sufficiently voluminous, nor sufficiently rigidly mounted, and possibly not provided with an exhaust-cock of sufficiently rapid or sufficiently constant action.

Furthermore, the adiabatic expansion is throughout better, *i.e.*, γ is larger, as the chamber is more bulky. In the small brass tube or the shallow cell, for instance, the expansion as actually produced and determined by the value of γ is nearly isothermal. In all cases the method by compression gave very low results, owing clearly to the unavoidable influx of relatively cold air during compression.

The mean results for γ useful for practical purposes are sufficiently given in figs. 62 and 64, when corrected with reference to equation (2).

As the micrometer can be set to 5×10^{-5} cm. on restoring the center of ellipses back to the fiducial sodium line selected, the displacement method is not much less sensitive than the ring method (sensitiveness limited by half a wave-length, or about half the given datum) and the former has the advantage of never losing count. This feature of the experiments was eminently satisfactory.

A curious result is the evanescence of several (2 to 5) rings subsequent to the adiabatic expansion. They vanish in the sense of an increase of the micrometer displacement ΔN. This phenomenon is apparently refer-

able to a non-instantaneous appearance of strain for the given stress in solid parts of the air-chamber. It ceases too soon to be called viscous in the ordinary sense, and it probably has an immediate bearing on Kelvin's " fatigue " of elasticity.

For the coronal fog-chamber (the largest one used above), it is then possible to write for dry air, $\gamma = 1.37$, and for wet air, $\gamma = 1.29$, in case of all the experiments usually made with coronas (drops of pressure exceeding 10 cm.). The data are the mean results obtained with Clement and Desormes's method.

This large difference in the values of γ for dry and for wet air, *cæt. par.*, suggests a method for the measurement of the quantity of fog precipitation per cubic centimeter of nucleated air, when suddenly cooled. An equation for this purpose will be considered elsewhere.

In conclusion, it is necessary to endeavor to account for the excessive values of ΔN and the correspondingly low values of γ given by the interference method as compared with the method of Clement and Desormes. Equation (2), assumed for experimental purposes, it will be remembered, contains no correction for the dispersion of air. It remains, therefore, to resume equation (2′), in which the constant b between the C and E lines has the mean value of $b_0 = 10^{-14} \times 1.64$ for a plenum of air. Equation (2′) may be written

$$\mu_0\left(1+\frac{2b_0}{\mu_0\lambda^2}\right)=\mu\left(1+\frac{2b}{\mu\lambda^2}\right)+\frac{\Delta N}{e} \tag{24}$$

where b_0 and b correspond to an air-column of length e at high (p_0) and low (p) pressure, respectively, and ΔN is the displacement of the micrometer. The simplified Cauchy equation $\mu = a + b/\lambda^2$, however, is inconvenient for the expansion of equation (6) above

$$\mu - 1 = p/C\vartheta \tag{6}$$

at a fixed wave-length λ, since the constants a and b both essentially enter. It is quite sufficient, moreover, to use an equation of interpolation of the form

$$\mu - 1 = B/\lambda^x \tag{25}$$

and to compute x for known values of μ between the B and F lines of the spectrum. When this is done

$$B = .0002101 \qquad x = .0341$$

are mean values applying near the D line, as the table shows.

Equation (1) now takes the form

$$\frac{\Delta N}{e}=\mu_0-\mu-\left(\frac{d\mu_0}{d\lambda}-\frac{d\mu}{d\lambda}\right)\lambda=\mu_0-\mu+\frac{x(B_0-B)}{\lambda^x} \tag{26}$$

or from (6) and (25)

$$\mu_0 - 1 = \mu - 1 + \frac{\Delta N}{e} - \frac{x}{C}\left(\frac{p_0}{\vartheta_0}-\frac{p}{\vartheta}\right) \tag{27}$$

But for adiabatic expansion

$$\frac{p_0}{\vartheta_0}-\frac{p}{\vartheta}=\frac{p_0}{\vartheta_0}\left(1-\left(\frac{p}{p_0}\right)^{1/\gamma}\right) \tag{7'}$$

which in (26) gives

$$\mu_0-1=\mu-1+\frac{\Delta N}{e}-\frac{x}{C}\left(1-\left(\frac{p}{p_0}\right)^{1/\gamma}\right)\frac{p_0}{\vartheta_0} \tag{28}$$

Furthermore, in view of adiabatic expansion, equation (7) above

$$\frac{p}{(\mu-1)^\gamma}=\frac{p_0}{(\mu_0-1)^\gamma} \tag{7}$$

and after inserting equations (6) and (7), equation (28), when solved for γ, becomes

$$\gamma=\frac{\lg(p/p_0)}{\lg\left(1-\frac{C\vartheta_0}{e(1+x)p_0}\Delta N\right)} \tag{29}$$

or solved with respect to ΔN, it is

$$\Delta N=(1+x)\frac{ep_0}{C\vartheta_0}\left(1+\left(\frac{p}{p_0}\right)^{1/\gamma}\right) \tag{30}$$

The last equation follows at once from (26), (7'), and (25). If p and p_0 refer to the pressures of fog and vacuum chambers, the coefficient $(1+x)$ must be inserted before ΔN as in the corresponding equations above. The results obtained in this way are computed for the small tube fog-chamber (tables 40 and 41 above) and for the large coronal fog-chamber (tables 62, 63, 64, 65) and marked corrected.

The mean value of γ obtained by the interference method on exhausting the coronal fog-chamber is now

$$\gamma=1.33 \text{ (dry air)} \qquad \gamma=1.23 \text{ (wet air)}.$$

These values are still below the data obtained by the Clement and Desormes method, but the reason for this may possibly be due to the different conditions involved. The latter refer to the mean volume of air, whereas in the interference method the pencil passes through a definite layer of air, in the present experiments unfortunately too near the bottom or walls of the chamber. The interferometer did not at the time admit of the introduction of bulky chambers, large in their vertical dimensions, though such alterations have since been made with success.

THE PRODUCTION OF ELLIPTIC INTERFERENCES IN RELATION TO INTERFEROMETRY

PART III

By CARL BARUS

Hazard Professor of Physics and Dean of the Graduate Department in Brown University

WASHINGTON, D. C.

Published by the Carnegie Institution of Washington

1914

CARNEGIE INSTITUTION OF WASHINGTON
Publication No. 149, Part III

PRESS OF J. B. LIPPINCOTT COMPANY
PHILADELPHIA, PA.

PREFACE.

The accompanying report contains a variety of investigations made at widely different times, but in all of which the displacement interferometer was used as a basis of measurement. It is thus a continuation of the work in the Carnegie Publications No. 149, 1911 and 1912.

In Chapter XII, the distance apart of the doublet interference patterns, obtained with plates of doubly-refracting crystals, is used for computing the corresponding ordinary and extraordinary indices of refraction of these crystals, in the case of light traveling through them in different directions. As quartz gives particularly beautiful and well-placed images, measurements were made in greatest number by means of it, though other bodies were also studied. It is an essential feature of the method that the center of ellipses is never lost, but may be brought back into coincidence with the fiducial sodium line of the spectrum by the proportionate displacement of the mirror on the micrometer. Hence plates of glass or crystal of any thickness, or indeed columns of any length, are available for measurement. These wide limits of application are peculiarly favorable to certain accurate measurements. For instance, if a glass column 1 meter long is inserted, and the micrometer reads to but 0.5×10^{-4} centimeter, $\mu-1$ (where μ is the index of refraction) would be measurable to one part in a million. The method should therefore be useful to answer refined questions in refraction.

Chapter XIII contains a number of miscellaneous measurements made with the displacement interferometer, or bearing upon it. Thus the ease with which it lends itself to the comparison of screws of any length is illustrated by many trials; a simple type of long screw micrometer is designed and investigated; a method for the measurement of very small increments of angle, consisting essentially of mounting two small mirrors in parallel and symmetrically to the axis, is tested; advantages in obtaining elliptic interferences when the reciprocating opaque mirrors are concave are discussed, etc. Furthermore, investigation is made of the availability of the interferometer in measuring certain acoustic displacements, such as occur in the Dvorak and Mayer experiments and telephone plates. It is then shown that by replacing the opaque mirrors of the interferometer by mirrors attached to the synchronized and reciprocating plates of modified telephones an induction balance of a peculiar kind may be constructed. If, for instance, one of these mirrors vibrates synchronously with the other towards and away from it, the ellipses remain in the field without displacement; if, however, the mirrors move in the same direction, the ellipses necessarily vanish. Hence, if there is a gradually increasing retardation in the electric circuit of one telephone only, the ellipses will alternately appear and vanish for identical intervals of retardation. The experiments attest the feasibility of so mounting the telephone mirrors on the interferometer that the balance may be realized. Finally, by the above method, an attempt is made to study double refraction resulting from dielectric polarization, in solids and in liquids, while in allied sections the prismatic spectrum is

studied on a Rowland spectrometer and certain peculiar results are shown in the resolution of interference fringes resembling the elliptic type.

Chapter XIV treats briefly of the interferometry of highly exhausted air carrying electric current. The adjustment used is that originally proposed by Mach, in which the rays do not retrace their path, but move along the sides of a parallelogram. The long exhaustion tube carrying current is placed in one of these sides, the light passing from end to end, and the effect of presence and absence of current on the interference pattern is determined. Thus far the exhaustions available were insufficient, so that the experiment in its final developments will be resumed at some time in the future. It is worth an inquiry to ascertain whether the motion of the cathode rays in a given direction may not produce some preponderating modification of the properties of the ether in that direction.

Chapter XV deals with the refraction of air at high temperatures investigated by the displacement interferometer (provided with water circulation), by comparing the refraction of a vacuum and of a plenum of air at each given temperature. As the system is not very sensitive to pressure, very perfect exhaustion need not be reached, but the need of sealed apparatus makes the experiment difficult at high temperatures. This chapter is but a beginning of experiments of this kind, which are naturally very difficult. It is curious that the refraction of a Bunsen flame through which a beam of light passes symmetrically may be approximately found by this means.

Finally, in Chapter XVI the displacement interferometer is applied to the electrometer. A large number of forms of the instrument are designed and the results of each are tested in detail. All of these are comprehended by the closed cylindric electrometer, in which a closed cylindric charged needle is capable of displacement along the axis of a closed cylinder, consisting of two symmetrically insulated halves, oppositely charged. The suspension of the needle is of the pendulum type. If the ends of each cylinder are removed, the instrument reduces to the cylindrical pattern, in which the movable cylinder may be within or without the fixed cylinder. If the cylindrical mantle is removed, the instrument is of the disk form, the simplest case of which is the absolute electrometer. All of these instruments may, with less sensitiveness, be used idiostatically. None of them, however, are exceptionally sensitive, the disk form, which is most so, and at the same time most treacherous, being characterized by a displacement of about 10^{-3} centimeters per volt, in favorable cases.

Far greater sensitiveness is therefore secured by adapting the device of two small light parallel mirrors for the measurement of angle (as referred to above) to the needle of the quadrant electrometer. When this is properly done, an instrument capable of measuring 10 to 20 millionths of a volt per vanishing interference ring may be constructed, provided a satisfactory environment is at hand. The chapter contains a great variety of experiments with each of these forms of apparatus.

My thanks are due to Miss A. I. Burton for efficient assistance both in the observations and in the editorial work and drawing.

CARL BARUS.

BROWN UNIVERSITY, *February* 1, 1914.

CONTENTS.

CHAPTER XII.—*The Indices of Doubly-refracting Crystals, Determined by Displacement Interferometry.*

PAGE

98. Introduction. Method. Fig. 65 169
99. Equations. Fig. 66. Table 69 171
100. Dispersion constants. Table 70 173
101. Oblique incidence. Fig. 67. Table 71 175
102. Oblique incidence. Round quartz cut normal to the axis. Table 72 177
103. Oblique incidence. Quartz rouge, cut normal to the axis, rhomboidal. Figs. 68, 69. Table 73 178
104. Oblique incidence. Quartz cut parallel to the axis. Fig. 70. Tables 74, 75, 76 181
105. Data for crown and for flint glass. Table 77 182
106. Apparatus remodeled. Table 78 183
107. Results for different spectrum lines. Fig. 71. Table 79 185
108. Conclusion 187

CHAPTER XIII.—*Subsidiary Experiments.*

The Prism Spectrum on the Rowland Spectrometer.

109. Introductory. Apparatus. Fig. 72. Table 80 189
110. Data. Fig. 73. Table 81 191

The Comparison of Two Screws.

111. Introductory 192
112. Method. Figs. 74, 75, 76 192
113. Data. Fig. 77. Table 82 194
114. Conclusion 197

Observations with the Simple Screw Micrometer.

115. Apparatus. Figs. 78, 79 197
116. Observation. Figs. 80, 81, 82 198

The Resolution of Interference Fringes.

117. Experiment. Figs. 83, 84 201
118. Explanation. Fig. 85 202

The Measurement of Small Increments of Angle.

119. Apparatus. Fig. 86 203
120. Experiments. Table 83 204

Elliptic Interferences with Concave Mirrors.

121. Apparatus. Fig. 87 205

Acoustic Displacements.

122. Mayer and Dvorak's experiment 206
123. Telephonic displacements. Table 84 208
124. Reciprocating and synchronized telephones. Apparatus. Figs. 88, 89 209
125. The same. Measurements. Tables 85, 86, 87 210

Change of Refraction Resulting from Dielectric Polarization.

126. Introductory 213
127. Apparatus. Figs. 90, 91 214
128. Equations 215
129. Data. Solid 216
130. Data. Liquid 216

CHAPTER XIV.—*The Interferometry of Air Carrying Electrical Current.* PAGE

131. Introduction ... 217
132. First experiments. Apparatus. Fig. 92 ... 217
133. The same. Results. Table 88 ... 219
134. Second experiments. Apparatus. Fig. 93 ... 219
135. The same. Results. Table 89 ... 221

CHAPTER XV.—*The Refraction of Hot Gases.*

The Refraction of Air at High Temperatures.

136. Introductory. Fig. 94 ... 223
137. Small apparatus ... 224
138. Equations ... 225
139. Data. Table 90 ... 226
140. Long tubes. Figs. 95, 96 ... 227
141. Data. Fig. 97. Tables 91, 92 ... 229

The Refraction of the Bunsen Flame.

142. Method ... 231
143. Conclusion ... 233

CHAPTER XVI.—*Electrometry with the Displacement Interferometer.*

Cylindrical and Disk Electrometers.

144. Introductory ... 235
145. Cylindrical electrometer. Movable cylinder without. Figs. 98, 99 ... 235
146. Cylindrical electrometer. Movable cylinder within. Figs. 100, 101, 102, 103 238
147. Equations. Absolute electrometer ... 241
148. Equations. Cylindrical electrometer ... 242
149. Equations. Disk electrometer ... 243
150. The closed field electrometer (disk and cylinder combined). Fig. 104 ... 244
151. Corrections. Figs. 105, 106, 107, 108. Tables 93, 94, 95, 96 ... 245
152. Experiments. Cylindrical electrometer; movable cylinder within. Figs. 109, 110. Tables 97, 98, 99, 100, 101, 102 ... 250
153. Cylindrical electrometer; movable cylinder within. Summary ... 254
154. Experiments. Cylindrical electrometer; movable cylinder without. Fig. 111. Table 103 ... 255
155. Disk electrometer. Apparatus. Figs. 112, 113 ... 256
156. Experiments with the disk electrometer. Fig. 114. Tables 104, 105, 106 ... 257
157. The same. Further experiments. Fig. 115. Tables 107, 108, 109 ... 260
158. Case of the inclosed disk. Fig. 116. Tables 110, 111 ... 262
159. Case of the unsymmetric disk. Fig. 117. Tables 112, 113, 114, 115 ... 264

The Quadrant Electrometer.

160. Apparatus. Figs. 118, 119 ... 266
161. Observations. Tables 116, 117 ... 269
162. Water damper. Tables 118, 119 ... 271
163. Drift forces ... 271
164. Conclusion ... 273

CHAPTER XII.

THE INDICES OF DOUBLY-REFRACTING CRYSTALS, DETERMINED BY DISPLACEMENT INTERFEROMETRY.

98. Introduction. Method.—In the following paper I shall make a further application* of the displacement interferometer, in endeavoring to investigate a method for the determination of the two refractions of a crystalline plate, with a degree of accuracy approaching the spectrometer and eventually to exceed it. The work is to be extended to all directions of the ordinary and extraordinary ray within the crystal. Inasmuch as the center of ellipses is never lost, but may always be brought back again to the fiducial and coincident sodium lines by moving the micrometer, however remote the center may be, a crystal (or indeed a column of any thickness) may be placed in one of the component beams and the micrometer equivalent of the difference resulting from presence and absence of the crystal may be ascertained. This makes the method quite sensitive; for the two micrometer readings for the presence of air and crystal, respectively, may differ by many centimeters, if desirable, and each reading may be taken to 0.00005 centimeter. If it were easily possible to determine the thickness of the crystal with the same degree of precision, the conditions would be enhanced; but this is not at once attainable, for ordinary plates, to more than 0.0001 centimeter, even apart from the errors of the two micrometer screws involved. The case of columns is more favorable.

Furthermore, the method in its direct applications requires an accurately plane parallel plate, however thick. If the faces are at even a slight angle, the beam passing through them will be deflected by the introduction of the crystal and will not be returned in its own path. This requires a readjustment and therefore a correction for the displacement of the mirror difficult to estimate without special appliances. It is to be accentuated, however, that the method for normal incidence admits of a plate of any thickness, *i.e.*, of a long column of glass with plane parallel end faces, so that this method of measuring the index of refraction must ultimately exceed in sensitiveness the method of the spectrometer, while even the importance of the readjustment in question becomes of less consequence. It will thus be available for answering refined questions relative to this index in glass, etc., under conditions where the spectrometer fails of application. It is in this direction that the results are to be prosecuted as soon as the preliminaries discussed in the present paper have been clarified.

It is also probable that if the deviation of the ray *mm* due to non-parallel faces in the crystal is corrected, not at the micrometer mirror *M*, but at

* The earlier papers on elliptic interferometry will be found in the Carnegie Publications, No. 149, 1911, Part I, and 1912, Part II.

the other opaque mirror N, beyond the grating, the discrepancy in question will vanish. For in this case, on restoring the interferences by rotating N, the air path of *both* component beams mm and nn is equally incremented.

The plate crystal X is mounted on a horizontal axle ab, normal to the interfering beam mm in question. The angle of incidence of the beam is changed by rotating the plate in definite steps and the amount of rotation read off on the attached fixed graduated circle C, with its plane parallel to the beam and its axis normal to it. Angles of 0°, 10°, 20°, 30°, 40°, and even 50° were usually available on either side of the normal position. The crystal, mounted in a cork plate, was at first conveniently held by a spring clip; but later* more elaborate means for mounting the plate parallel to the axis of rotation were adopted. The normal position is found with certainty by slightly rotating the crystal around the horizontal axis in either direction, until the interference rings in the field of view change their direction of motion. This is the minimum thickness e. The same operation is then performed around the vertical axis, both adjustments being usually easy and the result satisfactory.

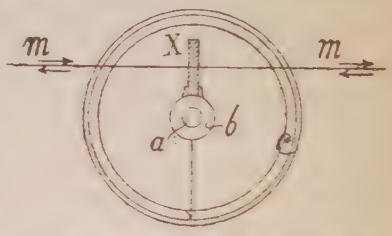

FIG. 65.—Apparatus for rotating crystals.

With the angle i given, the corresponding angle of refraction r, *i.e.*, the angle of the ray with the optic axis of the crystal cut normally to this axis, may be computed when the index of refraction for the given case is known. Hence the refraction in different directions r, both for the ordinary and extraordinary rays, follows, as far as about $r=30°$ from the optic axis, in the above apparatus. Plates are not usually large enough for a larger internal angle on the one hand, while the errors of measurement multiply on the other; but by selecting a plate cut parallel to the axis, the final 30° of the quadrant may be found. To obtain the intermediate 30° a plate cut obliquely to the axis or else a plate of large area would be necessary.

When the plate is cut parallel to the axis and the difference of the refractive indices (as in quartz) is not too large, the two interferometer ellipses, corresponding to the ordinary and extraordinary rays, are in the field at once, making an exceedingly beautiful design. Their distance apart may then be found micrometrically in terms of the refraction of the ordinary ray, giving an acceptable datum even in case of an imperfect, *i.e.*, slightly wedge-shaped, plate. In other words, the ordinary and extraordinary rays encounter the same conditions and their difference of path remains practically unimpaired.

To distinguish between the two families of intersecting ellipses it is necessary to polarize the incident beam in the vertical and horizontal

* It will be shown below that the eccentric mounting of the crystal, as in fig. 65, is not, as a rule, advisable.

planes respectively, seeing that the crystal is revolvable about the horizontal or vertical axis. When the plate is true and the mounting trustworthy, there need never be difficulties due to elliptical polarization, for the vertical and horizontal vibrations pass unchanged. If, however, rotary polarization occurs, the case of the oblique path is more complicated, but it does not interfere with the measurement.

The present method inherently presupposes a knowledge of the dispersion of the crystal; but as this term is of the nature of a correction, the coefficient in the simplified Cauchy equation of two terms may at the outset be inserted. For accurate work Cauchy's equation as far as the fourth power of wave-length must be used. It will be shown, moreover, that the method is self-contained, by affording means for determining the coefficients of the equation in question. Initially, no more than a measurement of the refraction of the extraordinary ray in terms of the ordinary ray will be attempted. The dispersion constant found for these rays from data for two Fraunhofer lines may then be used for all wave-lengths lying between.

99. Equations.—If e', I, R, μ', denote the thickness, the angles of incidence and refraction, and the index of refraction of the grating, and e, i, r, μ, the corresponding quantities for the plane parallel plate inserted in one of the component beams of the interferometer; if, furthermore, b' and b denote the corresponding coefficients in the simplified dispersion equation of Cauchy, $\mu = a + b/\lambda^2$, so that

$$-\lambda d\mu/d\lambda = 2b/\lambda^2$$

the coördinates of the micrometer in the absence of the plate will be, if μ_a is the absolute index of refraction of air,

$$N' = e'\mu'\left(\cos R + \frac{2b'}{\lambda^2\mu' \cos R}\right) + e\mu_a \quad (1)$$

where $e\mu_a$ is the air path coextensive with the thickness of the plate in its normal position AA, fig. 66, I being the incident beam of light. If the plate is inserted at an angle of incidence i, in the position given by BB, and the center of ellipses is then returned to the same fiducial line D of the spectrum, by moving the opaque mirror of the micrometer over a distance ΔN, nothing has been changed at the grating and the first term of the right-hand member of equation (1) remains unchanged. It therefore vanishes so far as ΔN is concerned. Hence we may write

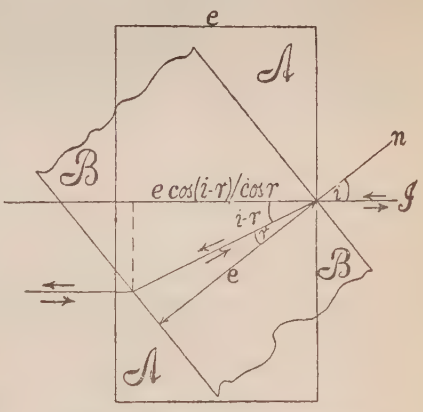

FIG. 66.—Diagram showing path increments.

$$\mu_a(e + \Delta N) = \frac{e}{\cos r}\left(\mu + \frac{2b}{\lambda^2}\right) + e\mu_a\left(1 - \frac{\cos(i-r)}{\cos r}\right) \quad (2)$$

as fig. 66 shows. For not only has the path e been increased by the introduction of the oblique plate, but the air-path is also longer. Hence, on removing $e\mu_a$,

$$\mu=\mu_a\left(\frac{\Delta N\cos r}{e}+\cos(i-r)\right)-\frac{2b}{\lambda^2} \tag{3}$$

In this equation the quantities μ, r, refer to the same fiducial spectrum line of wave-length λ, to which the center of ellipses is always to be restored by moving the micrometer. Whenever the incidence at the plate is normal, $i=r=0$,

$$\mu=\mu_a\left(\frac{\Delta N}{e}+1\right)-\frac{2b}{\lambda^2} \tag{4}$$

an equation more generally useful and particularly so in case of long columns.

If the dispersion of air can not be disregarded, μ_a must be replaced by $\mu_a(1+2b''/\lambda^2\mu_a)$, μ_a and b'' referring to a plenum of air. Thus if all quantities are to be considered, the equation is

$$\mu=\mu_a\left(\frac{\Delta N\cos r}{e}+\cos(i-r)\right)-\frac{2}{\lambda^2}(b-b'') \tag{5}$$

The value of b for the crystals is usually of the order of 4×10^{-11}, whereas the value for air is of the order of 1.6×10^{-14}, so that the dispersive effect of air is usually negligible, being not more than 0.00001. Again, the value of ΔN for a plate about 0.6 cm. in thickness is usually of the order of 0.3 to 0.6 cm. and a single reading should be correct to 0.00005 cm. The error should not be larger, therefore, than a few parts in 10,000, so that the minimum error of μ should not exceed 5 units in the fourth place.

Finally, the last term $2b/\lambda^2$ is of the order of 0.02 and if it is determinable by the method of §100 to about 1 per cent, this error also can only affect the fourth place. There remains the case of $\cos r$, which in the most unfavorable case of large incidence can not be wrong by more than 0.4 per cent per degree misread, and the effect would even then be but 2 units in the third place of μ. Whenever $i=r=0$, *i.e.*, for normal incidence, the values of μ are acceptable at once. Table 69, for instance, gives data under varying conditions.

TABLE 69.—True plate of quartz cut normal to the axis. $e=0.5996$ cm. $i=0°$ (normal incidence). $\mu_0=\mu_a+\Delta N/e-2b/\lambda^2$. D line fiducial. Sunlight. $10^{10}\times b=0.421$

Method.	$\Delta N\times10^4$	μ_0
Short collimator. Ellipses centered	0.34025	1.54350
No collimator. Sunlight and slit: Ellipses not centered	.34000	1.54309
Ellipses centered but distorted	.34020	1.54342
Ellipses centered	.34040	1.54376
Weak objective as collimator: Ellipses less distorted	.34015	1.54334
With large telescope	.34050	1.54392
Short collimator. Sharp ellipses	.34040	1.54376
Concave lenses added to collimator	.34060	1.54408

In this table the absolute value of μ depends upon the value of e (which was calipered), on the relation of the two screws of the micrometer and of the caliper, on the alignment of the micrometer screw which is difficult to adjust, on the value accepted for the dispersion constant b, etc. The fact that it is here appreciably different from the normal value, 1.54423, has therefore no significance. The values of ΔN are the chief exhibit. They possibly show some difference with the obliquity (convergence and divergence in the vertical plane) of the incident rays of light. It is probable, however, that the slight difference of values of ΔN found is due simply to the distortion of ellipses in the different cases. In some of these it was hard to define the center. One may argue that in case of a clear center the obliquity of rays is without influence on the result.

The beam, in case of sunlight, is sheet-like, with its long dimension vertical. Much of it is apt to be lost on successive reflection. Results obtained with the arc lamp and a collimator objective which places the focus relatively to the vertical plane on the opaque mirrors M and N furnishes a rapier-like beam, which may easily be made to penetrate tubes and columns. It is thus far preferable and the results better. The sodium line is invariably present as a line of reference for measurement.

Since $\cos r = \sqrt{\mu^2 - \sin^2 i/\mu}$, equation (5) is essentially of the fourth degree and can be solved only by approximation. If $\Delta N/e = x$ and $\sin i = y$ the equation reads, when b'' is neglected,

$$\mu - \mu_a \cos(i-r) = x\mu_a\sqrt{1 - y^2/\mu^2 - 2b/\lambda^2} \qquad (6)$$

The approximation is therefore rapid, since $\mu - 1$ (nearly) is computed successively in terms of μ, which is always relatively much more accurate than $\mu - 1$.

100. Dispersion constants.—In the equation in the normal form (4) for two wave-lengths λ and λ', b may be eliminated or determined; for if $y = 0$ (normal incidence, detected with certainty by the inversion in the motion of the rings, as described above) and $\mu = A + b/\lambda^2$ is assumed for a sufficiently narrow range of the spectrum near the D line,

$$A = \mu_a(1 + x\lambda^2 - x_1\lambda_1^2)/(\lambda^2 - \lambda_1^2) \qquad 3b = \mu_a\lambda^2(x - x_1)/(1 - (\lambda/\lambda_1)^2) \qquad (7)$$

If the value of x is restored, since for the two wave-lengths $\Delta N = N' - N$ and $\Delta N_1 = N_1' - N_1$, where N' refers to glass and N to air,

$$e(x_1 - x) = N_1' - N_1 - (N' - N) = N_1' - N' - (N_1 - N)$$

or briefly

$$e(x_1 - x) = \delta N' - \delta N$$

whence

$$b = \frac{\mu_a\lambda^2}{3e} \quad \frac{\delta N' - \delta N}{1 - (\lambda/\lambda_1)^2} \qquad (8)$$

Here $\delta N'$ and δN are the differences of micrometer readings for the two spectrum lines λ and λ', for glass in place and for glass removed, respectively. ΔN_1 and ΔN need not therefore be known, *i.e.*, the glass plate need not be

scrupulously plane parallel, as it is merely necessary to get the glass difference and the air difference for two successive lines, however far apart the air and glass positions may be for either line. Equation (8) also follows at once from (3) by inserting the equivalent of μ for the two spectrum lines. Table 70 gives a series of data obtained in this way.

TABLE 70.—Data for the dispersion constant b in $\mu = a + b/\lambda^2$ for a series of media.

Medium.	e	Line.	$10^3 \times \Delta N'$	$10^3 \times \Delta N$	$\lambda \times 10^6$	$\lambda' \times 10^6$	$b \times 10^{11}$
Common plate	0.7641	$D - b_1$	16.55	7.80	58.93	51.84	4.53
Do.....	.7641	$D - b_1$	....	....	58.93	51.84	4.60
		$E - F$	....	....	52.70	48.61	5.46
Flint glass....	.6720	$D - b_1$	24.05	7.90	58.93	51.84	9.52
		$E - F$	18.97	6.70	52.70	48.61	9.64
Crown glass..	.6946	$D - b_1$	15.95	7.90	58.93	51.84	4.70
		$E - F$	12.35	6.70	52.70	48.61	4.26

Granting the approximate form of Cauchy's equation, the error of b thus obtained should be well within 1 per cent. Its influence on μ should not exceed one unit in the fourth place. Unfortunately, however, the equation in question is not warranted to this extent, when the lines of the spectrum are as far apart as D and E, for instance. The question relative to b will be resumed in §107. Meanwhile I may observe that the equation with three constants, $\mu = A + b/\lambda^2 + c/\lambda^4$, leads to

$$3b\left(\frac{1}{\lambda_1^2} - \frac{1}{\lambda_2^2}\right) + 5c\left(\frac{1}{\lambda_1^4} - \frac{1}{\lambda_2^4}\right) = \mu_a \frac{\Delta N_1 - \Delta N_2}{e} \qquad (8')$$

and would need three spectrum lines for the determination of b and c. This is a cumbersome procedure, but from the nature of the problem is nevertheless probably the only resort, particularly in the case where a long column of glass, crystal, or liquid is to be investigated, for exceptionally accurate indices of refraction.

In conclusion, it is worth while to determine the value of μ_e in terms of μ_0 found from the normal position, when the difference of these indices (as in quartz) is not large. In fact, since $d(\Delta N) = e dx$,

$$\frac{d\mu}{d(\Delta N)} = \frac{\mu \cos^2 r}{e\mu \cos r/\mu_a - \Delta N \sin^2 r + e \sin r \sin (i - r)} \qquad (9)$$

Equation (9) may be reduced, with questionable advantage, by replacing μ in the denominator by its value from (3) to

$$\frac{d\mu}{d(\Delta N)} = \frac{\mu \cos^2 r}{(e + \Delta N) \cos 2r - 2eb \cos r/\mu_a \lambda^2}$$

If $i = r = 0$, this reduces to

$$\frac{d\mu}{d(\Delta N)} = \frac{\mu_a}{e} \qquad (10)$$

If in equation (9) the value of μ_0 is introduced, the corresponding value of μ_e may be computed from the ΔN and $\Delta N'$ which put the two ellipses,

respectively, on the fiducial sodium line. The result gives a fair value for μ_e, even when μ_0 varies with the incidence i due to errors of adjustment, seeing that μ_0 must be constant and is found from the normal position. See equation (11).

101. Oblique incidence.—In the first experiments no distinction was made between the ordinary and extraordinary rays, and these data may therefore be waived here.

In table 71 the object used was a plate cut normal to the axis, $e = 0.6100$ cm. thick, but not sufficiently plane parallel. In other words, it required angular adjustment of the opaque mirror when the plate was inserted and again when it was removed. This introduces an indeterminable error, as plane parallelism is a prime condition for the accurate application of the present method. The incident light was polarized in the vertical plane, before reaching the slit, the *D* line being as usual fiducial. When viewed through an analyzer, the light reaching the telescope in case of the more oblique positions of the plate on its horizontal axis was elliptically polarized in one of the superimposed spectra, the latter showing the usual channeled structure with more dark bands as the effective thickness increased. With obliquity decreasing through zero, moreover, the black bands between crossed Nicols moved in opposite directions when the normal position was passed. For the polarizer at 45° both families of ellipses were in the field at once. Either one or the other set could be excluded by rotating the analyzer. In the absence of this, the field showed the ordinary or the extraordinary set of ellipses separately, on rotating the polarizer 90°. In the further absence of the polarizer, one frequently observes dislocated rings, the dislocation being in multiple along equidistant vertical planes. In such loci the ordinary and extraordinary rings, therefore, successively passed into each other. In general, a figure which is blurred without polarizer is resolved into two clean figures by the aid of it, one being definitely displaced with reference to the other.

TABLE 71.—Double refraction of normal quartz. Rays not parallel in vertical plane. Opaque mirrors silvered on back. Plate thick, oblong, and slightly wedge-shaped. $e = 0.6100$ cm. Horizontal axis of rotation for i. $\mu_0 = 1.54423$; $\mu_e = 1.55338$; $b \times 10^{10} = 0.421$.

i	r	ΔN_0	Observed μ_0	ΔN_e	Observed μ_e	$10^5 \times \delta\mu$	Computed $10^5 \times \delta\mu$	Corrected $\mu_e = \mu_o + \delta\mu$
°	°							
0	0	0.34855	1.54759	0.34855	1.54759	0	0	1.54423
10	6.47	.35140	1.54671	.35158	1.54684	13	29	1.54436
20	12.80	.36103	1.54545	.36130	1.54588	43	43	1.54466
30	18.88	.37868	1.54485	.37935	1.54588	103	104	1.54526
40	24.60	.40300	1.54100	.40405	1.54258	158	157	1.54581
50	29.73	.43833	1.53820	.43978	1.54027	207	207	1.54630

Seeing that the plate was not quite plane parallel and that in addition to displacement ΔN, a slight rotation of the micrometer mirror was needed

to restore the ellipses on inserting the plate (equivalent to an appreciable increment of ΔN), the large value of μ for the normal position is to be anticipated. I have not thus far tested the way to correct this discrepancy.* One would have to evaluate the rotation of mirror horizontal or vertical in terms of the displacement ΔN or else make the compensation instrumentally.

The second feature is the very rapid increase of ΔN and therefore of μ with the angle of incidence i. The reason for this has yet to be succinctly stated, but it is due to the slightly wedge-shaped plate. When this is rotated on an eccentric axis, as in fig. 65, even if the axis is parallel to the plate, different parts of the crystal, of successively increasing thickness, are penetrated by the beam of light. Nevertheless both μ_0 and μ_e may be found, since the former is constant and would be given for a plate, while the latter is determinable from equation (9). Hence

$$\mu_e = \mu_0 + \mu \cos^2 r(\Delta N_e - \Delta N_0)/(e\mu \cos r - \Delta N \sin^2 r + e \sin r \sin (i-r)) \quad (11)$$

Again μ_0 and μ_e may be computed as in the table and μ_e found by adding the difference for a given i to the constant value of μ_0. Values of $\delta\mu$ found by both of these methods are frequently instanced in the tables, the one found by equation (11) being called computed $\delta\mu$.

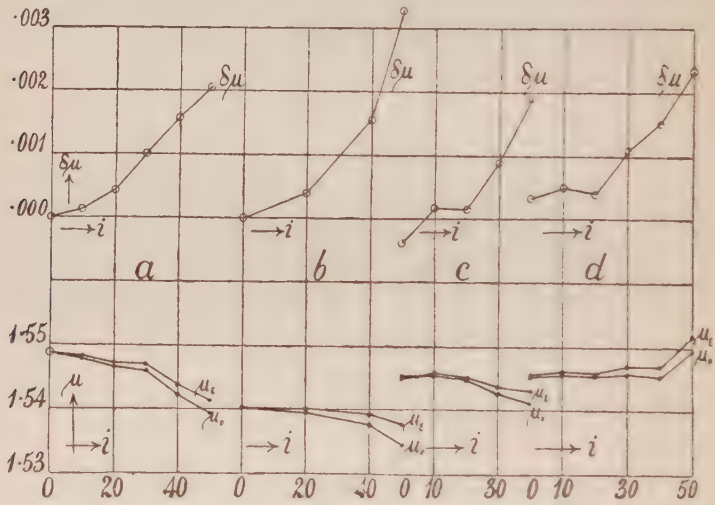

FIG. 67.—Observed indices of refraction and variation at different incidences.

The difference is slight and due to the fact that the direct computation of μ_e, as compared with the method by way of equation (9), has not been carried to a sufficient degree of successive approximation.

If in table 71, μ_0, μ_e, $\delta\mu = \mu_e - \mu_0$, be constructed as depending upon r, the angle between the axis and the ordinary ray (or more directly upon i,

* It is probable that if the adjustment for non-parallel faces is made, not at the micrometer mirror M, but at the distant mirror N, no appreciable discrepancy will be introduced. But the distant mirror is not easily accessible at the position of the observer.

the angle of incidence), the data appear as in fig. 67, *a*. The irregularity in μ at 30° is due to some error in the adjustment; nevertheless the values of $\delta\mu$ are not appreciably influenced by it. The results are naturally less trustworthy as i is larger.

It will be seen that the observations for $\delta\mu$ as such make a satisfactorily smooth series, even beyond the fourth place of decimals. If v refers to the velocity of light in the crystal, and o and e refer to ordinary and extraordinary rays,

$$v_o/v_e = 1 + \delta\mu/\mu_0$$

The observed order of change is apparently sufficient. As a whole and for large r the interpretation is complicated because of the occurrence of rotary polarization along the axis.

102. Oblique incidence. Round quartz cut normal to the axis.— This plate was 0.3100 cm. thick and cut approximately normal to the axis. Like the preceding plate it was slightly wedge-shaped. It therefore required rotation of the micrometer mirror, as well as the displacement ΔN on being inserted into the beam of light, in order to bring the ellipses back to the fiducial line. Table 72 shows the results on the same plan as the preceding. The second series is reproduced in fig. 67, *b*.

TABLE 72.—Thin quartz plate, round, cut normal to the axis. $e = 0.3100$ cm. Horizontal axis of rotation. $\mu_0 = 1.54423$; $b \times 10^{10} = 0.421$.

I.				II (later).		
i	r	ΔN_0	Obs. μ_0	i	r	ΔN_0
°	°			°	°	
0	0	0.17280	1.53360	0	0	0.17450
10	6.47	.17470	1.53427	20	21.80	.18128
20	12.80	.17995	1.53436	40	24.60	.20331
30	18.88	.18855	1.53289	50	29.73	.22101
40	24.60	.20210	1.53307			

II (later).					
Obs. μ_0	ΔN_e	Obs. μ_e	$10^5 \times \delta\mu$	Comp. $10^5 \times \delta\mu$	Corr. $\mu_e = \mu_0 + \delta\mu$
1.53910	0.17450	1.53910	0	0	1.54423
1.53855	.18141	1.53895	40	41	1.54463
1.53662	.20385	1.53819	157	159	1.54580
1.53330	.22218	1.53657	327	329	1.54750

This plate was at first supposed to be too thin to admit of the determination of the difference of μ_0 and μ_e, satisfactorily; in fact, the ordinary ray in the first series shows the usual increase of index with i, regarding which the remarks of the preceding paragraph apply. However, the second series

of data, found at a later date for both ordinary and extraordinary rays, is in good agreement with the preceding table, particularly in relation to $\delta\mu$. The data are smooth and consistent, even as far as $i = 50°$, which is not the case in table 71. This is probably owing to the large surface of the present plate.

103. Oblique incidence. Quartz rouge, cut normal to the axis, rhomboidal.—This is the only quartz plate found to be adequately plane parallel to admit of both of the measurements for ΔN (presence and absence of plate), without readjusting the mirrors by rotation. It would thus have been possible to obtain the true ΔN without appreciable error, but unfortunately the surface was too small for much inclination. The data are given in table 73.

TABLE 73.—Thick (rouge) quartz, lozenge-shaped, cut normal to the axis. $e = 0.5996$ cm. Plane parallel plate. Rays not parallel in vertical plane. Opaque mirrors silvered on back. $\mu_0 = 1.54423$; $b \times 10^{10} = 0.421$.

	i	r	ΔN_o	Obs. μ_0	ΔN_e	Obs. μ_e	$10^5 \times \delta\mu$	Comp. $10^5 \times \delta\mu$	Corr. $\mu_e = \mu_e + \delta\mu$
I. Horizontal axis of rotation.	0°	0°	0.34059	1.54422	0.34037	1.54385	−37	−37	1.54386
	10	6.47	.34395	1.54431	.34407	1.54448	+18	+20	1.54441
	20	12.80	.35379	1.54369	.35389	1.54385	16	16	1.54439
	30	18.88	.37011	1.54150	.37067	1.54239	89	88	1.54512
	40	24.60	.39543	1.53993	.39679	1.54183	190	207	1.54613
III. Vertical axis of rotation.	0°	0°	0.34049	1.54406	0.34069	1.54439	33	33	1.54456
	10	6.47	.34404	1.54445	.34434	1.54495	50	50	1.54473
	20	12.80	.35414	1.54426	.35439	1.54466	40	41	1.54463
	30	18.88	.37211	1.54465	.37280	1.54575	110	109	1.54533
	40	24.60	.39825	1.54422	.39925	1.54575	153	152	1.54576
	50	29.73	.43781	1.54827	.43944	1.55063	236	237	1.54959
IV. Vertical axis of rotation.	0°	0°	0.34065	1.54433	0.34065	1.54433	0	....	1.54423
	10	6.47	.34388	1.54419	.34388	1.54419	0	....	1.54423
	20	12.80	.35371	1.54356	.35407	1.54414	58	....	1.54481
	30	18.88	.37153	1.54375	.37217	1.54475	100	....	1.54523
	40	24.60	.39750	1.54309	.39818	1.54412	103	....	1.54526
V. Vertical axis of rotation.	0°	0°	0.34048	1.54403	0.34048	1.54403	0	....	1.54423
	30	18.88	.37198	1.54445	.37248	1.54525	80	....	1.54503
	50	29.73	.43423	1.54308	.43583	1.54540	232	....	1.54655
VI. Vertical axis of rotation. Sunlight.	0°	0°	0.34040	1.54390	0.34040	1.54390	0	....	1.54423
	20	12.80	.35400	1.54402	.35400	1.54402	0	....	1.54423
	30	18.88	.37153	1.54375	.37208	1.54462	87	....	1.54510
	40	24.60	.39770	1.54339	.39870	1.54490	151	....	1.54574
VII. Vertical axis of rotation. Electric arc.	0°	0°	0.34040	1.54390	0.34040	1.54390	0	....	1.54423
	20	12.80	.35360	1.54338	.35394	1.54393	55	....	1.54478
	30	18.88	.37109	1.54305	.37183	1.54422	117	....	1.54540
	40	24.60	.39723	1.54268	.39823	1.54418	150	...	1.54573
VIII. Biquartz. Line of separation horizontal. Vertical axis of rotation. $e = 0.748$, Small face.	0°	0°	0.42503	1.54442	0.42503	1.54442	0	....	1.54423
	20	12.80	.44233	1.54497	.44248	1.54515	18	....	1.54441
	30	18.88	.46425	1.54472	.46468	1.54525	53	....	1.54476

A variety of normal values was adduced in table 69. The earlier results of table 73 are constructed in fig. 67 under *c*. In case of the third series (fig. 67, *d*, and fig. 69), fourth series (fig. 68, *a*, and fig. 69), and fifth series (fig. 68, *b*, and fig. 69), the apparatus used had been totally changed. The quartz plate was now rotated around a vertical axis and a more accurate circle was installed for the measurement of the angle of incidence, *i*. Furthermore, the endeavor was made to mount the crystal parallel to the axis of rotation, by providing the axle with a fine axial perforation. A straight, snugly fitting steel wire could be sunk into this, against which the quartz plate was to be pressed, before fastening it. The wire was then removed. The position normal to the ray of light was found as before, by horizontal and vertical rotation, until the motion of ellipses changed sign. It would

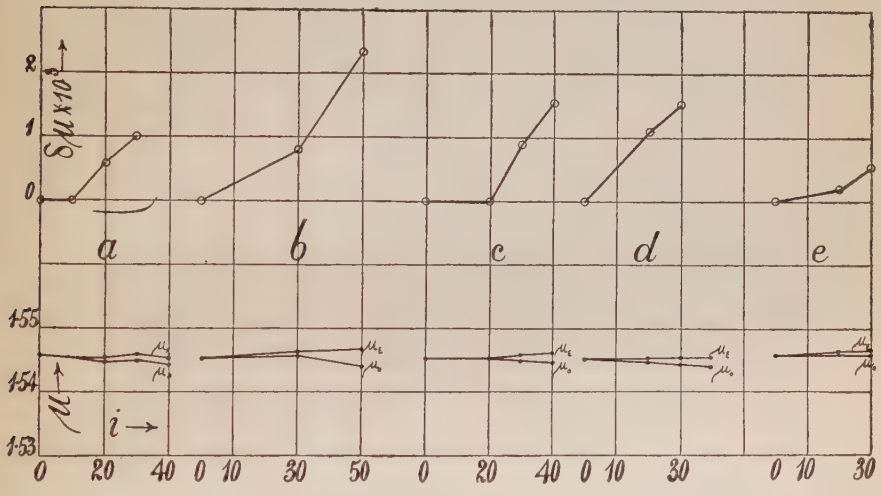

FIG. 68.—Observed indices of refraction and variation at different incidences.

have been a further improvement to mount the crystal so that the axis, instead of passing through one face, would pass symmetrically between the faces. The spot of light would not then move along the face appreciably. The data as a whole are of the same order of value and show the same character as the preceding results, obtained with a horizontal axis of rotation. No effect is therefore to be ascribed to the adjustment, though from a theoretical point of view one might be inclined to look for a difference. Practically the vertical axis, being parallel to the slit, is in some respects advantageous, as less surface of glass is required. The circle for measuring *i* was accurately graduated.

In Series III the change of μ as far as $i = 40°$ is but one unit in the fourth place; beyond this, for $i = 50°$, light passed partially outside the crystal and the data are approximate. Series IV and Series V show similar behavior, even as far as $i = 50°$. In fact Series III to V, both as to μ_0 and μ_e, are a marked improvement over Series I and II, in so far as the indices

themselves are concerned. It is curious that the corresponding values of $\delta\mu$, obtained by difference, did not come out as smoothly as in the earlier tables, though the order of value is throughout the same. Probably slight dislocations of the parts of the interferometer itself in an agitated laboratory are the cause of these discrepancies.

Final measurements, Series VI and VII of table 73, were made with the apparatus further modified, as stated in §106. In particular the mirrors used were silvered in front, so as to obviate discrepancies (though such an effect is here probably negligible, since the spot of light does not move on the plane of the mirror) from the two wedges of glass which lie in front of

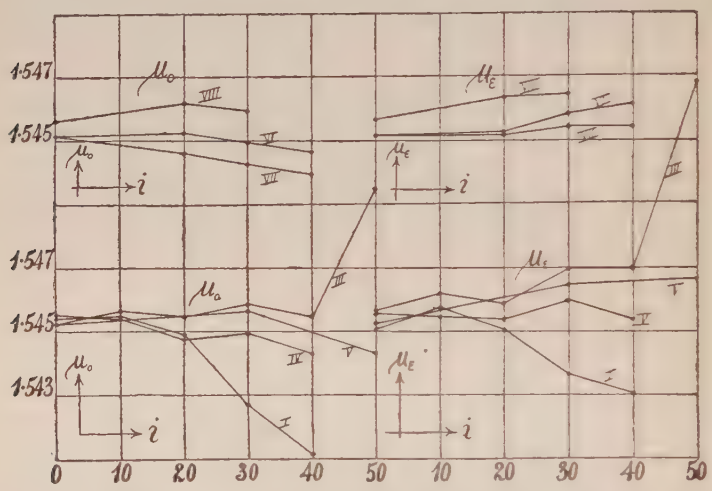

FIG. 69.—Observed indices of refraction and variation at different incidences.

the silver surface in the former case. The axis for varying i was vertical. A contrast is made between sunlight (using no collimator objective) and the electric arc.

The new results for μ are smoother, but in general not much of an improvement on preceding work. They represent the average limits of the method and show that the mounting of the crystal parallel to the axis, preferably with the latter passing symmetrically between the faces, finally becomes the chief obstacle to further development. The direction of this axis is immaterial. The results are given in fig. 68, *c* and *d*, and fig. 69.

Finally, certain measurements, table 73, VIII, fig. 68, *c*, made with a biquartz "rouge," may be inserted here. The right and left turning crystals were identically thick and respectively above and below the horizontal plane corresponding to the center of ellipses. The crystal was too small for satisfactory work, but no difference could be detected in the ellipses corresponding to right-handed and left-handed rotation, the biquartz behaving like a single homogeneous crystal.

104. Oblique incidence. Quartz cut parallel to the axis.—Table 74 and fig. 70, *a*, *b*, *c*, give the results for the parallel quartz. The index of refraction should, therefore, in the normal position, $i = 0°$, show maximum difference, $\delta\mu$. The only available plate was not quite plane parallel and rotational adjustment was required between the two readings for ΔN. This again throws the absolute values out. The mean thickness of the plate was $e = 0.4918$ cm. The surface was too small for much rotation.

TABLE 74.—Rectangular quartz plate parallel to the axis. $e = 0.4918$ cm. Rays not parallel in vertical plane. Opaque mirrors silvered on back. Horizontal axis of rotation. $\mu_0 = 1.54423$; $\mu_\varepsilon = 1.55338$; $b \times 10^{10} = 0.421$.

i	r	ΔN_o	Obs. μ_o	ΔN_e
°	°			
0	0	0.27919	1.54388	0.28431
10	6.47	.28165	1.54336	.28653
20	12.80	.28930	1.54193	.29395
30	18.88	.30315	1.54069	.30785
35	21.80	.31260	1.53991	.31730

The differences $\delta\mu$ between the corrected ordinary and extraordinary index are somewhat in excess of the true value, the observed ordinary index being about 4 units in the fourth place too large and the observed extraordinary 6 units too small. Apart from these absolute differences, however, the values of $\delta\mu$ make a smooth curve to the fifth place of decimals,

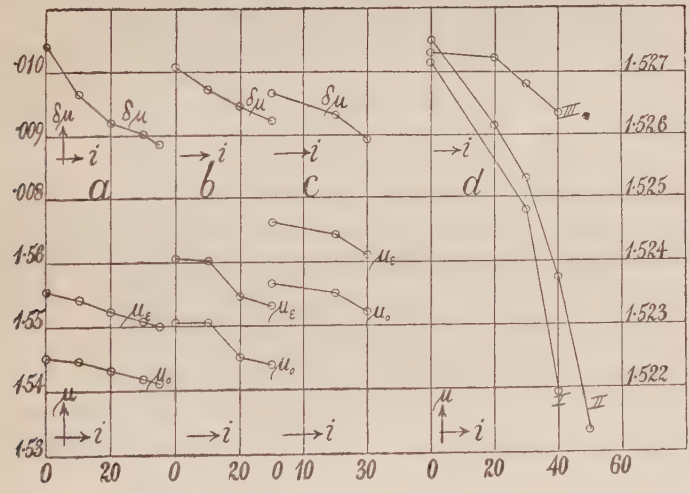

FIG. 70.—Observed indices of refraction and variation at different incidences.

as shown in fig. 70, *a*, and $\delta\mu$ decreases with the obliquity, *i.e.*, from the maximum difference of μ_0 and μ_e, as it should. Unfortunately the need of readjustment for air and the quartz medium leaves an uncertain element in these data.

The work was repeated shortly after this with the results given in table 75 and fig. 70, *b*.

TABLE 75.—Quartz plate parallel to the axis. Conditions as in table 74. $\mu_0 = 1.54423$; $\mu_e = 1.55338$; $b \times 10^{10} = 0.421$.

i	r	ΔN_0	Obs. μ_0	ΔN_e
°	°			
0	0	0.28193	1.54946	0.28690
*10	6.47	.28468	1.54949	.28960
20	12.80	.29038	1.54408	.29516
30	18.88	.30425	1.54280	.30904

*Readjusted.

This series is poor in relation to μ_0 and μ_e, as it was necessary to readjust the mirror twice. The values of $\delta\mu$, however, are nevertheless in accord with the data of the preceding table.

In the following experiments, table 76 and fig. 70, *c*, with the same plate of quartz, the lens of the collimator was removed and sunlight thrown directly on the slit. Light rays parallel in the vertical plane thus pass through the plate; but the ellipses in this case were neither sharp nor easily identified.

TABLE 76.—Quartz plate parallel to the axis. Sunlight and slit without collimator lens. $\mu_0 = 1.54423$; $\mu_e = 1.55338$; $b \times 10^{10} = 0.421$.

i	r	ΔN_0	Obs. μ_e	ΔN_e	Obs. μ_e
°	°				
0	0	0.28490	1.55549	0.28965	1.56515
20	12.80	.29535	1.55393	.30005	1.56325
30	18.88	.30855	1.55109	.31320	1.56002

In view of the difficulty of observation, these results are not easily interpreted in so far as the corrected absolute values are concerned. The data for $\mu_e - \mu_0$ are too low as compared with the preceding series, but they come nearest to the true value, while the individual indices of refraction μ_0 and μ_e are much too high. As a whole, the results for the plate cut parallel to the axis have failed to turn out well, owing to the fact that this plate was appreciably wedge-shaped.

105. Data for crown and for flint glass.—To exclude the peculiarities due to double refraction a few experiments were made with rectangular plates of crown and of flint glass. Neither of them was adequately plane parallel and separate adjustment (rotation of the micrometer mirror) for the air and for the plate medium was necessary.

To determine the dispersion constant, it is necessary to use the method of equation (8), §100, since the total reflectometer, in case of flint glass at least, is quite unavailable. The results, which were also discussed in §100, were crown glass, $10^{10}b = 0.470$; flint glass, $10^{10}b = 0.952$.

The results of table 77, like those for the ordinary ray in the preceding table, show the same variation of μ with r, the cause of which has been

ascribed to the appreciably wedge-shaped glass plates. Furthermore, a dispersion equation with three constants would have been preferable, if not necessary.

TABLE 77.—Plates of crown glass, $e=0.6946$ cm., and of flint glass, $e=0.6720$ cm. $b \times 10^{10}$ (crown glass) $=0.4698$; $b \times 10^{10}$ (flint glass) $=0.952$.

Crown glass			Flint glass	
i	ΔN	μ	ΔN	μ
°				
0	0.38876	1.53307	0.42965	1.58501
10	.39255	1.53306	.43355	1.58482
20	.40366	1.53221	.44672	1.58600
30	.42328	1.53125	.46880	1.58698
40	.45384	1.53157	.50103	1.58764

106. Apparatus remodeled.—The change in the direction of the axes of rotation for i, from the horizontal to the vertical, seems to be without effect, as has already been tested in table 73. Hence the vertical axis is to be preferred throughout the measurements. Being parallel to the slit, it requires a smaller face of crystal for a corresponding variation of i and none of the rays need be cut off on rotation. In any case, the axis should pass as nearly as possible through the line of symmetry of the crystal, *i.e.*, midway between the faces, to avoid the wedge-effect. The plate is made parallel to the axis by the device of the perforated axle and normal to the beam by aid of the motion of the interference rings for two planes of rotation. Errors introduced by inequalities of the screws for the measurement of ΔN and e will here be disregarded, as they are not significant and their effect may be corrected at the end of the work. (See Chapter XIII, p. 192.)

The first improvement consisted in providing all the mirrors and plates with a firmer spring, so that a tremor of the table might effect no permanent disadjustment, however small. Flexure of the table due to a weight must be scrupulously avoided during the measurements. The feet of the micrometer should be provided with vertical and horizontal (parallel to the mirror) adjustment screws, so that the final placing of the mirror may be made elastically, straining the arm which holds the micrometer to a very small extent. This secures much finer and easier adjustment than is possible by actuating the three leveling screws of the mirror. The ellipses may now be placed with certainty in the center of the field and they appear with maximum sharpness. Moreover, if the support of the micrometer is under strain, it is clutched more securely, so that the micrometer screw may be manipulated with the hand with less tremor to the image.

The opaque mirrors, which in the above experiments were silvered on the rear, were replaced by a similar set silvered on the front face. In this way the possibility of a sharp edge of glass at either mirror is avoided, care being taken to obtain a specially even coat of silver. Finally, tests were made with parallel rays of light, the objective of the collimator being

removed and the slit used alone either with sunlight or a distant arc light. The rays are then parallel in their projection on a vertical plane, but not in relation to a horizontal plane, because of diffraction of the slit.

Results so obtained are given in table 78 and fig. 70, *d*. The measurements were made with a selected piece of crown glass cut from a large sheet of common plate, which had been tested throughout its length and a suitable part taken. For this purpose it is merely necessary to examine the white undeviated slit images. If they are not displaced appreciably in any direction by the introduction of the plate into one of the component beams, the part of the plate used will probably be serviceable. The final test may be made with the ellipses themselves, which must be clear for both positions of the micrometer N and N_0, in the presence and absence of the plate.

TABLE 78.—Selected plate glass. $e=0.7641$ cm. $b\times10^{10}=0.453$; $2b/\lambda^2=0.2609$.

I. Sunlight. Horizontal axis.				II. Electric arc. Horizontal axis.			III. Electric arc. Vertical axis.		
i	r	ΔN	μ	r	ΔN	μ	r	ΔN	μ
° 0	0°	0.42238	1.52713	0°	0.42265	1.52749	0°	0.42250	1.52729
20	....	.....	.....	12.80	.43855	1.52614	12.80	.43938	1.52720
30	18.88	.45965	1.52481	18.18	.46006	1.52530	18.88	.46125	1.52679
40	24.60	.49033	1.52194	24.60	.49184	1.52374	24.60	.49403	1.52634
50	....	.....	.....	29.73	.53586	1.52134	....	.....	.....

In table 78 the first series was obtained, as already intimated, with parallel rays of sunlight, the objective of the collimator being removed. The ellipses in this case are liable to be small and cramped, so that this method (without lenses) is otherwise much inferior to that of the series in which the arc lamp was used in the usual way. The axis of rotation for varying i for the plate was eccentrically horizontal, even here an undesirable adjustment.

The values of μ obtained in the first series with sunlight are definitely below the second with electric light. They agree more nearly as i approaches zero, so that the effect is probably not due to obliquity of the rays, but to the eccentric axis. At $i=0°$ and as far as 30° the indices of refraction are alike to four units in the fourth place, which would be satisfactory.

In the belief that the marked variation of μ with i in Series I and II is referable to the eccentric axis of rotation, even in nearly plane parallel plates, the experiments were repeated with a carefully constructed vertical axis adjustable parallel to the faces. The graduated circle, moreover, was much finer, showing the values of i to tenths of a degree.

The new facilities in adjustments for rotation to secure different angles of incidence, taken as usual on both sides of $i=0°$, the mean value being used, have so much improved the values of μ (see fig. 70, *d*), that the suspicion aroused against the eccentric horizontal axis of rotation is verified. In fact, in the latter case different parts of the plate are successively put

into the beam obliquely when i changes. Any variation in thickness of the plate thus enters the data as a systematic discrepancy. In Series III, the values of μ at $i=0°$ and $i=20°$ differ by less than one unit of the fourth place, which is an altogether satisfactory result. Beyond 20° the error increases rapidly, as is to be expected.

It thus appears, in conclusion, that for very long columns of glass the values of the index of refraction should be obtainable with any refined degree of accuracy desirable, as suggested in §98.

107. Results for different spectrum lines.—In §100 the method for computing the approximate dispersion constant b was indicated. There is, however, a difficulty inherent in this method, inasmuch as for the case where μ is to be found for four or more places of decimals the abbreviated Cauchy equation is insufficient. It is necessary, in other words, to use the more extended form $\mu=A+\frac{b}{\lambda^2}+\frac{c}{\lambda^4}$.

Leaving this for the present, it is interesting to compare the results obtainable by the interferometer with the standard data of Mascart, de Lépinay, and others.* For this purpose the quartz of table 73 was mounted at normal incidence and the micrometer readings for the C, D, E, b, F lines of the spectrum taken in succession, both for the presence and absence (air) of the quartz plate. The differences of corresponding values (quartz and air), δN for the same line, were then reduced to the value of ΔN for the D line in table 73, so that the ΔN for each spectrum line was obtained in succession for the computation of μ. In other words, the values of δN are shifted so that for the sodium line $\delta N_D=0$.

The table shows that the value of μ thus computed differs from the value of Mascart μ_M by 14 units in the fourth place in case of the extreme C and F lines. The reason of this is the approximate value of b taken. To find what the value of b should have been in each case put $\mu_M=M$ and $\mu_a(\Delta N/e+1)=S$; then

$$(M-S)\lambda^2=-2b \qquad (12)$$

These data are also given in the table and show a very appreciable variation in the march of b from the C to the F line.

Table 79 contains three series of values made at different times. The agreement of the first two is very good, but the difficulty in recognizing the Fraunhofer lines among the stationary interferences has not been quite overcome.

If the mean value of b is computed from Mascart's data between the C and D and the D and E lines and compared with the computed mean of the table, the results are

	C to D	D to E
Mascart	$b\times10^{10}=0.421$	0.407
Interferometer	$b\times10^{10}=0.433$	0.412

* See Landolt and Boernstein's Tables.

a difference of about 3 and 1 per cent, respectively. But the C line in the interferometer is difficult to observe, as the stationary interferences are very prominent in the red. Between D and E, however, the agreement is as close as the method warrants.

TABLE 79.—Values of b as compared with the data of Mascart. Quartz as in table 73. $\Delta N_D = 0.34059$ cm. $i = r = 0°$. $\mu = \mu_a(\Delta N/e + 1) - 2b/\lambda^2 = S - 2b/\lambda^2$. Assumed $b \times 10^{10} = 0.415$.

		δN	$\delta N - \delta N_D$	ΔN	S	μ	M	Difference	$S - M$	$b \times 10^{10}$
I	C	0.01079	−0.00353	0.33706	1.56259	1.54332	1.54188	−0.00141	0.02071	0.446
	D	.01432	.0	.34059	1.56847	1.54457	1.54423	− .00034	.02424	.421
	E	.01897	+ .00465	.34524	1.57623	1.54635	1.54718	+ .00083	.02905	.403
	b	.01995	.00563	.34622	1.57785	1.54697	1.54770	+ .00073	.03015	.405
	F	.02325	.00893	.34952	1.58337	1.54825	1.54966	+ .00141	.03371	.398
II	C	.01008	− .00362	.33697	1.56243	1.54316	1.54188	− .00128	.02055	.443
	D	.01370	.0	.34059	1.56847	1.54457	1.54423	− .00034	.02424	.421
	E	.01838	+ .00468	.34527	1.57628	1.54640	1.54718	+ .00078	.02910	.404
	b	.01940	.00570	.34629	1.57798	1.54710	1.54770	+ .00060	.03028	.407
	F	.02255	.00885	.34944	1.58323	1.54811	1.54966	+ .00155	.03357	.397
III	C	.00317	− .00353	.33706	1.56259	1.54332	1.54188	− .00144	.02071	.446
	D	.00670	.0	.34059	1.56847	1.54457	1.54423	− .00034	.02424	.421
	E	.02515	+ .00437	.34496	1.57577	1.54589	1.54718	+ .00129	.02859	.397
	b	.02725	− .00535	.34594	1.57739	1.54651	1.54770	+ .00119	.02969	.399
	F	.03550	.00855	.34914	1.58273	1.54761	1.54966	+ .00205	.03307	.391

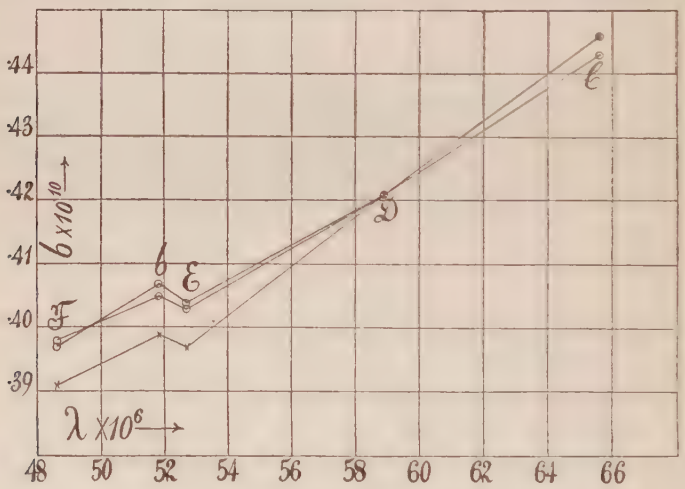

FIG. 71.—Variation of the dispersion coefficient with wave-length.

The results of b so found show the difficulty encountered in using the method of §100. The equivalent of the distance apart of C and D and D and E on the micrometer is too great to warrant the simplified Cauchy equation there used. It also shows, however, that the outstanding error of the above results is referable to the approximate value of b used. For the

D line in table 79 the mean result for b is $10^{-10} \times 0.421$. This value was therefore used in reducing the quartz data above.

108. Conclusion.—The above results, taken as a whole, bear out the surmise that it must be possible to determine the refraction of solid and liquid media by means of displacement interferometry with any degree of accuracy desirable, depending ultimately on the length of the refracting column employed. The center of ellipses is never lost but may be brought back to the fiducial Fraunhofer line if the micrometer screw is sufficiently long and the end faces of the medium are plane parallel. If the latter is not the case, and the angle of wedge is not too large, the discrepancy may be corrected by compensation. For this purpose the distant mirror N and not the one at the micrometer M and controlling the beam passing through the medium is to be rotated to restore the ellipses.

The coefficient $d\mu/d\lambda$ may be obtained by the same method with an adequate degree of accuracy, by using successive Fraunhofer lines. In the case of work of precision, the Cauchy equation as far as the fourth power of wave-length is necessary and three Fraunhofer lines are needed to determine the two essential constants. For this purpose it is immaterial whether the plate is slightly wedge-shaped or not.

If the optical constants of doubly refracting media are to be observed, the plates are to be mounted for rotation around an axis parallel to the slit and passing symmetrically between the faces. Otherwise the wedge effect is liable to produce excessive distortion in the results. If columns are to be used, plane parallel faces are to be cut at a definite angle to the optic axes, as the columns can not be rotated.

The position of minimum thickness of the plate or crystal may be recognized from two rotations at right angles to each other, and the reversal of the motion of the interference rings. It is thus easy to place the axis of rotation at right angles to the beam.

The interferometer used in the above experiments was an improvised apparatus, made of ¼-inch gas-pipe, through which water continually circulated. The angle between the component or interfering beams being but 30° or less, the micrometer was sufficiently close to the observing telescope to admit of easy manipulation. The arms have since been increased to over 1 meter in length, each, and the available free depth below the beam is 15 cm. There seems to be no difficulty of increasing these dimensions in any degree. In spite of the lightness of the apparatus, tremor of ellipses does not seriously hamper the observations. Suppose now a glass column 1 meter long with plane parallel end faces is placed in one of the beams. The micrometer displacement which restores the center of ellipses to the fiducial sodium line will be of the order of 50 cm., measurable, so far as the interferences are concerned, to 5×10^{-5} centimeter. Hence $\mu - 1$ must be measurable with an accuracy of 1 part in a million.

* Described in Am. Journ. of Sci., XXXIII, 1912, pp. 109–219.

CHAPTER XIII.

SUBSIDIARY EXPERIMENTS.

THE PRISM SPECTRUM ON THE ROWLAND SPECTROMETER.

109. Introductory. Apparatus.—Having certain experiments to make with the spectra of prisms of small angle, I attempted to find the indices in terms of wave-length on a modified Rowland adjustment, as described in a preceding paper.* In such a case the wave-length of the grating spectrum would at once be given in terms of the position of the carriage which supports the ocular. The refraction of the prism is found in terms of the same data, provided the Fraunhofer lines are available for adjustment.

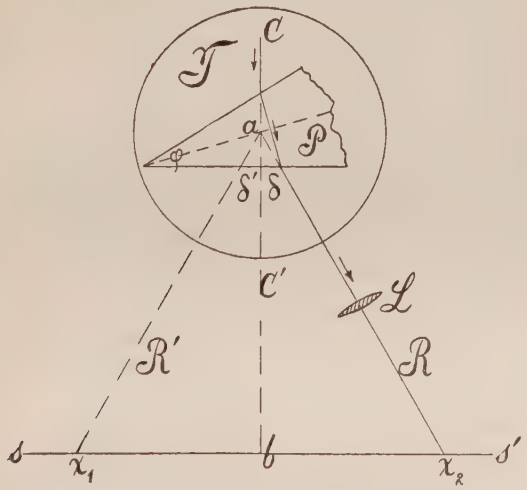

FIG. 72.—Adjustment of prism.

In fig. 72, ss' and CC' are the two fixed rails, symmetrically normal to each other, and R the sliding oblique rail of fixed length, swiveled at the axles a and x. If the grating were placed at a, normal to CC' or to R, the wave-lengths would be computed from

$$\lambda = D(x_2 - x_1)/2R \qquad (1)$$

which is either $D \sin \theta$ or $D \sin i$, respectively. I may therefore insert a slight digression here. In the figure the light is supposed to come from a white source beyond C, and to be collimated in the direction CC'. L is a weak achromatic lens carried by the rail R and placed so that Lx is the principal focal distance. For a transmission film grating of about 15,000

* American Journal of Sci., C. and M. Barus, xxxi, pp. 85–95, 1911.

lines to the inch, such as those made by Mr. Ives, the rail R is easily adjusted to a suitable length, while at the same time equation (1) reduces to

$$10^6\lambda = (x_2 - x_1)/2$$

This is a great convenience in practice. The rail in such a case is slightly less than 167 centimeters long. For a grating of 10,000 lines to the inch, it would be about 250 centimeters long, while about half this length would make $10^6\lambda = x_2 - x_1$.

By providing the ends of the rail aR with a right and left screw respectively or a stiff turnbuckle, the adjustment is secured with considerable precision. Table 80 shows a few measurements with the spectrometer so adjusted, sunlight being used.

TABLE 80.—Data for $x_2 - x_1$ and λ

Line.	I.			II.			III.		
	$x_2 - x_1$	$10^6 \times \lambda$ approx.	$10^6 \times \lambda$ comp.	$x_2 - x_1$	$10^6 \times \lambda$ approx.	$10^6 \times \lambda$ comp.	$x_2 - x_1$	$10^6 \times \lambda$ approx.	$10^6 \times \lambda$ comp.
B	137.35	68.68	68.77	137.00	68.50	68.65	137.35	68.68	68.68
C	131.10	65.55	65.64	131.00	65.50	65.65	131.20	65.60	65.60
D	117.70	58.85	58.93	117.60	58.80	58.93	117.85	58.93	58.93
E	105.20	52.60	52.67	105.15	52.58	52.69	105.40	52.70	52.70
b	103.45	51.73	51.80	103.40	51.70	51.81	103.60	51.80	51.80
F	97.00	48.50	48.57	96.95	48.48	48.58	97.20	48.60	48.60
G	86.10	43.05	43.11	86.00	43.00	43.10	86.05	43.03	43.03

The successive series show a different degree of approach to the true value and in the last the requirements have been met quite adequately. The parts of the apparatus were improved from available laboratory furniture and the scale was read to 0.1 mm. by estimation. For the identification of unknown lines, an approximation of this kind has proved invaluable.

Suppose now the grating is removed and the prism P placed on the horizontal table T, so that the plane bisecting the prism angle contains the axis a, at one end of the rod R. Let the prism be placed so that the angle δ may be the angle of minimum deviation for the given color, or the ray within the prism be normal to the place $a\varphi$. Finally, let R' and δ' be the corresponding position on the other side of the undeviated ray Cb, the prism having been suitably reversed and being again at minimum deviation. Then

$$\sin \delta = (x_2 - x_1)/2R \qquad (2)$$

For comparison, since $\lambda = D(x_2 - x_1)/2R$ would be the corresponding wavelength of the grating spectrum,

$$D = \lambda/\sin \delta \qquad (3)$$

is the grating space of the normal spectrum, coincident at the given Fraunhofer line λ, with the prismatic spectrum. Naturally the two spectra are turned in opposite directions.

To determine φ, the prism is rotated until the plane φa of the prism coincides with the direction $C'C$ and the positions x_1' and x_2' of the rays reflected from the two faces of the prism, respectively, are taken. Then in the same way

$$\sin \varphi = (x_2' - x_1')/2R \qquad (4)$$

From equations (2) and (4), which give δ and φ, respectively, the index of refraction μ is as usual

$$\mu = \frac{\sin (\varphi+\delta)/2}{\sin \varphi/2}. \qquad (5)$$

110. Data.—The following observations were made to illustrate this equation.

TABLE 81.—Refraction of a prism. $\varphi = 30°$; $R = 168.3$ cm. $10^6 D$ (computed) $= 176.55$; $1/D = 5664$ lines /cm^2.

Line.	I				II			
	$10^6 \times \lambda$	$x_2 - x_1$	δ	μ	$10^6 \times \lambda$	$x_2 - x_1$	δ	μ
B	.....	.....	.....	.....	68.7	111.25	19.30°	1.611
C	65.63	111.35	19.32°	1.612	65.63	111.65	19.37	1.614
D	58.93	112.35	19.50	1.618	58.93	112.45	19.52	1.618
E	52.70	113.55	19.72	1.624	52.70	113.75	19.75	1.626
b	51.84	113.80	19.76	1.626	51.84	114.00	19.80	1.627
F	48.61	114.60	19.91	1.630	48.61	114.85	19.95	1.632
G	43.08	116.70	20.28	1.641	43.08	116.90	20.32	1.643
	III				IV			
B	.....	.....	.....	.....	.....	.....	.....	.....
C	65.63	111.35	19.32°	1.612	65.63	111.05	19.26°	1.610
D	58.93	112.50	19.53	1.619	58.93	112.25	19.48	1.617
E	52.70	113.65	19.73	1.625	52.70	113.60	19.72	1.624
b	51.84	114.00	19.80	1.627	51.84	113.90	19.78	1.626
F	48.61	114.80	19.94	1.631	48.61	114.80	19.94	1.631
G	43.08	117.00	20.34	1.643	43.08	116.70	20.28	1.641

The chief difficulty here was the arrangement of ocular until the lines in the small spectrum of the 30° prism could be distinctly seen for measurement. This was finally accomplished by suitable magnification, as is shown by the successive series in fig. 73, in which Series II and IV are raised to keep them apart. The curves show the uncertainty in identifying the fine lines of the spectrum.

No attempt has here been made at accuracy, the scale being a millimeter scale on brass and the fractions of a millimeter estimated. Obviously the precision could now be increased at pleasure by sharper scale-reading. The difficulty in the work as a whole will ultimately be the measurement of R, the length between axles; but here, as this is about 169 centimeters, a reading of a little less than 0.2 millimeter would be needed to vouch for

the fourth place in μ, a result which is easily warranted. If a good grating is at hand whose space D is known, R may be found indirectly from the Fraunhofer lines of the solar spectrum.

Usually $x_2 - x_1$ is inconveniently large for so large a value of R, and this is particularly true when prisms of large angle are to be treated. Hence a smaller value of R is in general preferable, so long as its accurate length is still determinable. All this applies in an even greater degree to the measurement of the prism angle φ, in which case $x_2 - x_1$ is still larger than

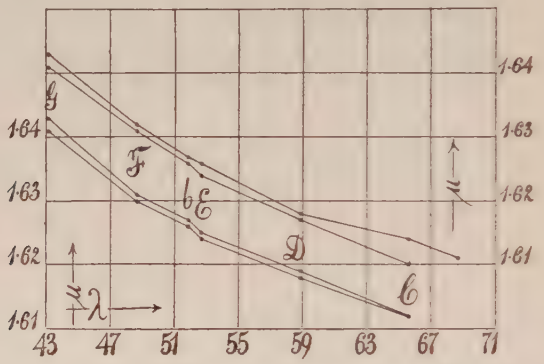

FIG. 73.—Dispersion and wave-length.

for δ. A plausible suggestion that an adjustment like the above might suffice without sunlight for the rectification of the spectrum does not seem feasible.

THE COMPARISON OF TWO SCREWS.

111. Introductory.—In work like the above, where two lengths are to be compared, a displacement ΔN measured with one micrometer, for instance, and a thickness e with another (a caliper screw), it becomes of importance to coördinate these data directly. This may be done with facility by mounting the opaque mirrors M and N on the two screws in question, shifting the ellipses away from the spectrum line with the first screw at N and returning them to the identical line with the other screw at M, through successive consecutive steps of their length. The screws must now be identically reversed in relation to the fixed beam of light and a similar series of complete data investigated. The true relation is the geometric mean of the two results at each step.

112. Method.—In fig. 74, let M and N be the opaque mirrors, actuated by the micrometer screws at angles α and α', respectively, to the beams of light m and n, *i.e.*, the normals of the mirrors. C is the collimator, G the grating, and T the telescope. Let the latter be clamped, so that the direction TG is fixed throughout the experiment, as is also CG. It must be possible to remove the mirrors M and N, together with their micrometer screws, without changing the angles α and α', in order that they may be identically reversed.

Let S be the pitch of the screw at M, for instance, s the corresponding equivalent (approximate pitch) at N. Then

$$S \cos \alpha = s \cos \alpha' \tag{1}$$

Now let the mirrors be reversed, the angles α and α' and the beams m and n being reproduced, in virtue of the fixed direction GT. In this case

$$S \cos \alpha' = s \cos \alpha \tag{2}$$

Hence

$$S^2 = ss' = s^2(1+k). \tag{3}$$

Since k is very small,

$$S = s(1+k/2) = \tfrac{1}{2}(s+s'), \text{ nearly.} \tag{4}$$

In order that the reversal may be properly made, the tablets carrying the micrometers M and N with the attached mirrors should be truly horizontal, so that merely an adjustment of each in azimuth is necessary. The sharp white line which is the direct reflection from the mirror N is

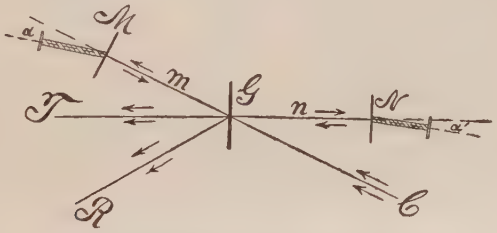

FIG. 74.—Interferometer for comparing screws.

first restored to the cross-hairs of the fixed telescope, after which the reflection from M is restored to the same image, the two lines merging into a single vertical sharp line. The slit images should now also coincide horizontally in the field, *i.e.*, the two images of any specks of dust or cross lines in the slit should cover each other. If this is not the case the tablets carrying M and N must be provided with three adjustment screws, so that condition of mirror normal to the beams of light may be reëstablished without changing α and α'. In other words, the adjustment screws of the mirrors on the micrometer must be left untouched.

When this is done, the ellipses will be seen in the direction of the diffracted rays R as soon as the proper distances m and n have also been reëstablished, by moving either mirror alone. The arrangement of mirrors on the tablet should therefore be as nearly as possible symmetric, even when different forms of screws are compared.

A simple type of micrometer screw, or attachment suitable to any screw to be tested, will also be used below and may be described here. S, fig. 75, is the micrometer screw in question, with its graduated head at H, revolvable in the socket R, this being adjustable with three screws as usual, on

the tablet at either N or M, fig. 74. The mirror M, fig. 75, is separately adjustable with three screws (horizontal and vertical axes), s, s, and a strong spring is suggested at p. The whole arrangement Mps is firmly fixed to the end of the screw S. In this case the mirror rotates with the screw as it advances and the latter is therefore necessarily normal to the component beam m, an adjustment secured by the set screws at s in the usual way, the effect of the operations being observed in the telescope T in fig. 74. The approximate adjustment is conveniently made with sunlight returned by reflection from the mirror to a screen 20 or 30 feet distant. Suppose, fig. 76, the mirror is nearly normal to the screw; let the intersection of the incident ray, the screw axis, the normals, and the reflected rays with the

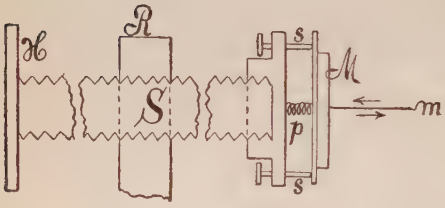

75

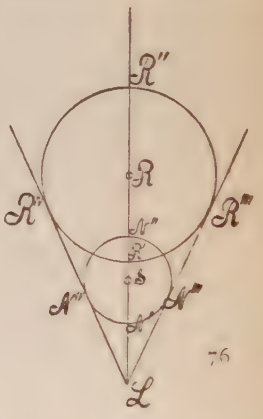

76

FIG. 75.—Simple screw micrometer with slide.
FIG. 76.—Diagram for adjustment.

screen, all lines prolonged if necessary, be at $L\,S\,N'$ and R, respectively. If the screw is rotated 360° the normal will trace a circle N' to N^{iv}, the reflected ray a similar circle R' to R^{iv}. If the normal N' coincides with the axis of the screw S, the reflected ray will be at the center R of the circle $R'\,R''$. Hence the center is to be sought by rotating the screw. The mirror is now adjusted so that the reflected ray is at R. Then N is at S, as required. With successive trials this succeeds very well.

113. Data.—Table 82 contains a comparison of the screws of two slide micrometers, one of them old but with an excellent slide, the other with a good new screw but an imperfect slide. As a result of this it was impossible to keep the ellipses adequately sharp throughout the whole motion of the screw. In fact, it was necessary to make a readjustment of mirrors M and N from time to time, *i.e.*, to take a fresh start, so that the comparison proceeded rather in sections. Moreover, the motion of the slide not strictly parallel to itself appears in the data as an error of the screw, and virtually it is so.

The discrepancy may, however, be corrected without reëstablishing a fresh zero, by removing the effect of any slight rotation at one mirror (due to an imperfect slide or other causes) by the adjustment screws at the tablet

of the other mirror, until the sharp lines of the ellipses are quite restored. This is, in fact, a method of compensation by which the excess of length due to incidental rotation of one mirror (at M) is manually imparted to the other (at N). Care must be taken to keep the angles α and α' unchanged.

TABLE 82.—Comparison of two micrometer screws.

I. Clockwise.			II. Counterclockwise.		
New.	Old	Diff.	New.	Old.	Diff.
cm.	*cm.*	*cm.*	*cm.*	*cm.*	*cm.*
0.00	0.0		1.35	1.34645	
		0.04910			0.04940
.05	.04910		1.30	1.29705	
		.04940			.04970
.10	.09850		1.25	1.24735	
		.05020			.04965
.15	.14870		1.20	1.19770	
		.05020			.05010
.20	.19890		1.15	1.14760	
		.04970			.05000
.25	.24860		1.10	1.09760	
		.04995			.04980
.30	.29855		1.05	1.04780	
		.05050			.05015
.35	.34905		1.00	.99765	
		.04995			.04935
.40	.39900		.95	.94830	
		.04975			.04960
.45	.44875		.90	.89870	
		.04985			.05035
.50	.49860		.85	.84835	
		.05010			.05020
.55	.54870		.80	.79815	
		.04950			.05015
.60	.59820		.75	.74800	
		.04970			.04990
.65	.64790		.70	.69810	
		.04975			.05020
.70	.69765		.65	.64790	
		.05025			
.75	.74790		III. Mirrors reversed		
		.04965			
.80	.79755		0.75	0.74790	
		.04985			0.05180
.85	.84740		.80	.79970	
		.04935			.05130
.90	.89675		.85	.85000	
		.04970			.04970
.95	.94645		.90	.89970	
		.04980			.04975
1.00	.99625		.95	.94945	
		.04985			.04995
1.05	1.04610		1.00	.99940	
		.04905			.04965
1.10	1.09515		1.05	1.04905	
		.04985			.04985
1.15	1.14500		1.10	1.09890	
		.04940			.04995
1.20	1.19440		1.15	1.14885	
		.04965			.05000
1.25	1.24405		1.20	1.19885	
		.04965			.05015
1.30	1.29370		1.25	1.24900	
		.04900			.05010
1.35	1.34270		1.30	1.29910	
		.04965			.05015
1.40	1.39235		1.35	1.34925	

In other respects the comparison, so far as the experiment is concerned, was satisfactory (see fig. 77), very little difficulty in adjusting and reversing being encountered. With two good slides the work would have proceeded smoothly from end to end of the screws, which were several inches long.

The first screw had a pitch of 0.05 cm., the micrometer reading to 0.00010 cm.; the second a pitch of 0.025 cm., the micrometer reading to 0.00005 cm. The former was turned in steps of a single pitch, and the value which brought the center of ellipses, originally coincident with the given Fraunhofer line, back to coincide with it, was read off on the finer screw.

In table 82 the successive sections have to be coördinated, as a fresh fiducial mark was determined in terms of the preceding whenever the ellipses lost adequate clearness. To find the relation of the two screws, the mean of the initial and final halves of each series was computed by deduct-

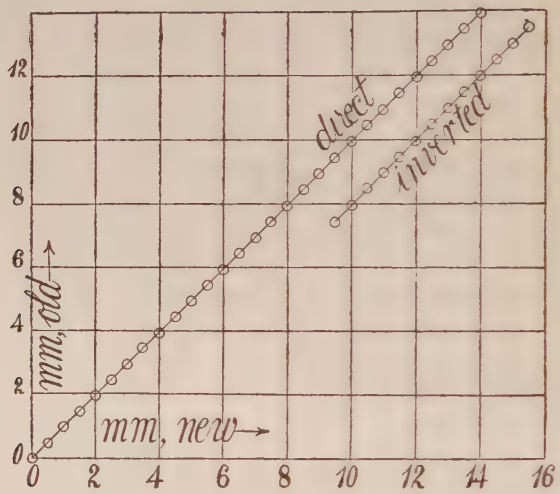

FIG. 77.—Comparison of screws.

ing the corresponding observations from each other and averaging the result. In this way the ratio r of the old appears in

Series I clockwise $r' = 0.9962$
" III mirrors reversed $r'' = 0.9997$

Thus the true relation is finally

$$r = (r' + r'')/2 = 0.998$$

Usually a large part of the difference of values of the two screws is to be ascribed to the angles of alignment α and α', if no special means are taken to orientate them accurately. With the ratio $r = S_1/s$ given, the ratio of the alignment angles would follow, but this is of little value. In fact, if $\alpha' = \alpha + d\alpha$, then

$$d\alpha = (1 - r)\frac{2 - \alpha^2}{2\alpha}$$

where α^2 may be neglected in comparison with 2. Hence $d\alpha$ increases as α decreases, numerically. The real problem of finding α for the measuring micrometer is naturally not touched by such a method, in case of two slide micrometers. It is given at once, however, when one of the microm-

eters is of the form of fig. 75, where α' (say) is necessarily zero. Hence if the screws are identical $\cos \alpha = 1/r$. Virtually, however, $S \cos \alpha = s$ is the effective absolute value of the micrometer screw calibrated in this way in terms of s. This is a particular reason for the development of such an apparatus, fig. 75, to serve the purposes of comparison and standardization.

114. Conclusion.—The advantage of the present method is that steps of any size, quite arbitrarily, are admissible and there is no danger of ever losing count. A rigorously linear slide is presupposed. If the slide is slightly circular, even with very large radius, the ellipses are soon blurred and lost. To restore the ellipses by rotation of mirror is possible, but in any case precarious.

OBSERVATIONS WITH THE SIMPLE SCREW MICROMETER.

115. Apparatus.—The screw micrometer without slide of the type of fig. 75 was made out of an old millimeter micrometer screw, which I used many years ago in determining the expansion of molten magmas. The screw was somewhat worn, though, held in place by an adjustable lock nut (not shown in fig. 75), it was still serviceable. The tripod of the micrometer was first adjusted, so as to bring the nearly normal reflected ray in the direction through the grating, roughly. Thereafter the final adjustment was made at the rotating mirror (special screws) at the end of the screw. Calling this mirror N, the corresponding mirror M (Fraunhofer slide) of the interferometer was placed so that the spot (cross-wire) in the direct image of the slit from M fell at the center of motion of the corresponding spot of the image from N, when the micrometer screw of the latter was rotated. The mirror N was now adjusted for coincidence of the two spots, using its adjustment screws for horizontal and vertical axes. The operation was then repeated. It is difficult to keep the spots from N quite stationary. One has better success on merely endeavoring to let the image from N rotate in a very small circle in the field of the telescope and return to its initial position after a complete rotation. In this way the following data were found, an example of many similar results sufficing the present purposes. The screw at N was turned in steps of about 1 mm. and their value found at the micrometer at M, by shifting the displaced center of ellipses back to the sodium line. In fig. 78 the observations have been raised to the same line at the points between which fresh adjustment was made. This line, curiously enough, is not horizontal, as it should be, but inclined by the amount of about 0.0037 cm. per centimeter of length of either screw. The explanation of this seems to be that the trial screw is not straight but slightly bent, so that at each turn slightly more of the screw is needed to bring the reflected image again into coincidence in consequence of flexure. The amount of this superposed error is 0.0037 cm. per centimeter of length. Otherwise, coincidence of the reflected images would ensue after each complete turn of the trial screw.

The object of the present test was in the main an endeavor to find some means of replacing the slide of a micrometer, as these slides are difficult to grind sufficiently true for interference work. In fact, the results obtained are encouraging enough to suggest that a screw mounted not on one but on *two supports*, *a* and *b*, fig. 79 (the sockets of the latter to be adjustable by being horizontally split), would probably meet the severe requirements of the interference problem, in the complete absence of a slide. The parts of this screw *SabS*, if of metal, must of course be ground together. The endeavor will therefore presently be made to avoid metal sockets. The effect of errors in the obliquity of faces of the grooves of the screws, or

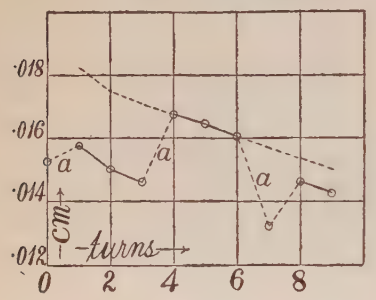

FIG. 78.—Comparison of screws.

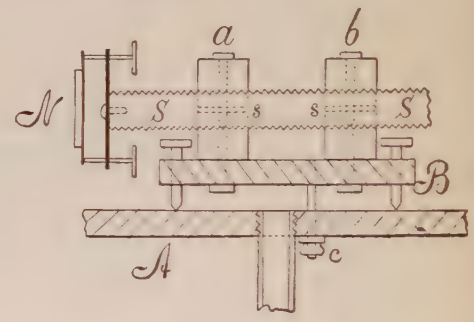

FIG. 79.—Simple screw micrometer with two lugs.

a residual wobble such as appears in fig. 75, would thus be minimized. Naturally the mirror *N* should be a good plate and reflection take place from the central part opposite the axis of the screw.

116. Observation.—A large number of experiments was now made with a screw of the type fig. 79, principally with brass screws, carefully cut but not ground in the laboratory and at first running in brass sockets.

The results with these screws were only moderately successful, so long as an unbroken socket was used. With the tools at hand it was not possible to cut the screw sufficiently loose to move easily for micrometer purposes, and at the same time sufficiently tight to be free from wobble. A single result (fig. 80), among many, may be shown as an example, obtained with the same screw as above, but readjusted on two sockets, the abscissas denoting the individual turns determined by one rotation as seen in the telescope, the ordinates the difference of value read off on the two drums of the screws. Here again the difference of reading of the drums of the screws is not constant, but diminishes by about 0.0038 cm. per linear centimeter, due to some superimposed error, attributable (as above) to flexure of the screw axis. The

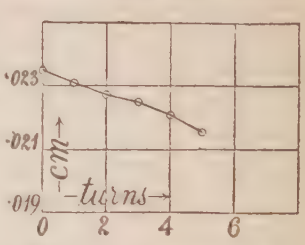

FIG. 80.—Comparison of screws.

reflected images do not register a complete turn for successive coincidences. Though the above datum is somewhat smaller, the difference is probably referable to the total change of mounting needed in the second case.

Success was eventually reached by slotting the sockets (no longer of metal) parallel to the axis of the screw on one side and drawing the two halves of the nut together or pushing them apart by a set screw. This slot at *s* should run nearly across the lugs *ab* in fig. 79 so that the two parts are held together elastically. The first experiments were made with screw No. 5, in which the lugs are of indurated fiber. Screws so cut (each nut one-quarter to one-half inch thick) are usually too tight at first, but they cling admirably. The necessary ease of motion was secured by the set screws at *a* and *b*, fig. 79, which here slightly push the socket apart. The ease with which a brass screw 10 inches long and a pair of sockets of the kind in question may be cut and mounted and their admirable precision of motion when tested by the interferometer are astonishing.

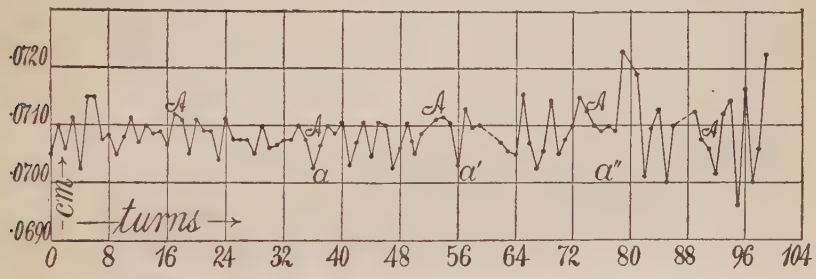

FIG. 81.—Comparison of screws.

Fig. 81 shows a comparison of screw No. 5 with the Fraunhofer micrometer, using about 3 inches of the former. The adjustment of the mirror of the latter (No. 5) was left incomplete, so that the directly reflected ray described a small circle in the telescope. The coincidence of images of the two mirrors *M* and *N* was secured at the beginning of each of the turns, by the initial adjustment, so that the ellipses reappeared with each complete turn, after the Fraunhofer micrometer had also been displaced. Owing to the length (3 inches) of the new screw used, it was necessary to use the Fraunhofer screw four times in succession, by introducing thick glass compensators into the ray coming from the new screw. These were made with thick plates of glass and added at the places indicated by *a*, *a′*, *a″*, in the figure. The total thicknesses of the piles of plates were: at *a*, 2.10 cm., 3 plates; at *a′*, 5.60 cm., 8 plates; at *a″*, 8.60 cm., 12 plates.

Owing to the number of reflections (24 faces in the last case), the image gradually became more colored and less intense, so that the adjustment was gradually less certain. At the same time the shift of ellipses was less sensitive. It was, however, wholly due to dimness of the interferences that adjustment was more difficult, a result which could have been avoided by using a single plate of thick glass (about 9 cm.); but this was not at hand.

Finally a few adjustments of the Fraunhofer mirror were made for incidental reasons not connected with the precision of motion of the screw (as shown at *A* in figure). In other words, through the 3 inches of screw used no effect of flexure or other serious discrepancy could be detected, the ellipses returning in full strength after each complete turn.

The fluctuation of the curve which represents the equivalent of 1/36 inch in centimeters (*i.e.*, 0.0705 cm.) is largely within 0.0005 cm. at the beginning of the work, when seeing was good. This is about one division of the drum of the micrometer screw, or about 1/141 of the pitch of the screw No. 5 and is largely referable to the difficulty of setting the head of the new screw at zero, the disk and graduation having been improvised. It furthermore contains all errors of the Fraunhofer screw, and finally all errors in judgment in bringing the centers of ellipses back to the sodium line. Nevertheless, throughout the whole length examined the new screw retains a satisfactory mean pitch. The whole operation of comparison can easily be completed in one afternoon.

A similar screw with the two lugs but ¼ inch thick and about 3½ inches apart was now tested. The mirror mechanism was made lighter and the adjustment screws finer (56 threads to the inch), the object being to quite eliminate, if possible, the circular motion of the reflected ray. This was not quite accomplished, owing perhaps to an insufficiently plane mirror; but on rotating the screw in successive arcs of 90° the ellipses were available in three of the positions, though they were too blurred in the fourth for use. For final adjustment, besides a more perfect mirror (which need be only ½ inch in diameter), finer adjustment screws than the above would be desirable. The new comparison as a whole is given in fig. 82

FIG. 82.—Comparison of screws.

in the same way as above. The fluctuation is on the average within about 0.0003 cm., or half a scale part of the drum of the Fraunhofer micrometer and 1/236 of the circumference of the drum of the new screw. This uncertainty is almost wholly due to the difficulty of setting the latter with this precision, as the head was improvised in the laboratory for the purposes here in view.

To summarize: There seems to be no doubt, therefore, that a screw, satisfying the requirements of the interferometer and trustworthy to about 0.0001 cm. and a length of even a foot or more, could be constructed by the above method. It is necessary to begin with a straight rod for this purpose (or preferably with a tube) of a larger diameter, say 1 or 2 cm. The adjustable mirror at the end should be light, which was not the case in the above apparatus, ordinary thick plate glass 1½ inch square being

used. The adjustment screw with orthogonal axes must be of very fine pitch if the image is to be stationary. Such a screw of low pitch, carefully cut in brass and running in sockets of indurated fiber, can be made in almost any laboratory.

The final advantage of this type of micrometer is the fact that the normal to the mirror is necessarily a prolongation of the axis of the screw and also coincides very nearly with the incident and reflected ray. There are thus no unknown angles between screw axis and normal to the mirror and exchange of screws at M and N is no longer necessary.

THE RESOLUTION OF INTERFERENCE FRINGES.

117. Experiment.—The following remarks apply to interference fringes produced preferably by the bi-prism, though Young's slits and the other methods of course show the same results. The experiment is straightforward, as is given in fig. 83, but the effect obtained is at first quite unexpected.

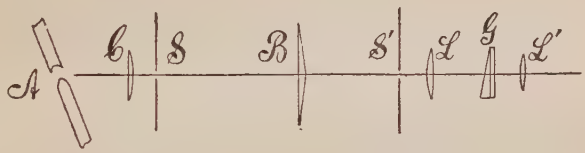

FIG. 83.—Adjustment of bi-prism.

In fig. 83 the arc light A passing the condenser C and the slit S, falls on the bi-prism B and then upon the direct-vision spectroscope $S'G$ (preferably of the grating form like that of Mr. Ives), where S' is the slit, G the grating with attached prism, L and L' the collimator and eyepiece, respectively. Both slits S and S' must be as fine as possible, the spectrum seen being just short of darkness to obtain the sharpest effects, though the results are perfectly distinct, if more washed, for wider slits.

What one would expect to see as the spectroscope $S'G$ is moved across the field from left to right is the usual form of channeled spectrum, with

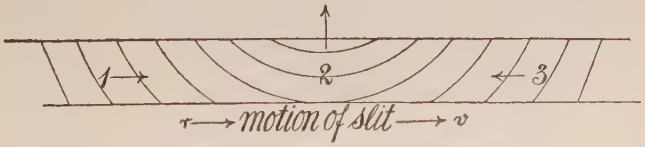

FIG. 84.—Spectrum with circular interferences.

the fringes moving horizontally from end to end of it. What actually appears, however, is a succession of intercepts between an upper and a lower horizontal, of broad concentrically circular or oval absorption bands, all of a very large radius, the displacement being on the plan shown in fig. 84, or the reverse. In other words, the spectroscope reveals the similarly intercepted arcs of large absorption bands. The arcs if essentially

horizontal move up and down, if essentially vertical right and left. They are never quite vertical, and they become thinner and more crowded toward the ends of the spectrum. The groups 1, 2, 3 appear in succession.

The phenomenon is exceptionally sensitive to changes in the approximate verticality of the slit, so that if the spectroscope is slightly rotated on its axis, all the groups may reappear in turn.

118. Explanation.—To interpret this phenomenon it is convenient to plot the order n of a given fringe in terms of its distance x from the center of fringes, where $n = (c/r(\lambda/2))x$, r being the virtual distance of the fringes on the screen, here the slit of the spectroscope, from the virtual position of the two slit images for the wave-length λ. There will be dark bands for a given color λ, as fig. 85 shows, whenever $n = 1, 3, 5$, etc. The two lines drawn show the limits of the spectrum for any distance of fringe x and the heavy horizontal lines the number of dark bands to be expected. Thus

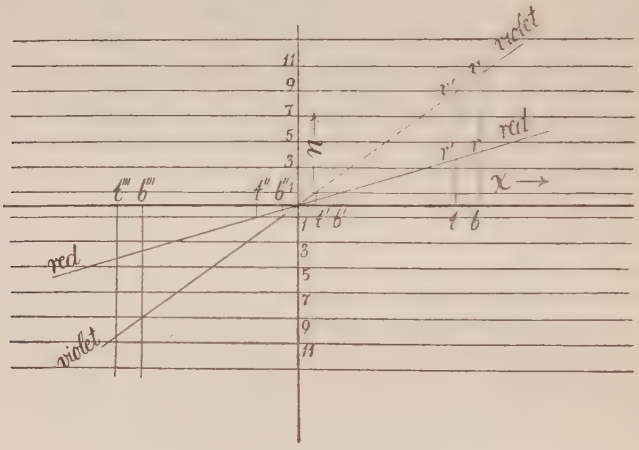

FIG. 85.—Diagram showing color distribution.

for the value of x corresponding to vr, there will be three black bands in the spectrum, their color distribution depending upon their position between v and r. As the slit moves from right to left from the positive to the negative values of x, bands will enter the red end and leave the violet end, for a positive value of x, and do just the reverse for a negative value of x.

The question now arises as to what will happen if the fine slit is not quite parallel to the fine interference fringes, crowded together as they are in a vertical band about half an inch in breadth. The oblique but fine slit in such a case corresponds to a succession of values of x depending upon the obliquity and length of the slit, and the diagram, fig. 85, therefore, shows the case for only one point in the length of the slit. It is thus necessary to introduce the third dimension corresponding to the breadth of spectrum, at right angles to the plane of fig. 85, which plane may be sup-

posed to correspond to the bottom point of the slit. If the horizontal projection of the oblique line of the effective slit is *tb*, the spectrum corresponding to the top point of the slit will be *v'r'*, so that all the bands have been displaced toward the violet. Since the internal points of the slit correspond to the intermediate spectra between *vr* and *v'r'*, the spectrum will thus contain curved black bands with the tops toward the violet and their bottoms toward the red. Precisely the opposite will be the case for a negative value of *x*, *i.e.*, on the other side of the center of interference fringes. If the slit moves, the general motion of bands will remain as already explained, only there must now be successive changes of form.

Thus if the slit takes the position *t'b'* (same distance apart from top to bottom of spectrum) there can be but one black band in the spectrum, running from the red at the bottom to the violet at the top and being therefore nearly horizontal. At *t'' b''* a single band must run from the violet at the bottom to the red at the top, *i.e.*, with reversed slope, so that clearly with the projected slit symmetrical to $x=0$ the bands if appearing (as they do in multiple in a proper position of the bi-prism *B*, fig. 83, close to the spectroscope *S'G*) must be quite horizontal in the middle and curved upwards, or the reverse, at both ends.

Following fig. 85 for a given obliquity and length of slit, all conditions may be easily computed. It is clear, moreover, that the bands can never be closed curves, but are limited to arcs cut off by the band of spectrum from a series of concentric closed curves. In this respect they differ from the elliptic interferences, which they in many respects recall; but the ellipties are essentially closed curves moving as a whole in the same direction.

THE MEASUREMENT OF SMALL INCREMENTS OF ANGLE.

119. Apparatus.—In connection with electrometry (see below, §160 and elsewhere), the measurement of small angles or small variations of an angle is often necessary and the following method was tested with such an end in view. The adjustments are simple in design, but in application they often give some difficulty. Two light mirrors, *m* and *n*, are attached to the rotating body, *bb*, pivoted in such a way that their faces are as nearly as possible parallel, so that the incoming component beam of light *L*, from the interferometer, is reflected at the same angle *i* at each mirror. The beam then strikes the fixed mirror *N* of the interferometer normally and retraces its path, meeting the component beam from the mirror *M* at the grating in the usual way.

To obtain sufficient parallelism in the two mirrors, a beam of sunlight usually suffices and it is merely necessary to make the undeviated beam *L* and the reflected beam *L'* coincide at a distant screen, the mirror *N* being absent. In other words, the light reflected from the mirror *m* is to cover the shadow of the disk. If the revolving body is substantial, *m* and *n* may be adjusted around the vertical and horizontal axes, as usual, by aid of three screws. In case of a light body it was found convenient

to clutch the two stems of the mirrors m and n in slots cut in the ends of bb with a fine scroll saw, and after adjustment to hold them in place with wax, applied by melting.

The angle i, which is to change by a very small quantity only, must be determined by rotating bb on a divided arc, for instance until n is parallel to L, which is sufficient, $90°-i$ being thus given. Usually it is possible and far preferable to rotate the mirror n on bb, until the beam retraces its path toward the grating. In such a case i may be read off directly. From this, a, the normal distance apart of the mirrors, may be found from their fixed oblique distance, mn.

Since $\delta = 2a \cos i$, the variation of the angle i in terms of the variation of the path difference δ for different orientations m and n is found to be

$$-di = d\delta / 2a \sin i.$$

Hence for the given value of the increment di, $d\delta$ will be larger as $2a \sin i$ is numerically larger. Hence a and i should have the largest values available. It is more convenient to make i about 45° and to increase the sensitiveness by increasing a. If i is measured in degrees,

$$-d\delta / di = 0.035a \sin i$$

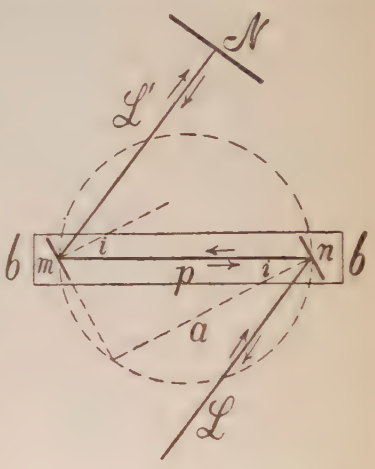

FIG. 86.—Parallel mirror adjustment for micrometry of angles.

120. Experiments.—To put this apparatus to a practical test, a pair of light mirrors m, n was mounted and made parallel by sunlight as stated, on the index arm bb of a divided circle. The latter was clamped on one arm of the interferometer, in front of the stationary mirror M, this being about 1 meter from the grating. Table 83 gives an example of the results obtained, the total range of the angle i being about 10°, after which the reflected images passed beyond the limits of the small mirrors. The index with its mirrors was moved in steps of about 0.5, 1, or 2 degrees, in different cases, steps which were read off directly on the circle, and therefore necessarily unequal as compared with the refined measurement on the interferometer, the circle being only about 3 inches in diameter. The normal distance apart of the mirrors was 4.5 cm. and the angle i on the average about 50°. The initial value of i was found by normal reflection.

Table 83 shows the successive angles of incidence i, the successive displacements ΔN of the micrometer between each, and finally the observed and computed value of displacement per degree of arc.

The irregularities in table 83 are merely due to the setting of the index arm of the divided circle, where an uncertainty of 0.1° was inevitable. It was not thought worth while to repeat the work without a definite pur-

pose. It appears from the table that if 10^{-4} centimeter is guaranteed on the interferometer, the twelve-hundredth part of a degree, *i.e.*, about 3 seconds of arc, is guaranteed; or if the installation is sufficient for the use of the interference rings, 1 second of arc per ring would be the sensitiveness of the above apparatus, where $a = 4.5$ cm. and i has the value of

TABLE 83.—Comparison of the displacement at the micrometer and the increment of angle.

i	$\Delta N \times 10^3$	Observed $d\delta/di$	Computed $d\delta/di$
54°	0.2408	0.1204	0.1258
52	.2438	.1219	.1224
50	.2212	.1106	.1189
48	.1151	.1151	.1161
47			
53	.2529	.1264	.1274
55			

about 50°. As a may without inconvenience easily be increased ten times, there would thus be no difficulty in measuring well within 0.1 second of arc, the displacement being 0.1 second of arc per ring.

ELLIPTIC INTERFERENCES WITH CONCAVE MIRRORS.

121. Apparatus.—In the course of the work, the production of elliptic interferences with the opaque mirrors identically concave presented itself and it was thought worth while to test the adjustment. Figure 87 is a

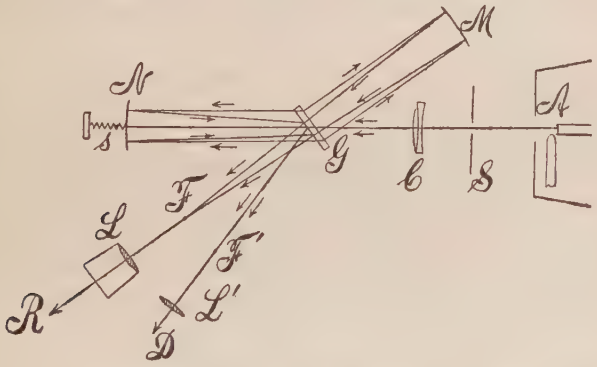

FIG. 87.—Adjustment for elliptic interferences with concave mirrors.

diagram of the parts of the interferometer, S being the slit illuminated by the arc lamp (screened), A and C the collimating lens, G the grating with its ruled face toward the impinging light. The beam reflected from G strikes the concave mirror M and is then reflected to the focus at F. The transmitted beam reaches the concave mirror N on the micrometer

screw, and is in its turn doubly reflected to the same focus F. If now the undeviated beams R are in superposition, horizontally and vertically (fine wire across slit to facilitate the former), and the mirrors M and N are adjusted for equivalent distances, the diffracted beam D coming to the focus F' will be made up of two superimposed spectra which show the interferences in question. Lenses L and L' are available for magnifying the phenomena respectively; or an observing telescope with reinforced objectives for short distance vision may be used with advantage.

The mirrors used had an area of only about $\frac{1}{8}$ inch square, each, and were cut from the common concave mirrors used in connection with Kelvin's galvanometer, each mirror being a quadrant. Nevertheless the spectra and ellipses obtained were adequately sharp and luminous for practical use in the portion of the interference pattern near the center of ellipses. The remote parts of the pattern, *i.e.*, the fine interference lines, did not come out well, for reasons doubtless connected with the quality of the mirrors. It is probable that the parts of a silvered concave spectacle lens would have been preferable throughout. However, it is astonishing that mirrors so small and necessarily not of high grade should give the phenomenon as satisfactorily as was the case.

Though the adjustment is easily made, two difficulties were encountered which are not incident to the case of plane mirrors and parallel rays. If the axis of the micrometer screw at N is not parallel to the axis of the beam, the mirror M will shift laterally and with it the focus at F, destroying the coincidence of spectra and the interferences. Again, if the mirrors are as usual silvered on the back, there are many slit images from both surfaces and they are not very unequally bright when the mirrors are small. One soon succeeds, however, in recognizing the bluish image from M and the yellowish image from N in correspondence with the position of the face of the grating, which are more serviceable for effective coincidence than the others. In view of the near foci $F\,F'$, the images in the telescope are highly magnified and the ellipses are apt to be stretched in their vertical dimension.

If the grating G is replaced by a half-silvered plate of glass and the mirrors M and N replaced by as identically concave gratings as possible, set at the same fixed angle of incidence, a variation of the present method well worth the trouble of special test suggests itself. F would then be the focus of spectra and the interferences observed at L. These interferences would naturally be on a large scale and this fact suggests many applications.

ACOUSTIC DISPLACEMENTS.

122. Mayer and Dvorak's experiment.—A variety of acoustic experiments was made for the detection of small forces, in cases where the interferometer seemed to be particularly adapted. The forces acting on a sounding resonator, discovered by A. M. Mayer in this country and by Dvorak abroad, seemed to fall within the scope of the method. Accord-

ingly a paper cylinder (resonator), open at one end and closed at the other, was suspended horizontally from the bifilar pendulum shown in fig. 98, so that any longitudinal displacement due to acoustic pressure could be detected and the corresponding forces estimated. The cylinder used in the final experiments was 6 cm. in diameter; hence with an area of 28.3 sq. cm. It was about 14 cm. long, so as to be in resonance with a König tuning fork of 522 vibrations. The mass of the cylinder and appurtenances was 3.132 grams and the pendulum suspension 18.5 cm. long. The mirror was adjustably attached at the closed end.

When placed on the interferometer the ellipses were easily obtained, though the tremors of the laboratory kept them in continual slight motion, so that measurement by the interference rings was out of the question. The resonator was excited by placing the mouth of the box of the tuning fork near the mouth of the suspended resonator. During this interval the ellipses vanished at once, as a whole, showing that the vibrations of the *body* of the resonator were so intense as to destroy the visibility of the interference pattern. They reappeared, however, again at once, as soon as the tuning fork ceased to sound, without showing the occurrence of any discernible vibration. Hence there could not have been any appreciable deflection of the resonator or the forces, if any, are below the limit of measurement.

The experiment was now modified by making the head of the resonator thicker and more rigid. For this purpose a disk of cardboard was fixed within the resonator by cement. The cylinder was also provided with a mica vane damper submerged in oil, and the whole apparatus surrounded by a case of tin plate to guard against air-currents. To avoid interferences due to the nearness of the operator, the resonator was excited with the tuning fork *at a distance*, the sound being conveyed through a hole in the case, after having passed through a 2-inch metal pipe about 10 feet long.

The results, however, were not different from the above. When the tuning fork sounded, the ellipses vanished, owing to the tremor of the whole system of mirror and resonator. When the fork was suddenly stopped, the ellipses reappeared at once, and in place, showing no gradually decreasing oscillation to the point of equilibrium, such as would have occurred had there been any appreciable deflection.

It appears, therefore, that the deflection of the resonator, if any, could not have been larger than $\Delta N = 10^{-4}$ centimeter, and since in the first experiment $M = 3.132$ grams, the deflecting force could not have exceeded $F = Mg\Delta N/l = 0.017$ dyne, equivalent to a pressure $p = 0.0006$ dyne per square centimeter. In the second experiment, since $M = 8.316$ grams,

$$F = 0.045 \text{ dyne}, \quad p = 0.0016 \text{ dyne/cm}^2$$

would have been recognized. Acoustic pressure difference would therefore have to be less than this value.

In the later experiments of Dvorak and in the work of Rayleigh, Lebedew, M. Wien, and others the neck of the resonator is the seat of the forces

actually observed. The above resonator was therefore closed with a disk of cardboard having a hole about 2 cm. in diameter at its center. The experiments made were like the preceding and showed the same negative results. The work was therefore abandoned as not sufficiently promising for further research by this method. The method of Davis of detecting acoustic pressure within the organ pipe seemed equally difficult of adaptation.

123. Telephonic displacements.—The endeavor was then made to determine the displacement of the telephone plate, by attaching a mirror at its center and fixing it on the interferometer confronting the micrometer mirror. It was supposed that ellipses might be visible even when the plate vibrated, at the elongations of the displacements, but this was not the case, even after several attempts in relocating the mirror. The vibrations

TABLE 84.—Deflection of telephone blade. 2 strong cells. $L=20$; $b=1.1$; $d=0.062$; $E=2.1\times10^{12}$; $F=7.2\times10^{3}\Delta N$.

R ohms.	i amperes.	$\Delta N\times10^{3}$ cm.	r ohms.	F dynes.
500	0.0066	0.6	100	4.3
60	.024	2.25		16.2
200	.103	1.35	87	9.7
40	.027	3.05		22.0
100	.019	2.05	117	14.8
20	.032	3.25		23.4
80	.021	2.30	124	16.6
10	.034	3.50		25.2

were always accompanied by rotation of mirror, as a result of which the interferences were lost. With direct current of reasonable intensity the ellipses were not appreciably displaced. The tremors of the laboratory were too great to admit of the use of interference rings and strong currents were apt to rotate the mirror.

The plate was then replaced by a steel hack-saw blade, 20 cm. long, 1.1 cm. wide, and 0.062 cm. thick, held by two horizontal arms clutching the ends of the blade, immediately in front of the magnet of the telephone (see fig. 88). The mirror was cemented to the center of the blade near the magnet so that the mirror moved parallel to itself. But even here the ellipses vanished when alternating currents were used to put the mirror in vibration, showing that rotation accompanies the vibrating plate; otherwise the ellipses should have been glimpsed at the elongations. It is probable that the whole supporting adjustment securing the telephone, as well as part of the interferometer, is put into vibration. Direct currents, however, now gave deflections ΔN of a reasonable order of value, as may be seen from table 84, chosen from many similar results. R ohms is the resistance in circuit, and r that of the telephone coils, ΔN centimeters is the displacement of mirror for the current i in amperes. If ΔN varies as i, $(R+r)\Delta N$ is constant. This appears to be nearly the case, the dis-

crepancies being rather due to incidental disturbances in the adjustment and to difficulties in reading the ellipses. It is interesting to compute the forces F involved, supposing the saw blade vertically loose at its end (which was nearly the case),

$$F = 4Eb(d^3/L^3)\Delta N$$

The values of F are given in the table, so that the table may be summarized by putting the displacement about $\Delta N = 0.11$ cm. and $F = 740$ dynes per ampere of current, when ΔN is less than 0.002 cm., after which a rapid decrease of sensitiveness begins. A number of experiments of the same kind gave practically identical results. It is curious that for such small displacements i and ΔN are not proportional throughout.

In place of the saw blade a narrow strip of thin tin plate was next used, the strip being 20 cm. long, 8 cm. broad, and 0.029 cm. thick. The experiment showed $\Delta N = 0.001$ cm. for $i = 0.04$ ampere, which is equivalent to a sensitiveness of 0.072 cm. per ampere, not a marked advance on the preceding case when the distance from the magnet is taken into account. This means that less iron is available for attraction in the thin spring, or that, if it were the purpose to increase the sensitiveness, an iron armature should be mounted on the spring just in front of the magnet.

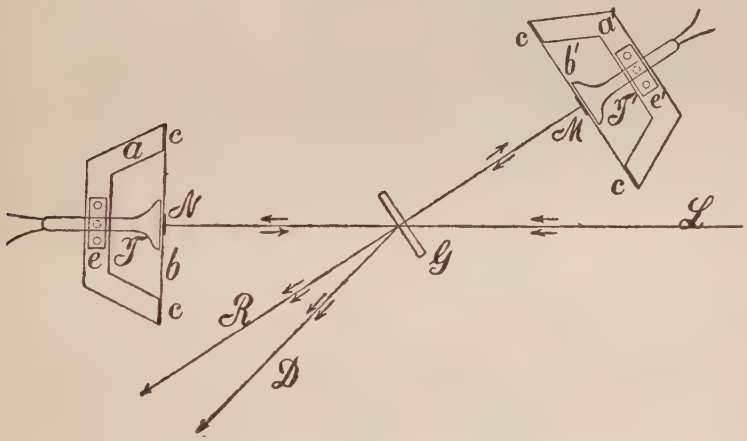

FIG. 88.—Telephonic induction balance on interferometer.

124. Reciprocating and synchronized telephones. Apparatus.—The next step in development was the insertion of the second telephone T, carrying the micrometer N (fig. 88) and furnishing with the mirror M, also on a telephone plate, the two component beams of the interferometer. The two identical saw blades of the preceding case were used in preference. In the diagram L is the entering beam of white light, G the grating, R the undeviated, and D the diffracted rays. The telephone T is held in a wooden yoke a, eventually brass-faced at cc. To these plates the saw blades bb * are screwed down. The telephones are adjustably secured at e. The

* Barus, American Journal (3), III, 1897, pp. 107–116.

yokes a, a' are fixed in short vertical ends of gas pipe clamped to the arms of the interferometer, admitting of sufficient vertical and horizontal rotation for rough adjustment. The fine adjustment for horizontal and vertical coincidence of the slits is made at a by three leveling screws (horizontal and vertical axes), and the yoke is additionally mounted on the plate of the micrometer screw. It is this contrivance which is to be specially designed and which at present constitutes the difficulty of the method; for the telephone T must be rigidly placed and yet be delicately adjustable and movable on a micrometer.

The electrical interferometer or induction balance* so obtained should be capable of exhibiting the phenomena illustrated by fig. 89, where the telephone T is within the resistances R and R', whereas T' is in immediate connection with the battery by the key K. Hence, if $R=R'=0$, both telephones are simultaneously affected and the plates vibrate symmetrically towards and from each other as at a. The ellipses should therefore remain in the field. When $R=R'$ is increased sufficiently the time must arrive when both plates move in the same direction in parallel as at b, the lag being half a period. The ellipses should therefore vanish. For a further increase of $R=R'$ the lag will become equal to a whole period and case a is reproduced, etc.; or two different circuits coupled together may act separately on T and T' and the time element of the coupling be determined, since the ellipses vanish for lags of an even number of half periods and appear for lags of an odd number of half periods.

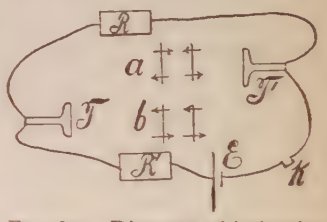

FIG. 89.—Diagram of induction balance.

125. Reciprocating and synchronized telephones. Measurements.—In the first experiments with the apparatus, the blades were screwed down on wood surfaces, not brass-faced, and purposely fixed just short of loosely. Table 85 contains an example of the results which are of the same nature as the preceding.

TABLE 85.—Two telephones. Deflection $\Delta N+\Delta N'$ summational. 2 storage cells. Blades as in table 84.

R	i	$\Delta N\times 10^3$	r
400	0.0067	0.80	122
100	.0133	2.00	
300	.0080	1.15	231
60	.0155	2.10	
200	.0100	1.80	171
0	.0200	2.75	

Some of the observations are not good, as is shown in the values of r, which should be constant. Probably the blade was too loose. The sen-

* Barus, American Journal (3), III, 1897, pp. 219–222. Note on the excursion of the diaphragm of a telephone.

sitiveness is nearly constant and equivalent to about $\Delta N = 0.14$ cm. per ampere, not twice the preceding value, because the blades were probably further from the magnet.

On connecting the two telephones differentially so that the deflections proceeded in opposite directions, practically no displacements of ellipses was obtained. Thus at $R = 100$ ohms, $\Delta N = 0.0001$ cm.; at $R = 50$, $\Delta N = 0.00015$ cm., etc.—a difference which could have been removed by more carefully spacing the saw blades in front of the magnets of the telephones.

The expectation that, on applying alternating currents, the ellipses would remain in place in case of differential adjustment, was, however, frustrated. They practically vanished, either because the support as a whole was put in vibration whenever the telephone sounded, or because the upper harmonics play along the length of the saw blade. In either case the practical solution is not yet at hand, even for the case of identical counter-motion of the two mirrors

In the following experiments the yoke holding the saw blade was faced with brass and the blades rigidly screwed in place. An example of the results is given in table 86. Sensitiveness was increased by approaching the blades closer to the magnet of the telephone. This table still shows the same uncertainty as to $r = \frac{R\Delta N - R'\Delta N'}{\Delta N' - \Delta N}$, which can only be ascribed to the small value of the denominator of the equation, as the current i is roughly proportional to ΔN. Thus half a drum division, which may easily be due to slight changes of adjustment, would have corrected the first value of r. The sensitiveness is greater than before, being $\Delta N = 0.185$ cm. per ampere, owing to smaller distances between magnets and armatures.

TABLE 86.—Yokes brass-faced. Rigid blades. $E = 2$ volts. Mirrors traveling in same direction.

R	i	$\Delta N \times 10^3$	r
300	0.0040	0.55	112
50	.0080	1.40	
220	.0050	.85	171
20	.0091	1.65	
100	.0067	1.20	200
0	.0100	1.80	

On commutation, *i.e.*, when the mirrors moved in opposite directions, the displacement ΔN showed small values similar to the preceding case. Alternating currents, however, did not now quite wipe out the ellipses. In the differential adjustment they were fairly clear, showing the advantages of the new form of apparatus.

In the final experiments the steel springs were iron-faced (armatures in the rear and just in front of the telephone magnet and immediately behind the small mirrors). This armature of soft iron, 3 cm. long, 1 cm. wide,

0.3 cm. thick, increased the strength of the forces involved and probably had a tendency to wipe out the possibility of nodes in the middle of the spring, *i.e.* at the mirrors, and thus of eliminating rotation at this place. The results given in table 87 seem to bear out this surmise. The irregularity of the values of r has not been overcome, although the observations were more definite than heretofore. It fails of explanation even if the currents are supposed to be not proportional to the displacements. It is rather due to some actual but irregular difference in the position of the mirrors before and after the displacement produced by the current. When the mirrors travel in opposite directions, ΔN is not quite zero, which simply means that one blade is a little nearer the magnet than the other.

TABLE 87.—Iron-faced springs. $E=2$ volts.

I. Mirrors traveling in same direction. Telephones in series.				II. Mirrors traveling in opposite directions. Telephones in series.		
R	$i\times10^3$	$\Delta N\times10^3$	r	$i\times10^3$	$\Delta N\times10^3$	r
400	3.3	0.60	177	3.3	0.00	...
100	6.7	1.25		6.7	.25	...
300	4.0	.88	252	4.0	.05	...
50	8.0	1.60		8.0	.40	...
200	5.0	1.07	191	5.0	.20	...
0	10.0	2.20		10.0	.50	...
III. N cut out; M alone vibrating.				IV. M cut out; N alone vibrating.		
R	$i\times10^3$	$\Delta N\times10^3$	r	$i\times10^3$	$\Delta N\times10^3$	r
400	4.0	0.45	59	4.0	0.15	...
100	10.0	1.30		10.0	.73	
300	5.0	.75	129	5.0	.25	33
50	13.3	1.80		13.3	1.00	
200	6.7	.90	81	6.7	.57	102
0	20.0	3.10		20.0	1.70	

In Series I the sensitiveness is about $\Delta N=0.2$ cm. per ampere and the data are fairly regular. In Series II, however, the case of opposed vibrations, the displacements begin after the current has reached a relatively large value, and the ensuing sensitiveness would be about $\Delta N=0.07$ cm. per ampere. Correspondingly the telephone M showed a reasonably regular march with the sensitiveness of 0.14 cm. per ampere, while for the fixed telephone N the displacement does not begin with the current, the mean sensitiveness being thereafter about 0.1 cm. per ampere. No doubt the way in which the blades are incidentally clamped, whether with or without a small initial strain, has much to do with this. The sensitiveness for the two telephones in series is naturally reduced by the double resistance. It appears from this that for small currents (less than 0.003 ampere) the

telephone if differentially connected should show no displacement. This was in fact the case on introducing the alternating current from a small induction coil. The ellipses were nearly as clear for two telephones in series as in the absence of current, if the mirrors vibrated in opposite directions; while the ellipses vanished almost completely when the mirrors vibrated in the same direction. Unfortunately the case of telephones in parallel was not tried, though it would probably have made no difference.

It was now attempted to equalize the displacements of the two telephones with the results for mirrors traveling in opposite directions and the telephones in series (2 volts applied)

$$R=0 \qquad i=0.01 \qquad \Delta N=0.0025 \text{ cm.}$$

The sensitiveness is increased to 0.25 cm. per ampere, because the weaker action of one of the telephones was strengthened. On using alternating currents, however, there was not much advantage observed for the new adjustment, probably because only weak currents could be used in both this and the preceding case.

To conclude: It has been possible to devise an induction balance consisting of two modified telephone plates vibrating synchronously on the interferometer in such a way that if the vibrations are in opposite directions the ellipses remain in the field, while they gradually vanish for vibrations more and more in the same sense. Some experiments to apply this apparatus in various practical directions were begun, but the work was discontinued for the present, as it is not in line with the main purpose of the present paper.

CHANGE OF REFRACTION RESULTING FROM DIELECTRIC POLARIZATION.

126. Introductory.—The experiments made on the value of Kerr's constant subsequently to the fundamental researches of the discoverer of the phenomenon are very numerous. It will suffice here to refer to the summary by Prof. L. Graetz in Winkelmann's Handbuch, vol. 4, p. 168 *et seq.* If d is the optical retardation due to an electric field f in a column of length e

$$d=Bef^2 \tag{1}$$

where B is Kerr's constant. If μ_0 and μ_e be the indices of refraction for the two rays due to the presence of the electrical field

$$d=e(\mu_0-\mu_e) \tag{2}$$

or

$$\mu_0-\mu_e=Bf^2 \tag{3}$$

If $\mu_0-\mu_e$ can be measured as above, the value of B would depend only on the measurement of f in volts/cm.

The present paper, however, gives merely a superior limit to the amount of double refraction produced by electrostriction in glass. The accuracy with which the index of refraction may be measured in case of long columns of solids, or of liquids, with plane parallel ends, made it seem probable that the increase of index at right angles to the lines of electric force in a

glass condenser might be detected. If so, it could at once be measured absolutely. But the amount in the solid is so small that in the first experiments no displacement of the ellipses or motion of the rings was visible when a strong electric field was alternately applied and removed.

127. Apparatus.—Liquids were inclosed in glass tubes about an inch or more in diameter with a tubulure normal to the axis in the middle. The ends were ground flat and plate glass fitted to the ends. One of these plates was cemented on either with glue or resinous cement, as the occasion required; the other, when rubber was permissible, was put in place by pressing it against a thick rubber cushion, intervening, with three adjustment screws. In this way it was possible to put the two faces adequately in parallel by observations on the interferometer, *i.e.*, the direct images of the slit should coincide horizontally or vertically, no matter whether the column is present or absent in one of the interfering beams. In the later experiments, selected troughs of plate glass, to be described below, were used.

In case of glass, plates about 0.7641 cm. in thickness, 6 cm. long and 2.5 cm. wide, were placed with their solid faces in contact, as shown in fig. 90. A column about 11.4 cm. long was thus built up, with 15 plates

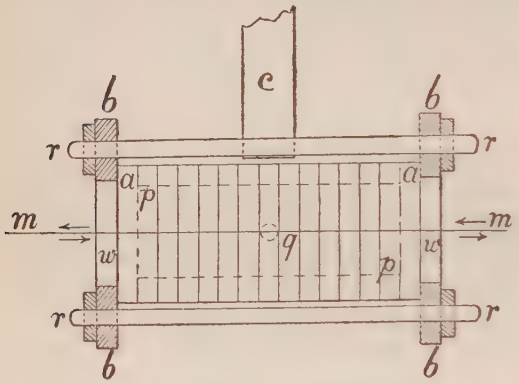

FIG. 90.—Pile of plates for Kerr effect, side view.

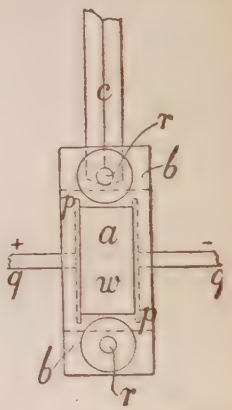

FIG. 91.—Pile of plates for Kerr effect, front view.

in contact and compressed by a rectangular screw clamp. *bbbb* (fig. 90), of hard rubber. The clutch of the longitudinal rods *rr* could be shortened by hard-rubber nuts at their ends. The rubber end-plates *bb* were provided with a window each, so that the interferometer beam could be passed through the column, before and after reflection at the opaque mirror on the micrometer. The whole arrangement was firmly held by a hard-rubber clutch *c*, suspended from a wall bracket. Suitable clamps admitted of raising and lowering and of two rotations. To supply the electrical field, the side faces of the glass plates were partially covered by copper plates *pp*, *pp*, confronting each other, and provided with terminals *q*, *q*. These plates were held in place with rubber cement (piccin), so that *ppapp* together form a

plate condenser, the glass dielectric being 2.5 cm. thick. The terminals q and q (see fig. 91) communicated with the prime conductors of a Holtz machine, and the insulation was sufficient to admit of sparks as long as 1.5 cm., even in the summer. The conductors of the Holtz machine were then pulled apart, so that a potential difference of 40,000 volts was assured. The maximum electrostatic field applied was thus about 16,000 volts/cm.

On placing the pile of plates between crossed Nicols with their principal sections at 45° to the lines of electrical force, no effect due to the presence or absence of the field could be discerned. There was usually a little permanent brightness due to stress in the insufficiently annealed glass.

When the plates were placed on the interferometer a sharp series of multiannular small ellipses was easily obtained. This part of the experiment was in every way satisfactory. The screw of the micrometer, however, was but 3.5 cm. long between the end positions of the slide (maximum displacement). The glass column would require a displacement of nearly twice this for the measurement of the index of refraction (shift of micrometer corresponding to presence and absence of the plate). But this index could be obtained with sufficient accuracy for the present purposes from a single plate, so that a thick compensator was introduced into the other component beam, n, of the interferometer, the compensator consisting of a pile of plates about 7 cm. thick. This reduced the effective thickness of the column to about 4.4 cm., requiring a play of screw of a little over 2 cm. to bring the center of ellipses to the fiducial sodium line, in case of the simultaneous presence and absence of the condenser and the compensator. On the other hand, the sensitiveness of displacement is not diminished, but corresponds to a column of glass 11.4 cm. long.

128. Equations.—Let the index of the uncharged transparent insulating column in the direction normal to the lines of electric force be μ_0; let the second index, due to electric stress of the charged plate, be μ_e. Let b be the constant of the simplified Cauchy equation for the wave-length λ. In the absence of the column let the center of ellipses coincide with the sodium line of the spectrum (air position); and let ΔN_0 and ΔN_e be the micrometer displacements which bring the center of ellipses back to the fiducial line when the transparent column is inserted, charged and uncharged, respectively. Then

$$\mu_0 - 1 + 2b/\lambda^2 = \Delta N_0/e \tag{4}$$

$$\mu_e - 1 + 2b/\lambda^2 = \Delta N_e/e \tag{5}$$

where e is the length of the column. Hence

$$\mu_0 - \mu_e = (\Delta N_0 - \Delta N_e)/e \tag{6}$$

and

$$(\mu_0 - \mu_e)/\mu = (\Delta N_0 - \Delta N_e)/e\mu \tag{7}$$

if μ is the mean index of the column (practically equal to either index).

As the evanescence of a ring corresponds to a shift $\Delta N = \lambda/2$, or roughly 30×10^{-6} cm., and as a change of one-fifth of this may certainly be detected, the limit of discernible $\Delta N_0 - \Delta N_e$ may be reckoned as 6×10^{-6} cm.

129. Data. Solid.—As has been stated, it is not necessary for the present purpose to determine the air position for long columns. For a plate $e=0.7641$ cm. in thickness showed a displacement of 0.4225 cm.; and hence by equation (1) the displacement for 15 similar plates, or a thickness of 11.46 cm., would be $\Delta N=6.34$ cm. Since no radial motion of ellipses was discernible, due to presence and absence of electric field,

$$\Delta N_0-\Delta N_e<6\times10^{-6}/6.34=9.5\times10^{-7}$$

Hence

$$\mu_0-\mu_e<9.5\times10^{-7}/11.46$$

or less than 8.3×10^{-8}. The index of refraction μ computed by equation (1) was roughly $\mu=1.53$; whence

$$(\mu_0-\mu_e)/\mu=5.4\times10^{-8}$$

Thus the change of index of refraction normal to the lines of force, in case of a field over 1 kilovolt per centimeter, is probably less than 10^{-8} of its value and quite beyond the scope of even the present sensitive adjustment of the interferometer.

These experiments were made in the summer, and considerable annoyance was encountered owing to the dampness of the laboratory. It is purposed, however, to repeat them in the dry laboratory in the winter months, and a report will then be made.

130. Data. Liquid.—In case of carbon disulphide, the absolute value of B is known from Lemoine's measurements and equal to $B=3.70\times10^{-7}$, if the field is given in electrostatic units. In case of a volt per centimeter B would then be roughly 4.1×10^{-12}. Hence for the above field of $f=16\times10^{-3}$

$$\mu_0-\mu_e=4\times10^{-12}\times256\times10^{9}=10^{-3}, \text{ nearly,}$$

which should be easily observable. In other words, since

$$\Delta N_0-\Delta N_e=e\Delta\mu=10.46\times10^{-3}=10^{-2}, \text{ nearly,}$$

displacement would be

$$10^{-2}/5\times10^{-5}$$

or 200 times the least perceptible value.

Unfortunately the expectations were doomed to disappointment, in view of the large variation of carbon disulphide with temperature. It was found impossible to obtain an adequately sharp image of the slit for the case of a beam of light passing twice through the column of carbon disulphide, in consequence of the convection currents set in motion by the heat of the beam. The slit image was invariably washed and unsteady, and to obtain the interferences under these conditions was out of the question. As these troughs were 10 cm. long and high, but only 1 cm. broad, it is possible that horizontal partitions of mica may in a measure remove these difficulties, but the complications introduced in this way are so great that further trials were for the present abandoned.

CHAPTER XIV.

THE INTERFEROMETRY OF AIR CARRYING ELECTRICAL CURRENT.

131. Introduction.—The following experiments, though leading (as was to be anticipated) to negative results, are nevertheless sufficiently interesting in their details to deserve to be reported. The object in view was direct test as to whether a rarefied column of air, through which a current of electricity is flowing, shows any perceptible change of its index of refraction. Such an effect might result from the occurrence of ionization, or from rise of temperature, or, finally (in the extreme case), from a possible influence of rapidly moving corpuscles on the velocity of light traveling in the same direction as the corpuscles. The means of exhaustion at present at my disposal were not sufficient to carry the vacuum much below 1 mm. of mercury; neither were exceptionally large potential differences employed, so that the experiment has not been pushed to a limit at which it might possibly show results. I shall hope to return to the work at some other time. The present paper attempts therefore to do no more than to describe the adaptability of the displacement interferometer for present purposes.

132. First experiments. Apparatus.—At the outset the interferometer was used without other modification than a marked elongation of the arms GM and GN, where G is the grating, M (the micrometer) and N the opaque mirrors. The component beams of light m and n were now 1 meter in length, each, so that a glass tube t, hermetically sealed at its ends with plate-glass windows, provided with a tubulure for exhaustion at E (the tube being nearly 1 meter in length), could be inserted in either beam. The arc light or sunlight enters at the slit S of the collimator C. The direct beam for adjusting the interferences is observed with the telescope at R, and the interfering diffraction spectra by the same telescope on being rotated into the position D. The sodium line from the two coincident spectra is an admirable fiducial mark to which the centers of ellipses, as they move across the field, are always referred. A fine horizontal wire across the slit enables the observer to place the spectra in coincidence both horizontally and vertically.

As in the earlier instrument, the arms m and n were made of gas-pipe, through which a current of water continually circulates, when necessary. Tremors, of course, could not be wholly eliminated; but the instrument, in spite of its lightness, was made firm by the aid of horizontal and vertical leveling screws, which imparted slight strains to the gas-pipe arms m and

n; *i.e.*, the ends at *M* and *N* were pushed away from the wall by horizontal screws, until sufficient strain of parts resulted, while at the same time they were lifted above the table carrying the tripod (below *G*), by similar screws acting vertically. The latter, moreover, were advantageous in bringing (raising or lowering) the center of ellipses into the center of the field, after an approximate adjustment had been made. Similarly the foot of the revolving arm, which supports the telescope at *D*, could be used for the same purpose with advantage.

An open collimator at *C*, *i.e.*, objective and slit each in opaque screens, is specially convenient, inasmuch as it allows the image of the slit *S* reflected at *M* to be visibly reproduced on the jaws of the slit. The occurrence of parallel light and of a beam of light normal to *M* are thus both put in evidence. If *m* is cut off, the same applies to the mirror *N* and beam *n*, though this is liable to be too dark, and the rough and fine adjustments are best made at the telescope, using a wide slit first. The collimator *C*

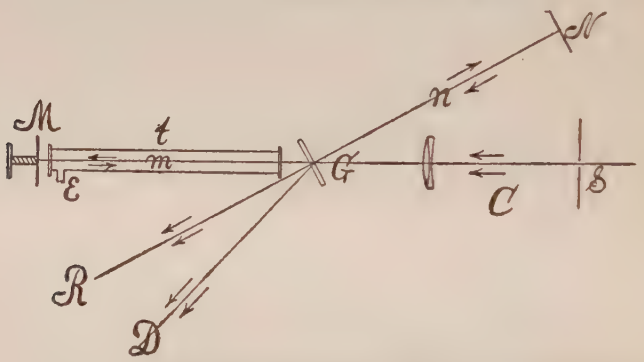

FIG. 92.—Diagram showing vacuum tube on interferometer.

should be long; in other words, the lens of long focal distance, so that the beam *m*, passing through the tube, may remain very short or spot-like in its vertical dimensions. Otherwise too much is cut off by the tube and reflection from *G* before the beam enters the telescope.

With the arc lamp the spectrum may be darkened, so that the sodium lines stand out clearly, by raising or lowering the arc behind the black screen, with a hole about 1 cm. in diameter for the passage of light. A small swiveled screen in front of the objective of the telescope, and approached from one side, greatly sharpens the interferences and the Fraunhofer lines by cutting off undesirable light and particularly the stationary interferences. Possibly the latter would disappear if the plate of the grating were made very thick. When water circulation is used, some time must elapse before the temperature conditions are adequately stationary. With distances *m* and *n* as long as the above, the ellipses are rarely perfect and frequently appear coarse and distorted. It is nevertheless easy to adjust the center of ellipses with an error not larger than 0.00005 cm., at the micrometer screw *M*, *i.e.*, to about the mean wave-length of light.

133. First experiments. Results.—The sealed glass tube, t, of length $e=89.49$ cm. within, having been inserted, the data for the refraction of air, found by alternately exhausting and filling it, were about as given in table 88.

TABLE 88.—Glass tube with plate-glass ends; diameter 4.5 cm.; length, 89.49 cm. Barometer, 75.59 cm. at 17.5°; temperature about 20°.

p_0	p	$10^5\Delta N$	$\mu-1$
75.59	0.32	2505	280
	.10	2495	279

Here ΔN is the displacement of the micrometer corresponding to the pressure difference p_0-p, at the constant temperature given, and μ the index of refraction of the air contained.

The induction coil was now attached and a current from 3 to 4 storage cells sent through the apparatus. Not the slightest shifting of ellipses or interference lines could be detected when the secondary current was alternately made and broken. The lines were very clear. The experiment was then repeated and the air-pump (Geryk) connected directly with the tube without accessory apparatus between. A coarsely stratified column and some cathode dark space was obtained. But the effect at the interferometer was again definitely negative.

The absence of an effect due to the current was to be expected, since the positive and negative currents and the direct and returning beam of light both traveled in opposite directions. The same is true for the ionization, which is too slight; yet it was supposed that some evidence of a temperature effect might be obtained; but there was none.

Since

$$p=C(\mu-1)\vartheta=C\Delta N\vartheta/e$$

where C is constant and ϑ denotes absolute temperature, therefore at constant pressure

$$\frac{d(\Delta N)}{\Delta N}=\frac{d\vartheta}{\vartheta}$$

If $d(\Delta N)=5\times10^{-5}$ cm., $\Delta N=25\times10^{-3}$ cm., $\vartheta=293°$, $d\vartheta=0.59°$; so that whatever rise of temperature may have occurred must have been much less than 0.6° C.

134. Second experiments. Apparatus.—In this experiment the direct and return beams m and n were separated, as shown in fig. 93, into m and m' and n and n', the beams traveling along contiguous sides of a rhombus. M and N are again the two opaque mirrors, the former with micrometer; C is the collimator, open as in fig. 92. The grating above the tripod of

the interferometer has been removed and replaced by a plate of glass P, of about the same thickness, while the grating is at G diametrically opposite, with its ruled face toward N. The normals of the mirrors are shown at p and p', and the telescope is either at R (direct ray) or at D (diffracted ray). It is here convenient to have two telescopes, one set at R and the other at D.

To secure this adjustment, the interferometer of fig. 92 is provided with a cross-arm of gas-pipe under PG, which can be clamped firmly in place on the standard of the tripod, below P in fig. 93, or G in fig. 92. The end of the arm below G, fig. 93, has a foot with a vertical set screw for imparting strain, and is braced with slight strain against rotation around the cross-arm. In the same way M must be laterally braced with slight strain against rotation around the arm under N or NP.

The arm of the telescope R, in fig. 92, is in this case turned about P, the telescope being simultaneously rotated until it occupies the position D in fig. 93. It is for this reason that two telescopes are used, as it would be much less convenient to provide a special axle moving about the foot of G.

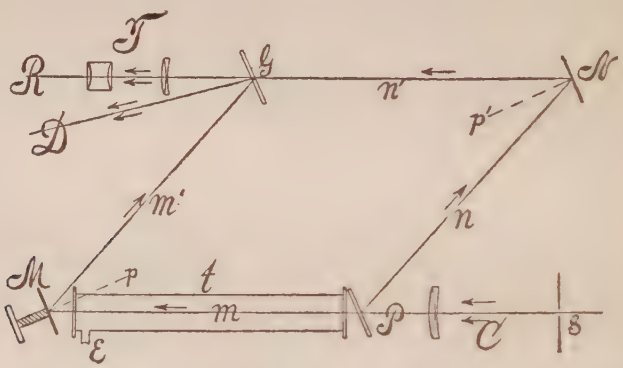

FIG. 93.—Displacement interferometer with separated pencils and vacuum tubes.

To adjust the apparatus the arms, m' and n', are first made roughly equal with a scale. P and G are then placed in the same line by a straight edge; the slit is widened so that the beam m passes directly through central parts of P and the reflection (spot) from the central parts of the mirror M is seen to strike the central part of the grating G. Proceeding thence, the beam is reflected into the telescope T approximately in position (both M and G being rotated horizontally and vertically for this purpose, finally by the adjusting screws). Next the beam reflected from P is made to strike the central parts of the mirror N (which it should do at once on very slight rotation of P), from which it is reflected to the central parts of the grating G, so that the two beams m' and n' may be across the same vertical line. Finally G is adjusted, until the two direct images coincide accurately (both horizontally and vertically) in the telescope, a fine hair having been drawn across the slit, as above.

Under these circumstances there will be four direct images in the telescope at R, due to front and rear reflection at P and G, neither of which is optical plate; but there will be but three spectra or three sodium lines visible at D, since the ray reflected at the rear face of G is not diffracted. To obtain the interferences, a single spectrum line from M must be placed fully in coincidence with either of the two lines from N; but to find them is nevertheless a matter of considerable difficulty. Since reflection takes place not from one and the same face of glass, but from the two independent faces P and G, the ellipses in the field of view are liable to be very eccentric. They thus appear as the merest hair lines, easily overlooked, even when M has (by trial) been moved into the correct position. In fact if the sodiun lines be called Na_m, Na_n, $Na_{n'}$, I have only been able to get interferences from two of these, say Na_m, Na_n, but not from Na_m $Na_{n'}$, after wasting much patience in the attempt. There may be some other reason for this which has escaped me. Na_m passes through three thicknesses of glass, whereas Na_n and $Na_{n'}$ pass through 1 and 3 thicknesses, respectively, and I have not been able to ascertain whether the self-compensating case or the other is the one which succeeds. In fact, the four lines m, m', n, n' are not necessarily coplanar, but will lie on a ruled surface, which is to be made as nearly plane as possible. Thus the plates P and G may be clamped to a long strip of plate glass, or other devices employed. These succeed adequately after some readjustment, but I have not been able to place the center quite in the center of the field of view. Experimentally this is not necessary, for the eye is quite as sensitive in placing the horizontal element of the circle in coincidence with the fiducial sodium lines (which it intersects at right angles), the inclination on the two sides being in opposite directions. Naturally the interference bands should be strong.

The micrometer screw of M, in this case, bisects the acute angle of the rhombus of $\varphi = 30°$, and the motion of the mirror over ΔN here cuts off $2\Delta N/\cos 15°$, from the beam of light. Moreover, at the grating the beam of light is shifted laterally when M advances, by an amount $\Delta N \tan 15°$, so that $2\Delta N \sec 15° \sin^2 15°$ is restored. Thus the path difference produced is generally $2\Delta y = 2\Delta N \cos \varphi/2$.

135. Second experiments. Results.—The data obtained in case of the rhombus are given in table 89.

TABLE 89.—Glass tube as in table 88. Barometer, 76.0 centimeters.

p_0	p	$10^5\Delta N$	$10^5\Delta y$	$\mu - 1$
76.0	0.4	1285	1241	287
....	....	1280	....	286

The data are of the same order as the preceding table, remembering that the tube is not twice traversed by the beam of light, as is the case with the adjustment of table 88.

The current from the induction coil was now passed through the exhausted tube and the circuit made and broken. Not the slightest effect could be observed, the interferences remaining stationary in all parts of the field, just as in the preceding case.

The endeavor must now be made to exhaust the tube to the highest degree possible, and to pass the current between electrodes of very high potential difference. To this I hope to return at some other opportunity.

CHAPTER XV.

THE REFRACTION OF HOT GASES.

THE REFRACTION OF AIR AT HIGH TEMPERATURES.

136. Introductory.—Inasmuch as the displacement interferometer admits of the determination of the index of refraction, no matter how large the excursions of the micrometer screw may be, it was thought interesting to examine the refraction of air and other gases at temperatures as high as may be applied. The gas for this purpose should be inclosed in a long hermetically sealed tube of metal (brass or iron) or porcelain, provided with glass plates at the ends. At very high temperatures this desideratum will have to be modified.

A number of difficulties at once present themselves because the effect of temperature on the glass plates, as well as the irregular distribution of temperature in the surrounding air, can not be eliminated unless the tube admits of exhaustion. In such a case difference readings (N_0, the position of the micrometer for a plenum of air, and N, corresponding to the position for a vacuum), at the same temperature, at once eliminate all discrepancies. The exhausted condition may alternate with the full condition of the tube and the result is enhanced, since the index is not very sensitive to pressure, *i.e.*, very perfect exhaustions need not be reached if the degree of exhaustion is known. Nevertheless the need of hermetically sealed windows is imperative, and this makes the experiment exceedingly difficult for temperatures approaching or exceeding red heat. In the present paper it is not the endeavor to go as far as this.

If the exhaustion at high temperature is not admissible, it is then necessary to determine the effect of temperature on the plates separately—an equally difficult problem, since difference readings can not be made. Changes of temperature in the air surrounding the tube become increasingly important. The cold-air column must also be kept in a water bath. Moreover, it is now absolutely essential that the arms of the interferometer be of absolutely invariable length for long periods of time. As in the preceding paper, they were made of gas-pipe provided with a continually circulating current of water from the hydrant.

The tube is inserted (fig. 94) so that one of the component beams mm' of the interferometer may pass through it axially. It is desirable for this purpose to have the collimator of long focus. The beam in such a case remains slender and narrow throughout its extent within the tube, and the clear space at the windows is not much over 2 cm. in diameter, when the outer diameter of the tube is over 3 cm. It is perhaps best to have the

focus of condensation in the vertical plane at the micrometer mirror. In its lateral dimensions the beam is almost without breadth, being sheet-like.

The tube and apparatus for heating were suspended from a wall bracket, quite free from the interferometer. To obtain the low temperature a current of cold water was circulated through the annular space *BB*—the same current, in fact, which traversed the arms of the interferometer being used. This water circulation might also be employed to keep the counter column of air at a constant low temperature. However, when the method of exhaustion is applicable such a safeguard is not needed; for in this case the time consumed is small enough to admit of the assumption of an average mean temperature in the region as a whole, during the interval of measurement.

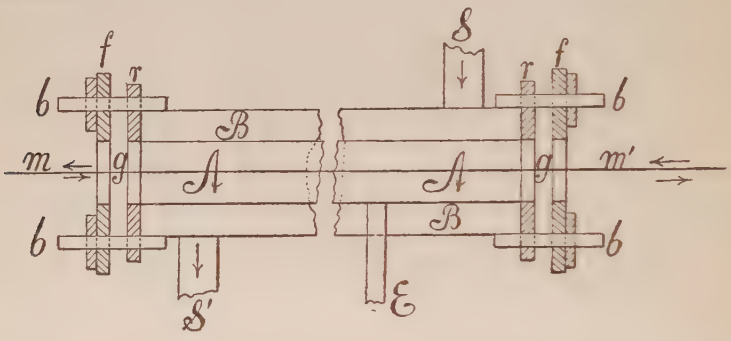

FIG. 94.—Heating apparatus for interferometry of air.

The high temperature was obtained from a current of steam taken from the steam-heating plant of the building. In later experiments it was found advantageous to generate the steam more quietly in a special copper boiler. The air was dried over phosphorus pentoxide.

To obtain a temperature of 200°, the limiting value in the present paper, a brazed vapor bath of naphthalene was available. In all these cases measurements may still be made with a mercury thermometer. At higher temperatures the direct determination by means of a thermo-couple will have to be resorted to, which introduces an additional difficulty, since the junction of the couple will also have to enter the hermetically sealed tube.

137. Small apparatus.—The interferometer is the same as that used in the preceding paper, the available length of arm being about 1 meter, and the free radius or vertical depth below the beam nearly 15 cm. It would be easy to increase these dimensions, but the apparatus in such a case becomes more sensitive to tremors and a greater distance is not needed. In the first experiments a short tube of brass 25.34 cm. long was used, adapted for measurements up to 100° C. only. The parts were soldered together, as shown in fig. 94, in longitudinal section. *A* is the cylindrical air-chamber provided with a tubulure *E* for exhaustion. *B* is the annular cylindrical steam or water chamber, the vapor or liquid entering at *S* and

escaping at S'. The tube should be jacketed without. The ring-shaped ends of the tube are turned smooth and provided with glass plates g pressed against rubber gaskets r by rings of fiber f and bolts bb, the inner ends of which are soldered longitudinally to the outside of the tube. It was at first difficult to keep the system quite tight, but it becomes so in the course of time.

138. Equations.—If we use the extended equation of Mascart, μ and μ_0 being the index of refraction at $t°$ and 0° C., respectively, at the pressure p in centimeters of mercury, and α the thermal coefficient

$$\frac{\mu-1}{\mu_0-1}=\frac{p}{76}\frac{1+\beta p}{1+\alpha t} \tag{1}$$

Since the coefficient β is very small ($\beta=0.0000017$, relative to centimeters of mercury), if the two observations at t and t' be made at about the same pressure p, the binomial $1+\beta p$ may be neglected so that, $p-p'=0$

$$\frac{\mu-1}{\mu'-1}=\frac{p}{p'}(1+\beta(p-p'))\frac{1+\alpha t'}{1+\alpha t}=\frac{N-N_0}{N'-N_0'} \tag{2}$$

where N_0 and N, N_0' and N' are the two positions of the micrometer for a plenum and a vacuum at the same temperature, at t and t', respectively. If for brevity the observed ratio

$$\frac{N-N_0}{N'-N_0'}=\frac{\Delta N}{\Delta N'}=R' \text{ and } \frac{N-N_0}{N'-N_0'}\frac{p'}{p}=R \tag{3}$$

$$\alpha=\frac{R-1}{t'-Rt} \tag{4}$$

If it were admissible to put $N_0=N_0'$ for the plenum of air and $\delta t=t'-t$, $\Delta N=N-N_0$, $\delta N=N-N'$, the equation

$$\alpha=\frac{\delta N}{\Delta N\delta t-t'\delta N}=\frac{1}{\Delta N\delta t/\delta N-t'} \tag{5}$$

might be used; but this is not the case. It shows, however, the difficulty of measurement, as δN is of the order of 0.0012 cm., ΔN of the order of 0.007 cm., if δt is about 80° C. Hence, since the smallest error of N is about 0.00005, the value of δN can not be trustworthy to more than 5 per cent, quite apart from the manifold other difficulties of measurement. Hence the need of using longer tubes than the present.

Equation (5) may, however, be remodeled by replacing

$$N-N_0 \text{ by } (N-N_0)/p=\Delta N/p \qquad N'-N_0' \text{ by } (N'-N_0')/p'=\Delta N'/p' \tag{6}$$

and putting $\delta t=t'-t$ and $\delta N=\Delta N-\Delta N'$, in which case equation (5) is generally applicable in the form given.

139. Data.—The results for α in table 90 show considerable differences for the reasons stated.

TABLE 90.—Refraction of air. Short tube, length $e=25.342$ cm. $\Delta N=N-N_0$ at low temperature, pressure interval p; $\Delta N'=N'-N_0'$ at high temperature, pressure interval p'. μ_0 refers to 0° centigrade and 76 cm.

t	p	$\Delta N\times 10^3$	$10^6\times(\mu-1)$	$10^6\times(\mu_0-1)$	t'	p'	$\Delta N'\times 10^3$	R	$10^3\times\alpha$
15.8°	67.94	5.56	219.4	260.1	100°	67.94	4.24	1.312	3.93
....	....	....	....	....	100	74.55	5.36	1.305	3.82
14.0	74.55	7.00	276.2	296.5	100	74.55	5.43	1.288	3.52
....	....	....	....	....	*100	76.91	5.62	1.286	3.48
18.9	75.98	6.90	272.1	291.6	100	75.98	5.48	1.259	3.40
16.2	75.93	7.01	276.4	293.6	100	75.98	5.48	1.280	3.54
18.9	74.67	6.95	274.1	298.9	100	74.67	5.41	1.284	3.75
....	....	....	....	....	100	74.67	5.50	1.263	3.45
....	....	....	....	....	100	74.67	5.41	1.284	3.75
....	....	....	....	....	100	74.67	5.39	1.290	3.83

*Corrected for p'/p; cold measurements not made on same day.

These observations are obtained from triplets, two at high pressure (barometer) alternating with one at low pressure (partial vacuum). The observations for ΔN, of the order of 0.007 cm., and those for $\Delta N'$, of the order of 0.0055 cm., should each be correct to about 1 per cent; but their difference δN, of the order of 0.0014 cm., will not be reliable to more than 4 per cent. Since

$$\frac{d\alpha}{d(\delta N)}=\left(\frac{\alpha}{\delta N}\right)^2\Delta N\delta t$$

the effect on α is of the order of 5 per cent, when $d(\delta N)$ denotes the limiting precision of 5×10^{-5} cm.

The values of α obtained from the successive series on different days, if we neglect the first crude results after which the details of the apparatus were gradually more and more perfected, range from $\alpha=0.0034$ to $\alpha=0.0038$, *i.e.*, over about 10 per cent, an interval twice as large as the estimated minimum error. It is difficult to find a reason for this. Undoubtedly the arms of the apparatus are continually varying in length, in view of the micrometric scale on which the observations of length measurement are made and in spite of the flow of cold water at nearly constant temperature. The atmospheric temperature also, both in front of and behind the steam tube as well as in the other arm of the apparatus (GN in fig. 92, Chap. XIV), is continually fluctuating around a mean value. The temperature and refraction of the plate-glass caps of the apparatus are changing slightly; but it does not seem probable that, in the short interval of time between the occurrence of a plenum of air and a vacuum in the refraction tube, there should be any discrepancy sufficient to increase the minimum error two times. The possibility of discrepancies from adiabatic expansion, moreover, can be disregarded in so thin a tube, and in the case of a vacuum they vanish naturally.

It is true that in the course of the work the ellipses gradually undergo change of form or of clearness. Some part of the apparatus or the supporting table is continually undergoing slight change of form. Similarly on successive days (different series in table 90) the values of α, though nearly identical and consistent on the same day, show marked differences due to undetected differences of adjustment, etc. The ellipses, if the steam tube is turbulent, are liable to be in incessant vibration, though in the last series this difficulty was practically conquered. Finally, the actual error may possibly reach twice the minimum error in the case of two single readings.

The only way of overcoming the elusive causes of error referred to must therefore consist in the installation of a long tube and the use of longer ranges of temperature. This is attempted in the next section, where a tube about 28 inches long shows about $\Delta N = 38.4$ scale parts or about 0.019 cm. at ordinary temperature, being thus nearly three times as large as the above. On the same scale of errors, it should therefore be possible to obtain α to a few per cent. Moreover, the rubber gasket, which at 100° and low pressures may essentially modify the air contained in the tube by vitiating it with sulphur fumes, should be abandoned. It is not impossible that such discrepancies may have entered the above data; but they were not considered serious, because at high exhaustions the difficulty cures itself, as there is an absence of gas; whereas at the large pressures sulphur is insufficiently volatile at 100° to be a menace. Anticipating the results of the next section, it is possible that the difference of values on successive days is due to the steam supply. To my surprise it was difficult to heat the air in the tube with glass ends, to 100° permanently, in spite of the jacketed steam bath, fed with a steady flow from the radiator pipe. Measurement of temperature on the inside of the tube at this stage of the work seemed superfluous and no such tests were made.

140. Long tubes.—To obtain a larger value of $\delta N = N - N_0 - (N' - N_0')$, longer tubes must be resorted to and the present experiments were therefore made with staunch brass gas-pipe, 28 inches long and 1 inch inside

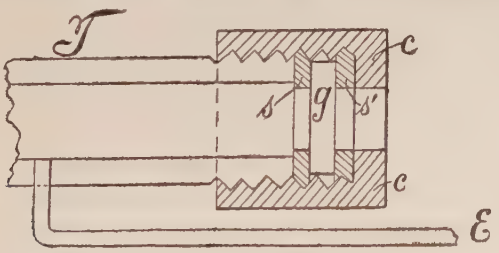

FIG. 95.—End of air tube.

diameter. To obtain a gas-tight joint for the plates of glass at the ends, the brass caps C (fig. 95) of the tube were perforated with axial holes about three-fourths inch in diameter and the inside of the ends turned smooth.

In this way they secured a round disk of plate glass g between gaskets s and s' of fiber. Before adjusting in place the inner gasket was slightly soaked in water and after placing the parts the cap was screwed down till the joint appeared air-tight and then left in this position to dry. The drying operation was assisted by repeated exhaustion over calcic chloride by the aid of the air-pump In proportion as the paper gasket dries, it shrinks, and the screws must be tightened. Eventually a good joint is obtained, practically tight at 100° and even at 200°. There is no further danger from contamination by gases which arise in the gasket. They seem, however, to shrink after exposure to high temperature. Although the joint is rarely quite tight, it is sufficiently so for work of the present character, where the phenomenon is not very sensitive to variations of pressure.

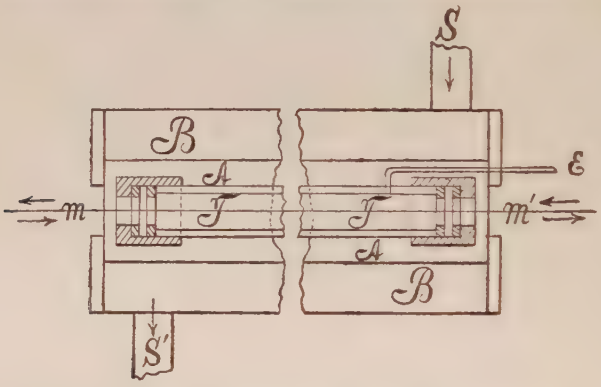

FIG. 96.—Heating apparatus for higher temperatures.

Fig. 96 shows the air-tube TT in place in the cylindrical axial channel of the annular vapor bath BB. In case of steam, the vapor entered at S and left at S'. The bath was jacketed with felt. A small hole was left in the end for the beam of light. The inner tube TT, wedged in place, was provided with a bent exhaust-pipe E, of thin brass or steel tubing, screwed into T. To make a tight joint, the end of E is covered with an adhesive coating of lead or a solder fusing at high temperature and then screwed into T before the latter is put into the chamber. The copper pipe may thus be fitted practically tight even without lead.

The vapor bath is suspended (with the tube inclosed) from an independent wall bracket as usual. There seemed to be no difficulty in causing the beam to traverse the tube twice, remembering that the collimator objective must be of long focus. For higher temperatures a brazed annular bath of sheet iron, similar in form to fig. 96 and containing the liquid to be boiled, replaced BB. This molten liquid was heated by burners placed below BB and a central pipe (not shown) on top provided for the escape and recondensation of the vapor. The bath was jacketed with asbestos on the sides and ends with the exception only of the small holes for the beam of light, mm, of the interferometer.

The glass ends of the tube extend nearly to the ends of the vapor bath. So long as the exhaustion method is applicable, there need be no correction for hot air at the ends of the chamber and outside of the tube, the distance being small. For the irregular temperature, distribution between the ends of the tube and the mirror and grating, respectively, remains constant on the average during the short time between the exhaustion and the reoccurrence of full supply of air in the tube. So also the arms, in view of water circulation, are of constant length for short intervals of time. In case of long periods, however, a time correction obtained from length measurements before and after on the interferometer would be needed; *i.e.*, in the absence of exhaustion. The inevitable flickering of the ellipses, due to air currents, proves no serious annoyance. They are steady enough for measurement and the change of aspect is rather a convenience, as it assists in bisecting the ellipses with the fiducial sodium line.

141. Data.—The results obtained at low temperatures, 22.5°, present no anomaly. They are given in table 91, as obtained on different occasions, a thermometer placed in the inner chamber of the cold steam bath showing the temperature. Each observation refers to a triplet, the observation for exhausted air lying between two observations for a plenum of air, in regular succession.

TABLE 91.—Refraction of air. Long tube, length $e=71.75$ cm. (air column), diameter 2.5 cm., windows 2 cm.

Barometer	t	p	$10^3\times\Delta N$	$10^6\times(\mu-1)$	$10^6\times(\mu_0-1)$	t'	p'	$10^3\times\Delta N'$	R	$10^3\times\alpha$
75.37 at 22°	22.5°	74.87	19.34	269.5	297.0	99.58°	74.87	17.27	1.13	1.75
.....	....	....	19.41	270.6	298.1	....	....	17.10	1.14	1.91
.....	....	....	19.80	276.0	304.1	....	....	16.94	1.15	2.07
.....	....	....	....	....	....	....	....	16.55	1.18	2.46
.....	....	....	....	....	....	....	....	16.30	1.20	2.71
.....	....	....	....	....	....	....	....	16.22	1.20	2.80
76.66 at 22°	22.5	74.87	19.52	272.0	299.7	95.5	75.96	16.09	1.23	3.40

The table also contains the high-temperature results, t' being the boiling-point of water for the day and p' the effective pressure.

The data of the table are exceedingly disappointing, as the errors made in measuring δN can not be greater than a few tenths of 1 per cent. Moreover, a long time was allowed to secure constancy of temperature and to reach the maximum value. The observations lasted thereafter for about an hour, and the bath was well jacketed on all sides, including the ends. Nevertheless the temperature of the steam was not even approximately reached by the air within the tube and the successively increasing values of α from 1.8 to 2.8 show that, even at the end of the experiments, temperature on the inside of the air-tube is still markedly rising. In fact, if the constant α be taken at 3.6, the initial and final temperatures would be 61°

and 80° instead of 99.6°. Unfortunately, so confident were the observers of the temperature constancy throughout the steam bath that no thermometer was put inside of the tube.

The experiments contained in the lower part of table 91 were made with great care as to the temperature limits to be reached. Thermometers at the end of the brass tube registered the heating there, and it is obvious that, for parts within, the temperature must be higher and probably normal. Hence, when the temperature of the ends and the boiling-point for the day differed by but a few degrees, observations were commenced and the mean values taken as the actual temperature. Thus t' can not be too large; and since

$$d\alpha/dt' = -\alpha^2\left(\frac{\Delta N}{\delta t} - 1\right)$$

α can not be too small. If all temperatures agree within a single degree the error can not much exceed 1 per cent.

Unfortunately the apparatus began to leak as the experiments proceeded, so that only the first result is reasonably trustworthy. The effect of this leak was to decrease the refraction of the plenum of air at 100° and hence to enormously exaggerate α, very probably owing to the ingress of water-vapor present in the air. These results were therefore discarded.

In the next experiments, table 92, a special copper boiler was installed and all steam tubes, etc., were jacketed. Efflux steam was more carefully condensed in order to leave the atmosphere without dry, and decrease the

TABLE 92.—Tube as in table 91. Barometer, 75.50 at 25°.

t	p	$10^3 \times \Delta N$	$10^6 \times (\mu - 1)$	$10^6 \times (\mu_0 - 1)$	t'	p'	$10^3 \times \Delta N'$	R	$10^3 \times \alpha$
22.7°	75.71	19.43	270.8	295.3	95.0°	75.15	16.15	1.19	2.87
....	....	....	....	....	96.0	75.11	16.03	1.20	2.96
....	....	....	....	....	96.5	75.15	15.90	1.21	3.09
....	....	....	....	....	96.5	75.17	15.96	1.21	3.03
....	....	....	....	....	97.0	75.15	16.02	1.20	2.93
....	....	....	....	....	97.0	75.10	15.80	1.22	3.18
....	....	....	....	....	97.5	75.14	15.54	1.24	3.48
....	....	....	....	....	98.0	75.17	15.67	1.23	3.31

burden on the drying tube. The air was taken from some distance from the apparatus. An additional advantage was secured in the use of the boiler, as the whole apparatus showed much greater freedom from tremors. Indeed, the experiment proceeded very smoothly throughout and, though it took some time before an adequately constant temperature was reached, exceptionally trustworthy results were anticipated. After two hours the temperature was still about a degree below normal at the end of the tube, the effect of which upon α would be about -1.6 per cent. This is not, therefore, the difficulty encountered. In other words, the observations for α in table 92 remain astonishingly small and present a degree of irregularity which can not easily be made out.

Even at the end of the experiments, however, the value of α has not yet reached a limiting value, as fig. 97, in which α and ΔN are graphically shown for successive observations, clearly evidences. To obtain such a result the experiment will have to be prolonged about half a day, and even greater safeguards taken at the ends of the tube.

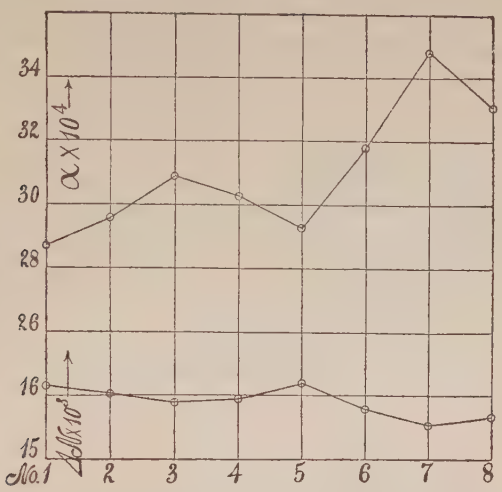

FIG. 97.—Displacement and temperature coefficients in successive experiments.

THE REFRACTION OF THE BUNSEN FLAME.

142. Method.—The following experiment is interesting as a rough application of the method. It aims at measuring the refraction of flaming gases and, so far as I am aware, is the first example of results of this kind. The attempt to determine the temperature of the flame would not be warranted so long as the temperature coefficient of the gases undergoing chemical ignition can not be known. The first result shows, however, that the refraction of flame gases is apparently peculiar, inasmuch as the flame behaves as if its index of refraction were less than 1. Such an outcome must be seriously considered, even if it can eventually be explained away.

The method consisted in first finding the micrometer displacement on the interferometer per centimeter of length of the column of air; thereafter, the displacement per linear centimeter for the given mixture of air and gas is ascertained by direct comparison with air; finally, the displacement of a column of the hot flaming gases per centimeter of length is found by comparison with cold air.

The cold-air tube at 20° C., for the length $e = 25.3$ cm., showed a total displacement of $\Delta N = 12.1$ scale parts or 0.00605 cm., as the equivalent of the difference in refraction between a plenum of air and a vacuum. Thus the air displacement per centimeter is $\frac{0.00605}{25.3} = 0.000239$, which is nearly equal to $\mu - 1$ at the given temperature (cold).

The gases of the burner, without being ignited, were now passed into a similar tube, 33.4 cm. long, at 21°. This tube was provided with glass plates at its ends, but there was room between them and the end of the tube for the escape of gas. The displacement at the micrometer due to the difference between the gas-content and the air-content of the tube was now found to be successively (observations being made in triplets) 0.87 and 0.92 scale parts, or 0.00045 cm., for the tube-length of 33.4 cm.; *i.e.*, $\frac{0.00045}{33.4} = 0.0000135$ per linear centimeter of gas column. The total displacement for the gas column per centimeter of length would be the sum, or $\Delta N = 0.000239 + 0.0000135 = 0.0002526$ cm. It was interesting to note the motion of the ellipses, while the contents of the tube changed from gas to air and back again. They are naturally both deformed and displaced during the transfer. The method must thus be applicable in case of a suitably designed apparatus for the measurement of the diffusion of gases into gases.

Finally the same beam of light of the interferometer was passed through the flame directly and at the top of the blue cone, the external mantle of flame being about 2.3 cm. in diameter. It was astonishing to find that the ellipses, though quivering violently, were still visible and available for rough measurement; but this is only the case when the beam of light passes normally through the flame. If it passes through or grazes either side of the mantle, it is naturally refracted away from one side or the other, respectively. The white slit image of the undeviated beam shows the nature of the result clearly. One of the two coincident images is drawn to one side of the stationary image, the latter corresponding to the beam not passing through the flame, and appears as a narrow band of white light, fluted with fine interference lines.

The displacement due to the flame was successively as follows:

Air.	Flame.	Diff.
45.7 46.8 }	44.6 }	−1.6
46.8 }	45.2 }	

equivalent to −0.00080 cm. for the flame diameter 2.3 cm.; or $\delta N = -\frac{0.00080}{2.3} = -0.00035$ per linear cm. The gradual advance of the air value is due to the expansion of the arms of the apparatus, resulting from the radiation of the flame. The value of δN is the mean of two triplets.

Comparing this with the preceding result,

$$\frac{\Delta N}{\delta N} = -\frac{0.0002526}{0.00035} = -0.72$$

Now since the flame temperature t' is given in terms of the room temperature t by the equation

$$t' = \frac{1/\alpha + t\Delta N/\delta N}{\Delta N/\delta N - 1}$$

where α is the thermal coefficient of the gas, the result $\delta N > \Delta N$ is impossible, since $\delta N = \Delta N$ would make $t' = \infty$

Hence the depth of flame (2.3 cm.) should be increased by the region of hot air around it, or $\delta N = \frac{1.6}{2.3 + x}$, where x is the increment of diameter, which is again apparently impossible, since the increase would have to be at least $2.3 + 1.7$ cm., or about 75 per cent. To avoid this assumption we must suppose, alternatively, that associated flame gases have an abnormally small refraction.

143. Conclusion.—Since the equation for the high temperature t' of the flame is of the form just given, δN can at most be equal to ΔN or $\Delta N/\delta N > 1$. Since experimentally the reverse of this is apparently the case and since

$$\frac{\mu - 1}{\mu' - 1} = \frac{\Delta N}{\Delta N - \delta N} = \frac{1}{1 - \delta N/\Delta N}$$

$\mu' - 1$ must be effectively negative or apparently $\mu' < 1$. Before endeavoring to account for this anomalous result, two other results may be mentioned. For a flame about 2 cm. in diameter the micrometer positions for air and flame were, respectively, 44.5 and 43.5 scale parts. This makes, per linear centimeter, $\delta N = 0.000375$ cm.

In the next experiment with a somewhat larger flame, water at constant temperature rapidly circulated through the arms of the interferometer. The micrometer positions in scale parts were successively

Air.	Flame.
9·7	7·5
9·7	7·4
9·7	

The difference is equivalent to 0.00113 cm., or $\delta N = \frac{0.00113}{2.3} = 0.00049$ cm. per linear centimeter of flame. As $\Delta N = 0.000253$ is the same value as above, the anomalously excessive value of δN again appears, in an even more pronounced degree. One should note that here there can be no thermal expansion of the arms of the apparatus as the result of flame radiation. Such an effect, moreover, is excluded when the measurements are made in triplets, as was done throughout.

To account for this result in the simplest manner and in the absence of a value for α, one may assume, as has been done, that the flame acts effect-

ively beyond the visible mantle (diameter e). Hence the limit of activity must be greater than $x/2$ beyond the flame on either side when

$$\Delta N = \frac{\delta N}{e+x}$$

In the last experiment, therefore,

$$x = \frac{1130}{253} - 2.3 = 2.2 \text{ cm.}$$

The flame at the excessively high temperature ($t = \infty$) would thus have to extend effective much more than 1 cm. beyond the mantle, which seems to be unreasonable.

The other alternative is the occurrence of $\mu < 1$ for the ignited gases, an even more anomalous result. It would mean that light travels more rapidly through a region of violent chemical reaction than through a vacuum, for which there is no other correlative instance. The question will have to be attacked in a different manner at some other opportunity.

CHAPTER XVI.

ELECTROMETRY WITH THE DISPLACEMENT INTERFEROMETER.

CYLINDRICAL AND DISK ELECTROMETERS.

144. Introductory.—The possibility of compensating any displacement of the mirror N by a corresponding displacement of the micrometer mirror M, *i.e.*, the fact that the ellipses are never lost in a properly adjusted apparatus, for any amount of motion of the mirror N, however sudden it may be, suggests the use of this method for electrometry. Some time ago I made experiments of this kind, using the device of the absolute electrometer for the purpose. A mirror was attached to the disk and the force of restitution was obtained from a pendulum suspension for parallel motion. Michelson's interferometer was employed. It appeared that for difference of potential of 1 volt the excursion, ΔN, would correspond to a distance apart of the condenser plates, d, in the given apparatus, as follows:

$d=$	1.0	0.1	0.01,
$10\Delta N=$	0.3	35	3,520, etc.

so that the apparatus was insensitive for small potentials, even with the use of the interferometer.

At first sight it seemed promising to change to the method of the quadrant electrometer. Here, however, the mirror can not be mounted on the needle unless a particular device of two mirrors is adopted; for even the slightest rotation is fatal to the interference measurements contemplated. A cylindric or lamellar form, such as is usually referred to in constructing the theory of the instrument, seemed to be alone available, but the sensitiveness here also, if torsion systems are excluded, is unexpectedly small, unless (as in Thomson's original apparatus) excessive charges are given to the needle, a procedure which introduces its own difficulties. Nevertheless I constructed the apparatus in a variety of forms, each of which will be described below, in turn, in order to ascertain in how far the sensitiveness which may be estimated from theory may be actually realized in practice; *i.e.*, to actually confront the instrumental difficulties of the problem, with a view to the use of the method in absolute measurements of potential.

145. Cylindrical electrometer. Movable cylinder without.—Figures 98 and 99, both sectional elevations, show the first form of electrometer in which the movable cylinder (usually highly charged) is external to the fixed cylinders h and i, carrying opposite charges. The latter are supported on hard-rubber pillars, u and v, rising from the adjustable feet q, of which r and s are the leveling screws and the set screw. The whole arises from a narrow base of brass plate AA. On this base the braced scaffolding of very thin brass pipe efg is also mounted, grasped above by the light cross-

rod *d*. This makes a light but very firm support for the two parallel horizontal rods of hard rubber *cc*, secured at *b* and carrying the revolvable brass rollers or reels *aa* snugly. From *aa* the threads of very thin copper wires *yy*, 0.007 cm. in diameter, depend, their lowest point being attached to the cylinder *kk*, making of it a pendulum. To obviate torsional vibration the wires *yy* converge on their front elevation from *aa* to the top *tt* of the cylinder, while in their side elevation they are rigorously parallel and

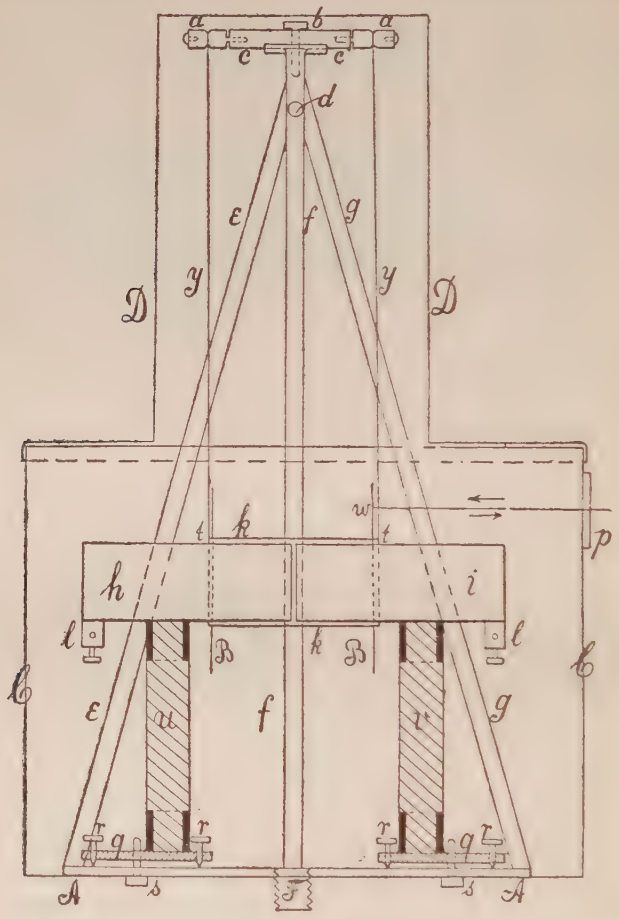

FIG. 98.—Cylindrical electrometer. Side view. Cylinder outside.

equally long. They may be lengthened or shortened by turning the close-fitting rollers *aa*, so that the cylinder *kk* may be placed accurately concentric to the cylinders *ih*. The latter may be mounted with a cylinder of wood passed quite through them, which is withdrawn after they are fastened. The clamp screws *ll* and those at the end of *a* are convenient for charging, the wires passing out of the light tin-plate cover *CCDD*, through hard-rubber cylinders at *Z*. The top *DD* may be lifted off. When

there is no danger of induction, *DD* may be removed. The ellipses of the interferometer, in a room free from draft, are quite adequately stationary even without *DD*, a surprising result.

The cylinder *kk* is either of very thin aluminum tubing, or preferably of gilt paper. The wires *yy* pass through small holes at the top ends. To secure adequate damping, thin circular rings of mica or of paper, *BB*, surround the ends, and the front one carries the light mirror *w*, which

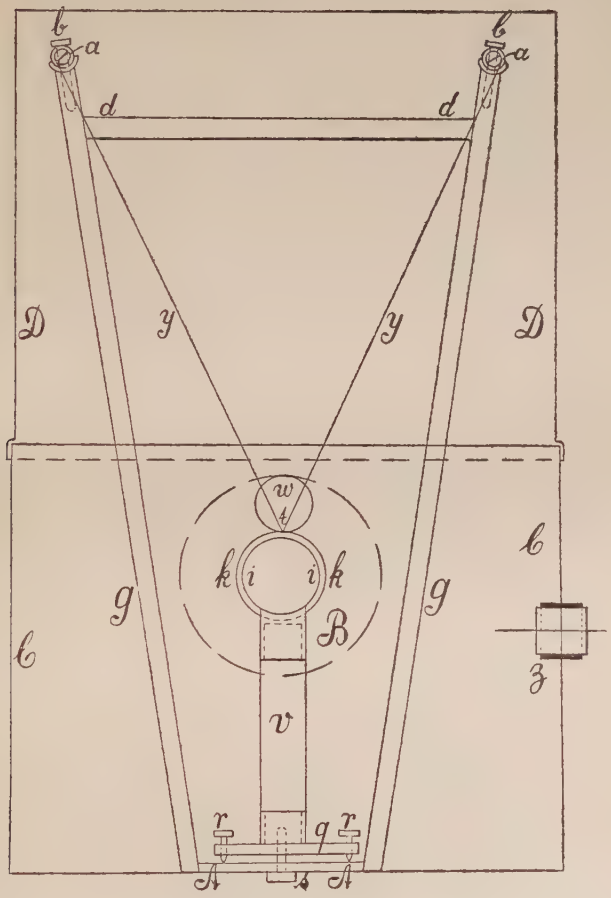

FIG. 99.—Cylindrical electrometer. End view. Cylinder outside.

reflects one of the component beams of the interferometer, as indicated at the glass window *p*. If liquid damping is desired, in the case of a heavy cylinder, wires ending in a vane may be dropped from one of these disks with the vane in a box of oil below. This was tried without apparent disadvantage, but a light paper cylinder and air damping is of course preferable, being far more sensitive. The mica *B* should be somewhat adjustable, so that the beam *p* may be given the proper direction, roughly. The methods for doing this will be described below.

The whole apparatus covered, at least as far as C, was then mounted on one arm of the interferometer by the aid of a large clamp of the ordinary pattern, the clamp having been screwed into the base A at F. As the arm is of gas-pipe, F is an ordinary nipple of suitable length. It is advisable to further support the tin case with wood uprights from the table to avoid the effect of tremors due to the vicinity of an active laboratory; but no great difficulty was here encountered. In fact, the ellipses of the interferometer were obtained in all cases after a preliminary rough adjustment of the mirrors with surprising ease, and they were quite as stable and available for measurement as if the mirrors had been rigidly fixed. Naturally this was quite contrary to our anticipations, but it is shown by the large number of experiments made, each of which required a new adjustment.

The measurement consists merely in a compensation of the displacement of the movable mirror on the electrometer, by the micrometric displacement ΔN of the mirror belonging to the other component beam. The center of the displaced ellipses in the field of the telescope is thus brought back to the fiducial sodium line. The compensation admits of an accuracy of about $\Delta N = 0.0001$ cm. without resorting to the interference rings. Other remarks on the optical method are given in the next paragraph.

146. Cylindrical electrometer. Movable cylinder within.—The framework and the mounting here are in general the same as in the preceding case and the movable cylinder *kk* is the same, but differently suspended. The fixed cylinders of the former apparatus, however, have been removed and replaced by the cylinders *h* and *i* of the present figures 100 and 101. These are mounted on higher hard-rubber supports *uv*, so that the interferometer beam *p* may have the same level as before.

The movable cylinder *kk* is fixed in the middle of the thin steel rod *tt* and suspended bifilarly from the threads *yy*, which are parallel in their side elevation, but triangular in their front elevation, as before. It must therefore have longer hard-rubber rods *cc*, though the suspension is in other respects the same. The interferometer mirror *w* was at first mounted in the end of the cylinder *kk*, where it meets the beam *p*. In a later construction it was thought advisable to mount the thin rod *tt* in the axis of the cylinder *kk*, the ends of the latter being closed. The mirror is then fixed to the end of *tt*. This has several advantages. The closed cylinder is very light and, together with the cylinders *h* and *i*, partially closed at their ends, admits of sufficient air damping; the mirror is accessible for adjustment and the axial rod *tt* is less subject to harmful induction. Other forms of instrument (disk pattern, closed field pattern) will be described below.

The general treatment of the displacement interferometer has been given in my earlier papers. The field of the telescope, after the appropriate two (of the four) undeviated images of the slit, from front and rear of the grating plate, have been put into coincidence horizontally and vertically (the images being usually bluish and yellowish), contains but three superposed

spectra, although there are four white images, two from the front and two from the rear of the plate. For the component beam reflected from the rear face of the grating is not diffracted. It is thus advantageous to eliminate the third spectrum also, and to keep only the two which are superimposed for interference in the field. This may be easily done as follows: the two component beams reflected from the mirror facing the ruled side of the grating plate usually appear as separated images on the mirror,

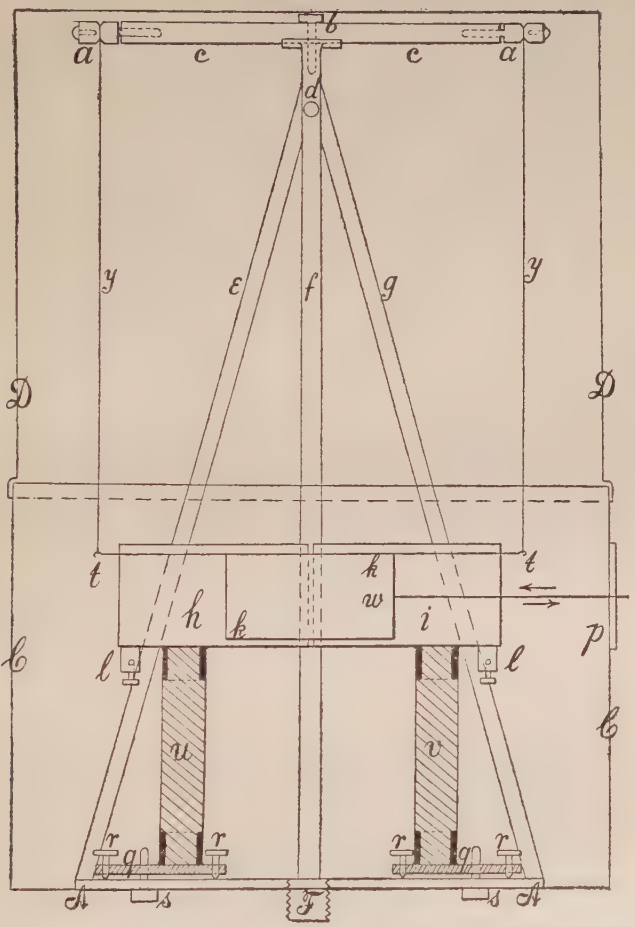

FIG. 100.—Cylindrical electrometer. Side view. Cylinder inside.

about one-eighth inch apart, and the one yellowish in color may be blotted out by a small screen near the mirror. As a result of this the stationary interferences which are due to the two beams from the same mirror also vanish. The spectrum is now clear and contains only the interfering superpositions, giving the ellipses their maximum definition.

In other respects the mounting on the interferometer is the same as before, and very little difficulty was experienced in obtaining the ellipses

The top of the case *DD*, here necessarily a square box, may usually be removed without disadvantage. If liquid damping is necessary in case of a heavy cylinder *kk*, the wire with vane may be dropped into a vessel of oil from the rear end of *tt*, the front carrying the mirror.

The usual method of connecting was used for potential measurements, one pole of the experimental cells being alternately earthed as well as one pole of the charging battery. A Mascart key was very useful. When the

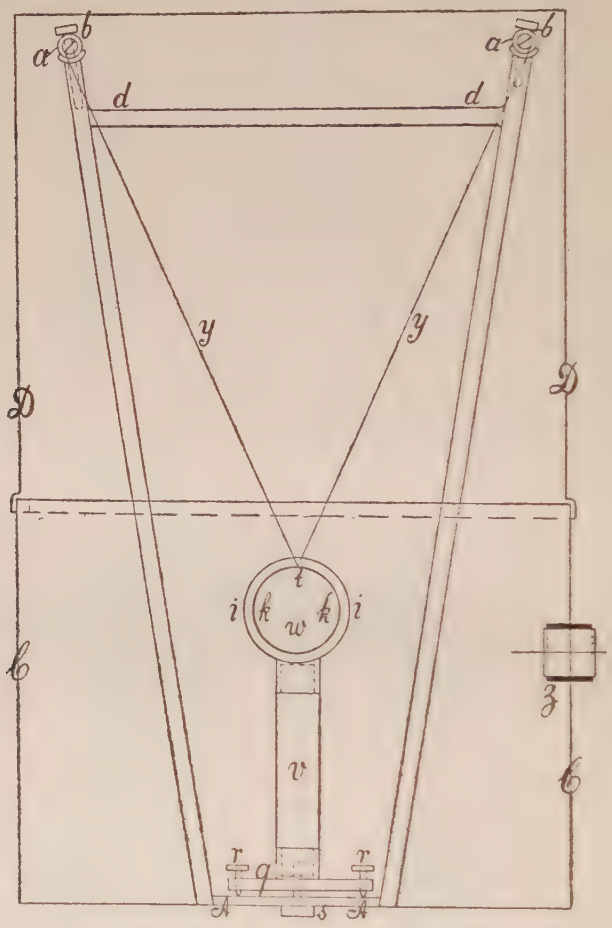

FIG. 101.—Cylindrical electrometer. End view. Cylinder inside.

needle swings to and fro the ellipses are visible at the extreme elongations of the deflection (if not too large) of the vibrating cylinder. They flash into the field of the telescope at the two ends of it, but are invisible between. The distance apart of the positions of visibility gradually diminishes until they coincide and the cylinder is stationary. If the ellipses are clear, slight motion does not interfere with the measurements, as the mean position is readily determinable in the displacement method. This would not, how-

ever, be the case had the evanescence of rings been made the basis of measurement, as in Michelson's interferometer.

When the needle or quadrants carry isolated charges to be removed by leakage, the electrometer is caged, and a caged key, shown in figs. 102 and 103, is necessary. This is a mercury key, c being the cup attached by a hard-rubber cylinder h and screw i to the base B, d being the clamp screw. The metallic connector is a supported on the hard-rubber stem g and screw k. The connector a turns in the axle b held by the brass cap e, the axle being connected by a thin flexible wire to the clamp screw f. The axle b is controlled by the observer at a distance by a long stick passing out of a hole in the cage. The cage is earthed.

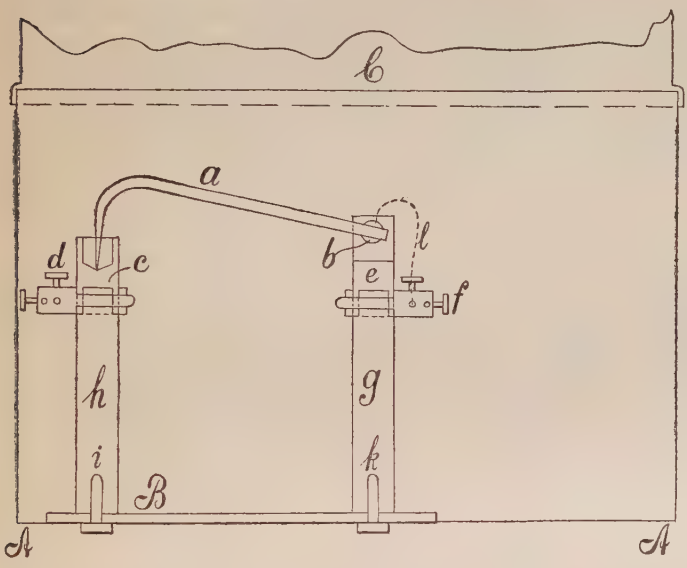

FIG. 102.—Electrometer key. Side view.

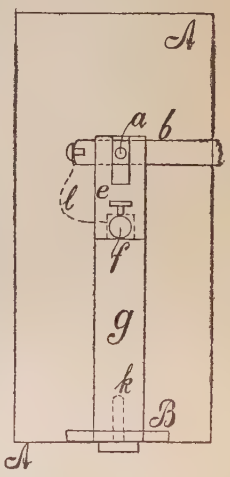

FIG. 103.—Electrometer key. End view.

147. Equations. Absolute electrometer.—It is convenient to include, for comparison, the equations for the absolute electrometer as used in the older paper (*l.c.*). If the condenser plates are at a distance d apart and A is the area of the disk; and further, m is the mass of the disk with appurtenances (mirror, etc.), l is the pendulum suspension, ΔN the micrometer displacement of the mirror corresponding to $V_2 - V_1$ or the potential difference in volts

$$\Delta N = 4.51 \times 10^{-10} \frac{Al(V_2 - V_1)^2}{d^2 m}$$

If the thickness and density of the disk are t and ρ

$$\Delta N = 4.51 \times 10^{-10} l(V_2 - V_1)/d^2 t\rho$$

which is independent of A if the disk is large. The apparatus is thus extremely insensitive for small potentials in spite of the interferometer, but its readings are absolute. If ΔN is to remain small in comparison with d,

the latter can not be made much less than 0.05 cm. For the case of a silvered sheet of mica one may estimate

$$t=0.2 \text{ cm.} \qquad \rho=3 \qquad l=100 \text{ cm.} \quad \text{or} \quad \Delta N=3\times 10^{-4} \text{ cm.}$$

per volt is about the limit of sensitiveness. Hence about one-third volt could be measured by displacement interferometry, or one-tenth volt per ring.

The small value of d could be eliminated as usual from two measurements where $d-d'$ is known.

148. Equations. Cylindrical electrometer.—The equations may be found in the usual manner, and as so little of the field is displaced during deflection they apply with acceptable accuracy. Virtually a small cylindrical shell of uniform field is supposed to disappear on one side to reappear on the other. Hence, let V_3, V_2, and V_1 be the potentials of the two fixed and a movable cylinder (needle) respectively. Let f_{12} denote the electric force between cylinders (2) and (1), f_{13} the force between cylinders (3) and (1), R the common radius of the fixed cylinders, and r that of the movable cylinder. Hence if $R-r$ is small, then

$$f_{12}=(V_1-V_2)/(R-r), \qquad f_{13}=(V_1-V_3)/(R-r)$$

If the displacement of the cylinder is dx, the changes of potential energy on the two sides are

$$dW_{12}=\frac{R+r}{R-r}\frac{V_1-V_2}{8}dx \qquad dW_{13}=-\frac{R+r}{R-r}\frac{V_1-V_3}{8}dx,$$

and hence the force acting in the direction x (if $W=W_{13}+W_{12}$) is after reduction

$$X=\frac{1}{8}\frac{R+r}{R-r}(V_3-V_2)\left(2V_1-(V_2+V_3)\right)$$

On the other hand, the restoring force is for small displacements

$$X=Mgdx/l$$

where M is the mass of the cylinder, l the length of the pendulum suspension; whence if $dx=\Delta N$, in electrostatic units,

$$(V_3-V_2)\left(V_1-\frac{V_3+V_2}{2}\right)=\frac{4Mg(R-r)}{l(R+r)}\Delta N$$

which is the required equation. Since, if t is the thickness, L the length, and ρ the density of the movable cylinder,

$$(V_3-V_2)\left(V_1-\frac{V_3+V_2}{2}\right)=\frac{8\pi Lt\rho(R-r)}{l(1+R/r)}\Delta N$$

the appurtenances, like mirror, etc., being disregarded, and where $1+R/r$ is slightly larger than 2. A given deflection ΔN will therefore correspond to smaller V_3-V_2 as $R-r$, L, t, are smaller and l and V are larger.

If the instrument is used idiostatically (electrostatic units)

$$(V_3-V_2)^2=\frac{8Mg(R-r)}{l(R+r)}\Delta N$$

If one pole of the cell $V_3 - V_2$ is earthed, $V_2 = 0$, and the deflections on commutation are ΔN and $-\Delta N'$,

$$V_3 = 300^2 \frac{4Mg(R-r)}{V_1 l(R+r)} \frac{\Delta N + \Delta N'}{2} = 300^2 \frac{8\pi L t \rho (R-r)}{V_1 l(1+R/r)} \frac{\Delta N + \Delta N'}{2} \text{ volts.}$$

If the cylinder V_1 is made of paper, the following dimensions seem to be reasonably convenient limits, so that, for $\Delta N = 0.0001$ cm.,

$$L = 5 \text{ cm.} \quad t = 0.2 \text{ cm.} \quad \rho = 1 \quad l = 100 \text{ cm.} \quad V_1 = 300 \text{ volts}$$

whence

$$V_3 = 3.8 \times 10^{-4} \text{ volts, or about } 10^{-4} \text{ volts per ring.}$$

One should thus be able to measure voltages even within 4×10^{-4}; but on trial the actual limits fall much within this. The use of wide apparatus has the advantage, only, of diminishing the effect of appurtenances like the mirror, etc. In the practical work below, however, these limits could not be reached, for reasons which will appear.

The idiostatic method under the same circumstances, $\Delta N = 0.0001$ cm., should just measure $V_3 = 0.5$ volt, so that alternating currents much within 1 volt will apparently be measurable. This method is naturally much less sensitive than the other, but its absolute character and its adaptation to alternating currents are of interest. The sensitiveness of the idiostatic electrometer as here designed and in the above case of the absolute electrometer would thus appear to have the same practical limit. In the way of absolute measurement nothing has been gained.

149. Equations. Disk electrometer.—In this case a charged disk with a guard ring (the apparatus to be described hereafter, §155, figs. 112 and 113) at potential V_1 is suspended bifilarly, as above, between the two concentric parallel disks of the condenser at potentials V_3 and V_2. The adjustment may be regarded as the extreme case of the cylinder electrometer with closed ends, and the equations will be, necessarily, nearly the same. Let d be the distance apart of the plates of potential V_3 and V_1, D the distance between the plates of potential V_3 and V_2, r the radius of the movable disk. The total energy W of the variable system is then, after reduction,

$$W = \frac{r^2}{8\pi} \left\{ \frac{(V_3 - V_1)^2}{d} + \frac{(V_1 - V_2)^2}{D-d} \right\}$$

and the corresponding mechanical force will be

$$X = \frac{r^2}{8} \left(\frac{V_1 - V^2}{D-d} + \frac{V_3 - V_1}{d} \right) \left(\frac{V_1 - V_2}{D-d} - \frac{V_3 - V_1}{d} \right)$$

which depends essentially on d as well as on D.

Let the disk be in the middle, or $2d = D$, and put $X = Mg\Delta N/l$ as above, where M is now the mass of the disk and appurtenances, ΔN the interferometer displacement, l the length of the bifilar pendulum, and g the acceleration of gravity. Then

$$(V_3 - V_2) \left(V_1 - \frac{V_2 + V_3}{2} \right) = \frac{MgD^2}{lr^2} \Delta N$$

Let $V_2=0$ and $M=\pi r^2 t\rho$, t being the thickness and ρ the density of the disk, the latter being sufficiently large so that the appurtenances may be ignored. Then on commutation and in electrostatic units, ΔN being the mean displacement,

$$V_3=\frac{MgD^2}{V_1 l r^2}\Delta N=\frac{\pi t\rho g D^2}{V_1 l}\Delta N$$

which (for a sufficiently large disk) is independent of its area.

To estimate the limiting sensitiveness the following apparently reasonable values may be inserted:

$V_1=\frac{1}{3}$els. $t=0.05$ cm. $\rho=1$ $D=0.1$ cm. $\Delta N=10^{-4}$ cm. $l=10^2$ cm.

whence

$$V_3=1.4\times 10^{-3}\text{ volts}$$

The limiting sensitiveness is thus of the same order as in the cylindrical case for the same V_1, as might have been anticipated. It is probable, however, that the present conditions may be more nearly realized in practice, as the apparatus is essentially simpler.

If $V_2=V_1=0$, the idiostatic case is identical with the absolute electrometer of §147.

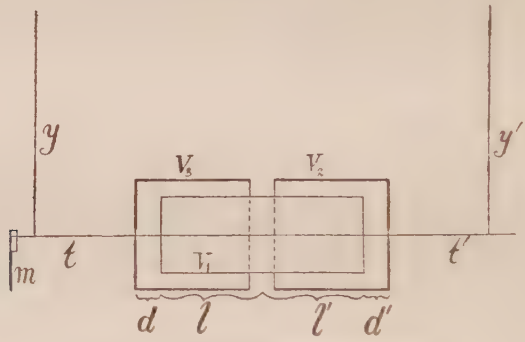

FIG. 104.—Closed field electrometer.

150. The closed field electrometer (disk and cylinder combined).—If the two cases of the preceding paragraphs be combined as in fig. 104, where the symbols of potential and distance are the same as before, the energy of the system is, in electrostatic units,

$$W=\frac{1}{8}\left\{(V_3-V_2)^2\left(\frac{r^2}{d}+L\frac{R+r}{R-r}\right)+(V_1-V_2)^2\left(\frac{r^2}{d'}+L'\frac{R+r}{R-r}\right)\right\}$$

and hence the forces become

$$X=\frac{1}{4}\left(\frac{r^2}{d^2}+\frac{R+r}{R-r}\right)(V_3-V_2)\left(V_1-\frac{V_2+V_3}{2}\right)=\frac{Mg}{l}\Delta N$$

If $V_2=0$, then

$$V_3=\frac{4Mg\Delta N}{V_1(r^2/d^2+(R+r)/(R-r))l}$$

after commutation, where L is the length of the cylinder. The sensitiveness of this apparatus depends very largely on d—that is, upon the disk—in any practical case; but it should be more nearly absolute. Experiments were not made. In fig. 104 the distances d, l, l', d', are used in the equations. Also

V_1 = the closed cylinder.
V_3, V_2 = the hollow half-cylinders with their open ends confronting each other, coaxially with V_1.
tt' = the horizontal steel wire fixed to V_1 and passing through perforations in the closed ends of V_2 and V_3.
m = the mirror (slot suspension).
y, y' = the bifilar pendulum supports.

151. Corrections.—The most important consideration to be made here is the effect attributable to the want of symmetry in the orientation of the disk or movable charge, supposing the latter and the plates are quite parallel. Let k be the axial distance of the uncharged disk from the plane midway between the condenser plates (guard ring). In such a case, if the electric displacement is ΔN, the quantity $\Delta = k + \Delta N$ must be added on one side and subtracted on the other, so that

$$d = \frac{D}{2} + \Delta \qquad d' = \frac{D}{2} - \Delta$$

Thus the displacing force is, after reduction:

$$X = \frac{r^2}{2}\left(\frac{V_1 - V_2}{D - 2\Delta} + \frac{V_3 - V_1}{D + 2\Delta}\right)\left(\frac{V_1 - V_2}{D - 2\Delta} - \frac{V_3 - V_1}{D + 2\Delta}\right)$$

which, if $a = V_3 - V_2$ and $b = 2V_1 - (V_2 + V_3)$, may be further reduced to

$$X = \frac{ab}{2}\frac{r^2}{D^2}\left(1 + 2\frac{\Delta}{D}\left(\frac{a}{b} + \frac{b}{a}\right)\right)$$

if $4\Delta^2$ is neglected in comparison with D, and where $X = Mg\Delta N/l$. If $\Delta = 0$, this reduces to the equation above.

If nothing is neglected and under the assumption of a uniform field, the equation is, for a positive charge, V_3, corresponding to a displacement $\Delta N'$ with $V_2 = 0$,

$$\frac{2Mg\Delta N'}{lr^2} = V_3(2V_1 - V_3)\frac{D^2 + 4\Delta^2}{(D^2 - 4\Delta^2)^2}\left(1 + \frac{2D\Delta}{D^2 + 4\Delta^2}\left(\frac{2V_1 - V_3}{V_3} + \frac{V_3}{2V_1 - V_3}\right)\right)$$

and for a negative charge, $-V_3$, corresponding to a displacement, $-\Delta N''$,

$$\frac{2Mg\Delta N''}{lr^2} = V_3(2V_1 + V_3)\frac{D^2 + 4\Delta^2}{(D^2 - 4\Delta^2)^2}\left(1 - \frac{2D\Delta}{D^2 + 4\Delta^2}\left(\frac{2V_1 - V_3}{V_3} + \frac{V_3}{2V_1 - V_3}\right)\right)$$

The mean of the equations, $\overline{\Delta N} = \frac{1}{2}(\Delta N' + \Delta N'')$, after reduction becomes

$$\frac{Mg\overline{\Delta N}}{l}\frac{D^2}{r^2}\frac{(1 + 2\Delta/D)^2}{V_1} = V_3$$

the corrected equation required, reducing to the above case, when $\Delta = 0$. The correction factor is thus $1/F = (1+2\Delta/D)^2$ and has been given in table 93 and fig. 105 for both positive and negative values of Δ.

TABLE 93.—Values of the factors F and $1/F$. $M = 1.0865$ g.; $D = 1.04$ cm.; $l = 23.5$ cm.; $r = 3.065$ cm.; $V_1 = 250$ volts.

$+\Delta/D$	F	$1/F$	$-\Delta/D$	F	$1/F$
0.10	1.44	0.69	0.10	0.64	1.56
.15	1.69	.59	.15	.49	2.04
.20	1.96	.51	.20	.36	2.78
.25	2.25	.44	.25	.25	4.00
.30	2.56	.39	.30	.16	6.25
.35	2.89	.35	.35	.09	11.11
.40	3.24	.31	.40	.04	25.00
.45	3.61	.28	.45	.01	100.00

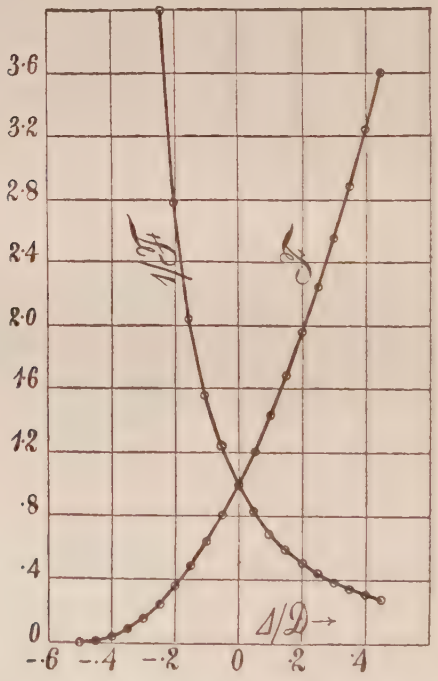

FIG. 105.—Graph showing reduction factors for different displacements.

It is now easy to discuss the conditions of equilibrium, for the forces X are given by the equations (second member referring to the pendulum and the third member to the electrical forces)

$$X = \frac{Mg\Delta N}{l} = V_1 V_3 \frac{r^2}{D^2} \frac{1}{(1+2\Delta/D)^2}$$

Hence, if $\Delta N=\Delta$, $k=0$, the condition under which the disk just moves, without interruption, from the guard ring to the condenser plates, *i.e.*, the limiting value of the potential products (V_1V_3), for stable positions for the disk, since

$$\frac{dX}{d(\Delta/D)}=\frac{MgD}{l}=(V_1V_3)\frac{r^2}{D^2}\frac{-4}{(1+2\Delta/D)^3}$$

is (in electrostatic units)

$$(V_1V_3)=-\frac{Mg}{4l}\frac{D^3}{r^2}\frac{(1+2\Delta/D)^3}{\Delta/D}$$

Assuming $V_1=250$ volts, the forces X for the pendulum and the electric field have been given in table 95 and fig. 106.

TABLE 94.—Electric forces. V_3 charged, $V_2=0$, $V_1=250$ volts. $M=1.0865$ g.; $D=104$ cm.; $l=2.3.5$ cm.; $r=3.065$.

V_3	$\frac{\Delta}{D}$	X	V_3	$\frac{-\Delta}{D}$	X
20	0.10	0.335	20	0.10	0.756
	.15	.286		.15	.985
	.20	.246		.20	1.340
	.25	.215		.25	1.930
	.30	.189		.30	3.016
	.35	.167		.35	5.361
	.40	.149		.40	12.063
	.45	.132		.45	48.252
100	.10	1.676	100	.10	3.779
	.15	1.428		.15	4.924
	.20	1.231		.20	6.700
	.25	1.073		.25	9.650
	.30	.943		.30	15.080
	.35	.835		.35	26.605
	.40	.745		.40	60.315
	.45	.659		.45	241.260
140	.10	2.346	140	.10	5.290
	.15	1.999		.15	6.893
	.20	1.723		.20	9.380
	.25	1.502		.25	13.510
	.30	1.320		.30	21.110
	.35	1.169		.35	37.327
	.40	1.042		.40	84.441
	.45	.923		.45	337.760

If, now, we insert the value of V_3 from the above equation and reduce, $-6\Delta/D=1$ or $-\Delta=D/6$

Hence the value of V_3 which corresponds to tangency is

$$V_3=\frac{Mg\,D^3}{lV_1r^2}\left(-\frac{1}{6}\right)\left(\frac{2}{3}\right)^2=\frac{2}{27}\frac{MgD^3}{lV_1r^2}$$

or $V_3=145$ volts, above which charge the disk passes continuously from guard ring to plate.

In fig. 106 the case of tangency is well indicated, the line referring to the gravitational forces and the curves to the electrical forces, supposing $V_1=250$ volts.

If the suspension is provided with a horizontal micrometer by which it can be shifted as a whole from k to k', taking the needle with it, k may be eliminated. But the expression is not simple.

Let $\sqrt{\Delta N}=x$, $\sqrt{\Delta N'}=x'$, and $k'-k=\kappa$. Then

$$k=\kappa x'/(x-x')+\left(\frac{D}{2}+x^2+x'x+x'^2\right)$$

It would be more convenient to find k from known potential V_1 and V_3.

The idiostatic method needs a corresponding correction, and if Δ^2 is neglected in comparison with D, then

$$\left(1-2\frac{\Delta}{D}\right)^2\frac{2MgD^2}{lr^2}\Delta N=V_3^2$$

As the new factor is practically k or constant, V_3^2 is linear with ΔN. If, as above indicated, the suspension is provided with a horizontal micrometer by which it can be shifted as a whole from k to k', taking the needle with it, k may be eliminated. But the expression is not simple. Let

$$\sqrt{\Delta N}=x,\ \sqrt{\Delta N'}=x' \quad \text{and} \quad k'-k=\kappa$$

Then

$$k=\kappa x'/(x-x')+\left(\frac{D}{2}-(x^2+x'x+x'^2)\right)$$

It would be more convenient to find k from known potential V_1 and V_3.

If $V_2=V_3=0$, and the disk V_1 is charged, the equation reduces to

$$\frac{2Mg(D^2-4\Delta^2)^2}{lr^2(D^2+4\Delta^2)}\Delta N=2V_1\frac{2D\Delta}{D^2+4\Delta^2}2V_1$$

or

$$V_3^2=MgD^2(1-4\Delta^2/D^2)^2\Delta N/4lr^2(\Delta/D)$$

The equation may be written in terms of the two forces X (gravitational and electric)

$$X=\frac{Mg\Delta N}{l}=\frac{4r^2}{D^2}V_1^2\frac{\Delta/D}{(1-4\Delta^2/D^2)}=\frac{4V_1^2r^2}{D^2}F'$$

where

$$F'=\frac{\Delta/D}{(1-4\Delta^2/D^2)^2} \quad \text{and} \quad V_1^2=\frac{MgD^2}{4lr^2F'}\Delta N$$

The value of the factor F' is shown in table 95 and fig. 107.

TABLE 95.—Values of the factor F' and $1/F'$. $M=1.055$ g.; $D=0.612$ cm.; $l=23.5$ cm.; $r=3.065$ cm.; $V_3=V_2=0$.

Δ/D	F'	$1/F'$
0.10	0.109	9.174
.15	.181	5.525
.20	.283	3.534
.25	.445	2.247
.30	.732	1.366
.35	1.345	.741
.40	3.086	.324
.45	12.465	.080

With the aid of table 95 the two forces X may be at once computed, and they are given for different values of V_1 in table 96 and fig. 108 under the supposition that k is equal to zero or $\Delta = \Delta N$; *i.e.*, that the disk is initially symmetric.

TABLE 96.—Electric forces. $V_3 = V_2 = 0$. V_1 charged. $M = 1.055$ g.; $D = 0.612$ cm.; $l = 23.5$ cm.; $r = 3.065$ cm.

V_1	Δ/D	X/r^2	V_1	Δ/D	X/r^2	V_1	Δ/D	X/r^2	V_1	Δ/D	X/r^2
20	0.10	0.005	40	0.10	0.021	70	0.10	0.064	100	0.10	0.130
	.15	.009		.15	.034		.15	.105		.15	.215
	.20	.013		.20	.054		.20	.164		.20	.335
	.25	.021		.25	.084		.25	.259		.25	.528
	.30	.035		.30	.139		.30	.426		.30	.870
	.35	.064		.35	.254		.35	.779		.35	1.590
	.40	.146		.40	.583		.40	1.786		.40	3.645
	.45	.592		.45	2.367		.45	7.248		.45	14.793

The curves, fig. 108, indicate a tangency of the curves X/r^2, above V_1, at least 100 volts. Below this, therefore, there are necessarily two available points of equilibrium of the disk, one unstable at $\Delta N = 0$ and the other in

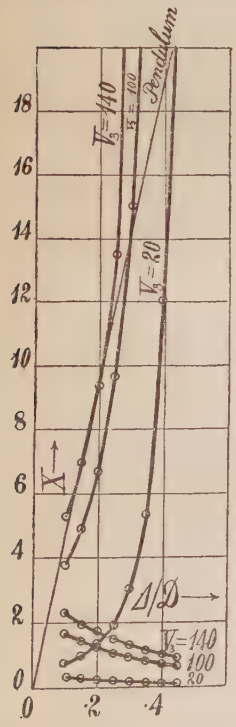

FIG. 106.—Graphs showing pendulum and electric forces at different potentials and displacements.

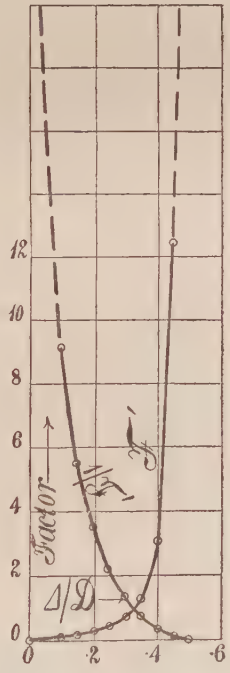

FIG. 107.—Graphs showing reduction factors at different displacements.

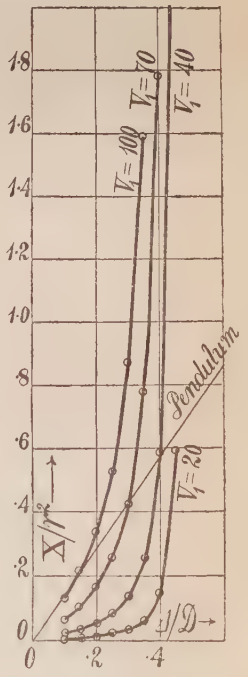

FIG. 108.—Graphs showing pendulum and electric forces at different potentials and displacements.

practice not very far from it. For high potentials the disk sweeps uninterruptedly from $\Delta N = 0$ into contact with the nearer plate, as the electric forces are now throughout in excess of the gravitational forces of restitution. In fact, the condition may be precisely stated, inasmuch as the values $dX/d\Delta$ may be easily derived. They are for the pendulum Mg/l and for the electric field

$$\frac{dX}{d\Delta} = \frac{4V_1^2r^2}{D^3} \cdot \frac{1+12\Delta^2/D^2}{1-4\Delta^2/D^2}$$

Equating them, we derive the voltage of transition, to be characterized by (V_1), as

$$(V_1)^2 = \frac{MgD^3}{4lr^2}$$

since $\Delta = 0$ at the origin. Hence above $(V_1) = 156$ volts the disk would move on any slight disturbance without interruption from the guard ring, $\Delta = 0$, to either plate of the condenser; but within (V_1) the apparatus is available for accurate measurement of V_1, if k is equal to zero by trial.

152. Experiments. Cylindrical electrometer; movable cylinder within.—Tests of the apparatus described were begun by using a rather heavy cylinder of aluminum, damped with a vane submerged in a cup of oil. The constants of the apparatus were as follows:

$M = 10.4$ g.	$l = 21$ cm.	$2R = 4.15$ cm.
$2r = 3.46$ cm.	$L = 6.7$ cm.	$V_1 = 250$ volts

The cylinder itself weighed but 6.546 grams; but air damping was quite inadequate, though the cylinder might easily have been etched to a more appropriate degree of thinness in acid.

TABLE 97.—Cylindrical electrometer; movable cylinder within (aluminum). $M = 10.4$ g.; $l = 21$ cm.; $r = 1.73$ cm.; $R = 2.075$ cm.; $V_1 = 250$ volts; $V_2 = 0$.

I			II			
Drum.	$10^3\Delta N$	V_2	Drum.	$10^3\Delta N$	V_2	Voltmeter.
5.2	1.29	95	4.7	1.18	74	70
4.1	1.02	75	3.3	.82	52	48
3.0	.74	54	2.5	.63	39	36
			1.4	.23	22	19
			.1	.03	2	0

The observations are given in table 97, showing the drum reading on the micrometer, the displacement ΔN on the micrometer and the voltages corresponding. The displacement is doubled by commutation. Compared with a voltmeter the data were too high, and the idiostatic method was inapplicable. In the second series of this table, the comparison with the

voltmeter shows that the observations are distributed as if an initial potential of 3 or 4 volts were superimposed upon them. These data are merely given to point out the difficulties in the use of a metallic cylinder, however thin. The apparatus containing such a cylinder is very insensitive, if liquid damping is resorted to, otherwise the swing of the needle is almost indefinitely long. It is interesting, nevertheless, to follow the ellipses which flash out at the extreme elongations of the vibrating cylinder.

It is therefore necessary to make use of paper cylinders, even if the possibility of securing more nearly accurate values of the diameter of cylinder is the advantage of the metallic appurtenance.

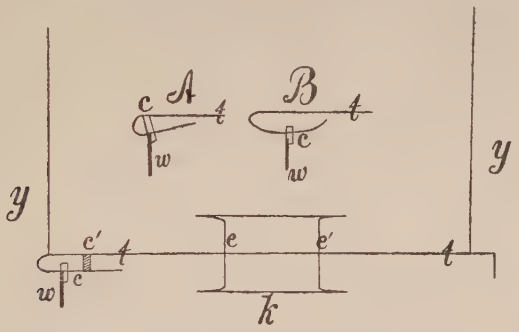

FIG. 109.—Suspension of inside cylinder of electrometer.

The gilt paper cylinder *k* was mounted as shown in fig. 109, *yy* being the bifilar suspension. The ends of the cylinder are closed by the reëntrant partitions *e* and *e'*, the object being to avoid the disk effect, by screening off the disk by the ends of the cylinder. The steel wire *tt* passes through the centers of the disks *ee'*, a drop of mucilage being sufficient for electrical contact and to keep the cylinder in place. The mirror *w* is attached by a bit of cork *c* to the bent end of the elastic rod. As the mirror must be adjustable around the horizontal axis (the apparatus, as a whole, may be rotated around the vertical), a second little piece of cork *c'* serves, when moved from left to right, to open the spring hook and rotate the mirror. Fig. 109, *A* and *B*, are other devices for this purpose. In the former a single piece of cork opens the spring and holds the mirror; in the latter the lower part of the hook is circular and the mirror is rotated on sliding the cork. Many other devices were tried, but probably a small piece of cork, slit vertically, and mounted on a straight rod, is as good as any. The difficulty in devising these parts is that both cork and mirror must be exceedingly light. No trouble was encountered in using a light plane mirror about one-fourth inch in diameter. To sharpen the ellipses the yellow image at the movable mirror should be screened off, leaving but the blue image and but two superposed spectra.

The first experiments were made with a cylinder of relatively small diameter having the constants, and showing the results as given in Series I of table 98.

TABLE 98.—Cylindrical electrometer; movable cylinder (gilt paper) within. $M = 1.613$ g.; $l = 21$ cm.; $R = 2.075$ cm.; $r = 1.66$ cm.; $V_1 = 250$ volts; $V_2 = 0$.

I.			II.			
Drum.	$10^3\Delta N$	V_3	Drum.	$10^3\Delta N$	V_3	Volt-meter.
16.4	4.1	55	6.6	1.65	22.0	19
10.3	2.6	34	9.2	2.29	30.6	29
9.7	2.4	32	9.4	2.36	31.6	30
5.3	1.3	18	10.0	2.50	33.4	32
.35	.1	1	16.1	4.02	53.7	52

Further experiments with the same instrument (somewhat improved), on being compared with the voltmeter, gave the values contained in Series II of the table.

A lighter gilt-paper cylinder, weighing with mirror, etc., $M = 1.049$ grams, $2R = 4.15$, $2r = 3.32$, was thereafter inserted, the other constants remaining the same as before. The behavior now was satisfactory throughout and the increased sensitiveness is shown in table 99, Series I.

TABLE 99.—Cylindrical electrometer; movable cylinder (gilt paper) within. $M = 1.049$ g.; $l = 21$ cm.; $R = 2.075$ cm.; $r = 1.66$ cm.

I. $V_1 = 250$ volts. $V_2 = 0$				II. Idiostatic method. $V_3 = V_2 = 0$			
Drum.	$10^3\Delta N$	V_3	Volt-meter.	Drum.	$10^3\Delta N$	V_1	Volt-meter.
9.1	2.27	19.7	15	4.77	2.38	102	101
18.8	4.71	40.9	41	2.83	1.41	78	81
28.7	7.17	62.3	61	1.81	.90	63	61
37.2	9.41	81.7	81	.73	.36	40	41
47.5	11.88	103.2	101				

The second part of the table contains the idiostatic results, in which the instrument, though less sensitive, is absolute.

The endeavor was then made to secure greater sensitiveness by increasing the diameter of the movable cylinder, and its constants were

$$M = 1.138 \text{ g.} \qquad 2R = 4.15 \qquad 2r = 3.83 \qquad L = 5 \text{ cm.}$$

so that the shell-like space between the cylinders was only $R - r = 0.16$ cm. thick. But with a charge of 250 volts the cylinder was pulled aside in contact with the stationary cylinders and observations had to be abandoned. With the idiostatic method, the results of table 100 were secured.

TABLE 100.—Cylindrical electrometer; movable cylinder (gilt paper) within. $M = 1.138$ g.; $l = 21$ cm.; $R = 2.075$ cm.; $r = 1.915$ cm. Idiostatic method; $V_3 = V_2 = 0$.

Drum.	$10^3\Delta N$	V_1
20.1	10.0	124
14.0	7.0	104
8.4	4.2	80
4.9	2.4	62
.8	.4	25

The march of results is fairly linear with the actual voltages, though the computed values of V_3 are necessarily inaccurate, actually in excess, owing to the fact that the small value, $R-r=0.16$ cm., is not vouched for in the case of the paper cylinder. The use of a smaller charging potential was tried with similar results.

TABLE 101.—Cylindrical electrometer; movable cylinder (gilt paper) within. $M=1.1050$ g.; $l=21$ cm.; $R=2.075$ cm.; $r=1.75$ cm.

I. $V_1=250$ volts. $V_2=0$.				II. Idiostatic method. $V_3=V_2=0$.			
Drum.	$10^3\Delta N$	V_3	Voltmeter.	Drum.	$10^3\Delta N$	V_1	Voltmeter.
0.8	0.2	1	2	0.15	0.08	15	15
2.9	.7	5	6	.50	.25	28	29
5.3	1.3	8	9	1.2	.60	43	41
9.3	2.3	15	15	2.2	1.12	60	61
23.3	5.8	37	41	3.7	1.87	77	81
33.9	8.5	53	61				
44.0	11.0	69	81				

The next cylinder to be inserted was of smaller diameter, and its constants and the records of results are given in table 101. In case of the charged needle the sensitiveness increases at the higher voltages, due no doubt to the growing asymmetry of the needle. Similarly the idiostatic method, fig. 110, *b*, in view of its small deflections, shows fairly regular results, though they diminish at high voltages.

In another adjustment, carefully made with reference to freedom and symmetry of cylinder, it was found that a charge of 250 volts could actually be carried, without deflecting the cylinder laterally into contact with the walls. The observations in Series II of table 102 were carried out in this way, and show the maximum sensitiveness obtained with short suspension.

TABLE 102.—Cylindrical electrometer; movable cylinder (gilt paper) within. $M=1.189$ g.; $l=21$ cm.; $R=2.075$ cm.; $r=1.90$ cm.

I. Idiostatic method. $V_3=V_2=0$				II. $V_1=250$ volts.			
Drum.	$10^3\Delta N$	V_1	Voltmeter.	Drum.	$10^3\Delta N$	V_3	Voltmeter.
8.75	4.37	87.8	88.0	7.0	1.74	6.1	5
5.35	2.67	68.6	68	8.7	2.17	7.6	7
5.80	2.90	71.5	70.5	13.2	3.31	11.6	11.5
2.90	1.45	50.5	50	18.1	4.53	16.0	15
1.70	.85	38	38	23.4	5.85	20.6	19

With a final closely fitting cylinder of gilt paper of a diameter probably as large as practicable, the data of table 102 and fig. 110, *a*, were found by the idiostatic method. These results for high voltages are quite satisfactory and the differences are more liable to be sought for in the voltmeter than

in the electrometer. It indicates the sufficiency of the equation assumed, apart from corrections for the ends of the cylinder, so that the latter can not be menacing.

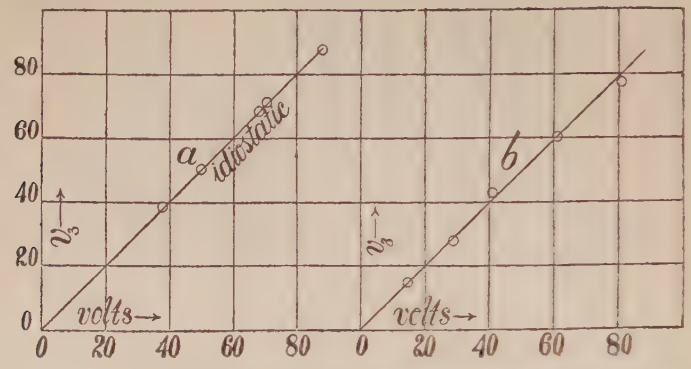

FIG. 110.—Observations with cylindrical electrometer. Cylinder inside.

Besides this, the method of the charged needle was tried. In this case, 250 volts was an excessive charge and the needle could no longer be freed from the stationary cylinder. With a charge of 87 volts (storage battery) and a single battery for V_3, the results were

$$10^3 \times \Delta N = 0.108 \qquad V_3 = 1.1$$

instead of 1.3 volts, the sensitiveness being thus 2×0.4 drum parts of double deflection per volt.

In addition to these experiments, a long suspension ($l = 150$ cm.), in which the sensitiveness would have been increased seven times or equivalent to 5×10^{-3} cm. per volt or 0.006 volt per vanishing ring, was installed. The ellipses were easily found, but were continually in motion, owing to the friction of air-currents moving across the wires. To make the adjustment available it would have been necessary to build a closed case around the bifilar suspension over 1.5 meters in height. It was not thought worth while to do this, and further experiments were abandoned.

153. Cylindrical electrometer; movable cylinder within. Summary.—The above experiments were made in the midst of the turmoil of a large city and near the engineering laboratories of a university. It is rather remarkable, therefore, that the ellipses were so easily found throughout and so easily made use of; but it was quite out of question to use the evanescence of rings by which the sensitiveness could have been increased over twenty-fold. Though the work was carefully done, it is intended merely to exhibit the general character of the method, inasmuch as the storage battery which was drawn upon was unavoidably in use elsewhere in the laboratory and the potential may have fluctuated.

The design of the apparatus with a movable inside cylinder is probably the least interesting of those used. Thus it is difficult to keep a paper

cylinder quite smooth or to give it a rigorous cylindrical shape, and the correction for the ends can scarcely be estimated. For high charges any asymmetry of the movable cylinder is liable to place it in contact with the fixed cylinders. Thus there is a limit of sensitiveness, from a purely instrumental point of view, not contemplated in theory. In the above experiments with short suspension (21 cm.), 7×10^{-4} cm. per volt was the largest double displacement practically obtained, which would mean about 0.04 volt per vanishing ring. With the long suspension 0.006 volt per ring may be estimated. It is far short of the theoretical datum of §148.

154. Experiments. Cylindrical electrometer; movable cylinder without. After a few preliminary experiments with the metal cylinder of aluminum, the gilt-paper cylinder was tried and was at once successful. The mirror was attached to the paper wing needed for damping by the aid of a bent piece of thin steel wire, cemented on so as to give a horizontal axis on passing through the perforation of the bit of cork holding the mirror. For a vertical axis the whole apparatus is rotated (*cf.* figs. 98 and 99). The results are given in table 103 and fig. 111, *a*.

TABLE 103.—Cylindrical electrometer; movable cylinder (gilt paper) without. $M = 2.075$ g.; $R = 1.75$ cm.; $r = 1.59$ cm.; $l = 21$ cm.; $V_1 = 250$ volts.

I.				II. $M = 1.0930$ g.			
Drum.	$10^3 \Delta N$	V_3	Volt-meter.	Drum.	$10^3 \Delta N$	V_3	Volt-meter.
11.2	2.79	18.7	18	24.9	6.22	21.9	21
22.9	5.72	38.2	38	47.3	11.82	41.6	41
35.3	8.83	59.1	58				
27.6	6.90	46.1	48				

The differences in this table are more liable to be of the voltmeter than of the electrometer. The needle easily carried a potential of $V_1 = 250$ volts. With $V_3 = 100$ volts, the needle became asymmetric and observations could no longer be taken. The sensitiveness is about 0.0003 cm. of double displacement per volt for the short suspension, so that 0.1 volt per ring is the equivalent datum. The present form is thus easily made as sensitive as the preceding form, besides being much simpler in general design and installation.

The experiment was now pushed a step further in the direction of sensitiveness by using an even lighter paper cylinder with paper wings, the needle having the constants given in the second series of table 103 and fig. 111, *b*. The sensitiveness is now about 0.0006 cm. of double displacement per volt, twice that of the preceding case, as it should be. This apparatus did not, however, behave as satisfactorily as the other, there being greater tendency of the movable cylinder to cling to the stable parts, whenever V_1 was high. In case of smaller potentials or of the idiostatic method

there would be no difficulty in this respect. No doubt if greater time and patience were spent on the work (a cylinder of celluloid suggests itself) the final result could be somewhat improved; but the limit found (6×10^{-4} cm. or 20 rings per volt) will not easily be exceeded.

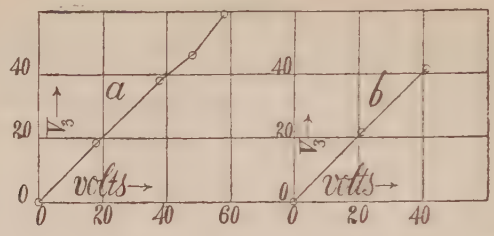

FIG. 111.—Observations with cylindrical electrometer. Cylinder outside.

155. Disk electrometer. Apparatus.—The disk electrometer deserves special attention because it is simpler in design and practically more sensitive than the cylinder types; but at the same time it is more treacherous, and without special precautions there is danger of short-circuiting the highly charged disk, while the sensitiveness is enormously variable in response to any unsymmetrical position of the disk. The instrument used is shown in figs. 112 and 113, in sectional side and front elevation. V_1 is

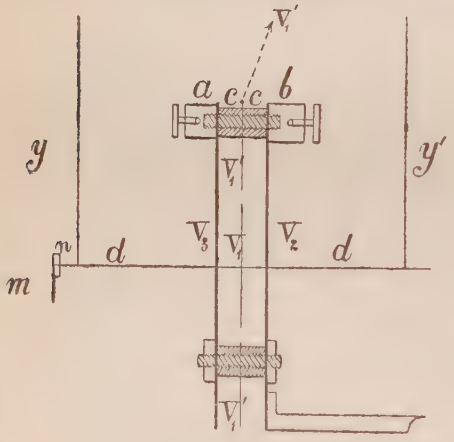

FIG. 112.—Disk electrometer. End view.

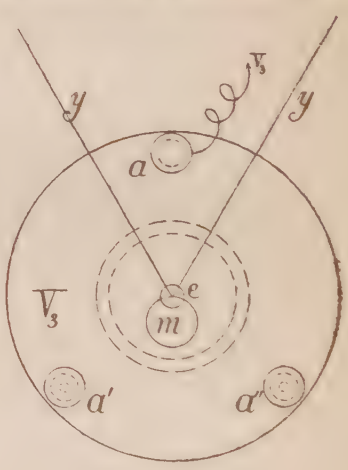

FIG. 113.—Disk electrometer. Front view.

the charged disk on the bifilar suspension of very thin copper wire yy', 0.007 cm. in diameter. The disk is made of thin mica, silver-plated, carried by the horizontal axial steel rod dd, and surrounded by the guard ring of very thin copper V_1'. Parallel to the disk and equidistant (d) from it are the plates V_3 and V_2 of the condenser at a distance D apart, so that D is twice d. The plate V_2 is earthed and firmly held on the arm of the interferometer. The plates V_3 and V_2 are spaced at three points

by hard-rubber gaskets, *cc*, through the holes of which hard-rubber screws are passed, the plates being ultimately secured by nuts *a*, *a'*, and *a''* on the outside of the plates. The nuts *a* terminate in clamp screws. The guard ring V_1' and the suspension wires *yy'* are in metallic connection at the tops of the suspension, the latter being the same already shown in figs. 98 and 99. The small mirror, *m*, is attached to a small plate of cork *n*, which is slotted parallel to the rod *dd*, the latter being clutched by the jaws of cork which make up the sides of the slot. In this way *m* may be rotated around a horizontal axis, while the apparatus as a whole may be revolved about a vertical axis.

If the grating is capable of being raised or lowered, it is not difficult to adjust the apparatus and find the ellipses. The damping of the disk is naturally good, though it may be improved by surrounding it with the case shown in fig. 98.

156. Experiments with the disk electrometer.—The experiments were begun with but a small distance, *D*, between the plates of the electrometer. In such a case the disk can carry but a slight potential before it is drawn across to the condenser plates and short-circuited. In fact, though the mica disks may be made very light, the annoyance of short-circuiting is correspondingly increased and the great advantage of sensitiveness can not for this reason be realized unless the idiostatic method is used. This is the case in table 104 and fig. 114, *e*.

TABLE 104.—Disk electrometer. $M=1.055$ g.; $D=0.612$ cm.; $l=23.5$ cm.; $r=3.065$ cm. Idiostatic method: $V_3=V_2=0$.

	Drum.	$10^3\Delta N$	V_1	Volt-meter.	10^3k
I	11.7	5.84	22.3	18	82
	79.7	39.82	58.3	38	207
II	2.38	1.19	19.4	18	25
	9.75	4.87	39.3	38	10
	22.47	11.23	59.6	57.5	11
	51.5	25.75	90.2	84	23
	82	41.01	113.9	104	27

Larger voltages threw out the coincidence of spectra, so that the ellipses could not be obtained because of asymmetry. The table shows that whereas the magnitude V_3 is of fair order of value for small potentials, it rapidly becomes excessive, owing to the fact that $k+\Delta N$ is no longer negligible in comparison with *D*. The ΔN in such a case is algebraically added to the original asymmetry of the disk, if *d* is greater or less than $D/2$. The importance of this superposition increases as the square of the potential and is thus serious at high voltages. A second and more careful adjustment of the same disk showed (by the use of the idiostatic method) a much more favorable succession of values (fig. 114, *f*), while at the same time there

is necessarily marked reduction in sensitiveness. The uncorrected V_3 is thus much nearer the actual value and more gradually fails as the high voltages are approached. The constants k computed for the first series are not only large, but differ unexpectedly. In a measure it is probably indicated that the larger deflection proceeds from a position of increased asymmetry. In agreement with this, data for k in the second series are

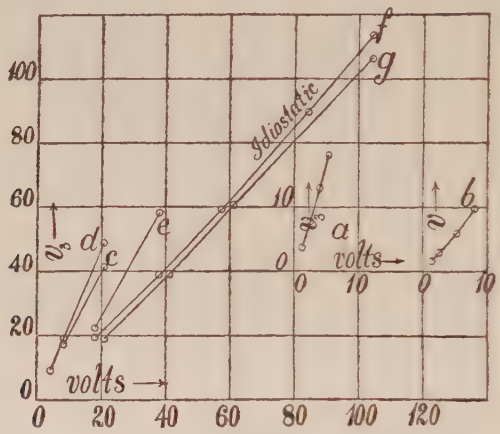

FIG. 114.—Observations with disk electrometer.

satisfactory and but slowly increase. The use of the apparatus for absolute measurement of potentials above 20 volts in case of a carefully adjusted disk is therefore not inadmissible.

TABLE 105.—Disk electrometer. $M=1.055$ g.; $D=0.612$ cm.; $l=23.5$ cm.; $r=3.065$ cm.; $V_1=101$ volts.

Drum.	$10^3\Delta N$	V_3	Volt-meter.
9.6	2.4	3.8	1.3
20.4	5.1	7.9	2.6
33.4	8.36	13.1	4.0
46.8	11.7	18.3	5.3

The disk was now charged with the storage battery to 101 volts and a number of small potentials measured at the plates. The results are given in table 105 and fig. 114, *a*, showing that the computed and uncorrected values are about three times as large as the true voltages. The sensitiveness is here surprisingly large, almost 8 drum parts of 2×10^{-3} cm. per volt, *i.e.*, 70 rings per volt. The distribution of results is nevertheless obviously linear and proportional to the true voltages. To account for this result by aid of the equation

$$V_3=\frac{Mg\Delta N}{lV_1}\frac{D^2}{r^2}(1-2\Delta/D)^2$$

is not impossible, if the asymmetry is such as to make the terms in Δ/D essentially negative. Yet in the case of a large value of Δ, the results are so lacking in probability that a lack of uniformity or of variation in the field is more liable to be in question.

On spacing the plates further, $D=1.04$ cm., and carefully adjusting the disk it carried a charge equivalent to $V_1=250$ volts easily, so long as V_3 did not exceed about 20 volts. On increasing the potential above this, short-circuiting accidentally occurred which destroyed the apparatus. The single datum obtained was $\Delta N=0.0273$, for which $V_3=49.8$ instead of 18 volts, the excessive result being due to causes of the kind just discussed.

A new and lighter disk was thereupon introduced, weighing but 0.607 gram. As it failed to carry a charge quite as large as $V_1=250$ volts, the only available smaller one, $V_1=104.5$ volts, was given to it. The data found are contained in table 106 and reproduced in fig. 114, *b*.

TABLE 106.—Disk electrometer. $D=1.04$ cm.; $l=23.5$ cm.; $r=3.065$ cm.

	Drum.	$10^3\Delta N$	V_3	Voltmeter.		Drum.	$10^3\Delta N$	V_3	Voltmeter.
I. $V_1=104.5$ volts. $M=0.607$ g.	2.9	0.73	1.8	1.3	III. $V_1=250$ volts. $M=1.086$ g.	104.1	26.02	49.0	21
	5.0	1.25	3.1	2.5		40.6	10.14	19.1	8.3
	9.9	2.48	6.2	5.2		19.2	4.79	9.0	4.1
	15.7	3.92	9.9	8.0	IV. Idiostatic method; $V_3=V_2=0$. $M=1.086$ g.	0.77	0.38	19.1	21
II. $V_1=250$ volts. $M=1.086$ g.	88.9	22.2	41.8	21		3.30	1.65	39.4	41
	36.3	9.1	17.1	8.2		7.95	3.97	61.1	61
						24.20	12.10	106.7	104

The uncorrected results for V_3 are here much nearer the true values, *i.e.*, about 1.2 times too large, than was the case in the preceding table, so that the correction for asymmetry is probably applicable. The mean trend of the locus is through zero. Sensitiveness is naturally much lower than above, showing $\Delta N=5\times10^{-4}$ cm. per volt The experiment well indicates how markedly dependent the constants of the instrument are on the position of the disk. Similar examples will be given below.

The same disk was now weighted with a rider, making the total mass 1.086 grams, with the object of charging it to 250 volts. The data for V_3 are given in the second series of table 106 and in fig. 114, *c*. The uncorrected results, while maintaining proportionality, are about twice too large.

A later adjustment gave the values in Series III and fig. 114, *b*, which are again two times too large. In spite of the effective weight of the disk, sensitiveness has risen in both cases to about 10^{-3} cm. per volt, which is quite out of proportion with M/V_1 and in contrast with the nearly normal values of V_3 in the first series.

The data obtained idiostatically, where the deflections are essentially small, are contained in the fourth series of table 103 and show an excellent agreement with the true voltages, as is indicated in fig. 114, *g*. Discrepancies are as liable to be in the voltmeter as in the electrometer. The

values of k given for this table show how nearly a true condition of symmetry was attained, as its mean value from the equation

$$V_3^2 = \frac{2MgD^2}{lr^2}\Delta N\left(1-2\frac{\Delta}{D}\right)^2$$

is but -0.0085 cm.

The data of table 106, as a whole, illustrate very well the peculiarities of the disk method, giving evidence both of its relatively great sensitiveness (the double displacements being even 2×10^{-3} centimeters per volt) on the one hand, and the variation of sensitiveness as the result of a more or less unsymmetric position of the disk on the other. The ratio of observed and actual voltages is fairly constant. The question then arises as to the degree to which the latter difference may be corrected. There is, in many cases, a peculiar shift of the zero of displacement for the uncharged apparatus which is not easily accounted for; though, from another point of view, it is truly astonishing that a suspended disk should adjust itself to a given position with an accuracy comparable with the wave-length of light. In the experiments detailed, such difficulties were eliminated by taking mean results, but usually the position in question was actually stable. If the shortcomings in question can be overcome, the practical limits of the apparatus as here constructed should, for short suspensions (23 cm.), be about 0.015 volt per vanishing ring.

157. Further experiments with the disk electrometer.—The interesting feature of the preceding result is the large range of variability in the sensitiveness of the apparatus. It was therefore thought worth while to throw further light upon the investigation by purposely tipping the apparatus, in order that the disk might lie on one side or the other of the guard ring. The same voltage (4 Leclanche cells, 5.7 volts) was evaluated for each position of the disk, which, being light, did not admit of a potential much in excess of $V_1 = 101$ volts. Table 107 is a record of the results in which the deflections were also taken for the case $V_3 = V_2 = 0$, with the total significant potential on the disk.

TABLE 107.—Experiments with eccentric disk. $M = 0.6075$ g.; $D = 1.04$ cm.

$V_2 = V_3 = 0$; $V_1 = 101$ volts.				$V_1 = 101$ volts; $V_2 = 0$			
Position of disk.	Drum.	$10^3\Delta N$	$10^3 k$	Drum.	$10^3\Delta N$	V^2	Voltmeter.
Tipped forward...	+28.5	+14.2	+81	13.82	3.46	9.0	5.7
Intermediate.....	−25.0	−12.5	−71	7.33	1.83	4.8	5.7
Tipped rearward..	−71.2	−35.6	−203	7.3	1.82	4.8	5.7
Slightly forward..	+16.2	+ 8.1	+46	7.5	1.87	4.9	5.7
More forward....	+11.2	+ 5.6	+32	11.8	2.95	7.7	5.7

Applying to the first half of the table the approximate equation

$$k/\Delta N = \frac{MgD^3}{4lr^2V_1^2} - 1$$

the results were as shown in the column under k. It is not, however, quite as consistent as was anticipated, inasmuch as the same value of k did not reappear when the apparatus was tipped back apparently to its original position. Moreover, the central position does not clearly correspond to $k=0$. Hence it seems that $k=0$ is determined by the geometry of a non-uniform field. Neither do the values of V_3 correspond very closely to the values of k. The apparatus is more sensitive when the disk V_1 is on the side of the plate V_3 and about equally so when central or when on the side of $V_2=0$. In the latter cases V_3 as computed comes out for the first time distinctly less than the datum given by the voltmeter, the usual tendency being in the direction of excessive values.

TABLE 108.—Experiments with eccentric disk. $M=1.086$ g.; $D=1.04$ cm.

$V_2=V_3=0$; $V_1=250$ volts.				$V_2=0$; $V_1=250$ volts.			
	Drum.	$10^3\Delta N$	10^3k	Drum.	$10^3\Delta N$	V_3	Voltmeter.
I	+29.05	+14.52	+13.9	126.9	31.72	59.9	20.5
				49.1	12.27	23.0	8.2
				23.2	5.81	10.9	4.1
				12.6	3.15	5.9	2.0
II	+35.15	+17.57	+16.7	103.0	25.75	48.5	20.5
				39.4	9.84	18.5	8.2
				18.3	4.58	8.0	4.1
III	−45.1	−22.55	−21.5	107.75	26.94	50.7	20.5
				42.9	10.72	20.2	8.2

The light disk is difficult to manipulate, as its weight is scarcely sufficient to stretch the wires. In the experiments of table 108 and fig. 115, *I*, the disk was therefore weighted with a rider and a similar series of data was taken, although $V_1=250$ volts was carried by the disk only in cases where its position was nearly central. Consequently the adjustments made contain but a slight departure from that position.

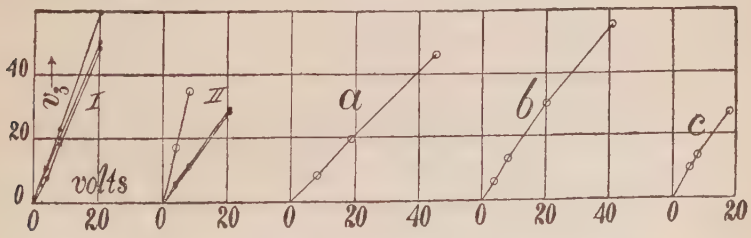

FIG. 115.—Observations with disk electrometer.

The disk in the three adjustments was therefore successively placed on the two sides of the central position within fractions of a millimeter. The addition of a rider did not make it essentially more stable, as slightly greater displacements drove it quite across, into contact with one or the other of the plates of the condenser. This was even the case on the addition of heavier riders. The computed values of V_3 are in all cases two or

three times the true values, though the proportionality is maintained except in the second series. The effect of k on V_3 does not appear.

Finally, the disk was made still heavier by the addition of a second rider of 0.709 gram. Nevertheless (as indicated) it was still unstable, except very near the symmetrical position. It was possible, however, to secure a change of sign in deflection. The results are given in table 109 and fig. 115, *II*.

TABLE 109.—Experiments with eccentric disk. $M=1.791$ g.; $D=1.04$ cm.

	$V_2=V_3=0$; $V_1=250$ volts.			$V_2=0$; $V_1=250$ volts.			
	Drum.	$10^3\Delta N$	10^3k	Drum.	$10^3\Delta N$	V_3	Voltmeter.
I	+110.25	+55.12	+122.6	21.85	5.46	16.9	4.1
				45.0	11.25	34.8	8.2
II	− 24.5	−12.25	− 27.2	7.6	1.90	5.9	4.1
				14.4	3.60	11.2	8.2
				37.8	9.46	29.3	21.0
III	− 47.27	−23.63	− 52.6	6.8	1.71	5.3	4.1
				14.0	3.51	10.9	8.2
				36.4	9.11	28.2	21.0

In the first of these adjustments k comes out over a millimeter distant from the symmetrical position in one case and about 0.5 mm. on the other side in another. In the first case, V_3 is over four times the true value, the highest ratio heretofore obtained, although the sensitiveness (2.8×10^{-3} cm. of double deflection per volt) is not much in excess of the earlier values. The second and third series are again near the true value in spite of not inconsiderable values of k. Apart from the abnormally large sensitiveness the curves are regular in proportion to the voltage.

158. Case of the inclosed disk.—With the object of obtaining a more uniform field, the disk electrometer was now modified as shown in fig. 116, where V_3 and V_2 are the plates of the condenser and V_1 is the disk inclosed in the short cylindric or drum-shaped tube within the guard ring V_1'. The disk, as before, is supported by the axial fine steel wire tt', passing through perforations in V_3 and V_2 and suspended by the bifilar system yy'. The disk is again well damped naturally. V_2 is usually earthed. The difficulty with this design is the impossibility of observing the disk, with a view to its symmetric adjustment. By pushing tt' longitudinally, the disk may be seen in the space between plate and tube and some adjustment made; but this is not quite adequate. The plates and guard ring are spaced as before by three hard-

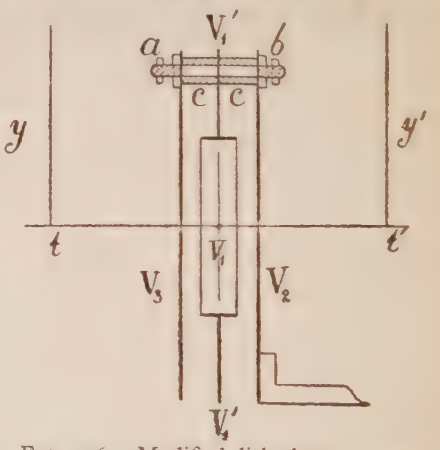

FIG. 116.—Modified disk electrometer.

rubber rings *cc*, with a hard-rubber screw passed through the perforations. On the outside are the brass connectors *a* and *b*. V_1' and *yy'* are in metallic connection at all times.

Experiments were begun with the light disk, $M = 0.607$ gram, which was charged to 110 volts, as it would not carry an appreciably higher voltage. Consequently a rider was thereafter added, making $M = 1.086$ grams, and the disk charged as far as 250 volts. The results are given in table 110 and fig. 115, *a*.

TABLE 110.—Experiments with inclosed disk. $M = 1.086$ g.; $D = 1.04$ cm.; $l = 23.5$ cm.; $r = 3.065$ cm.

V_1	Drum.	$10^3 \Delta N$	V_3	Voltmeter.
34	4.2	1.05	8.1	8.5
250	42.0	10.5	19.7	19.0
	97.9	24.5	46.0	45.5

These results, though obtained under very different conditions, are practically coincident and the discrepancies are as liable to be in one instrument (voltmeter) as the other.

Some time after, an accidental earth developed in the storage battery and destroyed this electrometer. The old disk was then again inserted and the experiments detailed in table 111 were made.

TABLE 111.—Experiments with inclosed disk. $M = 1.060$ g.; $D = 1.04$ cm.; $l = 23.5$ cm.; $r = 3.065$ cm. $V_1 = 250$ volts.

	Drum.	$10^3 \Delta N$	V_3	Voltmeter.
I...	6.4	1.59	5.8	4.0
	14.2	3.55	13.0	8.2
	33.3	8.32	30.6	20.5
	60.4	15.10	55.4	41.0
II...	10.2	5.12	9.4	6.0
	14.6	7.31	13.4	8.6
	29.5	14.77	27.1	18.5

The error of asymmetry in the first series is marked, showing inadequate adjustment. The curve, fig. 115, *b*, moreover, is not straight, as the disk did not move quite parallel to itself. An improvement of those imperfections was then attempted, as shown in the second series of the table and in fig. 115, *c*, but not successfully. The curve is again not quite straight. The experiments as a whole are unsatisfactory, inasmuch as the disk only just sustained the potential of 250 volts and became unstable on slight readjustment. An appropriately lower potential was not available. Further work was therefore abandoned. It is probable that table 110, where

the conditions were more favorable, gives the better account of the behavior of the present apparatus.

To summarize: the enormous variation of the sensitiveness of the disk electrometers as depending upon the position of the disk, k, has therefore failed of interpretation; *i.e.*, the correction for V_3 does not seem to follow the above equations. The field is therefore probably far from uniform, possibly consisting of a conical tube of force between plate and disk on the side toward which the disk leans and of a more nearly cylindric tube on the opposite side, where the tube must pass through the circular perforation in the guard ring. The result is an empiric instrument in which the deflections are proportional to the voltages to be measured, of enormously increased sensitiveness, even 2×10^{-3} cm. per volt, but not yet sensitive enough to be immediately valuable for practical purposes. The idiostatic instrument, for voltages above 20 volts (after the disk has been adjusted for $k=0$ by comparing the positions of the charged and uncharged disk), may in some cases be useful.

159. Case of the unsymmetric disk.—The cause of the departure from linearity in the preceding experiments is to be referred to a slight asymmetry in the disk, whereby an effect varying as the square of voltage of the disk is superimposed on an effect varying as its first power. To eliminate the non-linear term, it should be sufficient to obtain no deflection in the case of earthed plates, when the needle is successively charged and uncharged. In fact, the charged non-symmetrical needle between earthed plates introduces an interesting method of electrometry as follows.

Let k be the amount of non-symmetry for a disk whose mean distance from the plates D cm. apart would be $d=D/2$. Hence for any displacements ΔN, the distance of the disk from the condenser plates will be

$$d=D/2+(k+\Delta N) \qquad D-d=D/2-(k+\Delta N)$$

Hence the displacement force is (after reduction)

$$X=\frac{V_1^2r^2}{2}\,\frac{k+\Delta N}{D/2}\,\frac{1}{D^2/4-(k+\Delta N)^2}=\frac{Mg\Delta N}{l}$$

As $(k+\Delta N)^2$ may usually be neglected in comparison with $D^2/4$ the equation becomes

$$V_1^2\equiv=\frac{MgD^2}{4lr^2}\,\frac{\Delta N}{k+\Delta N}$$

This equation fails when $k+\Delta N=0$, which practically means that $k=0$. When ΔN is also zero, V_1^2 is indeterminate and the sign of the deflection depends upon chance conditions. If k is large as compared with ΔN, which will usually be the case, V_1^2 will vary linearly with ΔN.

To use this method, k must therefore be known, and it may be determined with the aid of a given voltage preliminarily. The following experiments have been made in this way.

TABLE 112.—Disk electrometer. $M=1.055$ g.; $D=0.612$ cm.; $l=23.5$ cm.; $r=3.065$ cm.; $V_2=V_3=0$; V_1 increasing. Mean $k=0.04771$.

Drum.	$10^3\Delta N$	10^3k	Volt-meter.	Cor-rected V_3
1.38	0.69	50.9	18	18.6
5.85	2.92	46.0	38	37.4
14.60	7.30	46.1	57	56.6
40.75	20.37	47.8	85	85.1
94.9	47.45	65.0	104	110.0

TABLE 113.—Disk electrometer. $M=1.055$ g.; $D=0.674$ cm.; $l=23.5$ cm.; $r=3.065$ cm.; $V_2=V_3=0$; V_1 increasing. Mean $k=0.04778$.

Drum.	$10^3\Delta N$	10^3k	Volt-meter.	Cor-rected V_3
1.02	0.51	50.6	18	18.5
4.17	2.09	44.6	38	36.8
10.47	5.24	45.9	57	56.5
26.82	13.41	46.5	85	84.1
47.27	23.64	51.2	104	103.4

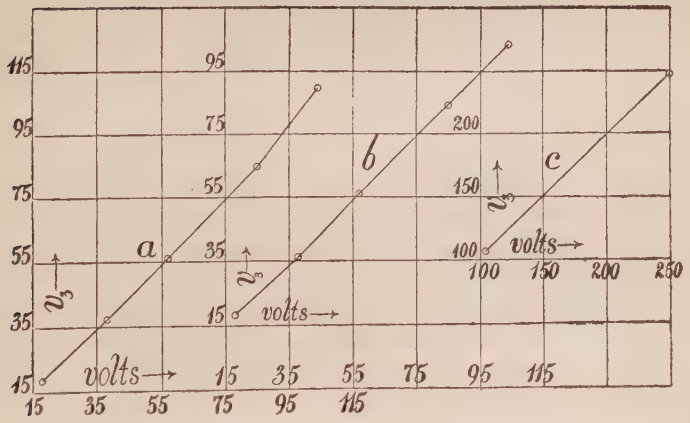

FIG. 117.—Observations with unsymmetric disk electrometer.

In both these tables and fig. 117, *a* and *b*, the asymmetry of the disk was about 0.5 mm., for the plates were over 6 mm. apart. The equation employed answers the requirements as closely as the observations could be made. At high voltages (100 volts) there is liable to be divergence, while at low voltages the displacement ΔN is too small for accurate work, seeing that the underlying equation is quadratic.

In tables 114 (fig. 117, *c*) and 115, tentative experiments are recorded as obtained with a light disk, $M = 0.6075$ gram. In table 114 it was weighted by a rider, so as to be available in measuring 250 volts and over. In table 115 the disk was used without a rider. The distance apart of the plates is over a centimeter.

TABLE 114.—Disk electrometer. $M = 1.0865$ g.; $D = 1.04$ cm.; $l = 23.5$ cm.; $r = 3.065$ cm.; $V_2 = V_3 = 0$.

	Drum.	$10^3 \Delta N$	$10^3 k$	Voltmeter.	Corrected V_3
V_1 decreasing: Mean $k = 0.005468$ cm.	10.85	5.42	5.2	250	247
	1.13	.56	5.8	104	107

TABLE 115.—Disk electrometer. $M = 1.0865$ g.; $D = 1.04$ cm.; $l = 23.5$ cm.; $r = 3.065$ cm.; $V_2 = V_3 = 0$.

	Drum.	$10^3 \Delta N$	$10^3 k$	Voltmeter.	Corrected V_3
V_1 increasing:	3.0	1.50	25.6	57	57
I. Mean $k = 0.030$ cm.	13.1	6.58	34.6	104	110
II. Mean $k = 0.049$ cm.	4.9	2.47	44.0	57	57
	17.0	8.49	54.6	104	100

The asymmetry occurring in table 114 is slight and the apparatus is therefore insensitive. In the second series of table 115 the disk was purposely made unsymmetric, without, however, increasing the sensitiveness or value of k as much as would have been supposed. For if ΔN is small as compared with k, $dV/d(\Delta N)$ should increase as $1/k$. In general, the *angular* orientation of the disk and irregularities at the edge of the guard ring and disk may introduce discrepancies of this kind. An apparatus like the present, intended for actual measurement, should be provided with a micrometer suspension, for shifting the disk as a whole in the direction of its axis, and with more elaborate means for sighting with a view to horizontal and vertical parallelism of the disk with the plates of the condenser than was the case with the improvised apparatus here treated. It has been stated that it is an inversion of the present displacement which is superimposed on the displacement in case of a permanently charged needle, and which thus demands an apparatus tested for absence of non-symmetry, if the voltages are to be proportional to the displacements.

THE QUADRANT ELECTROMETER.

160. Apparatus.—The method of measuring small angles given in §119 may be used in measuring very small voltages or small increments of potential, by attaching a pair of light mirrors, in parallel, to the needle of a quadrant electrometer. In the first experiments this was an improvised

instrument constructed by myself, the quadrants being of sheet copper fitted and soldered together and supported on cylinders of hard rubber. The bottom of the stem of the needle was submerged in sulphuric acid, as in Kelvin's instrument, and the suspension was bifilar. The insulation was throughout excellent. The needle was kept charged to about 200 volts with a Zamboni pile, any variation of charge being indicated by Elster and Geitel's electroscope.

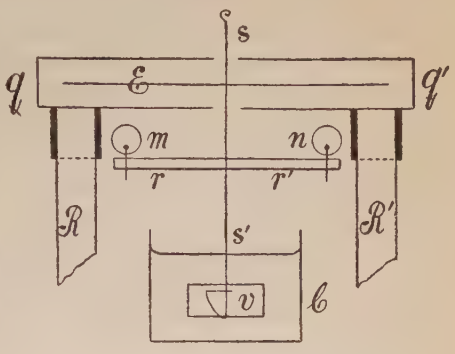

FIG. 118.—Quadrant electrometer adapted for parallel-mirror interferometry.

In fig. 118, qq' shows a pair of quadrants in vertical section, E the needle on the stem ss', the lower end of which is platinum, bent as shown, thus making a clip to hold the light mica vane v (if necessary) submerged in sulphuric acid of the vessel C charged by the Zamboni pile; RR are the hard-rubber supports of the quadrants. At a suitable distance below them the light parallel mirrors m and n (less than 1 cm. in diameter each) are supported by the light cross-piece of hard rubber rr attached to the stem ss' of the needle. The axial line of the needle E is parallel to the line rr between the mirrors, and the latter are placed at a horizontal angle of about 45° to rr.

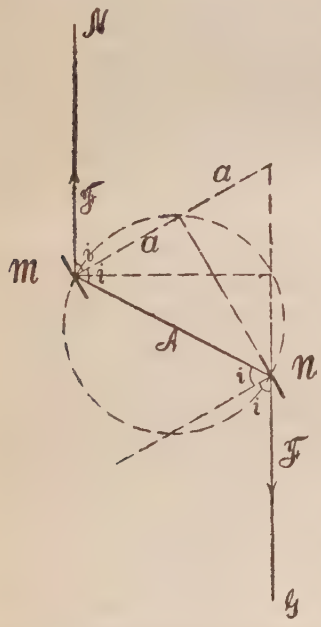

FIG. 119.—Diagram showing displacement and deflection in parallel-mirror interferometry.

To adjust m and n to adequate parallelism, each is supported by an attached fine needle, fitting snugly in a vertical groove in the ends of rr. The needle, as a whole, is to be clamped at rr in a suitable support and sunlight is to be used. When the horizontal beam reflected from m to n, and thence to a distant white screen, falls within the direct shadow of n, the needles are fixed in place by resinous cement. The mirrors should be equally high.

The quadrant electrometer with the needle in position was now placed with the aid of three long foot-screws on a circular platform just below the iron arm holding the fixed interferometer mirror M, and the reflection took place as shown in fig. 119 or in fig. 86 above. In effect the arc light from a collimator reflected from the front face of the grating (blue image due to scattering) is next reflected at n, thence to m, whence it goes to N and returns by the same route, passing, however, from n through the grating

to the observer's telescope. The case surrounding the electrometer must therefore be provided with a front and rear window. With so many reflections (altogether ten, including the one at the grating and the effect of the two windows) this beam is considerably weakened, and it is advisable to use black glass and not a silver mirror at the micrometer *M*. It is preferable, moreover, to use the glass side of the mirrors at *m* and *n*, as the silvering is liable to be brighter in the rear and the effect of the thin glass plate is of no consequence. This, in fact, was the greatest difficulty encountered, as the mirrors *m* and *n* were not at first adequately silvered and polished. Even when the direct image of the slit is clear the spectrum is apt to be dull and the ellipses are hard to find.

The adjustments, when so many conditions have to be met, were not easy of attainment. The electrical installation should first be completed and the needle in place between the quadrants, the electrometer being placed so that the beam from the interferometer strikes *n* (see figs. 118 and 119). A white screen behind *n*, catching the light passing beyond the edges and showing the shadow of *n*, facilitates this adjustment, the slit being opened wide. If possible, sunlight should here be used. The electrometer is now rotated as a whole around the vertical, until the light reflected from *n* strikes *m*, and a similar screen behind the latter in the line *mn* is necessary here. Next the mirror *N* is adjusted to normality, a white screen behind *m* in the direction *Nm* being essential, whereupon the light is reflected from *n* again toward the grating. As the pencil must pass through the grating (*G*) again, this is mounted to be capable of being raised or lowered and rotated around the vertical and horizontal (adjustment screws); but these are the usual adjustments on the interferometer. It follows that the electrometer must also be capable of being raised and lowered on its long foot screws, as already indicated.

Naturally sunlight, being steadier, is preferable to arc light, seeing that the range in which reflection takes place is limited by the area of the small one-fourth inch mirrors. Direct sunlight, without concentration, is adequate. It has been stated that both mirrors must be well silvered. Moreover, the spectrum should be so placed by raising and lowering the source of light and inclining the grating together with *N* that the higher orders of direct spectra are not in the same plane with the spectra superposed for interference. When the adjustments described are well made, there is no further difficulty in finding the solitary ellipses. As there is compensation owing to the two glass plate windows in case of the electrometer, the ellipses are liable to be enormous, practically vertical straight lines which are displaced with correspondingly great rapidity by the micrometer screw and are therefore hard to find. Hence some counter compensation at the micrometer mirror is desirable, in order that centers may appear and the displacement may be slower. A compensating plate about 1 cm. or less in thickness, with the *vertical* focus of the light from the slit on the stationary mirror, produces very clear and sharp ellipses, admirably adapted for measurement.

161. Observations.—The stems of the mirrors m and n on rr were about 4.5 cm. apart. Hence, since $i=45°$, $a=4.5/\sqrt{2}$ and if δ is the path difference

$$\frac{d\delta}{di}=0.0175\times 2a\sin i=0.079 \text{ cm. per degree.}$$

Supposing that 1 volt gave a deflection of 45° and that 10^{-4} cm. are measurable at the micrometer, the sensitiveness should be $10^{-4}/45\times 0.079$ or about 3×10^{-5} volts; *i.e.*, about 10^{-5} volts per vanishing interference ring. It would thus seem probable that with a lighter needle and a more delicate suspension the possibility of measuring 10^{-6} volts would not be out of the question. The following observations show that these surmises are correct so far as the method is concerned.

The great hardship encountered in the present work was the unavoidable agitation of the laboratory, and this unfortunately is insuperable. After the ellipses were found they were always in motion, so that the displacement work was bound to be rough and the use of interference rings out of the question. As the rings, however, may easily be obtained and used under suitable conditions, and as the purpose of the present paper is merely to test the method, the annoyances in question are of less consequence.

To obtain small potentials, a thin bare German-silver wire about 1 meter long was stretched and insulated on a board and the ends supplied with a constant potential difference of one volt. Two points of the wire, 1 or more centimeters apart, were then used as a source of potential, the wires from these points leading to a Mascart key, which suitably earths and commutates the charged wires leading to the electrometer. A thermocouple might have been used; but the long wire is preferable because of its simplicity.

In the first experiments made, the suspension was a bifilar about 10 cm. long (each strand of several silk fibers) and about 0.5 to 1 mm. apart. No doubt the torsional stress of the fiber was here of an order commensurate with the bifilar force. The needle, being damped in concentrated sulphuric acid, moved very slowly and about 2 minutes were allowed for each deflection. It was thus possible to follow the ellipses on commutation, from one to the other extreme elongation, by moving the micrometer screw proportionally to the displacement of ellipses. As a rule the ellipses were quite clear all the way, showing that the adjustment for parallelism of mirrors on the needle by the aid of sunlight is adequate. The potential of the charge on the needle was of the order of 200 volts.

Table 116 gives the results for the case when the points tapped on the wire were 10 and 18 cm., respectively, apart, the equivalent potential differences being 0.10 and 0.18 volt. The deflections on commutation at the Mascart key were nearly on opposite sides of the middle position of the needle.

The zero of the needle shows the usual tendency to wander, due apparently to air-currents, etc., but also to variations of the Zamboni pile, as the electrometer was an improvised instrument, in which the

electrometric adjustments were not quite perfect. In the same way the displacement per volt, $\Delta N/\Delta V$, varies somewhat, though here it is also a question as to whether in all cases adequate time was allowed before reading the micrometer; for the needle damped by concentrated sulphuric acid was quite aperiodic. There may be some residual effect

TABLE 116.—Potentials of quadrant electrometer read off by displacement interferometer. Mirrors at about 45° and 4.5 cm. apart along the needle.

P. D. applied.	Sign.	cm.	ΔN	$\Delta N/\Delta V$	P. D. applied.	Sign.	cm.	ΔN	$\Delta N/\Delta V$
0.18	±	0.0755			0.10	−	0.0183	0.0614	0.6140
	−	.0256	0.1025	0.5700		+	.0797		
	+	.1281							
	±	.0810				−	.0224	0.0569	0.5690
						+	.0793		
	±	.0790							
	−	.0194	0.1018	0.5650		−	.0232	0.0558	0.5580
	+	.1212				+	.0790		
	+	.1232	0.1046	0.5810		−	.0226	0.0564	0.5640
	−	.0186				+	.0790		

due to the viscosity of the relatively thick silk-fiber suspension. The sensitiveness obtained in the two series of experiments was as nearly the same as was to be expected, though there must have been some instrumental discrepancy in the first adjustment of the second series. We may, therefore, put $\Delta N/\Delta V = 0.57$ cm. on the micrometer, so that $\Delta N = 10^{-4}$ cm. corresponds to 0.000170 volt, or the sensitiveness is about 0.000060 per vanishing interference ring.

The instrument was now improved by inserting a longer bifilar suspension, consisting of a single fiber of silk. The damper and other details were retained. The results are given in table 117, potentials being tapped from points of the long wire, which were respectively 5 and 10 cm. apart. Owing to the very large deflection, the ellipses were not equally clear throughout the whole displacement from elongation to elongation.

TABLE 117.—The same. Long (20 cm.) suspension. Single fiber of silk.

P. D. applied.	Sign.	cm.	ΔN	$\Delta N/\Delta V$	P. D. applied.	Sign.	cm.	ΔN	$\Delta N/\Delta V$
0.10	−	0.0158	0.1538	1.538	0.05	−	0.0015	0.1495	2.990
	+	.1696				+	.1510		
	−	.0136	0.1595	1.595					
	+	.1731	0.1609	1.609		−	.0093	0.1437	2.874
	−	.0122				+	.1530		

The instrument behaved much better in the present case and the sensitiveness has been much increased, particularly in the second series of observations. Since $\Delta N/\Delta V$ is of the order of 2.9 cm. per volt, 10^{-4}

cm. corresponds to 0.000035 volt, *i.e.*, to about 0.000010 volt per ring, so that under favorable circumstances a few millionths of a volt should already be discernible.

162. Water damper.—The endeavor was now made to dispense with the damper of concentrated sulphuric acid, the motion of the needle being too slow in such a case. Water was next used, which as a damping medium admitted of several small oscillations of the needle. The curious fact, however, was here encountered that the illuminated mirrors were rarely at rest and that it was nearly impossible to determine the amount of displacement. In some cases the limit of motion of the uncharged needle was of the same order as the displacement to be measured.

To give examples of this behavior table 118 has been inserted, and it shows the consecutive values found for a needle the vane of which was damped in water. It was not quite aperiodic, but nearly so. The sensitiveness was low because of the low charge on the needle. The irregularity of displacement is the result of the superposition of the motion of the needle on the deflection to be measured.

Thus the mean sensitiveness is 0.4300 cm. per volt or 1/12900, about 0.000076 volt per vanishing interference ring. In spite of many trials the drift of the zero could not be removed. The results were about the same on the ensuing day.

TABLE 118.—Needle with a water damper. Potential = 170 volts. Potential difference 0.1 volt.

Shortly after charging $10^3\Delta N$ cm.	33.4	38.4	36.6	53.8
	49.1	46.7	39.3	37.5
	53.0	40.5	45.3	
Next day.....	40.5	48.0	51.5	

The instrument was now made more sensitive by charging the needle to a higher voltage. The results are given in table 119.

TABLE 119.—Needle with water damper. Potential = 220 volts. Potential difference 0.1 volt.

$10^3\Delta N$.....	82.0	85.0	73.0	83.0

The sensitiveness is thus 0.81 cm. per volt or 0.000040 volt per vanishing ring. The sensitiveness has not reached the above case, but the needle moves more rapidly.

A variety of other experiments led to similar results and need not be given here. The next step in advance will therefore be an investigation of the drift in the charged and uncharged instrument.

163. Drift forces.—The presence, in other words, of a beam of light impinging upon the mirrors seemed to be accompanied by torque tending to move the mirrors on the needle *into the beam*, *i.e.*, from the dark to the bright side of the mirrors. Very little control of this force was possible

535.4 B24P

a39001 006974565b

23278